ugr | Universidad de Granada

LABORATORIO EVALUACIÓN NO DESTRUCTIVA

MECHANICS OF NONLINEAR ULTRASOUND IN TISSUE

BY:

Juan Manuel Melchor Rodríguez

A THESIS SUBMITTED TO UNIVERSITY OF GRANADA
IN PARTIAL FULFILMENT OF THE REQUIREMENTS FOR THE DEGREE OF
DOCTOR OF PHILOSOPHY

ADVISOR:

Prof. Guillermo Rus Carlborg

Department of Structural Mechanics & Hydraulic Engineering
University of Granada
Granada (Spain)

November 2015

Editor: Universidad de Granada. Tesis Doctorales
Autor: Juan Manuel Melchor Rodríguez
ISBN: 978-84-1306-181-8
URI: http://hdl.handle.net/10481/55701

El doctorando Juan Manuel Melchor Rodríguez y el director de la tesis Dr. Guillermo Rus Carlborg, garantizamos, al firmar esta tesis doctoral, que el trabajo ha sido realizado por el doctorando bajo la dirección del director de la tesis y hasta donde nuestro conocimiento alcanza, en la realización del trabajo, se han respetado los derechos de otros autores a ser citados, cuando se han utilizado sus resultados o publicaciones.

En Granada, a 16 de noviembre de 2015

Director de la Tesis	Doctorando
Fdo.: GUILLERMO RUS CARLBORG	Fdo.: JUAN MANUEL MELCHOR RODRÍGUEZ

Summary

The study of tissue from the point of view of mechanics provides a tool to understand and unveil its structure as well as its behavior at different scales. Linear theories based on the superposition principle are an approximation that is devoid of meaning at the micromechanical level. Nonlinear theories generalize this concept where the effect does not need to be a consequence of only the sum of its causes, that is, where the principle of superposition is not valid and they explain the phenomenology of the processes in more precise contexts i.e. weather prediction, cellular competition in biology and propagation of sound through a complex media.

Particularly, Nonlinear Ultrasounds (NLUS) depend on elastic and inelastic constants different from Young's or Elastic's Modulus E and Poisson's Coefficient ν, which can be quite more sensitive to damage and hiperelastic properties in tissues, as they depends on their microestructure.

Throughout History, there are a disparity of unified criteria to consider the Third Order Elastic Constants (TOEC). Landau and Lifshitz in 1941, proposed for the first time in their book "Theory of Elasticity" [1] the TOEC as an exercise or proposed problem, following a series expansion of Hooke's law from the energy.

From the 70's, several visionary researchers on nonlinear waves as Zarembo and Gol'dberg field observed experimentally nonlinear elasticity constants by the finite amplitude techniques. Independently, they were raised theoretical models as Westervelt and Khokhlov, Zabolotskaya and Kuznetsov (KZK), where by making use of resolution proceses mainly based on perturbation theory an analytical solution were established and sometimes comparing with elasticity models. Progress in Science is subject to the application or unification of theories only by standing *on the shoulders of giants*. Since then, a large number of different references and criteria to encompass nonlinear elastic constants with the corresponding conversion have been published.

In trying to systematize the above, we have found many inconsistencies and contradictions. For example, following a reasonable basis to explore the relationship between nonlinear elasticity and nonlinear acoustics, there are several definitions of the nonlinear acoustic parameter of first order β (without physical meaning), several TOEC, Westervelt, Burgers and KZK Partial Differential Equations PDE or Nonlinear acoustic models only valid for the case of fluids or solids further with various different solutions suggested.

Therefore it is important to develop a general theory, consistent from the viewpoints of (1) mathematics, (2) the theory of continuum mechanics, (3) of the physics of wave propagation and (4) experimental engineering, that unifies all previous developments.

- ▷ **(1) Mathematics:** A framework of PDE should be derived from a consistent series in terms of invariants to rotations and translations are explicitly developed and analyzed, and indexical and vector notation facilitates a clear and unambiguous expression. At this point the families of nonlinear PDE should be well classified to establish the best practice in the relationship between elasticity and acoustics.
- ▷ **(2) Continuum Mechanics:** The beginning of a new theory should be expressed without simplifications in a general context without small displacements, correctly defining all the concepts of stress, Piola-Kirchoff tensor, strain tensor, deformation gradient, energy, and related magnitudes.
- ▷ **(3) Physics of Waves:** The equation of nonlinear waves and definition of nonlinearity from acoustic pressure is solved using perturbation theory as iterative recursive method in converging to the equation of Westervelt and its generalization to multiple harmonics.
- ▷ **(4) Experimental Engineering :** To quantify different harmonics from an experimental point of view, the acoustic pressures are measured with hydrophones and oscilloscopes, in different configurations via harmonic generation methods, as well as nonlinear interactions of ultrasonic waves, exciting with different types of source waves, Primary (P), Secondary (S), and their combinations.

This thesis provides an unified derivation of the theories of nonlinear elasticity based on the classical continuum mechanics evidencing several misconceptions and errors commonly assumed in literature. It establishes a relationship with the classical nonlinear acoustics from a new perspective that is validated with the results by Hamilton and Norris [2].

This analysis leads us to unify criteria and break down of the definition of the parameter β previously mentioned, to develop an equation of Westervelt, generalized for harmonics of any order, and to establish a new theory of nonlinear acoustics, expanding into four types of nonlinearity, whose origin is based on the contribution of the liquid phase and the fiber or collagen phase, which is crucial to explain and understand the hyperelasticity and wave propagation in quasi-fluids and tissue. The potential impact of this technique involves a new approach in the tissue characterization with clinical applications due to the separation of nonlinear phases of tissue revealing their main mechanism that is relevant in the diagnosis and therapy of many tissue disorders.

The different results that arise as a consequence of this theory, are experimentally validated in several setups in different materials by developing new non-destructive evaluation techniques. They are (1) Non-linear mixing with a single transducer to measure and quantify the nonlinearity of water, (2) nonlinear mixing with two transducers in angle to characterize

aluminum, and (3) a new torsional sensor for characterizing hydrogels, silicones and tissues, which has been designed, optimized and prototyped.

Finally, this thesis proposes a possible explanation on how the nolinearity is caused by damage from microcracks. The Homogenization theory developed by Eshelby in 1956 [3], is used for this purpose. Subsequently, the case of a material is resolved with inclusions with geometric form of spheroids. Note that the theoretical and experimental scheme proposed could be relevant in the development of new medical devices for bone quality assessment and the osteoporosis diagnosis.

Resumen

El estudio de los tejidos desde el punto de vista mecánico proporciona una herramienta tanto para entender y conocer su estructura como su comportamiento a distintas escalas. La teorías lineales basadas en el principio de superposición o el efecto como suma de las causas, son una aproximación que queda exenta de sentido a nivel micromecánico. Las teorías nolineales generalizan este concepto donde el efecto no tiene porque ser solo suma de las causas, es decir el principio de superposición no es completo y explican la fenomenología de los procesos en contextos más precisos.

La Nolinelalidad Ultrasónica NL US en concreto depende de constantes elásticas e inelásticas diferentes al Módulo de Young o Elástico E, y Coeficiente de Poisson ν, que pueden ser mucho más sensibles a daño y propiedades hiperelásticas de tejidos que E, y ν, porque dependen de su microestructura.

Varios investigadores visionarios desde los años 70 como Zarembo y Gol'dberg, observaron experimentalmente nolinealidades acústicas mediante métodos de amplitud finita. Independientemente, se plantearon modelos teóricos como es el caso de la Ecuación en derivadas parciales nolineal PDE de Westervelt, Khokhlov, Zabolotskaya y Kuznetsov, KZK con procesos de resolución analíticos basados en la teoría de la perturbación. El avance en la ciencia viene sujeto a la aplicación o unificación de grandes teorías poniéndonos *a hombros de gigantes*. A lo largo de la historia, existen disparidad de criterios para unificar las constantes elásticas de tercer orden. El libro de Teoría de la Elasticidad de Landau y Lifshitz en 1957 [1] es el primer lugar donde se plantean las Constantes Elásticas de Tercer orden conocidas hoy en día como TOEC, en un ejercicio o problema práctico propuesto, a raíz del desarrollo en serie de la ley de hooke a partir de la energía. Dese entonces es posible encontrar numerosas referencias y diferentes criterios para englobar las constantes de la elasticidad nolineal con su correspondiente conversión.

Al tratar de sistematizar lo anteriormente expuesto, hemos observado múltiples inconsistencias, y contradicciones. Por ejemplo, a raíz de explorar un criterio razonable para vincular la nolinealidad elástica con la nolinealidad acústica, existen diferentes definiciones del conocido parámetro β, diferentes parámetros elásticos de tercer orden, ecuaciones de Westervelt, Burgers y KZK que valen solo en el caso de fluidos, sólidos, etc. que además sugieren distintas soluciones.

Por lo tanto es importante desarrollar una teoría generalizada, consistente desde el punto de vista (1) matemático, (2) de la teoría de medios continuos, y (3) de la física de la propagación de ondas y (4) de la ingeniería experimental, que unifique todos los desarrollos anteriores.

- ▷ **(1) Matemático:** Partiendo de un marco consistente en el sentido de los desarrollos en serie de la energía bien analizados cuyos invariantes frente a rotaciones y traslaciones estén explícitamente analizados y desarrollados y cuya notación indicial y vectorial facilite de forma clara y unívoca su expresión. En este punto las familias de ecuaciones en derivadas parciales nolineales deben quedar muy bien clasificadas de cara a establecer procedimientos óptimos en la relación entre Elasticidad y Acústica.
- ▷ **(2) Medios continuos:** Comenzando con la teoría sin simplificaciones en un contexto lo más general posible sin pequeños desplazamientos, definiendo correctamente todos los conceptos de tensión, tensor de Piola-Kirchoff, tensor de deformaciones, gradiente de deformación energía, etc...
- ▷ **(3) Física de ondas:** Teoría de la perturbación como método recursivo iterativo en la ecuación de ondas nolineal, definición de nolinealidad desde la presión acústica coincidiendo con la que interviene en la ecuación de Westervelt, generalización a múltiples armónicos, etc.
- ▷ **(4) Ingeniería experimental:** Cuantificación de diversos armónicos desde el punto de vista realista a partir de la presión acústica que medimos con osciloscopios, en diferentes configuraciones vía generación de armónicos, mezcla de ondas ultrasónicas, diferentes tipos de ondas, P, S, y su combinación, etc.

A lo largo del desarrollo de esta Tesis, hace un desarrollo unificado de las teorías de nonlinealidad elástica basadas en la mecánica de medios continuos clásica. Se establece una relación con la nolinealidad acústica clásica desde una nueva perspectiva que valida los resultados de Hamilton y Norris en su libro *Nonlinear Acoustics* [2]. Dicho análisis nos lleva a unificar y desglosar criterios de definición del parametro β previamente mencionado, a desarrollar una ecuación generalizada de Westevelt para armónicos de cualquier orden y a establecer una nueva teoría de nolinealidad acústica expandiendo en cuatro tipologías de nolinealidad, es debido a la contribución de la fase líquida y la fase de fibra o colágeno, en el caso de quasifluidos o tejidos, respectivamente. El impacto potencial de esta técnica supone un nuevo aporte en la caracterización tisular cuyas aplicaciones clínicas se deben a la separación de fases nolineales que revelan sus principales mecanismos, lo cual es especialmente relevante desde el punto de vista diagnóstico y terapéutico de muchos trastornos en el tejido.

Al tratar de explicar experimentalmente los distintos resultados que surgen como consecuencia de esta teoría, se desarrollan varios ensayos en distintos materiales, utilizando técnicas de evaluación no destructiva. Mezcla no lineal con un solo transductor para medir

la nolinealidad del agua, mezcla con dos para caracterizar aluminio y el diseño y optimización de un nuevo sensor de torsión para caracterizar hidrogeles, siliconas y tejidos.

Además en esta Tesis se plantea una posible explicación sobre como se origina la nolinealidad por daño a partir de microgrietas. Para ello se recurre a la teoría de homogeneización desarrollada por Eshelby en 1956 [3], y se resuelve el caso de un material con inclusiones con forma geométrica de esferoides. Cabe destacar que el esquema teórico y experimental propuesto podría ser relevante en el desarrollo de nuevos dispositivos médicos para la evaluación de la calidad ósea y el diagnóstico de la osteoporosis.

Acknowledgments

First of all, I would like to thank the advisor responsible for the direction of my thesis, Prof. Guillermo Rus Carlborg, head of the *Nondestructive Evaluation Laboratory* of the Department of Structural Mechanics and Hydraulic Engineering. He has played an essential role in the success of this dissertation, joining and confronting his respective expertise in fields of Mathematics, Physics, Engineering and Medicine. In particular, I thank his permanent dedication, predisposition and passion to the investigation and for teaching and passing me down this vision, his patience, guidance, rigor and constructive suggestions over the course of these years. I am grateful to Prof. Juan Soler to get transmitting me the passion for Applied Mathematics in the grade of Mathematics, in Master of Physics and Mathematics and in research. Also, Prof. Aurelio Peñalver to initiate me in the mathematical knowledge from High School. I want to thank Prof. Ricardo Ocaña who always oriented me on my work in Statistics his full dedication and interest. In addition, I also thank to Prof. Pascal Laugier and Dr. Sylvain Haupert for supervising my research stay at the *Laboratoire d'Imagerie Biomedicale, University Pierre et Marie Curie, Sorbonna, Paris VI*, for sharing their expertise on bone quantitative ultrasound, and for counting on me for future collaborations. I would like to thank William J. Parnell for their supervision in my short term stay of research at the *Faculty of Mathematics Alan Turing, University of Manchester* inside the group of Waves in Complex Media, his work is a continuos inspiration for me, the contribution of our work is a main source of mathematical ideas that are the pillars of this thesis. The role of several friends and family was essential in this period, thanks to Álvaro, Nuria, Dani, Luis, Curra, Socorro, Antonio, Ernesto, Tilman, Miguel, and El Pequeño Salvaje (Soundtrack of this thesis *please listen the cd audio files*) for your support and interest. Finally, I thank to all my colleagues and friends of the Nondestructive Evaluation Laboratory specially Paloma Massó, Nicolas Bochud, Laura Peralta, Roberto Palma, Rafael Muñoz, Juanchu Soto, Rubén Molina and Antonio Callejas for making the everyday life at the lab enjoyable, magic, avant-garde, and particularly for supporting me over the last years. Thanks team.

I would like to thank the University of Granada, Spain for the support and funding in my FPU grant, and particularly to give the pleasure to investigate within this interdisciplinary researchs area during four years. In addition, I acknowledge the Spanish Ministerio de Economía y Competitividad for projects DPI2010-17065, DPI2014-51870R Junta de Andalucía for projects P11CTS-8089 and GGI3000IDIB, CEI Biotic grant, the University of

Manchester via the Engineering and Physical Science Research Council (EPSRC) grant reference EP/I01912X/1, whose funding enabled me to take part to numerous international congresses and stays of research.

Specially dedicated to Mia, Caroline, Juan and Nati.
Peace, Love, Inspiration & Harmony

Abbreviations

NLUS	Nonlinear Ultrasounds
TOEC	Third Order Elastic Constants
KZK	Khokhlov, Zabolotskaya and Kuznetsov
PDE	Partial Differential Equations
P	Primary
S	Secondary
NDE	Nondestructive Evaluation
DAET	Dynamic Acousto Elasticity Testing
HIFU	High Intensity Focus Ultrasound
FUIS	Fast Ultrasound Image Simulation
BLT	Bolt-clamped Langevin Type
PZT	Lead zirconate titanate
PZT-5	Lead zirconate titanate type 5
FEM	Finite Element Method
FEAP	Finite Element Method software
GA	Genetic Algorithms
POD	Probability of detection
RPOD	Robust Probability of Detection
FFT	Fast Fourier Transform
SEF	Strain energy function
HS	Hashin-Shtrikman
NL	Nonlinear
FP	Forward problem
USGS	United States Goverment
IP	Inverse Problem
RMS	Root mean square
PMMA	Polymethylmethacrylate
CFRP	Carbon Fiber
FOEC	Fourth Order Elastic Constants
NF	Near field
LF	Low frequency
HF	High frequency

TOA	Time of arrival
PLA	PolyLactic Acid
END	Nondestructive evaluation

List of Symbols

Symbol	Description
E	Elastic's Modulus
ν	Poisson's Coefficient
β	Nonlinear acoustic parameter of first order
a	Initial position
x_i^0	Initial position
x_i	Final position
$\mathbf{x^0}$	Initial position
$\mathbf{x_i^0}$	Final position
$\mathbf{u}$	Displacements
u_i	Displacements
$\mathbf{F}$	Deformation Gradient
F_{ij}	Deformation Gradient
$\mathbf{E}$	Green-Lagrange strain tensor
ε_{ij}	Green-Lagrange strain tensor
δ_{ij}	Kronecker symbol
$\mathbf{I}$	Identity matrix
$\mathbf{T}$	Cauchy's stress
σ_{ij}	Cauchy's stress
W	the strain energy *per unit volume of the undeformed material*
$\mathbf{P}$	The nominal stress or first Piola-Kirchoff stress
P_{ij}	The nominal stress or first Piola-Kirchoff stress
$\mathbf{S}$	second Piola-Kirchoff tensor
S_{ij}	second Piola-Kirchoff tensor
tr$\mathbf{F}$	Trace of deformation gradient
F_{kk}	Trace of deformation gradient
$\otimes$	Tensorial product
$\mathbf{T}^L$	Linear stress
$\mathbf{T}^{NL}$	Nonlinear stress

Symbol	Description
σ_{ij}^{L}	Linear stress tensor
σ_{ij}^{NL}	Nonlinear stress tensor
I_1	First invariant of strain
I_2	Second invariant of strain
I_3	Third invariant of strain
W_I	Isotropic strain energy
λ	First Lamé constant
μ	Second Lamé constant or shear modulus
$\mathcal{A}$	Third order elastic constant of Landau
$\mathcal{B}$	Third order elastic constant of Landau
$\mathcal{C}$	Third order elastic constant of Landau
$\tilde{\mathcal{A}}$	New Third order elastic constant
$\tilde{\mathcal{B}}$	New Third order elastic constant
$\tilde{\mathcal{C}}$	New Third order elastic constant
C_{IJK}	Standard nonlinear coefficients
l	Third order elastic constant of Murnaghan
m	Third order elastic constant of Murnaghan
n	Third order elastic constant of Murnaghan
ρ_0	Unperturbed density
A	First parameter of Taylor expansion of the pressure in fluids
B	Second parameter of Taylor expansion of the pressure in fluids
$\mathbf{v}$	Velocity
D/Dt	Total derivative
ρ	Density
$f_{,i} = \frac{\partial f}{\partial x_i}$	Cartesian components of the displacement
$u_1(x_1, x_2, x_3) = u_1(x_1)$,	Particles only move along the x_1-direction
u_1	Displacements in one dimension
$u_{1,tt}$	Second derivative in time
$u_{1,11}$	Second derivative in space
M	$\lambda + 2\mu = \rho c_p^2$
c_p	Longitudinal (P-wave) velocity
β_H	First nonlinear wave parameter as defined Hamilton
$u^{(0)}$	Zero-order perturbation solutions
$u^{(1)}$	First-order perturbation solutions
k	Wave number
a	Amplitude of fundamental harmonic
ω	Angular frequency
f	Oscillation frequency
b	Amplitude of second harmonic
K	Compressional modulus
$A[\varepsilon, \varepsilon_{1,t}]$	Hysteretic elastic elements typically nonanalytic
β_G	First nonlinear wave parameter as defined Guyer

Symbol	Description
ω_a	Excitation frequency
ω_b	Excitation frequency
ω_c	Sum or difference of two excitation frequencies
ε_a	Amplitude of a excitation frequency
ε_b	Amplitude of a excitation frequency
ε_b	Sum or difference of two amplitudes of excitation frequencies
β_Z^l	First nonlinear longitudinal wave parameter as defined Zarembo
β_Z^τ	First nonlinear transversal wave parameter as defined Zarembo
δ	Second-order nonlinearity
$u^{(2)}$	Second-order perturbation solution
c	Amplitude of the third harmonic
B/A	Nonlinear acoustic parameter for fluids
c_0	Small signal sound speed
β_W	First nonlinear wave parameter as is defined in the Westervelt equation
v	Volumetric strain
D	Sound diffusivity
η	Viscosity
τ_{ij}	Terms outside the diagonal in the Cauchy stress tensor
$\eta^v \dot{v}$	Viscosity part in constitutive equation
σ^V	Stress Viscosity part
α	Viscosity by Stokes' law
D_{ij}	Deviatoric tensor
β^{vp}	Volumetric pressure first nonlinear acoustic parameter
β^{dp}	Deviatoric pressure first nonlinear acoustic parameter
β^{ds}	Deviatoric shear first nonlinear acoustic parameter
β^{cs}	Compound shear first nonlinear acoustic parameter
c_s	Transversal velocity of sound
A	Constant amplitude of the plane longitudinal waves
A_h	Constant horizontal amplitude of the plane transversal waves
A_v	Constant vertical amplitude of the plane transversal waves
θ	Angle of propagation
$\mathbf{T}$	Stress
$\mathbf{S}$	Strain
$\mathbf{D}$	Charge-density displacement
$\mathbf{E}$	Electric field
$\mathbf{C_E}$	Piezoelectric stiffness matrix

Symbol	Description
$\mathbf{e}$	Piezoelectric coupling coefficient matrix
$\mathbf{e}^T$	Piezoelectric coupling coefficient matrix transposed
$\varepsilon_{\mathbf{S}}$	Permitivity coefficient matrix
ϕ	Electric potential or voltage
$\mathbf{U}$	Displacement vector
$\ddot{\mathbf{U}}$	Acceleration vector
u_i^a	Three components of the displacements
ϕ^a	Voltage degree of freedom associated to node a
$\mathbf{M}$	Mass matrix
$\mathbf{K}$	Stiffness matrix
$\bar{\mathbf{F}}(\mathbf{t})$	Time history of the applied load
$\mathbf{D^*}$	Elasticity matrix that transforms effective strains to stresses including the electric field coupling at every point of the domain
$\mathbf{B}^{(e)}$	Strain-displacement matrix of the element (e), and the superscript T denotes the transpose operator,
$N_{,i}^a$, $i = 1, 2, 3$	Shape functions defined for each type of element
$H(t)$	Heaviside function
D_0	Distance to origin in the x axes
Lx, Ly and Lz	Size of prismatic block
$k*$	Stiffness
$I*$	Inertia
M_T	Applied torsional moment.
n	Piezoceramic elements
d	Distance from the center of rotation
F	Resulting force of the shear stress
$a \times b$	Area of the element
$u*$	Displacement between upper and lower sides separated distance l
G^*	Modified shear stiffness
r	Cylindrical or annular (ring-shaped) of radius
h	Height of the cylinder (in the axial direction)
e	Thickness of the ring (in the radial direction)
V	Readings from the sensors for the theoretical or synthetic case
V^x	Readings from the sensors for the experimental case
V^0	Readings from the sensors in the healthy state of the tissue is defined for calibration
RMS	Root mean square defined for a discrete function f in time domain $f(t_i)$ at N sampling points
γ	A residual defined from the misfit or discrepancy $\Phi^x - \Phi$ between the measurements.
f	Fitness function
ϵ	Small value
pat_{pr}	Severity of the pathologies in terms of shear stiffness and damping alteration in different tissue layers p considering a reference healthy tissue r
G	Shear modulus
$\tilde{G}$	Reference healthy tissue
ξ_i	random variable

Symbol	Description
Ω	Medium
Ω_0	Host or matrix
Ω_1	Inclusion phase
$\mathbf{C}^0$	Hosted elastic modulus tensor
$\mathbf{C}^1$	Inclusion phase elastic modulus tensor
$a_1 = a_2 = \ell$	Semi-axes of aligned spheroids
$\delta = a_3/\ell$	Aspect ratio of aligned spheroids
ϕ	Volume fraction
$f\{\cdot\}$	An argument of the function f
$\overline{f}^r$	Volume average over the rth phase
$\mathbf{I}$	Fourth order identity tensor,
$\mathbf{S}$	(uniform) Eshelby tensor
$\mathbf{D}^0$	Compliance tensor
$\bar{\mathbf{E}}^0 = \bar{\mathbf{E}}^\infty$	Strain in the far field,
N	Number of inclusions in the domain Ω
$\mathbf{H}$	"Extra stress" associated with the crack.
$\tilde{\mathbf{T}}^1_{NL}$	Nonlinear isotropic stress term
$\boldsymbol{\mathcal{U}}$	Nonlinear effects
K_0	Compressibility modulus of the host material
κ	Sharpness parameter
$\mathbf{I}_2$	Identity tensor of second order
β_1	Volumetric constitutive nonlinearity
β^l_{Gol}	Longitudinal nonlinear acoustic parameter as defined Gol'dberg
β^τ_{Gol}	Transverse nonlinear acoustic parameter as defined Gol'dberg
I_4	Anisotropic invariants of deformation
I_5	Anisotropic invariants of deformation
$\mathbf{M}$	Direction parallel to the x_3 axis
W_{TI}	Transversal isotropic strain energy
$\mathcal{A}, \mathcal{B}, ..., \mathcal{I}$	*Nine* nonlinear (third-order) moduli)
k, ℓ, m, n and p	Linear elastic coefficients usually taken for linear elasticity
A, B, Γ, Δ, E, Z, H, Θ, I, K, Λ, M, N, Ξ and O	Parameters related to anisotropy stress expression
E_{*i}	Young's modulus depends on direction
ν_i	Poisson's ratio depends on direction
Q_{ij}	Stiffness matrix in composites materials
I_6	Invariant of fourth order.
Pi_i	Nonlinear acoustic parameters of any order from $1, ..., n$
$U_a^{(0)}$, $U_b^{(0)}$	Amplitude of the fundamental wave at frequency
$U^{(1)_a}$, $U^{(1)_b}$	Amplitude of the second harmonic
$p_a^{(0)}$, $p_a^{(0)}$	Pressures of the fundamentals
$p_a^{(1)}$, $p_a^{(1)}$	Pressures of the second harmonics
p_+, p_-	Pressures of the sum and difference harmonics

Symbol	Description
φ	Phase
$\mathbf{k_1}$, $\mathbf{k_2}$	Direction of the beam propagation
q_3, n, m, n_2, q_5, q_2, q_1, q_4, l, p, l_1 and l_2	Mesh refinement parameters
S_0	Initial signal
S_r	Receiver signal
S_c	Signal transmitted
α_c	Correction factor
$\mathbf{C}^*$	Effective nonlinear parameter
k_j	Normalization constants
β_*	Misfit function
U_s	Displacement of the particles in the specimen
T_{sw}	Transmission coefficient from bone to water
v^{max}	Maximum strain in sample

Symbol	SI	Description
ρ	[kg/m^3]	Density
λ	[Pa]	Lamé's first constant
μ	[Pa]	Lamé's second constant
β	[-]	Nonlinear elastic coefficient of first-order
δ	[-]	Nonlinear elastic coefficient of second-order
E	[Pa]	Young modulus
ν	[-]	Poisson ratio
c, c_p, c_s	[m/s]	Longitudinal and transversal wave velocity
Z	[Ω]	Material impedance
A, B	[m]	Displacement's amplitude
k	[1/m]	Wave number
t	[s]	Time variable
x	[m]	Space variable
a	[m]	Thickness
α	[Np/m]	Attenuation coefficient
d	[m]	Position
T	[s]	Period
pw	[mm]	Piezoelectric ceramic width
pl	[mm]	Piezoelectric ceramic length
pt	[mm]	Piezoelectric ceramic thickness
dpe	[mm]	Disc piezoelectric ceramic eccentricity
dr	[mm]	Disc radius
rpe	[mm]	Ring piezoelectric ceramic eccentricity
rw	[mm]	Ring width
drt	[mm]	Disc and ring thickness

Contents

List of Figures

List of Tables

L'ordre matemàtic simula el món real,
crea un altre món de càlcul, i mental
regido por leyes extrañas
hipótesis, modelos
en un ordenador renacen
y musicamos las celestes aventuras
vemos en la pantalla nacer un mundo nuevo [...]

El rastro profundo del tiempo, materia
has representado la solidez
y tus átomos son casi vacíos has sido certidumbre y paradoja
o inérte y estéril
¡cuantas preguntas cuantas respuestas! [...].

Multiversos
David Jou y Antonio Arias, 2015

Part I

INTRODUCTION

1

Context and motivation

Ultrasonics based Nondestructive Evaluation (NDE) is an emerging technology with an enormous potential in the field of biomedical and industrial engineering. To rigorously advance this technology, it is necessary to develop the knowledge mathematical and physical models that ground it. Nonlinearity is the key to introduce us into a micro-mechanical level and understand it as the origin of damage or pathology in new terms. Ultrasound nonlinearity is a new diagnosis principle with potentially superior sensitivity. The potential of this multi-scale new paradigm gives us a significative tool to quantify several modulus and parameters that could be relevant in diagnosis and therapies.

Nonlinearity should be studied for this proposal from the root, from (1) a mathematical point of view, where a nonlinear system of equations is a set of simultaneous equations in which the unknowns appear as variables of a polynomial of degree higher than one or in the argument of a function which is not a polynomial of degree one, and (2) In physics and other sciences, where a nonlinear system, in contrast to a linear system, is a system which does not satisfy *the superposition principle: meaning that the output of a nonlinear system is not directly proportional to the input.*

As nonlinear equations are difficult to solve, nonlinear systems are commonly approximated by linear equations (linearization). This works well up to some accuracy and some range for the input values, but some interesting phenomena such as chaos and singularities are hidden by linearization. It follows that some aspects of the behavior of a nonlinear system appear commonly to be chaotic, unpredictable or counterintuitive. Although such chaotic behavior may resemble random behavior, it is absolutely not random. For example, some aspects of the weather are seen to be chaotic, where simple changes in one part of the

system produce complex effects throughout. This nonlinearity is one of the reasons why accurate long-term forecasts are impossible with current technology.

Nonlinear acoustics is a branch of physics and acoustics dealing with sound waves of sufficiently large amplitudes. Large amplitudes require using full systems of governing equations of fluid dynamics (for sound waves in fluids and gases) and elasticity (for sound waves in solids and quasifluids such as tissues). These equations are generally nonlinear, and their traditional linearization is no longer realistic [8, 9, 10, 11]. The solutions of these equations show that, due to the effects of nonlinearity, sound waves are being distorted as they travel. This is a key in understanding the interaction and propagation of ultrasound.

The understanding of nonlinearity from the point of view of the Theory of Elasticity carry out the study of constitutive equation from the energy potential. Landau-Lifshitz, Murnaghan, Hughes, Gol'dberg, Thurston and Zarembo were interested in the formulation of nonlinear elasticity since the beginning of the second half of twentieth century [1, 12, 13, 14, 15, 5]. The main context was the rotation and displacement invariance before and after the consideration of strain. They extracted the TOEC with different expressions, and in the case of Gol'dberg Thurston and Zarembo started with the relationship between TOEC and acoustics. At the end of twentieh century, there were several authors interested on that research due to the experimental developing of new techniques in ultrasonics as finite amplitude, multilayer approaches, where the new forms of nonlinearity in acoustics and the study different types of waves as shear and surface played an important role [16, 17, 18, 19, 20, 21, 22, 23, 24, 25].

Nowadays, there are several new approaches in this field due to the repercussion of many experimental proceses as Dynamic Acousto Elasticity Testing, (DAET), and the renewal importance of the realtionship between the propagation of waves in complex media [26, 27, 28]. Biomaterials and tissues can be understanding without non invasive radiations in vivo [29, 30, 31].

Analyzing the theoretical background from Hamilton Nonlinear acoustics book and different studies about nonlinear acoustics previously cited [2], there were some conflict criteria by different schools. For example, the TOEC definitions are not unique, they depend on the algebraic invariants from the energy function and at the end to a Taylor expansion. There are many definitions of stress and strain and the main point is the consideration of compatibility equation where the strain is formulated from displacements and the large displacements when are introduced are considered as geometric nonlinearity. This leads to find in literature an ambiguous definition of beta nonlinear acoustic parameter of first order beta [32]. Consequently, this allow us to unify acoustic and elastic nonlinearity as a common theory where all formulations in solids, crystals, liquids and tissues are contemplated. Starting from the Hamilton classic relationship between TOEC and beta, and being validated from Landau invariants, and nonlinear wave equation we extend to second order of nonlinearity in acoustic and elastic regime, and transversally isotropic case is considered too due to the nature of tissues. Considering all these contexts, is posible to derive the Westervelt equation

[33, 34] to higher harmonics. It could be interesting in the field of the understanding of wave propagation in fluids, and may to the development of the KZK equation that is actually used in High Intensity Focus Ultrasound (HIFU) as a mechanism of modellization for ultrasonic therapies against some solid cancers [35, 36]. Elastic and geometric nonlinearity manifest in ultrasonic waves in new interactions by nonlinear mixing and appearance of growing harmonics by harmonic generation technique, which are easily detected and isolated experimentally in the frequency domain.

Finally, a new paradigm is formulated in order to establish a new criteria allowing the separation and quantification of nonlinear parts due to the fiber or collagen and from the liquid or water. For this reason, is necessary to validate the new types of nonlinearity from experimental setups, non collinear mixing is [37] immersion tank with just one transducer. Then, a new device is constructed to try the angles of interaction of two P and S waves even for horizontal and vertical amplitudes and all combinations between them, based on Korneev's equations [38]. However, for the cases of quasifluids and tissues nonlinear torsional waves are investigated under the fundamentals of this theory. A torsional ultrasonic sensor is design optimized and fabricated to validate the results of the theory [39]. The main impact of this transducer is the direct application to preterm birth assessment, it consists of the quantification of shear modulus as the consistency changes in cervical tissue [40]. The nonlinear torsional parameters could be also relevant in the diagnosis of many diseases that may be influenced by biomechanical variables.

Alternatively, the origin of nonlinearity in materials from the physical point of view was studied by several authors taking into account atomistic potential arguments [41, 42]. In this thesis, a new plausible explanation is proposed introducing that could be due to the appearance of micromechanical damage. The microcrack inclusions inside a material are considered and studied from nonlinear propagation of ultrasonic waves. This perspective, based on the homogenization theory developed firstly by Eshelby in the beginning of second half of the twentieth century [43, 44, 45] and then by many authors [46, 47, 48, 49, 50], provides a new approach studied as a set of microcracks as density of them, which could explain osseous quality and fracture risk [51, 52, 53, 54, 55, 56]. An experimental approach is also proposed to link nonlinear acoustic properties and density of microcracks in osteoporotic bone.

2
Objetives

The need to understand the mechanics impels us to unify nonlinear elasticity as well as nonlinear acoustics and the different techniques and prototypes that could be useful as medical diagnostic tools and principles.

The mechanics of solids understood and controlled to characterize tissue, provides both diagnostic techniques based on ultrasonic propagation and new sensors reliable and sensitive criteria in the face to improve the understanding of the structural annd mechanical properties [57, 58, 59, 60, 61, 62, 63]. The interaction between ultrasound and tissue entails evaluation techniques that evolve as advances into the understanding of the subject and the development of the technology [64, 65, 66, 67, 68]. The methodology used to quantify the mechanical properties focuses on the application of the inverse problem to reconstruct both the linear constitutive characteristics as the nonlinear model-based ones [69, 70, 71, 72, 39].

To this end, this thesis aims at understanding nonlinear elastoacoustic parameters in tissue, rewrite nonlinear acoustic models designing and validating a new set of parameters and explore the posible origin of nonlinearity in terms of damage and microcracks. To reach this target, the following research steps are consider, in basis of hypothesis:

1. To unify nonlinear continuum mechanics, which implies a global definition of stress and strain taking or not taking into account geometric nonlinearity in the compatibility equation and considering the material, if it is solid, fluid or tissue. The different assumptions, govern the whole theoretical background of this thesis.

   Hypothesis 1: Nonlinear Elasticity can be understood from a consistent algebraic context where a material whose anisotropic or isotropic behavior could be univocally characterized. The parameters that appear in nonlinear classical extensions

are relevant in the study of different materials as solids, crystals, liquids or tissues.

Research objetive 1: Create a new consistent framework where all theories in nonlinear classical elasticity are connected and a set of conversion factors to link to the Third Order Elastic Constants.

2. To Unify nonlinear classical acoustics, is a key to understand the classical nonlinear elasticity parameter because with a strong relationship with nonlinear acoustics, is possible to measure experimentally with ultrasonic technologies [73, 74].

   Hypothesis 2: Nonlinear classical acoustics under an unification criteria is a important tool to understand mechanical parameters relatives to damage in the case of materials or pathology in the case of tissue. A consistent and unified view provides a new approach to design a set of relevant experiments in tissue mechanics.

   Research objetive 2: To unify nonlinear classical acoustic theories to exploring the relationship between this parameters an mechanical ones and extend this to other possible scenarios exploring its physical meaning.

3. Rewrite of nonlinear acoustics is a necessary task to contribute in the scope of the nonlinear acoustic unification. Several authors, give the inspiration idea of non uniqueness in this field but without a physical explanation [38, 75].

   Hypothesis 3: Fluid and matrix parts of tissue could be the origin of Nonlinearity in tissues. The extension of nonlinear classical acoustics theories would imply a new point in the understanding of nonlinear physical meaning.

   Research objetive 3: Define nonlinear constitutive constants with physical meaning from the point of view of the interaction of waves depending on fluid and matrix parts, rather than a power series expansion as proposed by Landau.

4. To formulate a posible explanation to the nonlinear origin based on microdamage and microcracks in solid state. This origin starts with developing of the homogenization techniques, constructing a theory that connects micromechanical and heterogeneous elasticity and nonlinear ultrasound tools is possible to derivate and quantify density of microcracks [76, 77].

   Hypothesis 4: The study of the theory of homogenization by Eshelby and its extension to nonlinear geometrical inclusions or microcracks suggests that using ultrasonic nonlinear techniques, an origin to the nonlinearity could be due to the microdamage.

   Research objetive 4: Extending the theory of Eshelby to solve various cases of geometrical inclusions and provide a method for measuring density of microcracks with a consistent relationship established between the acoustic nonlinearity and homogenization.

5. Validate if nonlinear parameters could be measured by ultrasonic experimental setups. Reviewing the experimental techniques measuring ultrasonic parameters, a set of test

should be taken into account in order to provide a full set of nonlinear acoustic reliable parameters [78, 79, 80].

Hypothesis 5: The different techniques in the literature used to measure nonlinearity may lead us to improve the form of measurement by setting different cases of waves that interact resulting in desired measurements. Collinear mixing, Nonlinear mixing and new designs may explore and determine these parameters.

Research objetive 5: Develop new experimental techniques from ultrasonic sensors and different setups that allow us to measure the deduced theoretically parameters.

6. Torsional sensor method and measurements, once designed, provide a novel tool to understand tissue from the quantification of shear modulus and nonlinearity in biomechanics field. This process carry out the mathematical design from a semi-analytical model, a computational simulation, an structural optimization based in a different set of criteria and the fabrication and improves. The measurements should be try in different materials which is a new technique.

   Hypothesis 6: Torsional waves have the capability of be sensitive to the changes of consistency in tissues through the quantification of shear modulus and nonlinear acoustic parameters decomposed into collagen or fibers part and liquid part.

   Research objetive 6: Evaluate the torsional wave feasibility and capability for assessing linear and nonlinear measurements.

3

State of Art

The need to model the soft tissue behavior in terms of mechanical characteristics, relies on the understanding of nonlinear elasticity. Specifically, transversally isotropic nonlinear elasticity plays a special role due to the complexity of the nature of biological tissues. Relevant studies confirm the importance of these mechanical properties depending on the direction of anisotropy [81, 82, 83, 84, 58, 85, 86, 87, 88].

3.1 Nonlinear elasticity

The chapter 4 presents the most frequent mathematical descriptions of nonlinearity in the literature. We propose that nonlinearity can be understood from three different perspectives: (1) at the continuum mechanics level, where the constitutive laws that relate stress and strain deviate from Hooke's law, (2) at the theoretical level, or wave equation level in chapter 5, where the nonlinear parameters are directly related to the observable harmonics that appear in oscillatory movements such as ultrasonics, and (3) at the micro-mechanics level, in which atomistic, clapping microcracks see chapter 9, thermoelastic effects and so on, are proposed hypothesis of mechanisms may originate the observable nonlinearity at the other two levels. As opposed to many reviews, here we start from the continuum mechanics level, since there is no consensus over the variety of mechanistic origins of nonlinearity. We consistently derive the most frequent wave nonlinearity parameters from the different continuum mechanics nonlinear definitions, which are based on Taylor expansions of the constitutive equations. This expansion makes no assumption on the nature of the nonlinearity, which can be proposed ad hoc. This formulation serves as a basis to quantitatively understand and interpret experimental observations.

The Eriksen and Rivlin are the classical Invariants assuming strain-energy [89, 90, 91], to find a consistent algebraic context based on a historical review of isotropic and composite materials modelling [92, 93, 94, 95, 96, 97, 98]. Murnaghan Invariants and Desdrade's studies in the case of the compresibility restrictions of the strain-energy function to quasifluids or tissues, concluding remarks of some subcases discussing the degree of phisically realistic terms [99, 100, 101]. Exist a several invariants theories as such as Citarelle *et. al.* [102, 103], Lu and Zhang [104], Criscione *et. al.* [105, 106], depending on the type of skin tissue, for materials with fiber tension, and for materials with a reference configuration with transversally isotropic behavior, respectively.

Nevertheless, it is interesting explore the relationship between all of the different Third Order Elastic Constants TOEC, in the standard, Murnaghan, Landau,...[2, 107, 99, 98, 108, 109], with details. It is also significant different techniques of how make measures of a set of properties and explore the range limits of these experimental parameters where the tissue perform its mechanical function [110].

3.2 Nonlinear acoustics

The nonlinear constitutive equation is commonly described there by making use of the Third Order Elastic Constants TOEC [1, 111, 13, 5, 112, 6, 100], which are then linked to the nonlinear ultrasound propagation under the one dimensional P-wave restriction [113, 114, 115, 116]. Classical and nonclassical types of acoustic nonlinearities are developed below, showing their effect on common stress-strain, strain-time and strain amplitude-frequency spectrum relations. [117].

The Westervelt equation due to its nonlinear acoustic nature, has recently been used in the field of ultrasound for medical purposes such as for lithotripsy [118, 34] or by Fast Ultrasound Image Simulation (FUIS) [119, 120] can simulate realistic ultrasound images in a short time or through the application of HIFU [121, 122, 123].

In the chapter 5 an environmental theory about propagation of nonlinear waves in one dimension is presented. Once exposed to classical Westervelt equation, the first parameter of acoustic nonlinearity is derived from the classical nonlinear Hamilton equation. The general equations of acoustic propagation in mechanical terms are presented, are developed for the first order. The second order is also resolved using perturbation theory that is briefly explained in the chapter 5 .

The aim of the chapter 5 is to extend the Westervelt equation to classical second order nonlinearity and generalize it to the case of any high harmonics. At the same time it has been characterized by coefficients in elastic and viscous terms. Finally, the Westervelt generalized equation involve an ideal environment to develop future applications as technological progress in the field of tissue ultrasound mechanics.

As it is analyzed in this thesis, the study of the coefficients of acoustic nonlinearity has recently been recovered again [124, 125, 126, 6, 100]. There is abundant literature relating the degree of nonlinearity, in terms of the first and second nonlinear parameter in the wave

equation, with the atomic potential, microcracks and damage generation on specific materials [127, 128]. Nevertheless, there is a lack of theoretical proposals on nonlinear serial developments with the capability to explain some experimental phenomena. Nevertheless, the present theoretical proposals on nonlinear serial developments has not got the capability to explain some experimental phenomena.

The chapter 7 proposes deepening on the study of classical nonlinear acoustics, spliting the general first order nonlinearity into five specific nonlinear phenomena, due to the interaction of the deviatoric and volumentric components with the wave mode, P or S. The concept is scalable to the third and higher harmonics [129, 21, 130]. Hysteretic and viscous terms are also consider at this moment, in order to make easer the analysis [131].

Given the recent interest generated on the nonlinear elasticity and its relation to the nonlinear wave propagation [15], this chapter analyses the connection between the Landau third order elasticity constants TOEC and second order parameters of acoustic nonlinearity. Under this point of view, it can be considered that the parameters of constitutive nonlinearity are explicitly described in terms of those of acoustic nonlinearity and viceversa.

3.3 Possible origins of nonlinearity

Alternatively, in nonlinear acoustics, when a sinusoidal ultrasonic wave at a given frequency is transmitted into a nonlinear medium, the fundamental wave distorts as it propagates, generating second and higher harmonics of the fundamental frequency [174]. Those acoustical manifestations of nonlinear behavior can be explained as follows: Due to the amplitude-dependent wave propagation velocity, the compression phase of a sinusoidal wave travels faster than the rarefaction phase, and thus the wave distorts after it has propagated for some distance through a nonlinear material being transformed into a saw-tooth wave. This steepening of the waveform in the time-domain causes an energy transfer from the fundamental frequency to higher harmonics. As a consequence, several higher harmonics can be observed as local maxima in the frequency-domain [175, 176]. Measurements of the amplitude of these harmonics thus provide a means for extracting the coefficient of second and higher order terms in the nonlinear stress-strain relation, and deliver valuable information on the material degradation that is far more sensitive than the linear acoustic properties. Measuring these amplitudes is commonly referred to as the finite-amplitude method, initially developed by Breazeale and Thompson [177]. The nonlinear coefficients are usually determined by measuring the second-harmonic generation and sometimes higher harmonics for the longitudinal waves, and can be used to characterize acoustic nonlinear properties of gases, liquids, and solids. For this technique, the through- transmission mode in immersion is usually preferred. Instead of using two transducers, it is opportune to replace the receiver by a needle hydrophone (with a nearly linear frequency response), in order to conveniently measure the second and higher-harmonics. A finite- duration burst of (nearly) pure tone - typically around 20 cycles long - is launched towards the specimen, and the progress of some stationary peaks near the end of the tone-burst is followed and selected to compute

the Fast Fourier Transform (FFT), and thus permits one obtain the second and higher-order harmonics amplitude.

Associated with this study is the question of whether ultrasonic testing can be employed successfully as an investigative tool to determine significant changes in these macrosopic properties and thus provide an indication of material degradation in the form of damage or microcracks. This would be an important diagnostic tool as an indicator for, e.g. early on-set of a number industrial applications [178] or medical diagnosis tools, such as osteoporosis[179]. As a result, nonlinear ultrasound techniques have been proposed since it appears that the nonlinear acoustic parameters are much more sensitive to an increase in microdamage [180, 179, 181].

The induced nonlinearity appears to be present at small strains, attributed to e.g. Hertzian contact and other microstructural effects. The nonlinearity manifests itself in terms of a Strain energy function (SEF) associated with the material, from which effective stresses are found via differentiation. This SEF is not quadratic in strain, thus giving rise to nonlinear stress-strain relationships and effective nonlinear elastic moduli. Of specific interest is how these moduli depend on the microstructure. In particular in the bone community, where the interest is on the dependence of these parameters on the presence of damage, usually assumed to be micro-cracks, Renaud et al. [181] state "*However, little work has been done on the relationship between crack density and level of elastic nonlinearity*" and in Muller et al. [179] "*From empirical evidence it is clear that micro-cracks are responsible for the enhanced nonlinear response...we have no quantitative link between damage quantity and nonlinear response.*" It therefore appears to be of importance to try to build theoretical models which can attempt to provide these links.

Most of conventional ultrasonic NDE methods are very sensitive to gross defects, but much less sensitive to distributed micro-cracks. Furthermore, general degradation of strength is often found in apparently flawless materials [182]. It is well known that material failure is usually preceded by some kind of nonlinear mechanical behavior before significant plastic deformation or material damage occurs [183]. Therefore, the degree of material degradation can be evaluated by measuring the nonlinearity of the ultrasonic wave that propagates through the target material. Thus, one can expect that the magnitude of the second and higher-order harmonics will appear differently in normal and degraded material, when the same amplitude of wave and the same propagation distance is used. For instance, the finite-amplitude technique has been proven to be useful for nondestructive detection of defects in ceramics [184], concrete structures [185, 186], composites [174], as well as fatigue cracks in metals, such as steels, titanium, and aluminum alloys [187, 188]. Such defects are due to internal stresses, micro-cracks, zero-volume disbonds, and usually precede the main cracking mechanisms and the subsequent failure of the material. The characteristics between such defects and common material heterogeneities (i.e. pores, grains, etc.) is that an internal interface separates the intact material and the inclusion. This contact interface can be either free (large pores, opened cracks), partially clamped ("clapping" mechanism

between the states opened/closed cracks), or ideally bonded, and is thought to be mostly responsible for the high nonlinear behavior of degraded materials [22]. Therefore, a considerable number of authors have been involved in laboratory experiments to show that cracks and imperfect interfaces can behave in a nonlinear fashion [189, 190], and have thus opened new opportunities to detect partially closed cracks that may not be identified by conventional linear methods. The potential of such models for describing interfaces, the nonlinear mechanical behavior of layered media has been investigated using almost only homogenization approaches [191].

The problem of determining the effective *linear* elastic properties of an inhomogeneous material has been studied extensively [192, 193, 194]. A popular approach in micromechanics is to characterize the heterogeneous medium via dispersions of inclusions, particularly those involving spheroidal or ellipsoidal inclusions [195, 196, 197] thanks to the result of Eshelby [198]. These methods include self-consistent methods [199], the differential scheme [200, 201], the Mori-Tanaka method [202] and bounding schemes [203, 204]. Extensions of these schemes to accommodate the case of cracked media in the linear (static) regime when the cracks are assumed open (traction free), have been carried out in numerous studies [205, 206, 207, 208, 209, 210, 211]. Also see the comprehensive micromechanical study in [192]. However, often overlooked is the effective *dynamic* response where cracks can be in either opened or closed states (or more complex loadings) depending upon whether, for example, the crack is in a compressive or tensile cycle of the propagating wave. Furthermore, the notion of *nonlinear* crack response can often be important.

As opposed to the linear case, significantly less work has been carried out in the area of the effective behaviour of *nonlinear* inhomogeneous materials. In the context of finite elasticity, variational approaches associated with the Hashin-Shtrikman (HS) approach have been developed [212, 204]. More recently some of the micromechanical approaches have been adapted to the finite deformation regime [213, 214, 215, 46].

For the particular case of incompressible dispersions with rigid or liquid inclusions the effective energy was approximated, and for a more general case, with a power-law-type shear energy [216], where the energy density depends only on the Von Mises equivalent stress. Other authors took into account higher-order moments of the local fields in individual phases to introduce the nonlinear effects in the effective properties. Computational investigations of the first and second moments of the strain fields were performed by Moulinec and Suquet [217]. Recently, a new homogenization procedure of nonlinear inclusions based on the Eshelby theory was developed by Giordano et al. [218], who obtained the bulk and shear moduli along with the nonlinear Landau coefficients of the overall material in terms of the elastic behavior of the constituents and of their volume fractions, all in the context of small strain. Two nonlinear types of inclusions were investigated, spherical and parallel cylindrical inclusions, both of which were embedded into a linear homogeneous and isotropic matrix. In this context the material is considered to behave in a constitutively nonlinear manner under small strains (i.e. it is geometrically linear).

3.4 Experimental techniques on nonlinear acoustics

Chapter 6 is aimed to organize the basis of a new perspective on the classical acoustic nonlinearity: to analytically solve the wave propagation on each case, to find its relation to the coefficients of elastic nonlinearity and to experimentally validate using the Dynamic Acusto-Elasticity Technique DAET or nonlinear mixing methods [132, 6, 133, 134, 135]. Then, some possible scenarios will be considered with numerically simulated results in order to understand the range of the values that has not been able to be experimentally measured until now.

The nonlinear manifestations usually observed in classical materials are ultrasonically quantified by nonlinear acoustic parameter of first order β. Many methods have been developed to measure β as is showed in previous chapters. One of the most common used techniques for solids and fluids is the finite amplitude method [136]. This method based on the second harmonic generation; measuring its amplitude, β can be experimentally obtained. Despite it does not need a complicated setup and is relatively easy to perform, there are some some drawbacks inherent to this method. The first limitation is that the second harmonic signal recorded by the receiver may not all be due to the material nonlinearity of the sample. Some of this measured nonlinearity may be due to the nonlinearity of the measurement system, particularly the use of amplifiers, which reduces the accuracy of the method. To overcome these limitations of the finite amplitude method, the methods based on the nonlinear mixing technique have been recently applied to measure the ultrasonic nonlinearity of different materials [137, 138, 139, 140]. The aim of chapter 8 is to extract β parameter with a new experimental setup based on nonlinear mixing. The novelty of this configuration resides on the use of just one transducer as transmitter. Such a configuration permits to avoid the need to amplify the signal beyond 10 V while canceling out system nonlinearities. First, an expression of β that can be experimentally measured from the amplitude of the generated harmonics is derived. Secondly, the harmonic generated by the two incident waves at different frequencies are experimentally investigated in water for different excitation powers and different transmitter-receiver distances.

3.5 Torsional ultrasonic transducer

The chapter 9 focuses on designing and optimizing a transducer capable of transmitting and receiving torsional ultrasound waves, intended for tissue characterization applications in the field of clinical diagnosis. The application of ultrasonic sensors in the clinical field is mainly covered by compressional waves [141]. However, torsional ultrasonic waves are proposed in this paper for the first time for shear stiffness based medical diagnosis. Torsional ultrasound is chosen as the physical magnitude for several reasons. First, it is a mechanical wave, controlled by and therefore most sensitive to the mechanical parameters than any other indirect measurement. Second, the novelty and impact of this application is rooted in the fact that torsional waves propagate at the S-wave speed c_s has been reported[142, 143, 144] to be significantly sensitive to consistence changes in quasifluids and

soft tissues (p-value ¡ 0.001 measured with ultrasound) and to consistency changes caused by tumors[145, 146]. Several authors have reported evidence about the potential of shear dynamic viscoelastic properties to characterize tissue condition [147, 148, 149, 150]. We propose a design of a transducer to record information on the mechanical shear modulus in tissues. The reason is that shear stiffness directly correlates with the tissue micro architecture, which is most sensitive to pathologies, whereas compressional waves are predominantly correlated with the fluid phase of the tissue, which remains mostly constant. The main challenge and novelty resides in the capability of separate P waves and S waves based on the frequency contents of each wave. In contrast to commercial shear transducers, torsional movement guarantees no P-wave generation at the boundary of the transducer, with is critical in quasi-fluids, where c_s is at least 10 times lower than c_p, and P-waves mask S-waves. This is reinforced by using a radially rigid sensor contact surface. The ensuing design comprises an emitting disc and a receiving ring. Previous torsional transducers exist with resonance frequency between [22-148] kHz, which are of the torsional Bolt-clamped Langevin Type (BLT), and consist of discs of alternating polarity piezoelectric elements and two elastic blocks fitted at each end, in order to generate torsional mechanical vibrations of the desired frequencies with the capability of measuring shear modulus [151, 152]. The concept of introducing a radiating head mass resembles the Tonpilz design, but has been modified fundamentally to generate a torsional movement instead of a flexural movement.[153].

The transducer design that we propose is composed by a combination of elastic and piezoelectric parts. Piezoelectric materials convert electrical signals into mechanical vibrations and viceversa. Piezoelectric ceramic materials, such as lead zirconate titanate (PZT) are widely used in solid-state actuators and sensors for various areas of nondestructive evaluation and bioengineering such as an optical scanners, precision positioning, noise and vibration sensing and cancellation, linear motors,... [154, 155, 156, 157, 158, 159]. For this reason, PZT-5 is adopted for our design.

The central focus of our contribution in this chapter is the optimization of the transducer design with the aim of maximizing the sensitivity to shear properties. There are several optimization criteria of ultrasonic sensors, where the conventional characteristics as impedance of the backing material and the thickness of piezoelectric material have been studied [160, 141].

Numerical approaches can be used to evaluate transducer designs for each of the design parameters required, to maintain transducer performance within a specified range [161, 162]. Our transducer is simulated with the Finite Element Method (FEM) using the FEAP software [163], revealing the main mechanisms, which are in summary a circumferential shear movement of the piezoceramic elements, a torsional relative movement between upper and lower discs and rings, an inertial mass by the discs and rings that control the resonant frequency and movement amplitude, and compressional eigenmodes at frequencies at least 100 times higher than the torsional frequency. The model is subsequently validated

with an analytical model, where the simplified differential equations of piezoelectric torsional motions are derived and solved in terms of the circumferential displacement and the electric potential, aimed at unveiling the main correlations between the design parameters of the numerical model, and the response. This strategy has previously been used in different designs [151]. We have introduced dermic and connective tissue in the finite element model in view of the first intended application, but it could be extended or modified to other kinds of soft tissues, whose properties are similar, and the result too. Our simulated values for the S wave velocity ranged $[20, 380]$ $[\mathrm{m/s}]$, and for P-waves $[1200, 1800]$ $[\mathrm{m/s}]$, while the thicknesses layers in dermic and connective tissue was allowed to range at $[0.3, 0.7]$ $[\mathrm{mm}]$. Genetic Algorithms (GA) [164] and FEM have already been used in the literature to optimize waveform and amplitude spectra of ultrasonic transducers [160, 165, 166], as well as other optimization criteria [167, 166, 157].

The issue of the probability of detection (POD) has only been addressed independently, under the name of identifiability, in statistics and mathematics, with a wide application in chemistry and physics. In the field of nondestructive characterization, the concept of POD has been discussed under the name of identifiability in relationship with the number of measurements and the number of degrees of freedom to establish a necessity condition to obtain a minimum criteria between the number of measurements and unknown variables[168]. Also, the inversion theory under a probabilistic formulation and the introduction of probability density functions in the model has been examined (see [169, 170]) to explain the robustness of the inversion. Other perspectives of probabilistic formulations have been presented providing a general overview of the statistical inversion theory, whose Bayesian and Kalman filtering exposition for nonstationary inverse problems is particularly useful, for example in the micro damage detection field [171]. Some of these rational approaches have been scarcely applied experimentally for the case of damage characterization [172, 173]. In this paper, a new design optimality criteria called Robust Probability of Detection (RPOD) is proposed in this paper as a methodology approach. It is defined with the goal of maximizing the transducer sensitivity to the tissue properties while minimizing the sensitivity to noise ratio of the multilayered shear elastic constants.

The universe works on a math equation that never really even ever really even ends in the end Infinity spirals out creation.

Never ending math equation
Modest Mouse, 2004

Part II

THEORETICAL CONTRIBUTIONS

4

Unifying theories of classical nonlinearity

4.1 Nonlinear elasticity

In order to classify the nonlinear acoustic behavior of solid and fluid materials, the principles of nonlinear elasticity are introduced. The general constitutive equations are considered, in tensile form to derive the one-dimensional wave equation with nonlinear elastic coefficients. The notation used here is introduced in a similar manner that Norris 1998 [107] changing a by x_i^0 as the initial position. Lagrangian (are used to locate a point in space with respect to a fixed basis) and Eulerian (used to label material points) coordinates are defined as $\mathbf{x}$ in vector notation, or x_i in index notation (final position) and $\mathbf{x^0}$, or $\mathbf{x_i^0}$ (initial position), respectively, and displacements as $\mathbf{u} = \mathbf{x} - \mathbf{x^0}$, or $u_i = x_i - x_i^0$. The deformation gradient tensor is $\mathbf{F} = \partial \mathbf{x}^0 / \partial \mathbf{x}$ in tensor notation or $F_{ij} = \partial x_i^0 / \partial x_i$ in index notation is introduced to quantify the change in shape of infinitesimal line elements in a solid body.

The associated Green-Lagrange strain tensor is $\mathbf{E} = 1/2(\mathbf{F}^T\mathbf{F} - \mathbf{I})$ or $\varepsilon_{ij} = 1/2(F_{ij}F_{ji} - \delta_{ij})$ where $\mathbf{I}$ is the identity matrix and δ_{ij} is the Kronecker's delta function (equal to 1 when index i=j and zero if $i \neq j$) or in terms of displacements:

$$\varepsilon_{ij} = \frac{1}{2}\left(\frac{\partial u_i}{\partial x_j} + \frac{\partial u_j}{\partial x_i} + \frac{\partial u_k}{\partial x_i}\frac{\partial u_k}{\partial x_j}\right) \tag{4.1}$$

Note that the last term is frequently neglected in ultrasonic literature because small strains are considered. However, it should be necessary taken into account to consistently link the harmonics amplitude to the continuum mechanics, as proved later in the Nonlinear (NL) wave equation. The latter is commonly defined Cauchy's stress as,

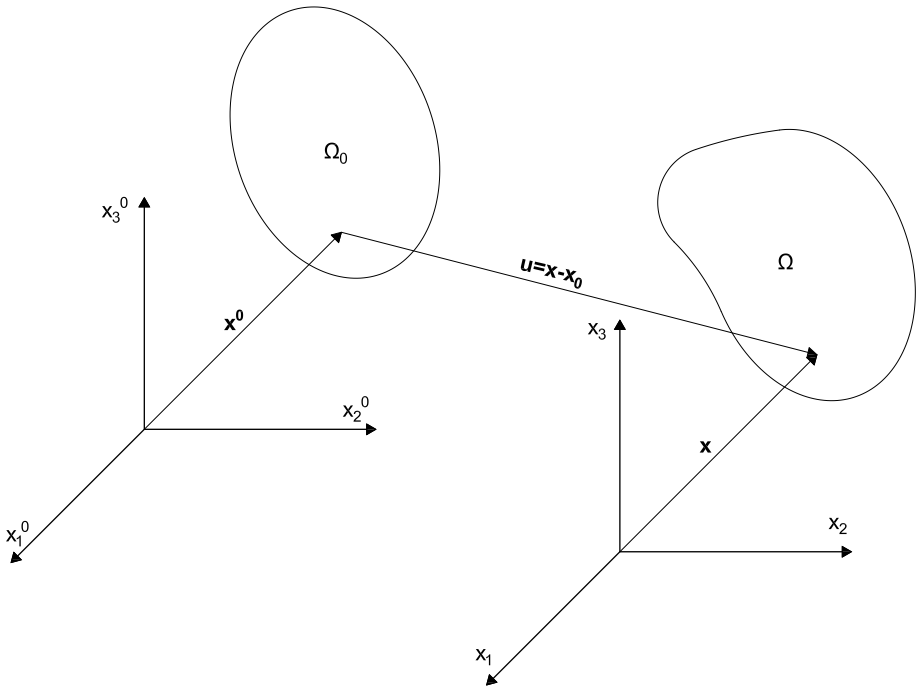

Figure 4.1: Classical representation of an undeformed and deformed body in both initial and final positions.

$$\mathbf{T} = \frac{1}{\det(\mathbf{F})}\mathbf{F}\frac{\partial W}{\partial \mathbf{E}} \cdot \mathbf{F}^T \quad \text{or} \quad \sigma_{ij} = \frac{1}{\det(F_{ij})} F_{ij} \frac{\partial W}{\partial E_{ij}} F_{ji} \tag{4.2}$$

where we have introduced the strain energy *per unit volume of the undeformed material* W.

The nominal stress or first Piola-Kirchoff stress $\mathbf{P}$ or P_{ij}, is defined as the force measured per unit surface area expressed in the reference configuration. the use of nominal stress and Green-Cauchy strain and them expansions establishes, so-called general nonlinear elasticity. It is linked to the Cauchy stress is given via,

$$\mathbf{P} = (\det \mathbf{F})\mathbf{T} \cdot (\mathbf{F}^{-1})^T, \qquad \mathbf{T} = \frac{1}{(\det \mathbf{F})}\mathbf{P} \cdot \mathbf{F}^T,$$

or

$$P_{ij} = (\det F_{ij})\sigma_{ij}F_{ji}^{-1}, \qquad \sigma_{ij} = \frac{1}{(\det F_{ij})}P_{ij}F_{ji}. \tag{4.3}$$

Consider a strain energy *per unit volume of the undeformed material*. Then,

$$\mathbf{P} = \frac{\partial W}{\partial \mathbf{F}}, \text{ or } P_{ij} = \frac{\partial W}{\partial F_{ij}} \tag{4.4}$$

noting that here we use the convention ($\frac{\partial W}{\partial \mathbf{F}}|_{\{ij\}} = \frac{\partial W}{\partial F_{ij}}$). Note that, for example, Ogden (1997) adopts [219] the transpose of this definition, mainly due to the fact that the nominal stress is usually measured [107, 8]. We eventually wish to write the strain energy in terms of the strain $\mathbf{E}$ so we write,

$$\begin{aligned} \mathbf{P} &= \frac{\partial W}{\partial \mathbf{E}} : \frac{\partial \mathbf{E}}{\partial \mathbf{F}} = \mathbf{F} \cdot \frac{\partial W}{\partial \mathbf{E}}, \\ &\text{or} \\ P_{ij} &= \frac{\partial W}{\partial \varepsilon_{ij}} : \frac{\partial \varepsilon_{ij}}{\partial F_{ij}} = F_{ij} \frac{\partial W}{\partial \varepsilon_{ij}}. \end{aligned} \tag{4.5}$$

and using the relations between stresses we obtain Equation 4.2. Importantly we note that $\mathbf{T} \neq \frac{\partial W}{\partial \mathbf{E}}$ in general in nonlinear elasticity.

We note that only when $\mathbf{E} \ll 1$, where strains are small, then $\mathbf{T} = \frac{\partial W}{\partial \mathbf{E}}$. This stress is usually noted as $\mathbf{S} = \frac{\partial W}{\partial \mathbf{E}}$ and called second Piola-Kirchoff tensor, since in that context geometric nonlinearity is neglected and only constitutive nonlinearity is retained [220]. Here we also remain in the context of small strain but we prefer to use an asymptotic methodology which retains *all* second order nonlinear (quadratic terms). We note that via Equation 4.1 we can obtain the expansions

$$\begin{aligned} \mathbf{F} &= \mathbf{I} + \mathbf{E} + O(\mathbf{E}^2), & \mathbf{F}^T &= \mathbf{I} + \mathbf{E} + O(\mathbf{E}^2), \\ & & &\text{or} \\ F_{ij} &= \delta_{ij} + \varepsilon_{ij} + O(\varepsilon_{ij}\varepsilon_{jk}), & F_{ji} &= \delta_{ij} + \varepsilon_{ij} + O(\varepsilon_{ij}\varepsilon_{jk}) \end{aligned} \tag{4.6}$$

and thus we find that,

$$\begin{aligned} \text{tr}\mathbf{F} &= 3 + \text{tr}\mathbf{E}, & \text{tr}(\mathbf{F}^2) &= 3 + 2\text{tr}\mathbf{E}, & \text{tr}(\mathbf{F}^3) &= 3 + 3\text{tr}\mathbf{E}, \\ & & &\text{or} & & \\ F_{kk} &= 3 + \varepsilon_{kk}, & F_{ij}F_{ji} &= 3 + 2\varepsilon_{kk}, & F_{ij}F_{jk}F_{ki} &= 3 + 3\varepsilon_{kk} \end{aligned} \tag{4.7}$$

whereby,

$$\det \mathbf{F} = 1 + \mathrm{tr}\mathbf{E} + O(\mathbf{E}^2)$$

or

$$\det F_{ij} = 1 + \varepsilon_{kk} + O(\varepsilon_{ij}\varepsilon_{jk}) \tag{4.8}$$

Finally note the importance of notation in the above, i.e. $\mathrm{tr}(\mathbf{F}^n) \neq (\mathrm{tr}\mathbf{F})^n$ where we note the standard definition for powers as for example $\mathbf{E}^2 = \varepsilon_{ij}\varepsilon_{jk}$ so that $\mathrm{tr}(\mathbf{E}^2) = \varepsilon_{ij}\varepsilon_{ji}$. We use brackets in order to make this notation clear when $n > 1$.

Defining a relationship between the strain energy W, and the strain ε_{ij}, a Taylor series expansion allows any degree of approximation to reality without loss of generality. The first term describes the linear elasticity,

$$\begin{aligned} W(\mathbf{E}) &= \mathbf{C} : \mathbf{E} \otimes \mathbf{E} + \mathbf{C} :: \mathbf{E} \otimes \mathbf{E} \otimes \mathbf{E} + ..., \\ &\text{or} \\ W &= \frac{1}{2!} C_{ijkl}\varepsilon_{ij}\varepsilon_{kl} + \frac{1}{3!} C_{ijklmn}\varepsilon_{ij}\varepsilon_{kl}\varepsilon_{mn} + ... \end{aligned} \tag{4.9}$$

where ":", denotes contraction operator (index-$ijjk$ contracts by Einstein summation to index-ik), and $\otimes$ is defined as the tensorial product which contract a pair of shared indices in two tensors. As a consequence, the stress can be decomposed into linear and nonlinear parts as,

$$\mathbf{T} = \mathbf{T}^L + \mathbf{T}^{NL} \quad \text{or} \quad \sigma_{ij} = \sigma_{ij}^L + \sigma_{ij}^{NL} \tag{4.10}$$

where σ_{ij}^L is consequence of Hooke's law.

In order to write down appropriate strain energy functions it is useful to define the invariants of deformation. "*A deformable medium is isotropic if, and only if,* $W(\mathbf{E})$ *is a function of three invariants* I_1, I_2 *and* I_3 *of* $\mathbf{E}$" (For more details see Murnaghan [12]). Then, for nonlinear elasticity, i.e. the case that we consider here we use,

$$\begin{aligned} &I_1 = \mathrm{tr}\mathbf{E}, && I_2 = \mathrm{tr}(\mathbf{E}^2), && I_3 = \mathrm{tr}(\mathbf{E}^3), \\ &&&\text{or,} \\ &I_1 = \varepsilon_{kk}, && I_2 = \varepsilon_{ij}\varepsilon_{ji}, && I_3 = \varepsilon_{ij}\varepsilon_{jk}\varepsilon_{ki}. \end{aligned} \tag{4.11}$$

These invariants are chosen explicitly in terms of the strain by writing det$\mathbf{F}$ (see Erigen [109]). For an isotropic material the form of the corresponding strain energy W_I was proposed by Landau as,

$$W_I = \frac{\lambda}{2} I_1^2 + \mu I_2 + \frac{\mathcal{A}}{3} I_3 + \mathcal{B} I_1 I_2 + \frac{\mathcal{C}}{3} I_1^3 + h.o.t. \tag{4.12}$$

where the coefficients $\mathcal{A}, \mathcal{B}$ and $\mathcal{C}$ are often referred to as the nonlinear, third-order *Landau coefficients* and $h.o.t.$ stand for the neglected fourth order effects (See [1, 107]). The combinations of invariants I_3, $I_1 I_2$ and I_1^3 are the three possible in third order. Let us consider the stress of second Piola Kirchoff as defined above, that arises in an isotropic material. Note that

$$\begin{aligned} \frac{\partial W_I}{\partial \mathbf{E}} &= \lambda(\mathrm{tr}\mathbf{E})\mathbf{I} + 2\mu\mathbf{E} + \mathcal{A}\mathbf{E}^2 + \mathcal{B}((\mathrm{tr}(\mathbf{E}^2))\mathbf{I} + 2(\mathrm{tr}\mathbf{E})\mathbf{E}) + \mathcal{C}(\mathrm{tr}\mathbf{E})^2\mathbf{I}, \\ &\quad \text{or} \\ \frac{\partial W_I}{\partial \varepsilon_{ij}} &= \lambda\varepsilon_{kk}\delta_{ij} + 2\mu\varepsilon_{ij} + \mathcal{A}\varepsilon_{ik}\varepsilon_{kj} + \mathcal{B}(\varepsilon_{kp}\varepsilon_{pk}\delta_{ij} + 2\varepsilon_{kk}\varepsilon_{ij}) + \mathcal{C}(\varepsilon_{kk}\delta_{ij})^2. \end{aligned} \tag{4.13}$$

Then, grouping in strain terms of invariants using Cauchy stress, see Equation 4.2, the nonlinear extension of the Hooke's law to the third order and isotropic materials can be written as,

$$\begin{aligned} \mathbf{T} &= \lambda\mathrm{tr}\mathbf{E}\mathbf{I} + 2\mu\mathbf{E} + \tilde{\mathcal{A}}\mathbf{E}^2 + \mathcal{B}\mathrm{tr}\mathbf{E}^2\mathbf{I} + 2\tilde{\mathcal{B}}\mathrm{tr}\mathbf{E}\mathbf{E} + \tilde{\mathcal{C}}(\mathrm{tr}\mathbf{E})^2\mathbf{I} \quad \text{or} \\ \sigma_{ij} &= \lambda\varepsilon_{kk}\delta_{ij} + 2\mu\varepsilon_{ij} + \tilde{\mathcal{A}}\varepsilon_{ik}\varepsilon_{kj} + \mathcal{B}\varepsilon_{kp}\varepsilon_{pk}\delta_{ij} + 2\tilde{\mathcal{B}}\varepsilon_{kk}\varepsilon_{ij} + \tilde{\mathcal{C}}(\varepsilon_{kk}\delta_{ij})^2 \end{aligned} \tag{4.14}$$

where λ and μ are the Lamé constants related to the Young modulus E, and Poisson ratio ν, as $\lambda = \frac{E\nu}{(1+\nu)(1-2\nu)}$ and $\mu = \frac{E}{2(1+\nu)}$, ε_{ij} is the strain tensor, ε_{kk} is the trace of the strain tensor, $\varepsilon_{ij}\varepsilon_{jk}$ is the square of the strain tensor, δ_{ij} is the Kronecker delta, and $\tilde{\mathcal{A}} = 4\mu + \mathcal{A}$, $\tilde{\mathcal{B}} = \mathcal{B} + \lambda - \mu$ and $\tilde{\mathcal{C}} = \mathcal{C} - \lambda$ are often referred to as the nonlinear, $\mathcal{A}$, $\mathcal{B}$ and $\mathcal{C}$ third order elastic constants [1]. The contribution in that the nonlinear stress never has been derived under these hypothesis, and the expression of TOEC impacts on the nonlinear theory even in the relationship between it and acoustics. Note that many authors defined other sets of third order elastic constants, by taking into account different combinations invariants i. e. in terms of Murnaghan l, m and n parameters, as a combination of three invariants in third order of energy function see Equation 4.13 with a different rule of derivation [12, 221, 108, 222]. See Table 4.1. below, note the standard nonlinear coefficients C_{IJK} are defined with the Voigt notation (where index is contracted with the rule $ijklmn = IJK$).

Table 4.2 ilustrates some experimental values of third order elastic constants [6, 126, 125, 223], using experimental acoustoelasticity techniques for Aluminum [6] and by other authors in Aluminum 7075 and Aluminum 2S samples using finite amplitude methodology and several ultrasonic setups.

Murnaghan (1951)	Standard, C_{IJK}
$l = \mathcal{B} + \mathcal{C}$	$c_{123} = 2\mathcal{C}$, $c_{111} = 2\mathcal{A} + 6\mathcal{B} + 2\mathcal{C}$
$m = \frac{1}{2}\mathcal{A} + \mathcal{B}$	$c_{144} = \mathcal{B}$, $c_{112} = 2\mathcal{B} + 2\mathcal{C}$
$n = \mathcal{A}$	$c_{456} = \frac{1}{4}\mathcal{A}$, $c_{166} = \frac{1}{2}\mathcal{A} + \mathcal{C}$

Table 4.1: Relations between third order elastic constants for isotropic solids

TOEC	AL7075 (GPa) Muir (2009)	AL7075 (GPa) Stobbe (2005)	AL7075 (GPa) Dubuget et al. (1996)	AL2S (GPa) Smith (1966)
$\mathcal{A}$	-334.5	-351.2	-282	-408
$\mathcal{B}$	-125.35	-149.4	-179	-197
$\mathcal{C}$	-60.5	-102.8	53	-114

Table 4.2: Literature values of Third-Order Elastic Constants experimentally determined.

A solid is characterized by a positive bulk and shear moduli but the signs of third order elastic constants are not univocal as shown in Table 4.2. In the case of fluids, since they have null shear modulus, the relationship is given by $\lambda = A$, $\mathcal{A} = 0$, $\mathcal{B} = -A$, and $\mathcal{C} = (A - B)/2$, where A and B are the parameters of Taylor expansion of the pressure in fluids,

$$p = A\left(\frac{\rho'}{\rho_0}\right) + \frac{B}{2!}\left(\frac{\rho'}{\rho_0}\right)^2 + \frac{C}{3!}\left(\frac{\rho'}{\rho_0}\right)^3 + ... \tag{4.15}$$

where ρ_0 is the unperturbed density. The parameters A and B, are also described by making use of the Westervelt and KZK nonlinear propagation models inside the acoustic nonlinearity of first order, (see [107]). Finally, Equation 4.1 can be written with respect to either coordinate system. Working in Eulerian coordinates, the equation of motion is

$$\frac{D\mathbf{v}}{Dt} = \nabla \cdot \mathbf{T},$$
$$\text{or, neglecting advection,}$$
$$\rho u_{i,tt} = \sigma_{ij,j} \tag{4.16}$$

where $\mathbf{v}$ is the velocity, D/Dt is the total derivative, $\mathbf{T}$ is the Cauchy stress defined above, and for the index notation, ρ is the density, $u_i = (x_1, x_2, x_3, t)$ and $\sigma_{ij,j}$, where we adopt the compact notation of derivative $f_{,i} = \frac{\partial f}{\partial x_i}$ with $i, j = 1, 2, 3$ are the cartesian components of the displacement and Cauchy stress, respectively.

5

Nonlinear propagation of ultrasound: Unification

The nonlinear wave propagation is particularized to one dimensional P-wave and S-wave equations to extract the nonlinearity parameter of first order β, which has been widely used in the literature. The second and hysteretic nonlinearity parameters are considered and characterized in the next subsections.

The contribution is a consistent derivation of the NL wave solutions based on clear continuum mechanics assumptions.

5.1 One dimensional P-wave equation

The one-dimensional nonlinear wave equation for solids is derived from the continuum model above. The nonlinear wave equation is reduced here to the classical theory and its fundamental solution up to third- and fourth-order is provided below.

In order to derive the effects of nonlinear elastic materials, the formulation of the kinematic relations can be written as in the following equation [5], as in Equation 4.1,

$$\varepsilon_{ij} = \frac{1}{2}(u_{i,j} + u_{j,i} + u_{k,i}u_{k,j}) \tag{5.1}$$

Under P waves restriction we note that $u_2 = u_3 = 0$, $u_1(x_1, x_2, x_3) = u_1(x_1)$, since particles only move along the x_1-direction, and $\varepsilon_{ij} = 0 \; \forall \; i, j \neq 11$,

$$
\begin{aligned}
\text{Kinematic relations :} \quad & \varepsilon_{11} = u_{1,1} + \tfrac{1}{2} u_{1,1} u_{1,1} \\
\text{Constitutive law :} \quad & \sigma_{11} = (\lambda + 2\mu)\varepsilon_{11} \\
& + (3(\lambda + 2\mu) + (2\mathcal{A} + 6\mathcal{B} + 2\mathcal{C}))\varepsilon_{11}^2 \\
& + O(\varepsilon_{11}^3) \text{ (neglecting attenuation)} \\
\text{Dynamic equilibrium :} \quad & \rho u_{1,tt} = \sigma_{11,1} \text{ (from Equation 4.2)}
\end{aligned} \tag{5.2}
$$

5.1.1 Nonlinearity of first-order

The case of the nonlinear wave equation up to the first-order nonlinearity is first considered. By making use of Equations 5.2 introducing Kinematic relations into Constitutive law and making use of Dynamic equilibrium as spatial derivative of stress we can obtain,

$$\rho u_{1,tt} = M u_{1,11} + (3M + 2\mathcal{A} + 6\mathcal{B} + 3\mathcal{C}) u_{1,1} u_{1,11} \tag{5.3}$$

If the second order wave equation (See [224]) is considered, Hamilton proposed to synthesize the 1D nonlinear wave equation to,

$$\rho u_{1,tt} = M u_{1,11}(1 - 2\beta_H u_{1,1}) \tag{5.4}$$

where u_1, $u_{1,tt}$ and $u_{1,11}$, are the displacements in one dimension, and the second derivatives in time and space respectively $M = \lambda + 2\mu = \rho c_p^2$, and c_p denotes the longitudinal (P-wave) velocity. Whereby the constant β_H (H is introduced to distinguish from other definitions of β by other authors) is,

$$\beta_H = -\frac{3}{2} - \frac{\mathcal{A} + 3\mathcal{B} + \mathcal{C}}{\lambda + 2\mu} \tag{5.5}$$

This is the standard relationship between third order elastic constants and first nonlinear wave parameter as defined Hamilton 1998, (See [2]). The linear part $-\frac{3}{2}$ coming from geometric nonlinearity and the NL part $-\frac{\mathcal{A}+3\mathcal{B}+\mathcal{C}}{\lambda+2\mu}$ from constitutive nonlinearity. Definitely, it is a contribution counterintuitive due to large strains of Cauchy stress tensor. Note that we have introduced the nonlinear coefficient β_H, in order to obtain a single nonlinearity parameter that described the acoustic harmonic generation. The perturbation theory [2] allows to decompose the wave displacement as,

$$u = u^{(0)} + u^{(1)} + ... \tag{5.6}$$

where $u^{(0)}$ and $u^{(1)}$ denote the zero-order and first-order perturbation solutions, respectively. The zero-order perturbation solution corresponds to the solution to the linear wave equation (that is, when $\beta_H = 0$). When considering a monochromatic plane wave propagating in a semi-infinite nonlinear elastic layer, the latter is given as,

$$u^{(0)}(x,t) = ae^{i(kx-\omega t)} \tag{5.7}$$

where k is the wave number, a is the amplitude of fundamental harmonic neglecting viscosity and $\omega = 2\pi f$ is the angular frequency of an oscillation frequency f. The nonlinear parameter of first order β_H can be determined by iteration from,

$$u^{(1)}_{1,tt} - c_p^2 u^{(1)}_{1,11} = 2c_p^2 \beta_H u^{(0)}_{1,11} u^{(0)}_{1,1} + h.o.t. \tag{5.8}$$

where $h.o.t.$ is neglected since they are of order $O(\beta^2)$. The former expression has the form of a classical partial differential equation with an inhomogeneous part. It is well-known that when the inhomogeneous part is linearly dependent to the general solution of the homogeneous part, the solution approach for the particular solution of $u^{(1)}$ must be multiplied by a sufficiently large power of x to become linearly independent. Thus, a particular solution may be obtained by substituting Equation 5.7 in $u^{(0)}$, whereby the right hand side becomes a forcing them that only allows a homogenous solution,

$$u^{(1)}(x,t) = bxe^{2i(kx-\omega t)} \tag{5.9}$$

where b is the amplitude of the second harmonic. From that solution, the nonlinear parameter of first-order β_H is derived as,

$$\beta_H = \frac{4b}{k^2 a^2 x} \tag{5.10}$$

5.1.2 Nonlinear acoustic parameter of first order defined by Guyer

A different definition of nonlinear parameter of first order was given by Guyer [225] from the following expansion of the constitutive law,

$$\sigma_1 = K(\varepsilon_{1,1} + \beta_G(\varepsilon^2_{1,1}) + O(\varepsilon^3_{1,1}) + A[\varepsilon, \varepsilon_{1,t}]) \tag{5.11}$$

where K is the compressional modulus, $A[\varepsilon, \varepsilon_{1,t}]$ are the hysteretic elastic elements typically nonanalytic and β_G is the nonlinear term. Note that it is only valid for fluids, since it coincides with that one of Hamilton Equation 5.3 if $\mu = 0$. Also, $\tilde{\mathcal{A}} = 0$ and $\tilde{\mathcal{B}} = 0$ from Equation 4.1, because all terms of strain tensor ε_{ij}, outside the diagonal are neglected which carries out this specific condition for fluids.

5.1.3 Nonlinear mixing

This is used to explain both harmonics generation and frequency mixing. To illustrate the second, if we consider two excitation frequencies, ω_a, ω_b, the solution of the wave equation yields a third output pair of waves frequencies $\omega_c = \omega_a \pm \omega_b$ with amplitude proportional to ε_a^2 that builds up over distance x to amplitude ε_c. Their amplitudes ε_a, ε_b and ε_c, are related by,

$$\beta_G \approx \frac{\varepsilon_c}{x\varepsilon_a^2} \tag{5.12}$$

5.1.4 *Nonlinear acoustic parameters of first order defined by Zarembo*

If we consider as invariants $I_1 = \varepsilon_{kk}$, $I_2 = 1/2(\varepsilon_{ij}\varepsilon_{ji} - \varepsilon_{kk}^2)$ and $I_3 = \det\varepsilon_{ij}$, classical invariants of Murnaghan, deduced from the characteristic polinomial of the strain tensor, the stress is defined as follows,

$$\sigma_{ij} = \frac{\rho}{\rho_0} Y \frac{\partial W}{\partial \varepsilon_{ij}} Y^T \tag{5.13}$$

where ρ and ρ_0 are the densities in the deformed and undeformed states, respectively, $\rho = \rho_0(1 + I_1)$, $Y = |u_{i,j} + \delta_{ij}|$. Note that Equation 5.13 is similar to the Cauchy stress defined in equation 4.2, however, in Equation 5.13 $\rho/\rho_0 = 1 + \varepsilon_{kk}$ and in Equation 4.2 its correspond to $1/(\det\varepsilon_{ij}) = 1 - \varepsilon_{kk}$.

The equation of motion results to apply spatial derivate of stress and the conversion of Murnaghan constants into Landau TOEC given in Table 4.1, stated as,

$$\begin{aligned}
\rho_0 u_{i,tt} - \mu u_{i,jj} - \left(K + \frac{\mu}{3}\right) u_{i,ki} &= \left(\mu + \tfrac{\mathcal{A}}{4}\right)\left(u_{k,jj}u_{k,i} + u_{k,jj}u_{k,i} + 2u_{i,jj}u_{k,j}\right) \\
&+ \left(K + \tfrac{\mu}{3} + \tfrac{\mathcal{A}}{4} + \mathcal{B}\right)\left(u_{k,ij}u_{k,j} + u_{j,kj}u_{i,k}\right) \\
&+ \left(K - \tfrac{2\mu}{3} + \mathcal{B}\right) u_{i,jj}u_{k,k} \\
&+ \left(\tfrac{\mathcal{A}}{4} + \mathcal{B}\right)\left(u_{j,kj}u_{k,i} + u_{k,ij}u_{j,k}\right) \\
&+ \left(\mathcal{B} + 2\mathcal{C}\right) u_{j,ij}u_{k,k}
\end{aligned} \tag{5.14}$$

If the wave front travels in x_1-direction, all the particles of the x_2x_3-plane do not depend on x_2 and x_3, and thus u_1 and u_2 are reduced to $u_1(x_1, t)$ and $u_2(x_1, t)$, respectively [5]. By making use of perturbation theory, the nonlinear interaction of wave propagation in one direction is obtained. Then, take the form,

$$u_{11,tt} - (c^l)^2 u_{1,11} = \beta_Z^l u_{1,11}u_{1,1} + \beta_Z^\tau(u_{2,11}u_{2,1} + u_{3,11}u_{3,1}) \tag{5.15}$$

$$u_{2,tt} - (c^\tau)^2 u_{2,11} = \beta_Z^\tau(u_{2,11}u_{1,1} + u_{1,11}u_{2,1}) \tag{5.16}$$

$$u_{3,tt} - (c^\tau)^2 u_{3,11} = \beta_Z^\tau(u_{3,11}u_{1,1} + u_{1,11}u_{3,1}) \tag{5.17}$$

where $(c^l)^2 = \left(K + \frac{4\mu}{3}\right)/\rho_0$ and $(c^\tau)^2 = \mu/\rho_0$ are the longitudinal and transversal square velocities, respectively. The Equation 5.16 corresponds to P-wave equation, primary wave equation and Equations 5.17 and 5.17 with the S-wave equation, secondary wave equation, in two polarizations that are related to the directions x_2 and x_3, respectively. The nonlinear longitudinal parameter of first order β_Z^l, (note that labeled Z side it correspond to Zarembo, 1951), is defined as follow in terms of Landau third order elastic constants,

$$\beta_Z^l = 3\frac{\lambda + 2\mu}{\rho_0} + \frac{1}{\rho_0}(2\mathcal{A} + 6\mathcal{B} + 2\mathcal{C}) \tag{5.18}$$

If in a similar way, the S-waves is considered in the u_2-direction $u_2(x_1)$, and $u_1 = u_3 = 0$, we obtain the nonlinear transversal parameter β_Z^τ defined as follows,

$$\beta_Z^\tau = \frac{\mu}{\rho_0} + \frac{1}{\rho}\left(\frac{\mathcal{A}}{2} + \mathcal{B}\right) \tag{5.19}$$

This definition establishes a relationship between nonlinear longitudinal and transversal parameters of first-order with the third order elastic constants. Note that the conversion of Murnaghan coefficients to Landau constants have been carried out by making use of the Table 4.1 above.

5.2 Nonlinearity of second-order

The case of the nonlinear wave equation up to the second-order nonlinearity (two nonlinear parameter β_H and δ) is considered now. Therefore, equation 5.6 is reduced to,

$$u_{1,tt} = c_p^2(1 - 2\beta_H u_{1,1} + 3\delta(u_{1,1})^2)u_{1,11} \tag{5.20}$$

The elastic coeffcient of second-order δ can be derived in the same manner as the first-order one β_H, resulting in,

$$u_{1,11}^{(2)} - \frac{1}{c_p^2}u_{1,tt}^{(2)} = -2\beta_H(u_{1,11}^{(0)}u_{1,1}^{(1)} + u_{1,11}^{(1)}u_{1,1}^{(0)}) - 3\delta u_{1,11}^{(0)}(u_{1,1}^{(0)})^2 \tag{5.21}$$

being $u^{(2)}$ the second-order perturbation solution by making use of Equation 5.6 up to $u^{(2)}$. Then, following the same framework, the solution for the δ parameter with monochromatic plane wave excitation is,

$$u^{(2)}(x,t) = ce^{3i(kx-\omega t)} \quad , \quad c = \tfrac{1}{2}\beta^2 k^4 a^3 x^2 + \tfrac{1}{6}\delta k^3 a^3 x \tag{5.22}$$

where c is the amplitude of the third harmonic.

5.3 Extension to nonclassical nonlinearity

Recent studies show that a broad category of materials share nonclassical nonlinear elastic behavior. Manifestations of nonclassical nonlinearity include stress-strain hysteresis and discrete memory in quasi-static experiments, and specific dependencies of the harmonic amplitudes with respect to the drive amplitude in dynamic wave experiments, which are remarkably different from those predicted by the classical theory. Nonclassical nonlinear effects are believed to be due to the presence of soft regions in hard materials (e.g., microcracks, micropores and soft bonding regions between material grains). They have been successfully reproduced by a model [226] and, later, by Guyer and McCall, based on a

Preisach-Mayergoyz space (PM space) representation [227, 228], in analogy with the treatment of magnetic hysteresis. Differences between nonclassical and classical Landau-type [1] nonlinear dynamic behavior include: a downshift of the resonance frequency, proportional to the resonance amplitude in the nonclassical case versus a quadratic amplitude dependence in the classical case; nonlinear attenuation versus amplitude independent attenuation; quadratic amplitude dependence of the third harmonic versus cubic in the classical case [229].

Given a harmonic excitation on a nonlinear constitutive material, the history of any variable (either the strain, stress or displacement) at any point will not necessarily be harmonic and can therefore be represented by,

$$\sigma = M(1 + \beta_H \varepsilon + \delta\varepsilon^2 + ... + \alpha(\varepsilon + \varepsilon \text{sgn}(\varepsilon_{1,t}))\varepsilon \tag{5.23}$$

The implications of the nonlinear classical and non classical contributions on the acoustic wave propagation are depicted in Figure 5.1, which highlights the effects on the stress-strain relations, the frequency spectrum and the deformation of the signal.

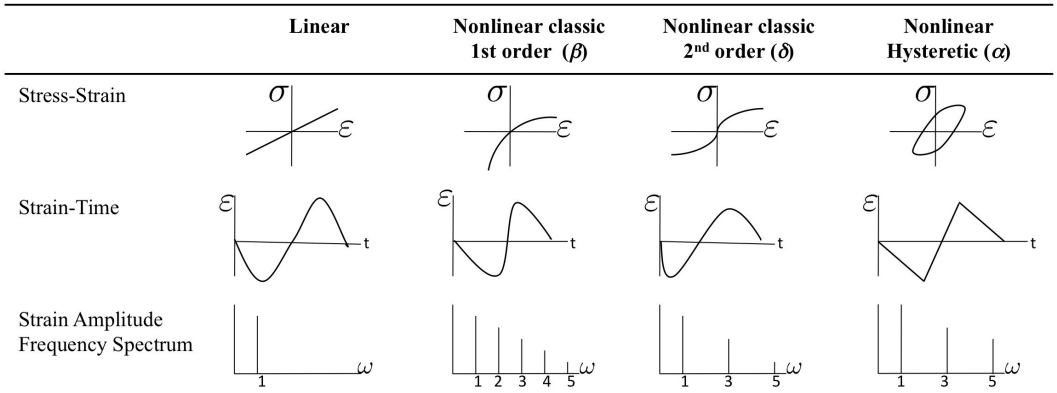

Figure 5.1: Nonlinear contribution to constitutive equation [4].

Note that Chapters 4 and 5 have direct application in nonlinear ultrasonics for early damage detection [230].

5.4 Connection with classical Westervelt model

To describe the level of nonlinearity in fluids or quasifluids, the nonlinear parameter B/A is usually provided, which originates in the Taylor series expansion of density in terms of pressure.

By using the relation $c_p^2 = \partial p/\partial \rho$ where p and ρ are sound pressure and density respectively, once can obtain from (Hamilton, Blackstock, and others, 1998) [107]:

$$p = A\left(\frac{\rho'}{\rho_0}\right) + \frac{B}{2!}\left(\frac{\rho'}{\rho_0}\right)^2 + \frac{C}{3!}\left(\frac{\rho'}{\rho_0}\right)^3 + ... \tag{5.24}$$

And from Equation 5.24, using the relation $c_p^2 = \frac{\partial p}{\partial \rho}$

$$\frac{c_p^2}{c_0^2} = 1 + \frac{B}{A}\left(\frac{\rho'}{\rho_0}\right) + \frac{C}{2A}\left(\frac{\rho'}{\rho_0}\right)^2 + ... \tag{5.25}$$

After a binomial expansion and leading root square,

$$\frac{c}{c_0} = 1 + \frac{B}{2A}\left(\frac{\rho'}{\rho_0}\right) + \frac{1}{4}\left[\frac{C}{A} - \frac{1}{2}\left(\frac{B}{A}\right)^2\right]\left(\frac{\rho'}{\rho_0}\right)^2 + ... \tag{5.26}$$

Equation of state with $\triangle\rho = \rho - \rho_0$, is considered now in terms of B/A ratio as follows,

$$p = c_0^2 \triangle\rho \left(1 + \frac{B}{2A}\frac{\triangle\rho}{\rho_0} + O\left(\left(\frac{\triangle\rho}{\rho_0}\right)^3\right)\right) \tag{5.27}$$

where ρ_0, is the ambient density and $c_0 = \sqrt{\frac{K}{\rho_0}}$, is the small signal sound speed. The values of B/A are usually calculated for selected fluids, liquefied gases,

$$\beta_W = 1 + \frac{B}{2A} \tag{5.28}$$

where β_W is defined now from the Westervelt equation that is explained in Equation 5.30 by making use of Taylor expansion of the pressure p in terms of volumetric strain v. Hydrostatic stress ($\sigma_{11} = \sigma_{22} = \sigma_{33}$) is defined in terms of pressure as,

$$p = -\frac{1}{3}(\sigma_{11} + \sigma_{22} + \sigma_{33}) = -\sigma_{11} \tag{5.29}$$

If we define p as a Taylor expansion of volumetric pressure being β the nonlinearity of first-order, from Equation 5.2 it results,

$$-p = -3Kv + 9\beta K v^2 + O(v^3) \tag{5.30}$$

Note that $M = K + \frac{4\mu}{3}$, so in the case of fluids and quasifluids (the limit of compressibility), $\mu = 0$ and $\mu \to 0$ respectively, $M = K$ is assumed. Then inverting Taylor expansion in terms of pressure and after second time derivative,

$$v = \frac{p}{3K} + \frac{\beta_W p^2}{3K^2} + h.o.t. \tag{5.31}$$

$$\dot{v} = \frac{\dot{p}}{3K} + \frac{2\beta_W}{3K^2} p\dot{p} + h.o.t. \tag{5.32}$$

$$\ddot{v} = \frac{\ddot{p}}{3K} + \frac{2\beta_W}{3K^2}(\ddot{p}p + \dot{p}) + h.o.t. \tag{5.33}$$

then using the kinematic relations in Equation 5.2, and space derivative, assuming small strains,

$$-3\ddot{v} = \ddot{\varepsilon}_{11} = \ddot{u}_{1,1} \tag{5.34}$$

introducing kinematic relations into pressure expansion, we obtain,

$$-p = Ku_{1,1} + K\beta_W u_{1,1}^2 + h.o.t. \tag{5.35}$$

assuming that high order terms are neglected ($O(u_{1,1}^3) = 0$), where β_W, is the Westervelt nonlinear parameter of first-order. So, the pressure may be defined as follows, by making use of Equations 5.34, 5.33 and 5.33,

$$-\frac{1}{3}\ddot{u}_{1,1} = \frac{\ddot{p}}{3K} + \frac{\beta_W}{3K^2}(\ddot{p}p + \dot{p}) + h.o.t \tag{5.36}$$

After second derivative of the pressure and introducing Dynamic equilibrium 5.2 leads,

$$\nabla^2 p = -\sigma_{11,11} = -\rho\ddot{u}_{1,1} \tag{5.37}$$

then the State Equation is deducted by comparing Equation 5.36 and Equation 5.37,

$$-\nabla^2 p = \rho\frac{\ddot{p}}{K} + \rho\frac{\beta_W}{K^2}(\ddot{p}p + \dot{p}^2) + h.o.t. \tag{5.38}$$

is possible to derive the classical nonlinear Westervelt equation. This equation is used in order to describe nonlinear sound propagation in dissipative fluids when cumulative nonlinear effects dominate local nonlinear effects. It is obtained from second order wave equation for progressive waves as,

$$\nabla^2 p - \frac{1}{c_0^2}\frac{\partial^2 p}{\partial t^2} + \frac{D}{c_0^4}\frac{\partial^3 p}{\partial t^3} = -\frac{\beta_W}{\rho c_0^4}\frac{\partial^2 p^2}{\partial t^2} \tag{5.39}$$

where D is the sound diffusivity that is not deducted at the moment, and β_W is the nonlinearity of first order coefficient.

5.4.1 Westervelt equation assuming large strains

Following the same framework that has been introduced in the previos section, the relationship between kinematic relations in Equation 5.2 and volumetric pressure second time-derivative 5.33 results,

$$-3\ddot{v} = \ddot{\varepsilon}_{11} = \ddot{u}_{1,1}(1 + u_{1,1}) + \dot{u}_{1,1}^2 \tag{5.40}$$

Introducing Kinematic relations into the pressure expansion neglecting displacement terms with power upper than third we obtain,

$$-p = Ku_{1,1} + \frac{1}{2}Ku_{1,1}^2 + \beta_W Ku_{1,1}^2 + O(u_{1,1}^3) \tag{5.41}$$

A series expansion of $u_{1,1} = -1 + \sqrt{1 - 6v}$ have been calculated in order to deduce the dynamic equilibrium in terms of volumetric part v. Then, is possible to establish the equilibrium in terms of pressure p by making use of constitutive equation inverted, that have been deducted in the previous section,

$$\nabla^2 p = -\rho \ddot{u}_{1,1} \tag{5.42}$$

whereby,

$$u_{1,1} = -3v - \frac{9}{2}v^2 - \frac{27}{2}v^3 + + h.o.t. \tag{5.43}$$

$$\dot{u}_{1,1} = -3\dot{v} - 9v\dot{v} - \frac{81}{2}v^2\dot{v} + h.o.t. \tag{5.44}$$

$$\ddot{u}_{1,1} = -3\ddot{v} - 9(\dot{v}^2 + v\ddot{v}) - \frac{81}{2}(2v\dot{v}^2 + v^2\ddot{v}) + h.o.t. \tag{5.45}$$

thus, by making use of Equations 5.32, 5.33 and 5.33 where volumetric pressure, its first and second time-derivatives were developed in terms of pressure and its first and second time derivatives,

$$\frac{1}{\rho}\nabla^2 p = \frac{\dot{p}^2}{K^2} + \frac{\ddot{p}}{K} + \frac{p\ddot{p}}{K^2} + \left(2\frac{\dot{p}^2}{K^2} + 6\frac{p\dot{p}^2}{K^3} + 2\frac{p\ddot{p}}{K^2} + 3\frac{p^2\ddot{p}}{K^3}\right)\beta + \left(6\frac{p^2\dot{p}^2}{K^4} + 2\frac{p^3\ddot{p}}{K^4}\right)\beta^2 \tag{5.46}$$

is posible to derive the classical Westervelt equation assuming large strains in this case, neglecting sound diffusivity part and third and high order terms as follows,

$$\nabla^2 p = \rho\left(\frac{\ddot{p}}{K} + \left(\beta + \frac{1}{2}\right)\frac{\dot{p}^2}{K^2}\right) \tag{5.47}$$

5.5 Extension to higher harmonics

In this section we have taken into account two parts, one with the assumption of fluid without viscosity, and the other the assumption of small displacements inside the compatibility equation with the wave propagating in one direction.

5.5.1 For fluid without viscosity in one direction and assuming small strains

- First simplification: For ideal fluid, shear moduli is equal to cero, $\mu = 0$ and neglecting viscosity means $\eta = 0$. In this case the terms outside the diagonal in the Cauchy stress tensor are zero, $\tau_{ij} = 0$ that implies,

$$\sigma_{ij} = \frac{1}{3}\sigma_{kk}\delta_{ij} = -p\delta_{ij} \tag{5.48}$$

  where δ_{ij} is the Kronecker's delta, and p is the pressure.
- Second simplification: is to consider the displacement in one direction, it means, $u_1 \neq 0$ and $u_2 = u_3 = 0$ that implies $\varepsilon_{11} \neq 0$ and $\varepsilon_{ij} = 0 \; \forall \; ij \neq 11$. In this case, the volumetric part is derived as,

$$v = -\frac{1}{3}(\varepsilon_{11} + \varepsilon_{22} + \varepsilon_{33}) = -\frac{1}{3}\varepsilon_{11} \tag{5.49}$$

where $\varepsilon_{11} = -v\delta_{11} + d_{11}$, and d_{11} is the deviatoric part of strain. Also small strains implies, $v = -\frac{1}{3}u_{1,1}$

- Third simplification affects to volumetric expression and its second derivative as follows,

$$\dot{v} = \frac{1}{3}(\dot{u}_{1,1} + \dot{u}_{2,2} + \dot{u}_{3,3}) \text{ and } \ddot{v} = -\frac{1}{3}\sum_{k=1}^{3}\ddot{u}_{k,k} \tag{5.50}$$

The linear elastic dependency is enriched with quadratic and cubic terms, following the series expansion concept put forth by Landau [1]. Only the volumetric part is datelined in terms of nonlinear acoustic parameter of second order β and nonlinear acoustic parameter of third order δ being scalar,

$$-p = -3Kv + 9\beta Kv^2 - 27\delta Kv^3 + h.o.t. \tag{5.51}$$

the constitutive Equation 5.51 could be introduced in Equilibrium Equation 5.2 as follows,

$$\rho\ddot{u} = \sigma_{ij,j} = \nabla(-p\delta_{ij}) = \nabla(-3Kv + 9\beta Kv^2 - 27\delta Kv^3 + h.o.t.) \tag{5.52}$$

If we consider the Constitutive Equation 5.32 in terms of volumetric part v, comparing coefficients of the polynomial series as follows,

$$\begin{aligned}
y &= a_0 + a_1x + a_2x^2 + ... = \sum_{n=0}^{\infty} a_n(x - x_0)^n \\
x &= \sum_{n=0}^{\infty} b_n(y - y_0)^n = \sum_{k=0}^{\infty} b_k[\sum_{j=0}^{\infty} a_j(x - x_0)^j]^k \\
b_1 &= \frac{1}{a_0} \\
b_2 &= -\frac{a_2}{a_1^3} \\
b_3 &= \frac{2a_2^2 - a_1a_3}{a_1^5} \\
b_4 &= \frac{5a_1a_2a_3 - a_1^2a_4 - 5a_2^3}{a_1^7} \\
b_n &= \frac{(-1)^{n-1}a_2^n - a_1^{n-2}a_n}{a_1^{2n-1}}
\end{aligned} \tag{5.53}$$

Thus, we obtain the constitutive law for v,

$$v = \frac{1}{3K}p + \frac{1}{3K^2}\beta p^2 + \frac{1}{3K^3}(2\beta^2 - \delta)p^3 + h.o.t. \tag{5.54}$$

Then, if we introduce first and second derivative in time, volumetric scalar expansions results,

$$\begin{aligned}\dot{v} &= \frac{1}{3K}\dot{p} + \frac{2}{3K^2}\beta p\dot{p} + \frac{1}{K^3}(2\beta^2 - \delta)p^2\dot{p} + h.o.t. \\ \ddot{v} &= \frac{1}{3K}\ddot{p} + \frac{2}{3K^2}\beta(\ddot{p}p + \dot{p}^2) + \frac{1}{K^3}(2\beta^2 - \delta)(2p\dot{p}^2 + p^2\ddot{p}) + h.o.t.\end{aligned} \tag{5.55}$$

by making use of Equation 5.42 $\ddot{v} = -\frac{1}{3}\ddot{u}_{1,1}$ and Equation 5.45, The westervelt equation for third order of nonlinearity with the assumption of small strains and viscosity neglected in one dimension, is deducted as follows,

$$\frac{1}{\rho}\nabla^2 p = \frac{1}{K}\frac{\partial p}{\partial t} - \frac{\partial p^2}{\partial t^2}\frac{\beta}{K^2} + \frac{\partial^3 p^3}{\partial t^3}\frac{(2\beta^2 - \delta)}{K^3} \tag{5.56}$$

5.5.2 For fluid without viscosity in one direction and assuming large strains

If we consider the case in which strains are related to large displacements, regarding to Equation 5.2, Kinematic relations 5.2 are derived as follows,

$$v = -\frac{1}{3}(u_{1,1} + \frac{1}{2}u_{1,1}^2) \tag{5.57}$$

A series expansion of $u_{1,1} = -1 + \sqrt{1 - 6v}$ have been calculated in order to deduce the dynamic equilibrium in terms of volumetric part v. Then, is possible to establish the equilibrium in terms of pressure p by making use of constitutive equation inverted 5.47, that have been deducted in the previous section,

$$\rho\ddot{u}_{1,1} = \nabla^2(-p) \tag{5.58}$$

whereby,

$$u_{1,1} = -3v - \frac{9}{2}v^2 - \frac{27}{2}v^3 - \frac{405}{8}v^4 + h.o.t. \tag{5.59}$$

$$\dot{u}_{1,1} = -3\dot{v} - 9v\dot{v} - \frac{81}{2}v^2\dot{v} + h.o.t. \tag{5.60}$$

$$\ddot{u}_{1,1} = -3\ddot{v} - 9(\dot{v}^2 + v\ddot{v}) - \frac{81}{2}(2v\dot{v}^2 + v^2\ddot{v}) + h.o.t. \tag{5.61}$$

So, the Westervelt equation for large strains for an ideal fluid neglecting viscosity terms, in one direction results as follows,

$$
\begin{aligned}
-\frac{1}{\rho}\nabla^2 p \;&= -9\left(\tfrac{\dot{p}}{3K}+\tfrac{p\dot{p}\beta}{3K^2}+\tfrac{p^2\dot{p}(2\beta^2-\delta)}{6K^3}\right)^2-9\left(\tfrac{p}{3K}+\tfrac{p^2\beta}{6K^2}+\tfrac{p^3(2\beta^2-\delta)}{18K^3}\right)\\
&\quad\left(\tfrac{\ddot{p}}{3K}+\tfrac{(\dot{p}^2+p\ddot{p})\beta}{3K^2}+\tfrac{(\dot{p}^3+2p\ddot{p})(2\beta^2-\delta)}{6K^3}\right)-\\
&\quad 3\left(\tfrac{\ddot{p}}{3K}+\tfrac{(\dot{p}^2+p\ddot{p})\beta}{3K^2}+\tfrac{(\dot{p}^3+2p\ddot{p})(2\beta^2-\delta)}{6K^3}\right)
\end{aligned}
\tag{5.62}
$$

This expression could be expand and simplified under the assumption that p/K is the unique factor no neglected up to third order. The others are approximately equal to zero because the order of bulk modulus is upper than the pressure. Then it results as follows,

$$
\begin{aligned}
\frac{1}{\rho}\nabla^2 p \;&= \tfrac{\dot{p}^2}{K^2}+\tfrac{3p\dot{p}^2}{K^3}+\tfrac{\ddot{p}}{K}+\tfrac{p\ddot{p}}{K^2}+\tfrac{3p^2\ddot{p}}{2K^3}\\
&\quad+\tfrac{2\dot{p}^2\beta}{K^2}+\tfrac{6p\dot{p}^2\beta}{K^3}+\tfrac{2p\ddot{p}\beta}{K^2}+\tfrac{3p^2\ddot{p}\beta}{K^3}\\
&\quad+\tfrac{12p\dot{p}^2\beta^2}{K^3}+\tfrac{6p^2\ddot{p}\beta^2}{K^3}-\tfrac{6p\dot{p}^2\delta}{K^3}-\tfrac{3p^2\ddot{p}\delta}{K^3}
\end{aligned}
\tag{5.63}
$$

Thus, grouping terms results,

$$
\frac{1}{\rho}\nabla^2 p \;= \tfrac{\ddot{p}}{K}+\left(\beta+\tfrac{1}{2}\right)\tfrac{\dddot{p}^2}{K^2}+\tfrac{3}{2}\left(1+2\beta+2(2\beta^2-\delta)\right)\tfrac{\dddot{p}^3}{K^3} \tag{5.64}
$$

5.5.3 For fluid with viscosity in one direction and assuming large strains

If we consider the case in which strains are related to large displacements, regarding to Equation 5.2, Kinematic relations 5.2 are derived as follows,

$$
v = -\frac{1}{3}(u_{1,1}+\frac{1}{2}u_{1,1}^2) \tag{5.65}
$$

A series expansion of $u_{1,1} = -1+\sqrt{1-6v}$ have been calculated in order to deduce the dynamic equilibrium in terms of volumetric part v. Then, is possible to establish the equilibrium in terms of pressure p by making use of constitutive equation inverted (39), that have been deducted in the previous section, but in this case we introduce $\eta^v\dot{v}$ as the viscosity part in the constitutive equation as,

$$
\sigma_{11,1} = \rho\ddot{u}_{1,1} - 3\eta^v\nabla^2\dot{v} = \nabla^2(-p) \tag{5.66}
$$

whereby,

$$
\ddot{u}_{1,1} \;=\; -3\ddot{v}-9(\dot{v}^2+v\ddot{v})-\frac{81}{2}(2v\dot{v}+v^2\ddot{v})+h.o.t. \tag{5.67}
$$

So, the Westervelt equation for large strains for an ideal fluid with viscosity terms, in one direction results as follows,

$$-3\ddot{v} - 9(\dot{v}^2 + v\ddot{v}) - \frac{81}{2}(2v\dot{v} + v^2\ddot{v}) - \eta^v \frac{1}{K\rho}\nabla^2\dot{p} = \frac{1}{\rho}\nabla^2(-p) \tag{5.68}$$

Note that nonlinear terms are neglected in the viscosity part, due to the harmonics generation is not expressed. Since one frequency is considered, $\frac{K}{\rho}\nabla^2\dot{p} = \dddot{p}$, Westervelt equation results as follows,

$$\frac{\ddot{p}}{K} + \left(\beta + \frac{1}{2}\right)\frac{\ddot{p^2}}{K^2} + \frac{3}{2}\left(1 + 2\beta + 2(2\beta^2 + \delta)\right)\frac{\ddot{p^3}}{K^3} - \eta^v \frac{1}{\rho^2}\dddot{p} = \frac{1}{\rho}\nabla^2(-p) \tag{5.69}$$

These results are an "open door" that suggest the main idea of the next section, introduce the extension to nonlinearity of second order into the Westervelt equation, and then upper harmonics translated to nonlinearities of high order. This process have been carried out based on binomial series expansion, discussing under different assumptions of the state of material and regime of strain.

5.6 Generalized Westervelt equation

Westervelt generalized equation is derived under the assumption of an ideal fluid without viscosity, since small displacements are considered inside the compatibility Equation 5.2. Analagously to the previous cases, the wave propagation along 1 direction is fixed. Then, an extension to high harmonics is derived.

5.6.1 For fluid without viscosity in one direction and assuming small strains

For an ideal fluid, where attenuation has been neglected, is possible to derive the generalized Westervelt equation for high harmonics by making use of the same three simplifications taking into account in Equations 5.48, 5.49 and 5.50.

- First simplification: For ideal fluid, shear moduli is equal to cero, $\mu = 0$ and neglecting viscosity means $\eta = 0$. In this case the terms outside the diagonal in the Cauchy stress tensor are zero, $\tau_{ij} = 0$ that implies,

$$\sigma_{ij} = \frac{1}{3}\sigma_{kk}\delta_{ij} = -p\delta_{ij} \tag{5.70}$$

  where δ_{ij} is the kronecker delta, and p is the pressure.
- Second simplification: is to consider the displacement in one direction, it means, $u_1 \neq 0$ and $u_2 = u_3 = 0$ that implies $\varepsilon_{11} \neq 0$ and $\varepsilon_{ij} = 0 \; \forall \; ij \neq 11$. In this case, the volumetric part is derived as,

$$v = -\frac{1}{3}(\varepsilon_{11} + \varepsilon_{22} + \varepsilon_{33}) = -\frac{1}{3}\varepsilon_{11} \tag{5.71}$$

where $\varepsilon_{11} = -v\delta_{11} + d_{11}$, and d_{11} is the deviatoric part of strain. Also small strains implies, $v = -\frac{1}{3}u_{1,1}$

- Third simplification affects to volumetric expression and its second derivative as follows,

$$\dot{v} = \frac{1}{3}(\dot{u}_{1,1} + \dot{u}_{2,2} + \dot{u}_{3,3}) \text{ and } \ddot{v} = -\frac{1}{3}\sum_{k=1}^{3}\ddot{u}_{k,k} \tag{5.72}$$

The linear elastic dependency is enriched with quadratic and cubic terms, following the series expansion concept put forth by Landau [1]. Only the volumetric part is datelined in terms of nonlinear acoustic parameter of second order β and nonlinear acoustic parameter of third order δ being scalar,

$$-p = -\sum_{i=1}^{n} 3^i K v^i \tag{5.73}$$

the Constitutive Equation 5.55 could be introduced in equilibrium Equation 5.2 as follows,

$$\rho\ddot{u} = \sigma_{ij,j} = \nabla(-p\delta_{ij}) = \nabla(-\sum_{i=1}^{n} 3^i K v^i) \tag{5.74}$$

If we consider the Constitutive Equation 5.55 in terms of volumetric part v, comparing coefficients of the polynomial series as follows,

$$\begin{aligned}
y &= a_0 + a_1 x + a_2 x^2 + ... = \sum_{n=0}^{\infty} a_n (x - x_0)^n \\
x &= \sum_{n=0}^{\infty} b_n (y - y_0)^n = \sum_{k=0}^{\infty} b_k [\sum_{j=0}^{\infty} a_j (x - x_0)^j]^k \\
b_1 &= \frac{1}{a_0} \\
b_2 &= -\frac{a_2}{a_1^3} \\
b_3 &= \frac{2a_2^2 - a_1 a_3}{a_1^5} \\
b_4 &= \frac{5a_1 a_2 a_3 - a_1^2 a_4 - 5a_2^3}{a_1^7} \\
b_n &= \frac{(-1)^{n-1} a_2^n - a_1^{n-2} a_n}{a_1^{2n-1}}
\end{aligned} \tag{5.75}$$

Thus, we obtain the constitutive law for v,

$$v = \frac{1}{3K}p + \frac{1}{6K^2}\beta p^2 + \frac{1}{18K^3}(2\beta^2 - \delta)p^3 + h.o.t. \tag{5.76}$$

Then, If we introduce second derivative in time, volumetric scalar expansions results,

$$\ddot{v} = \frac{1}{3K}\ddot{p} + \frac{1}{3K^2}\beta(\ddot{p}p + \dot{p}^2) + \frac{1}{6K^3}(2\beta^2 - \delta)(2\ddot{p}p + \dot{p}^3) + h.o.t. \tag{5.77}$$

by making use of Equation 5.58 $\ddot{v} = -\frac{1}{3}\ddot{u}_{1,1}$ and Equation 5.61, The Westervelt equation for third order of nonlinearity with the assumption of small strains and viscosity neglected in one dimension, is deducted as follows,

$$\frac{1}{\rho}\nabla^2 p = \frac{\partial^2}{\partial t^2}\left[b_0 p + \frac{1}{K}\sum_{i=1}^{n} a_i b_{n-i} p^{i+1}\right] \tag{5.78}$$

where

$$\begin{aligned} a_i &= \sum_{i=0}^{n} 3^{i+1}\Pi_i K \text{ and, } \Pi_i = \{1, \beta, \delta, ...\}_{i=1}^{n} \\ b_n &= \sum_{i=1}^{n} a_i b_{n-i} \\ b_0 &= -\frac{1}{a_0} \end{aligned} \tag{5.79}$$

5.6.2 For fluid with viscosity in one direction and assuming small strains

Generalized Westervelt equation is almost the same that in the equation 5.78 for fluid in one direction of propagation and assuming small strains. However, in this case viscosity term should be introduced in the same manner that in Equation 5.69, the case of the second order of nonlinearity.

$$\frac{\ddot{p}}{K} + \left(\beta + \frac{1}{2}\right)\frac{\ddot{p^2}}{K^2} + \frac{3}{2}\left(1 + 2\beta + 2(2\beta^2 + \delta)\right)\frac{\ddot{p^3}}{K^3} - \eta^v \frac{1}{\rho^2}\dddot{p} = \frac{1}{\rho}\nabla^2(-p) \tag{5.80}$$

where $\frac{1}{\rho}\nabla^2 p$ can be generalized as follows,

$$\frac{1}{\rho}\nabla^2 p = \frac{\partial^2}{\partial t^2}\left[b_0 p + \frac{1}{K}\sum_{i=1}^{n} a_i b_{n-i} p^{i+1} - \frac{\eta^v}{\rho^2}\frac{\partial p}{\partial t}\right] \tag{5.81}$$

where the coefficients of this generalization are the same than in the previous cases 5.79.

$$\begin{aligned} a_i &= \sum_{i=0}^{n} 3^{i+1}\Pi_i K \text{ and, } \Pi_i = \{1, \beta, \delta, ...\}_{i=1}^{n} \\ b_n &= \sum_{i=1}^{n} a_i b_{n-i} \\ b_0 &= -\frac{1}{a_0} \end{aligned} \tag{5.82}$$

Note that all cases of second and higher order in a classical context have been studied and extracted. However the case of generalization for large strains no, it keeps the same frameworks than the others.

The purpose introducing an analytical new approach where the nonlinear acoustic Westervelt equation is directly linked with the future applications in this field. Nowadays is technically almost imposible to develop a experimental procedure to obtain measurements physically significant upper than the third harmonics, but with the constant evolution of the ultrasonic technologies, some day could be relevant in the understanding of the matter.

5.7 Unification between β nonlinear parameters

The second research objetive of this Thesis connects with the unification of nonlinear acoustic parameter of first order and its explicit calculation from several literature values in different materials. Table 5.1 shows seven types of β parameters depending on author conception respect how are derived and the nature of the plane wave considered.

Nonlinear Classic 1^{st} order β	Relation with third order elastic constants	Harmonic amplitudes and strains	B/A ratio (Fluids)
β_H	$-\frac{3}{2}-\frac{\mathcal{A}+3\mathcal{B}+\mathcal{C}}{\lambda+2\mu}$	$\frac{4b}{k^2a^2x}$	-
β_G	$-\frac{3}{2}-\frac{\mathcal{A}+3\mathcal{B}+\mathcal{C}}{K}$	$\frac{E_c}{xE_a^2}$	-
β_Z^l	$3\frac{\lambda+2\mu}{\rho_0}+\frac{1}{\rho_0}(2\mathcal{A}+6\mathcal{B}+2\mathcal{C})$	-	-
β_Z^τ	$\frac{\mu}{\rho_0}+\frac{1}{\rho}\left(\frac{\mathcal{A}}{2}+\mathcal{B}\right)$	-	-
β_{Gol}^l	$3K+4\mu+(2\mathcal{A}+6\mathcal{B}+2\mathcal{C})$	-	-
β_{Gol}^τ	$K+\frac{4}{3}\mu+\frac{\mathcal{A}}{2}+\mathcal{B}$	-	-
β_W	$1+\frac{2\mathcal{C}+\mathcal{B}}{2\mathcal{B}}$	-	$1+\frac{B}{2A}$

Table 5.1: Relationship between various nonlinear classic first order β from literature and TOEC, harmonics amplitudes, and B/A ratio.

Note that to compare all definitions of β we have introduced $\beta_W = 1 + \frac{B}{2A}$ with de index W since Westervelt equation is commonly used in fluids with this relationship explicitly deducted by Hamilton, see [2]. The definition of Gol'dberg in 1960 is also introduced as longitudinal and transverse nonlinear acoustic parameter, β_{Gol}^l and β_{Gol}^τ, respectively. It was based on the study of β by Zarembo previously detailed, but with the purpose of analyzing the interaction between them [14].

5.8 Nonlinear acoustic parameter of first order values for metals, crystals, liquids and tissues

It is well known that there are not many references where Third Order Elastic Constants are experimentally obtained. However, in the case of metals and crystals have been calculated by Zarembo 1971 and Muir 2009. (See [5, 6]). Also, Third Order Elastic Constants have been calculated from Hamilton 1998 [2] since B/A ratio was determined in all cases from Equation 5.4 for liquids and biological tissues. Tables 5.2 and 5.3 shows TOEC for some metals and crystals, and tables 5.4 and 5.5 shows TOEC for liquids and biological tissues, respectively and in both the first parameter of no linearity β_H that has been taken with the

common Hamilton meaning from Equation 4.15. The first and second Lamé parameters λ and μ have been included also, using traction forces and NDT (Non-Destructive Testing) technics, with a database given by [231, 232, 233, 234, 63].

Metal	λ [GPa]	μ [GPa]	$\mathcal{A}$ [GPa]	$\mathcal{B}$ [GPa]	$\mathcal{C}$ [GPa]	β_H
AL7075	52.04	25.86	-334.5	-125.35	-60.5	5.93
Steel 60C2H2a	107.8	81.32	-760	-250	-90	4.42
Nickel Steel 535	154	124	-730	-230	-180	2.48
Polystyrene	2.8	1.2	-10	-8	-11	7.15
"Armco" iron	80	80	1100	-1580	1230	8.54
Glass (pyrex)	16.67	25	420	-118	-132	-0.51

Table 5.2: Beta value and Third-Order Elastic Constants associated to literature values of metals. TOEC were given by Zarembo and Muir (See [5, 6])

.

The first group of materials, solid metals, have been from references of Zarembo 1971 and Muir 2009, the nonlinear acoustic parameter β comprises between -0.51 for glass (pyrex), and 8.54 in the case of "Armco" iron.

Crystal	λ	μ	$\mathcal{A}$ [GPa]	$\mathcal{B}$ [GPa]	$\mathcal{C}$ [GPa]	β_H
NaCl	13.63	16	132	33	1.13	-6.56
NaF	57.66	29.7	304	76	2.74	-6.07
KBr	7.46	11.2	7.44	18.6	0.46	-6.63
KCl	9.54	12.14	82.8	20.7	0.62	-5.8
Si	65.08	51.14	-256	12	-2.67	-0.2
Ag	86.22	30.29	332	56	7.88	-4.96
Au	112.86	28.21	-48	-13	-9.71	-0.93
Cu	94.36	44.4	380	-3	-2.08	-3.51
SiO_2	16.09	31.24	870	-276	-12.25	-1.88

Table 5.3: Beta value and Third-Order Elastic Constants associated to literature values of crystals. (See Zarembo 1971 [5])

.

Table 5.3 shows the same parameters for solid crystals, this values have been calculated from Zarembo 1971. In all cases the nonlinear acoustic parameter β has been obtained with a minus sign and the minimum value corresponds to -6.63 for KBr and the maximum was obtained for SiO_2 with -1.88.

Liquid	λ [GPa]	μ [GPa]	$\mathcal{A}$ [GPa]	$\mathcal{B}$ [GPa]	$\mathcal{C}$ [GPa]	β_H
Distilled water	2.15	0	0	-2.15	-4.3	3.5
Methanol	0.82	0	0	-0.82	-3.53	5.8
Ethanol	1.06	0	0	-1.06	-4.98	6.2
Mercury	28.5	0	0	-28.5	-96.9	4.9
Glycerol	4.35	0	0	-4.35	-17.4	5.5

Table 5.4: Beta value and Third-Order Elastic Constants associated to literature values of liquids. (See Hamilton and Blackstock 1998 [2])

.

In the next type of materials, for the liquid state Table 6, they have been deduced from the extraction of experimental B/A parameter (see Hamilton and Blackstock 1998), this parameter is commonly calculated from finite amplitude technics. By making use of $\beta = 1 + \frac{B}{2A}$ relationship, and the mechanical properties assumptions for fluids $\mu \approx 0$, $\mathcal{A} = 0$ that implies $\mathcal{B} = -\lambda$ and $\mathcal{C} = \frac{B-A}{2}$ as was shown in section 1 is possible to deduce all nonlinear coefficients. The nonlinear acoustic parameter β comprise a minimum value of 3.5 for distilled water and a maximum value of 5.4 for the case of ethanol.

Biological Tissue	λ [GPa]	μ [GPa]	B/A
Haemoglobin	2.2	$\approx$0	3.6$\pm$0.3
Human liver	1.7	$\approx$0	7.6$\pm$0.8
Human breast fat	2.1	$\approx$0	9.91
Human spleen	2.9	$\approx$0	7.8$\pm$0.8
Human multiple myeloma	2.5	5$\pm$0.1	5.8$\pm$5
Collagen	0.07	0.77	4.3$\pm$1

Table 5.5: B/A parameter associated to literature values of biological tissues. (See [2, 7])

.

Assuming the references values of haemoglobin 2.2 [7], human liver has a Lamé of about 1.7 [GPa] [7], human breast fat with 2.1 [GPa] of Lamé parameter [7], 2.9 $\pm$ 1.8 [kPa] for the spleen [235], multiple myeloma 5.10$\pm$ 1.47 [Pa] [236], and 0.073, 0.77 for first and second Lamé parameters, respectively in the case of collagen [237], the values of Table 5.5 has been extracted. The results, of nonlinear acoustic parameter B/A varies between 9.91 for human breast fat and 4.3 for collagen.

Note that biological tissues are derived under the $\lambda >> \mu$ condition and μ can be relevant in the context of fiber phase. In fact, there is no manner to measure TOEC at the moment, this conclusion is one of the main contributions of this thesis, in Chapter 9.

5.9 General nonlinear elasticity for isotropic and transversely isotropic materials

Three invariants suffice for isotropic elasticity, see Equation 4.13, but for transverse isotropy we require an additional two, in terms of the anisotropy of the material. We define a vector $\mathbf{M}$, or δ_{i3} which defines the axis of transverse isotropy and thus define the additional invariants,

$$I_4 = \mathbf{M} \cdot \mathbf{EM}, \qquad I_5 = \mathbf{M} \cdot \mathbf{E}^2\mathbf{M},$$

or

$$I_4 = \delta_{i3}\varepsilon_{ij}\delta_{3k}, \qquad I_5 = \delta_{i3}\varepsilon_{ij}\varepsilon_{jk}\delta_{3k}. \tag{5.83}$$

Here we shall take $\mathbf{M}$ to be in the direction parallel to the x_3 axis, without loss of generality, just by an reference rotation.

Thus for a macroscopically anisotropic material the form of the corresponding strain energy W (see [238]) is,

$$W_{TI} = \frac{1}{2}(k-m)I_1^2 + mI_2 + \frac{1}{2}(n-4p-2\ell+k+m)I_4^2 + 2(p-m)I_5 + (\ell-k+m)I_1I_4 \quad (5.84)$$

$$+\frac{\mathcal{A}}{3}I_3 + \mathcal{B}I_1I_2 + \frac{\mathcal{C}}{3}I_1^3 + \mathcal{D}I_1I_4^2 + \mathcal{E}I_1I_5 + \mathcal{F}I_1^2I_4 + \mathcal{G}I_2I_4 + \mathcal{H}I_4^3 + \mathcal{I}I_4I_5 \quad (5.85)$$

where k, ℓ, m, n and p are the linear elastic coefficients usually taken for linear elasticity [239], they are introduced to simplify constitutive law in terms of invariants previously defined. Note that there are *nine* nonlinear (third-order) moduli $\mathcal{A}, \mathcal{B}, ..., \mathcal{I}$.

In the limit of isotropy, $k = \lambda + \mu, \ell = \lambda, m = \mu, n = \lambda + 2\mu$ and $p = \mu$. This gives rise to the leading order terms in (5.85) reducing to the form of those in (4.12). Additionally in this limit, we must have $\mathcal{D} = \mathcal{E} = \mathcal{F} = \mathcal{G} = \mathcal{H} = \mathcal{I} = 0$.

So if we consider the transversely isotropic material with quadratic nonlinearity. Following an analogous approach using 5.85-**??** with 4.15 we can group,

$$\mathbf{T} = \mathbf{T}^{L1} + \mathbf{T}^{L2} + \mathbf{T}^{NL1} + \mathbf{T}^{NL2} \quad (5.86)$$

where we have decomposed the stress into its linear (L) and nonlinear (NL) parts and contributions associated with isotropy 4.15 and anisotropy 5.86, defined by

$$\mathbf{T}_{L1} = (k-m)(\mathrm{tr}\mathbf{E})\mathbf{I} + 2m\mathbf{E}, \quad (5.87)$$

$$\mathbf{T}_{L2} = \mathcal{L}_1(\mathbf{M}\cdot\mathbf{EM})\mathbf{N} + 2(p-m)(\mathbf{NE}+\mathbf{EN}) + \mathcal{L}_2((\mathbf{M}\cdot\mathbf{EM})\mathbf{I} + (\mathrm{tr}\mathbf{E})\mathbf{N}), \quad (5.88)$$

$$\mathbf{T}_{NL1} = \mathcal{A}\mathbf{E}^2 + \mathcal{B}(\mathrm{tr}(\mathbf{E}^2)\mathbf{I} + 2(\mathrm{tr}\mathbf{E})\mathbf{E}) + \mathcal{C}(\mathrm{tr}\mathbf{E})^2\mathbf{I}, \quad (5.89)$$

$$\mathbf{T}_{NL2} = (\mathcal{D}I_4^2 + \mathcal{E}I_5 + 2\mathcal{F}I_1I_4)\mathbf{I} + (2\mathcal{D}I_1I_4 + \mathcal{F}I_1^2 + \mathcal{G}I_2 + 3\mathcal{H}I_4^2 + \mathcal{I}I_5)\mathbf{N}$$

$$+ 2\mathcal{G}I_4\mathbf{E} + (\mathcal{E}I_1 + \mathcal{I}I_4)(\mathbf{NE}+\mathbf{EN}), \quad (5.90)$$

where we used the notation $\mathbf{N} = \mathbf{M}\otimes\mathbf{M}$, or

$$\sigma_{ij}^{L1} = (k-m)\varepsilon_{kk}\delta_{ij} + 2m\varepsilon_{ij}, \quad (5.91)$$

$$\sigma_{ij}^{L2} = \mathcal{L}_1(\delta_{i3}\varepsilon_{ij}\delta_{3j})\delta_{i3}\delta_{j3} + 2(p-m)(\delta_{i3}\delta_{j3}\varepsilon_{ij} + \varepsilon_{ij}\delta_{33}) + \mathcal{L}_2((\delta_{i3}\varepsilon_{ij}\delta_{3j})\delta_{ij} + \varepsilon_{kk}\delta_{i3}\delta_{j3}), \quad (5.92)$$

$$\sigma_{ij}^{NL1} = \mathcal{A}\varepsilon_{ij}\varepsilon_{jk} + \mathcal{B}(\varepsilon_{ij}E_{ji})\delta_{ij} + 2\varepsilon_{kk}\varepsilon_{ij} + \mathcal{C}\varepsilon_{kk}^2\delta_{ij}, \quad (5.93)$$

$$\sigma_{ij}^{NL2} = (\mathcal{D}I_4^2 + \mathcal{E}I_5 + 2\mathcal{F}I_1I_4)\delta_{ij} + (2\mathcal{D}I_1I_4 + \mathcal{F}I_1^2 + \mathcal{G}I_2 + 3\mathcal{H}I_4^2 + \mathcal{I}I_5)\delta_{i3}\delta_{j3} + 2\mathcal{G}I_4\varepsilon_{ij} + (\mathcal{E}I_1 + \mathcal{I}I_4)(\delta_{i3}\delta_{j3}\varepsilon_{ij} + \varepsilon_{ij}\delta_{i3}\delta_{j3}), \quad (5.94)$$

and

$$\mathcal{L}_1 = n - 4p - 2\ell + k + m, \qquad \mathcal{L}_2 = \ell - k + m. \quad (5.95)$$

We note that in the isotropic limit, the anisotropic contributions $\mathbf{T}_{L2} = \mathbf{T}_{NL2} = 0$ and $\mathbf{T}_{L1}$ and $\mathbf{T}_{NL2}$ recover the isotropic forms Equation 4.15. (All derivations rules are detailed in the appendix B)

5.10 Nonlinear acoustic constant β calculated from nonlinear terms in transversally isotropic media

If the material constitutive law is extended to the anisotropic case, in addition to nonlinear, the stress can be split into four terms, as it is explained in Equation 5.96,

$$\mathbf{T} = \mathbf{T}_{L1} + \mathbf{T}_{L2} + \mathbf{T}_{NL1} + \mathbf{T}_{NL2} \quad (5.96)$$

By making use of the index notation, the previous equation is explicitly related as,

$$\begin{aligned}
\sigma_{ij}^{L1} &= A\varepsilon_{kk}\delta_{ij} + B\varepsilon_{ij} \\
\sigma_{ij}^{L2} &= \Gamma(\delta_{i3}\varepsilon_{ij}\delta_{3j})\delta_{i3}\delta_{3j} + \Delta(\delta_{k3}\varepsilon_{ij}\delta_{i3} + \delta_{i3}\varepsilon_{ij}\delta_{k3}) \\
&\quad + E(\delta_{k3}\varepsilon_{kp}\delta_{p3}\delta_{ij} + \varepsilon_{kk}\delta_{i3}\delta_{3j}) \\
\sigma_{ij}^{NL1} &= Z\varepsilon_{ij}\varepsilon_{jk} + H\varepsilon_{kp}\varepsilon_{pk}\delta_{ij} + \Theta\varepsilon_{kk}\varepsilon_{ij} + I(\varepsilon_{kk}\delta_{ij})^2 \\
\sigma_{ij}^{NL2} &= \delta_{ij}(K\delta_{k3}\varepsilon_{kp}\delta_{3p}\delta_{k3}\varepsilon_{kp}\delta_{3p} + \Lambda\delta_{k3}\varepsilon_{kp}\varepsilon_{pl}\delta_{3p} + 2M\varepsilon_{kk}\delta_{i3}\varepsilon_{ij}\delta_{3j} - E\varepsilon_{kk}\delta_{i3}\varepsilon_{ij}\delta_{3j}) \\
&\quad + \delta_{i3}\delta_{3j}(2K\varepsilon_{kk}\delta_{i3}\varepsilon_{ij}\delta_{3j} + M\varepsilon_{kk}\varepsilon_{kk} + N\varepsilon_{ij}\varepsilon_{jk} + 3\Xi\delta_{i3}\varepsilon_{ij}\delta_{3j}\delta_{i3}\varepsilon_{ij}\delta_{3j} \\
&\quad + O\delta_{i3}E_{ij}\varepsilon_{jk}\delta_{3j} - (\Gamma\varepsilon_{kk}\delta_{i3}\varepsilon_{ij}\delta_{3j} + E\varepsilon_{kk}\varepsilon_{kk})) + \varepsilon_{ij}(2N + 2E)(\delta_{i3}\varepsilon_{ij}\delta_{3j}) \\
&\quad + (\delta_{k3}\varepsilon_{ij}\delta_{i3} + \delta_{i3}\varepsilon_{ij}\delta_{k3})((\Lambda + E - \Delta)\varepsilon_{kk} + (O + \Gamma)\delta_{i3}\varepsilon_{ij}\delta_{3j}) \\
&\quad + \Delta(\delta_{i3}\delta_{3j}\varepsilon_{ij}\varepsilon_{jk} + \varepsilon_{ij}\varepsilon_{jk}\delta_{i3}\delta_{3j} + \varepsilon_{ij}\delta_{i3}\varepsilon_{kl}\delta_{k3} + \delta_{i3}\varepsilon_{ij}\delta_{k3}\varepsilon_{kl})
\end{aligned} \quad (5.97)$$

where A, B, Γ, Δ, E, Z, H, Θ, I, K, Λ, M, N, Ξ and O are parameters related to anisotropy stress expression showed below:

$$\begin{array}{llll} A = (k-m), & B = 2m, & \Gamma = \mathcal{L}, & \Delta = 2(p-m) \\ E = \mathcal{L}_2, & Z = \mathcal{A} + 4m, & H = \mathcal{B}, & \Theta = 2(\mathcal{B} - 2m + k) \\ I = \mathcal{C} - k + m, & K = \mathcal{D}, & \Lambda = \mathcal{E}, & M = \mathcal{F} \\ N = \mathcal{G}, & \Xi = \mathcal{H}, & O = \mathcal{I} & \end{array} \tag{5.98}$$

Once, specified constitutive anisotropic nonlinear third order law, two cases are considered, on one hand the case of uniaxial stress in direction 1 where all strains are different and on the other hand the case of uniaxial stress in direction 3 for the same strains in directions 1 and 2.

Case of uniaxial stress in direction 1, and all strains different

Case one of trasversally isotropic media occurs when $\sigma_{11} \neq 0, \sigma_{22} = 0, \sigma_{33} = 0$ and $\varepsilon_{11} \neq \varepsilon_{22} \neq \varepsilon_{33}$. Firstly, $\sigma_{11} \neq 0, \sigma_{22} = 0, \sigma_{33} = 0$ restriction is assumed. Then, constitutive nonlinear anisotropic law takes the next form,

$$\begin{aligned} \sigma_{11} &= (A+B)\varepsilon_{11} + A\varepsilon_{22} + (A+E)\varepsilon_{33} + (Z+H)\varepsilon_{11}^2 + 2H(\varepsilon_{22}^2 + \varepsilon_{33}^2) + (K+\Lambda)\varepsilon_{33}^2 \\ &\quad + \Theta\varepsilon_{11}(\varepsilon_{11} + \varepsilon_{22} + \varepsilon_{33}) + I(\varepsilon_{11} + \varepsilon_{22} + \varepsilon_{33})^2 \\ 0 &= A\varepsilon_{11} + (A+B)\varepsilon_{22} + (A+E)\varepsilon_{33} + (Z+H)\varepsilon_{22}^2 + 2H(\varepsilon_{11}^2 + \varepsilon_{33}^2) + (K+\Lambda)\varepsilon_{33}^2 \\ &\quad + \Theta\varepsilon_{22}(\varepsilon_{11} + \varepsilon_{22} + \varepsilon_{33}) + I(\varepsilon_{11} + \varepsilon_{22} + \varepsilon_{33})^2 \\ 0 &= (A+E)\varepsilon_{11} + (A+E)\varepsilon_{22} + (A+B+\Gamma+2\Delta+2E)\varepsilon_{33} \\ &\quad + (Z+H+\Theta+K+3\Lambda+2M+2K+3N+3E+3\Xi+3O+\Gamma+2\Delta)\varepsilon_{33}^2 \\ &\quad + 2H(\varepsilon_{11}^2 + \varepsilon_{22}^2) + (\Theta+2M-E+2K-\Gamma+2(\Lambda+E-\Delta))(\varepsilon_{11}+\varepsilon_{22})\varepsilon_{33} \\ &\quad + (I+M-E)(\varepsilon_{11}+\varepsilon_{22}+\varepsilon_{33})^2 \end{aligned} \tag{5.99}$$

and when $\varepsilon_{11} \neq \varepsilon_{22} \neq \varepsilon_{33}$, only linear terms are retained for substitution, since quadratic terms will generate vanish higher order terms,

$$\varepsilon_{33} = -\frac{A\varepsilon_{11} + (A+B)\varepsilon_{22}}{A+E} \tag{5.100}$$

$$\varepsilon_{22} = \frac{(A+E)^2 - A(A+B+\Gamma+2\Delta+2E)}{-(A+E)^2 + (A+B)(A+B+\Gamma+2\Delta+2E)}\varepsilon_{11} \tag{5.101}$$

Finally, constitutive law in one dimension for this first case is derived as follows,

$$\sigma_{11} = B(1-X)\varepsilon_{11} + \left(Z + H + 2HX^2 + (K + \Lambda + 1)\left(\frac{A + (A+B)X}{A+E}\right)^2 \right)\varepsilon_{11}^2 + \left(\Theta\left(1 + X + \frac{A + (A+B)X}{A+E}\right) + I\left(1 + X + \frac{A + (A+B)X}{A+E}\right)^2 \right)\varepsilon_{11}^2 \tag{5.102}$$

where $X = \frac{(A+E)^2 - A(A+B+\Gamma+2\Delta+2E)}{-(A+E)^2 + (A+B)(A+B+\Gamma+2\Delta+2E)}$.
The acoustic nonlinearity is measured by comparing the stress and strain in one direction, in our case for the direction 1. In order to define the acoustic β_H, the terms of stress that depend linearly and quadratically on the strain are grouped as,

$$\sigma_{11} = E_*(1 - \beta\varepsilon_{11})\varepsilon_{11} \tag{5.103}$$

where E_* is the young modulus. The acoustic nonlinearity parameter β_H is therefore derived to be,

$$\beta_H = -\frac{\left(Z + H + 2HX^2 + (K + \Lambda + 1)\left(\frac{A+(A+B)X}{A+E}\right)^2 \right)}{B(1-X)} - \frac{\left(\Theta\left(1 + X + \frac{A+(A+B)X}{A+E}\right) + I\left(1 + X + \frac{A+(A+B)X}{A+E}\right)^2 \right)}{B(1-X)} \tag{5.104}$$

and after the application of conversion given in the Equation (44), the next expression is obtained,

$$\beta_H = -\frac{\left(\mathcal{A} + 4m + \mathcal{B} + 2\mathcal{B}X^2 + (\mathcal{D} + \mathcal{E} + 1)\left(\frac{(k-m)+(k+m)X}{k-m+\mathcal{L}_2}\right)^2 \right)}{m(1-X)} - \frac{\left(2(\mathcal{B} - 2m + k)\left(1 + X + \frac{k-m+(k+m)X}{k-m+\mathcal{L}_2}\right) + (\mathcal{C} - k + m)\left(1 + X + \frac{k-m+(k+m)X}{k-m+\mathcal{L}_2}\right)^2 \right)}{m(1-X)} \tag{5.105}$$

where $X = \frac{(k-m+\mathcal{L}_2)^2 - (k-m)(k+\mathcal{L}_1+4(p-m)+2\mathcal{L}_2)}{-(k-m+\mathcal{L}_2)^2 + (k+m)((k+m)+\mathcal{L}_1+4(p-m)+2\mathcal{L}_2)}$

5.10.1 Case of uniaxial stress in direction 3, and equal strains in directions 1 and 2

The case two of transversally isotropic media is considered now and it occurs when $\sigma_{11} = 0, \sigma_{22} = 0, \sigma_{33} \neq 0$ and $\varepsilon_{11} = \varepsilon_{22} \neq \varepsilon_{33}$. Firstly, constitutive nonlinear law under $\sigma_{11} = 0, \sigma_{22} = 0, \sigma_{33} \neq 0$ condition is assumed as follows,

$$
\begin{aligned}
0 &= (A+B)\varepsilon_{11} + A\varepsilon_{22} + (A+E)\varepsilon_{33} + (Z+H)\varepsilon_{11}^2 + 2H(\varepsilon_{22}^2+\varepsilon_{33}^2) + (K+\Lambda)\varepsilon_{33}^2 \\
&\quad + \Theta\varepsilon_{11}(\varepsilon_{11}+\varepsilon_{22}+\varepsilon_{33}) + I(\varepsilon_{11}+\varepsilon_{22}+\varepsilon_{33})^2 \\
0 &= A\varepsilon_{11} + (A+B)\varepsilon_{22} + (A+E)\varepsilon_{33} + (Z+H)\varepsilon_{22}^2 + 2H(\varepsilon_{11}^2+\varepsilon_{33}^2) + (K+\Lambda)\varepsilon_{33}^2 \\
&\quad + \Theta\varepsilon_{22}(\varepsilon_{11}+\varepsilon_{22}+\varepsilon_{33}) + I(\varepsilon_{11}+\varepsilon_{22}+\varepsilon_{33})^2 \\
\sigma_{33} &= (A+E)\varepsilon_{11} + (A+E)\varepsilon_{22} + (A+B+\Gamma+2\Delta+2E)\varepsilon_{33} \\
&\quad + (Z+H+\Theta+K+3\Lambda+2M+2K+3N+3E+3\Xi+3O+\Gamma+2\Delta)\varepsilon_{33}^2 \\
&\quad + 2H(\varepsilon_{22}^2+\varepsilon_{11}^2) + (\Theta+2M-E+2K-\Gamma+2(\Lambda+E-\Delta))(\varepsilon_{11}+\varepsilon_{22})\varepsilon_{33} \\
&\quad + (I+M-E)(\varepsilon_{11}+\varepsilon_{22}+\varepsilon_{33})^2
\end{aligned}
\tag{5.106}
$$

and when $\varepsilon_{11} = \varepsilon_{22} \neq \varepsilon_{33}$, the previous Equation 5.106 takes this form,

$$
\begin{aligned}
0 &= (2A+B)\varepsilon_{11} + (A+E)\varepsilon_{33} + (Z+2H)\varepsilon_{11}^2 + H\varepsilon_{33}^2 + \Theta\varepsilon_{11}(2\varepsilon_{11}+\varepsilon_{33}) \\
&\quad + I(2\varepsilon_{11}+\varepsilon_{33})^2 \\
0 &= (2A+B)\varepsilon_{11} + (A+E)\varepsilon_{33} + (Z+2H)\varepsilon_{11}^2 + HE_{33}^2 + \Theta E_{11}(2\varepsilon_{11}+\varepsilon_{33}) \\
&\quad + I(2\varepsilon_{11}+\varepsilon_{33})^2 \\
\sigma_{33} &= 2(A+E)\varepsilon_{11} + (A+B+\Gamma+2\Delta+2E)\varepsilon_{33} \\
&\quad + (Z+H+\Theta+K+3\Lambda+2M+2K+3N+3E+3\Xi+3O+\Gamma+2\Delta)\varepsilon_{33}^2 \\
&\quad 2H\varepsilon_{11}^2 + (\Theta+2M-E+2K-\Gamma+2(\Lambda+E-\Delta))(2\varepsilon_{11})\varepsilon_{33} \\
&\quad + (I+M-E)(2\varepsilon_{11}+\varepsilon_{33})^2
\end{aligned}
\tag{5.107}
$$

The acoustic nonlinearity is measured by comparing the stress and strain in one direction, (in our case the x_3-direction). In order to define the acoustic β, the terms of stress that depend linearly and quadratically on the strain are grouped as,

$$
\varepsilon_{11} = -\frac{A+E}{2A+B}\varepsilon_{33} \tag{5.108}
$$

Then, the nonlinear anisotropic constitutive in 3-direction, is derived as follows,

$$
\begin{aligned}
\sigma_{33} &= -\left(2(A+E)\frac{A+E}{2A+B} + A + B + \Gamma + 2\Delta + 2E\right)\varepsilon_{33} \\
&\quad + (Z+H+\Theta+K+3\Lambda+2M+2K+3N+3E+3\Xi+3O+\Gamma+2\Delta)\varepsilon_{33}^2 \\
&\quad - 2H\frac{A+E}{2A+B}\varepsilon_{33}^2 - 2(\Theta+2M-E+2K-\Gamma+2(\Lambda+E-\Delta))\frac{A+E}{2A+B}E_{33}^2 \\
&\quad + (I+M-E)\left(-2\frac{A+E}{2A+B}+1\right)\varepsilon_{33}^2
\end{aligned}
\tag{5.109}
$$

and the acoustic nonlinear first parameter β_H is therefore derived to be,

$$\begin{aligned}\beta_H = & \frac{(Z+H+\Theta+K+3\Lambda+2M+2K+3N+3E+3\Xi+3O+\Gamma+2\Delta)}{\left(2(A+E)\frac{A+E}{2A+B}+A+B+\Gamma+2\Delta+2E\right)} \\ & - \frac{2H\frac{A+E}{2A+B}}{\left(2(A+E)\frac{A+E}{2A+B}+A+B+\Gamma+2\Delta+2E\right)} \\ & - \frac{2(\Theta+2M-E+2K-\Gamma+2(\Lambda+E-\Delta))\frac{A+E}{2A+B}}{\left(2(A+E)\frac{A+E}{2A+B}+A+B+\Gamma+2\Delta+2E\right)} \\ & + \frac{(I+M-E)\left(-2\frac{A+E}{2A+B}+1\right)}{\left(2(A+E)\frac{A+E}{2A+B}+A+B+\Gamma+2\Delta+2E\right)}\end{aligned} \tag{5.110}$$

By making use of conversion related to Equation 5.98 is possible to deduce that,

$$\begin{aligned}\beta_H = & \frac{\mathcal{A}+4m+\mathcal{B}+2(\mathcal{B}-2m+k)+\mathcal{D}+3\mathcal{E}+2\mathcal{F}+2\mathcal{D}+3\mathcal{G}}{2(k-m+\mathcal{L}_2)\frac{k-m+\mathcal{L}_2}{2(k-m)+2m}+k+m+\mathcal{L}_1+4(p-m)+2\mathcal{L}_2} \\ & + \frac{3\mathcal{L}_2+3\mathcal{H}+3\mathcal{I}+\mathcal{L}_1+4(p-m)}{2(k-m+\mathcal{L}_2)\frac{k-m+\mathcal{L}_2}{2(k-m)+2m}+k+m+\mathcal{L}_1+4(p-m)+2\mathcal{L}_2} \\ & - \frac{2\mathcal{B}\frac{k-m+\mathcal{L}_2}{2(k-m)+2m}}{2((k-m)+\mathcal{L}_2)\frac{k-m+\mathcal{L}_2}{2(k-m)+2m}+k+m+\mathcal{L}_1+4(p-m)+2\mathcal{L}_2} \\ & - \frac{2(2(\mathcal{B}-2m+k)+2\mathcal{F}-\mathcal{L}_2+2\mathcal{D}-\mathcal{L}_1+2(\mathcal{E}+\mathcal{L}_2-2(p-m)))\frac{k-m+\mathcal{L}_2}{2(k-m)+2m}}{2(k-m+\mathcal{L}_2)\frac{k-m+\mathcal{L}_2}{2(k-m)+2m}+k+m+\mathcal{L}_1+4(p-m)+2\mathcal{L}_2} \\ & + \frac{((\mathcal{C}-k+m)+\mathcal{F}-\mathcal{L}_2)\left(-2\frac{k-m+\mathcal{L}_2}{2(k-m)+2m}+1\right)}{2(k-m+\mathcal{L}_2)\frac{k-m+\mathcal{L}_2}{2(k-m)+2m}+k+m+\mathcal{L}_1+4(p-m)+2\mathcal{L}_2}\end{aligned} \tag{5.111}$$

Furthermore, two anisotropic cases have been analytically derived and linked to the nonlinear acoustic parameter β_H by a relationship based on constitute law. The next subsection shows a numerical validation for both isotropic and anisotropy material of this formulation.

Numerical example for transversally isotropic cases

The consistency of the obtained formulation is validated by numerical evaluations of the stress-strain curves for a set of realistic materials and setups. The obtained formulation for acoustic nonlinearity is validated for realistic cases, where some of the constants are known, whereas others are just invented for the sake of simulating realistic stress-strain curves, using the nonlinear Landau formulation versus the acoustic nonlinearity expression derived herein. First, the isotropic case is tested for a Polymethylmethacrylate (PMMA) material whose Young's modulus E_* is between 1800 and 3100 [MPa] and whose Poisson's ratio ν ranges between 0.35 and 0.4 (see Figure 2). As the coefficients $\mathcal{A}$, $\mathcal{B}$ and $\mathcal{C}$ have never been measured experimentally in the case of CFRP. However, the acoustic nonlinear coefficient β_H for this material typically varies in the range between 12 and 15 [31], and

hence, coefficients $\mathcal{A}$, $\mathcal{B}$ and $\mathcal{C}$ are assigned assumed values compatible with β_H (see figure 3). Furthermore, for the conversion of m and k variables depending on elastic constants, the following relationships are obtained,

$$m = \frac{E_*}{-3(1-2\nu)}, \qquad k = \frac{E_*}{-3(1-2\nu)^2} \tag{5.112}$$

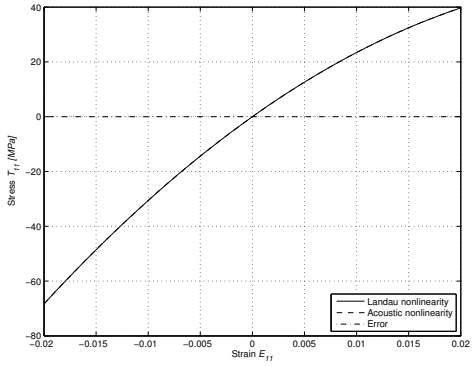

Figure 5.2: Landau acoustic example for isotropic case

Transversally isotropic cases has been validated using carbon fiber material whose Young's modulus and Poisson's ratio depends on direction E_{*i} and ν_i, respectively. As the coefficients $\mathcal{A}$, $\mathcal{B}$, $\mathcal{C}$, $\mathcal{D}$, $\mathcal{E}$, $\mathcal{F}$, $\mathcal{G}$, $\mathcal{H}$ and $\mathcal{I}$ have never been measured experimentally, to the knowledge of the authors, simulated values were simulated computationally with a nonlinear acoustic β_H assumed. Furthermore, for the conversion of values m, k, l, n and p depending on elastic constants, we obtained:

$$\begin{aligned} m &= \frac{Q_{11}-Q_{12}}{2}, & k &= \frac{Q_{11}+Q_{12}}{2}, & l &= Q_{13} \\ n &= Q_{33}, & p &= Q_{44} \end{aligned} \tag{5.113}$$

where,

$$\begin{aligned} Q_{11} &= \frac{E_{*11}(1-\nu_{23}\nu_{32})}{\nabla}, & Q_{12} &= \frac{E_{*11}(\nu_{21}+\nu_{31}\nu_{23})}{\nabla}, \\ Q_{13} &= \frac{E_{*11}(\nu_{31}+\nu_{21}\nu_{32})}{\nabla}, & Q_{33} &= \frac{E_{*33}(1-\nu_{12}\nu_{21})}{\nabla}, \\ Q_{44} &= G_{23} = \frac{E_{*23}}{2(1+\nu_{23})} \end{aligned} \tag{5.114}$$

are related to the stiffness matrix usually noted by Q_{ij} in composites materials where $\nabla = 1-\nu_{12}\nu_{21}-\nu_{23}\nu_{32}-\nu_{13}\nu_{31}-2\nu_{21}\nu_{32}\nu_{13}$. They have been deducted experimentally by the rule of mixtures method. It assumes that the modulus of a composite is the combination of the modulus of the fiber and the matrix that are related by the volume fraction of the

constituent materials [240, 241].

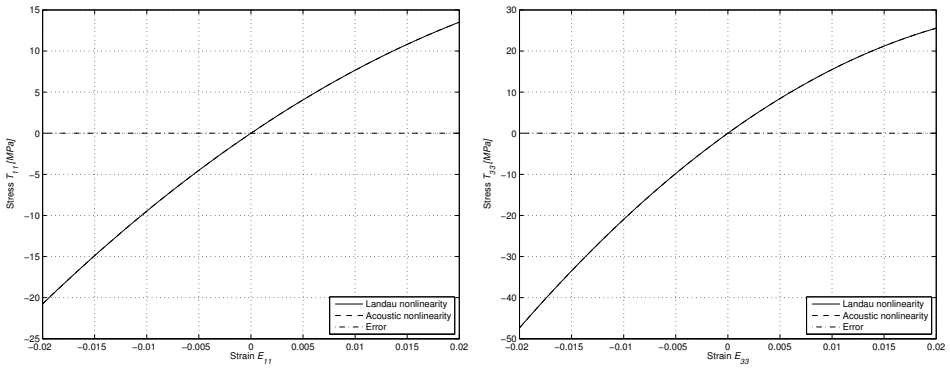

Figure 5.3: Landau acoustic example for transversally isotropic cases

Figure 5.3 shows stress-strain relationship with two anisotropy directions cases 11 and 33 using Third Order Elastic Contants and β_H nonlinear acoustic parameter as is extracted in Equations 5.105 and 5.111. Note that the values of Third Order Elastic Constants have been simulated computationally. Table 5.6 shows mechanical properties as Young modulus and Poisson coefficient for isotropic (PMMA material) and transversally isotropic cases (CFRP T300 N5208). Also, Third Order Elastic Constants and beta nonlinear acoustic parameter of first order is calculated computationally in both cases.

Properties/ Material	Ispotropy PMMA	Anisotropy CFRP T300 N5208 (2.1.)	Anisotropy CFRP T300 N5208 (2.2.)
Young Modulus [MPa]	2700	-	-
Poisson coefficient	0.384	-	-
β_H	13.247	10.569	14.952
S_{11} [MPa]	-	0.0055	0.0055
S_{12} [MPa]	-	-0.0015	-0.0015
S_{13} [MPa]	-	-0.0015	-0.0015
S_{33} [MPa]	-	0.0971	0.0971
S_{44} [MPa]	-	0.1395	0.1395
$\mathcal{A}$	22866	7450	73
$\mathcal{B}$	-34299	-2990	-2990
$\mathcal{C}$	-57165	-3850	-3850
$\mathcal{D}$	-	-40000	43080
$\mathcal{E}$	-	-10000	-10000
$\mathcal{F}$	-	1000	1000
$\mathcal{G}$	-	-1000	-1000
$\mathcal{H}$	-	1000	1000
$\mathcal{I}$	-	10000	10000

Table 5.6: Numerical example parameters

Note that $\mathbf{S}^*$, or S^*_{ij} is the compliance matrix, by making use of $\mathbf{Q} = \mathbf{S}^{*-1}$ relationship, Q_{ij} coefficient have been deduced introducing Equation 5.114 into Equations 5.105 and 5.111.

5.10.2 Isotropic derivation to fourth order elastic constants

It is possible to derive strain energy until fourth order, for macroscopically isotropic material based on a combination of invariants, just introducing $I_6 = \mathrm{tr}\mathbf{E}^4$, or $I_6 = \varepsilon_{ij}\varepsilon_{ik}\varepsilon_{kp}\varepsilon_{pi}$, in the same manner that it has been developed in the previous subsection. (For more details about derivation rules, see Appendix B).

$$W_I = \frac{\lambda}{2}I_1 + \mu I_2 + \frac{\mathcal{A}}{3}I_3 + \mathcal{B}I_1I_2 + \frac{\mathcal{C}}{3}I_3^3 + \frac{\mathcal{J}}{4}I_6 + \mathcal{K}I_1I_3 + \frac{\mathcal{L}}{4}I_2^2 + \frac{\mathcal{M}}{2}I_1^2I_2 + \frac{\mathcal{N}}{4}I_1^4 + ... \quad (5.115)$$

It must be noted that anisotropic terms are neglected in this step, by making use of asymptotic methodology which retain all third order (cubic terms). Via Equation 4.2 we can obtain the expansions,

$$\begin{aligned}
\mathbf{F} &= \mathbf{I} + \mathbf{E} - \frac{1}{2}\mathbf{E}^2 + O(\mathbf{E}^3),\\
\mathbf{F}^T &= \mathbf{I} + \mathbf{E} - \frac{1}{2}\mathbf{E}^2 + O(\mathbf{E}^3),\\
&\text{or}\\
F_{ij} &= \delta_{ij} + \varepsilon_{ij} - \frac{1}{2}\varepsilon_{ij}\varepsilon_{jk} + O(\varepsilon_{ij}\varepsilon_{jk}\varepsilon_{kl}),\\
F_{ji} &= \delta_{ij} + \varepsilon_{ij} - \frac{1}{2}\varepsilon_{ij}\varepsilon_{jk} + O(\varepsilon_{ij}\varepsilon_{jk}\varepsilon_{kl})
\end{aligned} \quad (5.116)$$

and thus from this we find that,

$$\begin{aligned}
&\mathrm{tr}\mathbf{F} = 3 + \mathrm{tr}\mathbf{E} - \frac{1}{2}\mathrm{tr}\mathbf{E}^2, \qquad \mathrm{tr}(\mathbf{F}^2) = 3 + 2\mathrm{tr}\mathbf{E}, \qquad \mathrm{tr}(\mathbf{F}^3) = 3 + 3\mathrm{tr}\mathbf{E} + \frac{3}{2}\mathrm{tr}\mathbf{E}^2,\\
&\text{or}\\
&F_{kk} = 3 + \varepsilon_{kk} - \frac{1}{2}\varepsilon_{ij}\varepsilon_{ji}, \qquad F_{ij}F_{ji} = 3 + 2\varepsilon_{kk}, \qquad F_{ij}F_{jk}F_{ki} = 3 + 3\varepsilon_{kk} + \frac{3}{2}\varepsilon_{ij}\varepsilon_{ji},
\end{aligned} \quad (5.117)$$

and

$$\begin{aligned}
\det\mathbf{F} &= \frac{1}{6}[6 + 6\mathrm{tr}\mathbf{E} + 3(\mathrm{tr}\mathbf{E})^2 - \frac{3}{2}\mathrm{tr}\mathbf{E}^2 + O(\mathbf{E}^3)]\\
&\text{or}\\
\det F_{ij} &= \frac{1}{6}[6 + 6\varepsilon_{kk} + 3\varepsilon_{kk}^2 - \frac{3}{2}\varepsilon_{ij}\varepsilon_{ji} + O(\varepsilon_{ij}\varepsilon_{jk}\varepsilon_{kl})]
\end{aligned} \quad (5.118)$$

Under these condition, the constitutive equation extended to FOEC (Fourth Order Elastic Constants), by making use of Cauchy stress definition in Equation 4.10, it has been assumed in the next form,

$$\mathbf{T} = \mathbf{T}^{L1} + \mathbf{T}^{NL1} + \mathbf{T}^{NL3} \tag{5.119}$$

where $\mathbf{T}^{NL3}$ has been noted with the index 3 to be differentiated from $\mathbf{T}^{NL2}$ in Equation 5.96 related to anisotropic nonlinear part of stress.

$$\begin{aligned}
\mathbf{T} &= \lambda \mathrm{tr}\mathbf{E}\mathbf{I} + 2\mu\mathbf{E} + \tilde{\mathcal{A}}\mathbf{E}^2 + 2\tilde{\mathcal{B}}\mathrm{tr}\mathbf{E}\mathbf{E} + \mathcal{B}\mathrm{tr}(\mathbf{E})^2 + \tilde{\mathcal{C}}(\mathrm{tr}\mathbf{E})^2 \\
&\quad + \tilde{\mathcal{J}}\mathbf{E}^3 + \mathcal{K}\mathrm{tr}(\mathbf{E}^3\mathbf{I} + \tilde{\mathcal{K}}\mathbf{E}^2\mathrm{tr}\mathbf{E}) + \tilde{\mathcal{L}}(\mathbf{E}\mathrm{tr}(\mathbf{E}^2)) \\
&\quad + \tilde{\mathcal{M}}_1\mathrm{tr}\mathbf{E}\mathbf{I}\mathrm{tr}(\mathbf{E})^2 + \tilde{\mathcal{M}}_2(\mathrm{tr}\mathbf{E})^2\mathbf{E}) + \tilde{\mathcal{N}}(\mathrm{tr}\mathbf{E})^3, \\
&\quad \text{or} \\
\sigma_{ij} &= \lambda\varepsilon_{kk}\delta_{ij} + 2\mu\varepsilon_{ij} + \tilde{\mathcal{A}}\varepsilon_{ij}\varepsilon_{jk} + 2\tilde{\mathcal{B}}\varepsilon_{kk}\varepsilon_{ij} + \mathcal{B}\varepsilon_{ij}\varepsilon_{ji} + \tilde{\mathcal{C}}\varepsilon_{kk}^2 \\
&\quad + \tilde{\mathcal{J}}\varepsilon_{ij}\varepsilon_{jk}\varepsilon_{jp} + \mathcal{K}\varepsilon_{ij}\varepsilon_{jk}\varepsilon_{ki})\delta_{ij} + \tilde{\mathcal{K}}\varepsilon_{ij}\varepsilon_{jk}\varepsilon_{kk}) + \tilde{\mathcal{L}}\varepsilon_{ij}\varepsilon_{ij}\varepsilon_{ji} \\
&\quad + \tilde{\mathcal{M}}_1\varepsilon_{kk}\delta_{ij}\varepsilon_{ij}\varepsilon_{ji}) + \tilde{\mathcal{M}}_2(\varepsilon_{kk})^2\varepsilon_{ij} + \tilde{\mathcal{N}}(\varepsilon_{kk})^3.
\end{aligned} \tag{5.120}$$

where $\tilde{\mathcal{J}} = \mathcal{J} + 2\mathcal{A} + \mu$, $\tilde{\mathcal{K}} = 3\mathcal{K} - \mathcal{A} + 4\mathcal{B} - 4\mu + \frac{\lambda}{2}$, $\tilde{\mathcal{L}} = \mathcal{L} + 2\mathcal{B} - \frac{\mu}{2}$, $\tilde{\mathcal{M}}_1 = \mathcal{M} - \mathcal{B} - \frac{\lambda}{4}$, $\tilde{\mathcal{M}}_2 = \mathcal{M} - 2\mathcal{B} + 2\mathcal{C} + \mu - 2\lambda$ and $\tilde{\mathcal{N}} = \mathcal{N} + \mathcal{C} - \frac{\lambda}{2}$ are referred to nonlinear constants extracted to Taylor expansion of the strain energy up to fourth order, see Equation 5.115 above. We have noted that $\mathbf{T}^L$ and $\mathbf{T}^{NL1}$ retain the same coefficients that Equation 4.10.

If we consider $\sigma_{11} \neq 0$ and $\varepsilon_{22} = \varepsilon_{33} = 0$ since $u_2 = u_3 = 0$ the case of wave propagation in one direction neglecting strain in directions 2 and 3, Equation 5.120 stated as,

$$\begin{aligned}
\sigma_{11} &= \lambda\varepsilon_{11} + 2\mu\varepsilon_{11} + \tilde{\mathcal{A}}\varepsilon_{11}^2 + 2\tilde{\mathcal{B}}\varepsilon_{11}^2 + \mathcal{B}\varepsilon_{11}^2 + \tilde{\mathcal{C}}\varepsilon_{11}^2 \\
&\quad + \tilde{\mathcal{J}}\varepsilon_{11}^3 + \mathcal{K}\varepsilon_{11}^3 + \tilde{\mathcal{K}}\varepsilon_{11}^3 + \tilde{\mathcal{L}}\varepsilon_{11}^3 \\
&\quad + \tilde{\mathcal{M}}_1\varepsilon_{11}^3 + \tilde{\mathcal{M}}_2\varepsilon_{11}^3 + \tilde{\mathcal{N}}\varepsilon_{11}^3.
\end{aligned} \tag{5.121}$$

Thus, by making use of the Equations 5.2, the nonlinear wave equation up to third order in terms of nonlinear elastic constants results as follows,

$$\begin{aligned}
\sigma_{11,1} &= (\lambda + 2\mu)u_{1,11} + 2\left(\frac{\lambda + 2\mu}{2} + \tilde{\mathcal{A}} + 2\tilde{\mathcal{B}} + \mathcal{B} + \tilde{\mathcal{C}}\right)u_{1,11}u_{1,1} \\
&\quad + 3(\tilde{\mathcal{A}} + 2\tilde{\mathcal{B}} + \mathcal{B} + \tilde{\mathcal{C}} + \tilde{\mathcal{J}} + \mathcal{K} + \tilde{\mathcal{K}} + \tilde{\mathcal{L}} + \tilde{\mathcal{M}}_1 + \tilde{\mathcal{M}}_2 + \tilde{\mathcal{N}})u_{1,1}^2u_{1,11}.
\end{aligned} \tag{5.122}$$

Furthermore, we can conclude that the relationship between nonlinearity of second order δ given by Equation 5.20 and nonlinear elastic constants up to fourth order is given by the next expression,

$$\delta = \frac{\tilde{\mathcal{A}} + 2\tilde{\mathcal{B}} + \mathcal{B} + \tilde{\mathcal{C}} + \tilde{\mathcal{J}} + \mathcal{K} + \tilde{\mathcal{K}} + \tilde{\mathcal{L}} + \tilde{\mathcal{M}}_1 + \tilde{\mathcal{M}}_2 + \tilde{\mathcal{N}}}{\lambda + 2\mu} \tag{5.123}$$

It must be noted that we have no found any reference or method where experimental or simulated values have been taken into account for the case of FOEC. We consider that it could be interesting to investigate physical values and relationship with structure of matter of all these parameters that was suggested firstly by Konyukhov in 1974 [242].

6

Classical nonlinear acoustics genesis: Fluid and matrix phases

The present theoretical proposals on nonlinear serial developments has helped to understand many nonlinear experimental phenomena. But new approaches can better interpret some others. This Chapter proposes deepening on the study of classical nonlinear acoustics, splitting the general first order nonlinearity into four specific nonlinear phenomena (measured with four new nonlinear constants), due to the interaction of the deviatoric and volumentric components of the deformation tensor with the wave mode, P or S. For instance, this can be useful to explain nonlinear propagation in materials constituted by two phases, as solid fibers embedded in a quasi-fluid matrix. This is the case of some tissues, where the propagation of shear waves in the liquid phase can be neglected against the solid propagation.

Fluids are composed of molecules that collide with one another and solid objects. The continuum assumption, however, considers properties such as density, pressure, temperature, and velocity to vary continuously from one point to another, and are averaged values over a REV (Reference Element of Volume), at the geometric order of the distance between two adjacent molecules of fluid. Solid and fluid materials are assumed to coexist at non-intersecting subdomains (phases) of the system. Solids will undergo not small deformations, due to the harmonic generation interest of this hypothesis, whereas fluids will flow as they are unable to withstand static shear stress. In this Chapter, the nonlinear acoustic theory will be rewrite in the common notation from linear elasticity governing equations in the case of isotropy and classical material.

6.1 Solid phase

Small deformations are not assumed, and plastic flow neglected, which leads to the linear elasticity governing equations that relate the quantities in Table 6.1.

Quantity	Symbol	Units
Displacement	u_i	m
Velocity	$v_i = \dot{u}_i = \frac{du_i}{dt}$	m/s
Stress	σ_{ij}	Pa
Strain	ε_{ij}	-
Body force	b_i	N/m^3
Space	x_i	m
Time	t	s
Lamé constants	λ, μ	Pa
Density	ρ	kg/m^3
Kinematic viscosity	$\gamma = \frac{\eta}{\rho}$	s^{-1}

Table 6.1: Variables in fluid mechanics

Equilibrium

$$\rho\ddot{u}_i + \gamma\rho\dot{u}_i = b_i + \sigma_{ij,j} \tag{6.1}$$

Compatibility

$$\varepsilon_{ij} = \frac{1}{2}(u_{i,j} + u_{j,i} + u_{k,i}u_{k,j}) \tag{6.2}$$

Constitutive

General case and non linear isotropic case adding viscosity terms as σ_{ij}^L, σ_{ij}^{NL}, and σ_{ij}^V respectively :

$$\sigma_{ij} = \sigma_{ij}^L + \sigma_{ij}^V + \sigma_{ij}^{NL} \tag{6.3}$$

If we develop the equation described above, introducing Third Order Elastic Constants in the Landau form, calculating from Cauchy stress, as in Chapter 4, it results,

$$\begin{aligned}\sigma_{ij} = &\underbrace{\lambda\delta_{ij}\varepsilon_{kk} + 2\mu\varepsilon_{ij}}_{\sigma^L} + \underbrace{2\eta\dot{\varepsilon}_{ij} - \frac{2}{3}\eta\delta_{ij}\dot{\varepsilon}_{kk} + \eta^v\delta_{ij}\dot{\varepsilon}_{kk}}_{\sigma^V} \\ &+ \underbrace{(\mathcal{A}+4\mu)\varepsilon_{ik}\varepsilon_{kj} + \mathcal{B}\varepsilon_{kp}\varepsilon_{pk}\delta_{ij} + 2(\mathcal{B}+\lambda-\mu)\varepsilon_{kk}\varepsilon_{ij} + (\mathcal{C}-\lambda)\varepsilon_{kk}^2\delta_{ij}}_{\sigma^{NL}}\end{aligned} \tag{6.4}$$

The solid and fluid constitutive equations can be derived as particular cases of the following general form, which, after being decomposed into volumetric and deviatoric constituents, each of them depends on the strain ε_{ij} (elastic component predominant in solids) and the strain rate $\dot{\varepsilon}_{ij}$ (viscous component predominant in fluids) [243],

$$\sigma_{ij} = \underbrace{-p\delta_{ij}}_{\text{volumetric}} + \underbrace{\tau_{ij}}_{\text{deviatoric}}, \; p = -\frac{1}{3}\sigma_{kk} \tag{6.5}$$

$$-p = -3Kv - 3\eta^v \dot{v} \tag{6.6}$$

$$\tau_{ij} = 2\mu D_{ij} + 2\eta \dot{D}_{ij} \tag{6.7}$$

where any tensor is split into volumetric (scalar) and deviatoric (tensor) parts by,

$$\varepsilon_{ij} = -v\delta_{ij} + D_{ij}, \quad v = -\frac{1}{3}\varepsilon_{kk} \tag{6.8}$$

Note that a pure fluid, by definition, can withstand no static shear stress, i.e. $\mu = 0$, which, after substitution yields the Fluid Constitutive Equation 6.7. Similarly, the elastic Constitutive Equation 6.3 is recovered by recalling that the compressibility modulus is related to $K = \lambda + \frac{2}{3}\mu = \rho c^2$ and relating (to be derived) a compound shear and volumetric viscosity with the damping, recalling that Kinematic viscosity ν are related to Dynamic viscosity η by the relation $\nu = \frac{\eta}{\rho}$. The attenuation (excluding scattering) α is related to viscosity by Stokes' law (modified to account for volumetric viscosity),

$$\alpha = \frac{\omega^2}{\rho c^3}\left(\frac{2}{3}\eta + \frac{1}{2}\eta^v\right) \tag{6.9}$$

The linear elastic solid constitutive equation $\sigma_{ij} = \lambda\varepsilon_{kk}\delta_{ij} + 2\mu\varepsilon_{ij}$ is recovered by neglecting nonlinear terms ans viscosity.

Microviscosity, also known as microscopic viscosity, is the friction experienced by a single particle undergoing diffusion because of its interaction with its environment at the micrometer length scale. In the field of biophysics, a typical microviscosity problem is understanding how a biomolecule's mobility is hindered within a cellular compartment which will depend upon size, shape, charge, quantity and density of both the diffusing particle and all members of its environment [244, 245].

6.1.1 Nonlinear constitutive equation

Following the series expansion concept put forth by Landau [1], only volumetric part is detailed in terms of the nonlinear parameter β,

$$-p = -3Kv + 9K\beta v^2 - 3\eta^v \dot{v}. \tag{6.10}$$

However, there is five combinations of nonlinear parameters β that may explain a different scenario of experimental calculations. These combinations could be expanded as exploring the whole set of combinations by quadratic terms as follows,

$$\sigma_{ij} = \underbrace{\underbrace{-3Kv\delta_{ij}}_{\text{pressure}} + \underbrace{2\mu D_{ij}}_{\text{shear}}}_{\sigma_{ij}^{L}\ (Linear)} \underbrace{\underbrace{-3\eta^{v}\dot{v}\delta_{ij}}_{\text{pressure}} + \underbrace{2\eta\dot{D}_{ij}}_{\text{shear}}}_{\sigma_{ij}^{V}\ (Viscous)} \tag{6.11}$$

$$\underbrace{\underbrace{+9K\beta^{vp}v^2\delta_{ij} + 9K\beta^{dp}D_{kp}D_{pk}\delta_{ij}}_{\text{pressure}} + \underbrace{4\mu\beta^{ds}D_{ik}D_{kj} + 4\mu\beta^{cs}vD_{ij}}_{\text{shear}}}_{\sigma_{ij}^{NL}\ (Nonlinear)} \tag{6.12}$$

where v and D_{ij} are the volumetric and deviatoric parts of the stress tensor defined in Equation 6.7. Four nonlinear parameters of first order have been defined as β^{vp}, β^{dp} as the volumetric, the deviatoric and the compound denoting the pressure components and β^{ds}, β^{cs} as the deviatoric, and compound denoting the shear components. Note that the combinations $vD_{kk}\delta_{ij}$ and $(D_{kk})^2\delta_{ij}$ have been neglected due to the definition of D_{ij}, where the deviatoric tensor contains trace equal to zero. The constants in function of K and μ accompanying nonlinear parameters have been chosen in accordance with Equation 9.47, as the quadratic power expansion.

With the aim to find a relationship between this nonlinear expansion of beta parameters and TOEC, we assuming now that the strains are separated in volumetric and deviatoric part to the second order, so ε yields,

$$\begin{aligned}
\varepsilon_{kk} &= -v\delta_{kk} + D_{kk} = -3v \\
\varepsilon_{ik}\varepsilon_{kj} &= v^2\delta_{ik}\delta_{kj} - vD_{ik}\delta_{kj} - vD_{kj}\delta_{ik} + D_{ik}D_{kj} \\
\varepsilon_{ij} &= -v\delta_{ij} + D_{ij} \\
\varepsilon_{kj} &= -v\delta_{kj} + D_{kj} \\
\varepsilon_{kp} &= -v\delta_{kp} + D_{kp} \\
\varepsilon_{pk} &= -v\delta_{pk} + D_{pk} \\
\varepsilon_{kk}^2 &= 9v^2
\end{aligned} \tag{6.13}$$

By making use of Cauchy stress described in Equation 6.7, in nonlinear regime, an equivalence is deducted in terms of Third Order Elastic Constants TOEC,

$$\begin{aligned}
(\mathcal{A}+4\mu)\varepsilon_{ik}\varepsilon_{kj} &= (\mathcal{A}+4\mu)(v^2\delta_{ik}\delta_{kj} - vD_{ik}\delta_{kj} - v\delta_{ik}D_{kj} + D_{ik}D_{kj}) \\
\mathcal{B}\varepsilon_{kp}\varepsilon_{pk}\delta_{ij} &= \mathcal{B}(3v^2 + D_{kp}D_{pk})\delta_{ij} \\
2(\mathcal{B}+\lambda-\mu)\varepsilon_{kk}\varepsilon_{ij} &= 2(\mathcal{B}+\lambda-\mu)(3v^2\delta_{ij} - 3vD_{ij}) \\
(C-\lambda)\varepsilon_{kk}^2\delta_{ij} &= (C-\lambda)9v^2\delta_{ij}
\end{aligned} \tag{6.14}$$

The above analysis is also valid combining nonlinear part of the stress with v and D_{ij} in the constitutive equation,

$$\begin{aligned}\sigma_{ij}^{NL} &= v^2(\mathcal{A}+9\mathcal{B}+9\mathcal{C}-2\mu-3\lambda)\delta_{ij}+D_{ik}D_{kj}(\mathcal{A}+4\mu)+D_{kp}D_{pk}\mathcal{B}\delta_{ij} \\ &\quad +vD_{ij}(-2\mathcal{A}+6\mathcal{B}-6\lambda-2\mu) \end{aligned} \tag{6.15}$$

Since the relationship is established in the nonlinear constitutive equation, nonlinear acoustic parameters of first order are explicitly deducted as follows in terms of Third Order Elastic Constants,

$$\beta^{vp} = \frac{\mathcal{A}+9\mathcal{B}+9\mathcal{C}-2\mu-3\lambda}{9K} \tag{6.16}$$

$$\beta^{dp} = \frac{\mathcal{B}}{9K} \tag{6.17}$$

$$\beta^{ds} = \frac{\mathcal{A}+4\mu}{4\mu} \tag{6.18}$$

$$\beta^{cs} = \frac{-2\mathcal{A}-6\mathcal{B}-2\mu-6\lambda}{4\mu} \tag{6.19}$$

For the viscous components, it is shown that the establish definition in Equation 9.47 matches Landau's one,

$$\begin{aligned} 2\eta\dot{\varepsilon}_{ij} &= 2\eta(-\dot{v}\delta_{ij}+\dot{D}_{ij}) \\ -\frac{2}{3}\eta\dot{\varepsilon}_{kk}\delta_{ij} &= 2\eta\dot{v}\delta_{ij} \\ \eta^v\dot{\varepsilon}_{kk}\delta_{ij} &= -3\eta^v\dot{v}\delta_{ij} \\ \mathbf{T}_V &= -3\eta^v\dot{v}\delta_{ij}+2\eta\dot{D}_{ij}=\sigma_{ij}^V \end{aligned}$$

6.2 Perturbation method

By adopting the acoustic nonlinear constitutive equation presented above Equations 6.7 in terms of deviatoric a volumetric parts, is possible to establish the three dimensional nonlinear equation of motion up to first-order nonlinearity in terms of four parameters β. This formulation, implies that beta parameter is not unique and it can be defined as the separation between pressure and shear waves written as, (See [246]),

$$
\begin{aligned}
\rho\frac{\partial^2 u_i}{\partial t^2} &= K\left(\frac{\partial^2 u_k}{\partial x_k \partial x_i}+\frac{\partial u_l}{\partial x_k}\frac{\partial^2 u_l}{\partial x_k \partial x_i}\right) \\
&+\mu\left(\frac{\partial^2 u_i}{\partial x_j^2}+\frac{\partial^2 u_j}{\partial x_i \partial x_j}+\frac{\partial^2 u_k}{\partial x_j^2}\frac{\partial u_k}{\partial x_i}+\frac{\partial^2 u_k}{\partial x_i \partial x_j}\frac{\partial u_k}{\partial x_j}-\frac{2}{3}\left(\frac{\partial^2 u_k}{\partial x_k \partial x_i}+\frac{\partial u_l}{\partial x_k}\frac{\partial^2 u_l}{\partial x_k \partial x_i}\right)\right) \\
&+2K\beta^{vp}\left(\frac{\partial^2 u_k}{\partial x_k \partial x_i}\frac{\partial u_l}{\partial x_l}\right) \\
&+9K\beta^{dp}\left(\frac{1}{2}\left(\frac{\partial^2 u_l}{\partial x_k \partial x_i}\frac{\partial u_l}{\partial x_k}+\frac{\partial^2 u_k}{\partial x_l \partial x_i}\frac{\partial u_k}{\partial x_l}+\frac{\partial^2 u_l}{\partial x_k \partial x_i}\frac{\partial u_k}{\partial x_l}+\frac{\partial^2 u_k}{\partial x_l \partial x_i}\frac{\partial u_l}{\partial x_k}\right)-\frac{2}{3}\frac{\partial^2 u_k}{\partial x_k \partial x_i}\frac{\partial u_l}{\partial x_l}\right) \\
&+4\mu\beta^{ds}\left(\frac{1}{4}\left(\frac{\partial^2 u_i}{\partial x_k \partial x_j}\frac{\partial u_k}{\partial x_j}+\frac{\partial^2 u_k}{\partial x_i \partial x_j}\frac{\partial u_k}{\partial x_j}+\frac{\partial^2 u_i}{\partial x_k \partial x_j}\frac{\partial u_j}{\partial x_k}+\frac{\partial^2 u_k}{\partial x_i \partial x_j}\frac{\partial u_j}{\partial x_k}\right)\right) \\
&+4\mu\beta^{ds}\left(\frac{1}{4}\left(\frac{\partial^2 u_k}{\partial x_j \partial x_j}\frac{\partial u_i}{\partial x_k}+\frac{\partial^2 u_j}{\partial x_k \partial x_j}\frac{\partial u_i}{\partial x_k}+\frac{\partial^2 u_k}{\partial x_j \partial x_j}\frac{\partial u_k}{\partial x_i}+\frac{\partial^2 u_j}{\partial x_k \partial x_j}\frac{\partial u_k}{\partial x_i}\right)\right) \\
&+4\mu\beta^{ds}\left(-\frac{1}{3}\left(\frac{\partial^2 u_k}{\partial x_k \partial x_j}\frac{\partial u_i}{\partial x_j}+\frac{\partial^2 u_k}{\partial x_k \partial x_j}\frac{\partial u_j}{\partial x_i}+\frac{\partial^2 u_i}{\partial x_j^2}\frac{\partial u_k}{\partial x_k}+\frac{\partial^2 u_j}{\partial x_i \partial x_j}\frac{\partial u_k}{\partial x_k}\right)+\frac{2}{9}\frac{\partial^2 u_k}{\partial x_k \partial x_i}\frac{\partial u_l}{\partial x_l}\right) \\
&+4\mu\beta^{cs}\left(-\frac{1}{6}\left(\frac{\partial^2 u_k}{\partial x_k \partial x_j}\frac{\partial u_i}{\partial x_j}+\frac{\partial^2 u_k}{\partial x_k \partial x_j}\frac{\partial u_j}{\partial x_i}+\frac{\partial^2 u_i}{\partial x_j^2}\frac{\partial u_k}{\partial x_k}+\frac{\partial^2 u_j}{\partial x_i \partial x_j}\frac{\partial u_k}{\partial x_k}\right)+\frac{2}{9}\frac{\partial^2 u_k}{\partial x_k \partial x_i}\frac{\partial u_l}{\partial x_l}\right)
\end{aligned}
\tag{6.20}
$$

where K is the Bulk modulus, μ is the shear modulus, ρ is the density and $\beta^{vp}, \beta^{dp}, \beta^{ds}$ and β^{cs} are the four nonlinear parameter of first order explained below in the constitutive expression. The relevance of this expression is directly linked with the separation of P and S waves and the possibility of design an experimental setup to extract new measurements. Applying the perturbation method [247], it allows to write the wave displacement as,

$$
u_i = u_i^{(0)} + u_i^{(1)} + \dots \tag{6.21}
$$

where $u^{(0)}$ and $u^{(1)}$ denote the zero-order and first-order perturbation solutions, respectively. The zero-order perturbation solution corresponds to the fundamental solution of the linear wave equation (that is, when $\beta = 0$). The first-order perturbation solution is denoted by $u^{(1)}$. Since the effect of the nonlinear term β is small, an approximate solution can be obtained by iteration. When considering two plane waves propagating in a semi-infinite elastic layer, the latter is given as,

$$
\begin{aligned}
u_1^{(0)} &= A\sin\theta\cos\left(\omega_1\left(\frac{\sin\theta x_1+\cos\theta x_2}{c_p}\right)-t\right) \\
u_2^{(0)} &= A\cos\theta\cos\left(\omega_1\left(\frac{\sin\theta x_1+\cos\theta x_2}{c_p}\right)-t\right) \\
u_3^{(0)} &= 0
\end{aligned}
\tag{6.22}
$$

or,

$$
\begin{aligned}
u_1^{(0)} &= -A_h \cos\theta \cos\left(\omega_1\left(\frac{\sin\theta x_1 + \cos\theta x_2}{c_s}\right) - t\right) \\
u_2^{(0)} &= A_h \sin\theta \cos\left(\omega_1\left(\frac{\sin\theta x_1 + \cos\theta x_2}{c_s}\right) - t\right) \\
u_3^{(0)} &= A_v \cos\left(\omega_1\left(\frac{\sin\theta x_1 + \cos\theta x_2}{c_s}\right) - t\right) \qquad (6.23)
\end{aligned}
$$

(6.24)

where A is the constant amplitude of the plane longitudinal waves, A_h and A_v are the constant amplitudes to the S-wave, for horizontal and vertical directions, c_p and c_s, are the velocity of compressional wave and shear wave respectively, θ is the angle of propagation and ω_1 is the angular frequency. Let us then consider the first-order perturbation equation,

$$
\begin{aligned}
\rho\frac{\partial^2 u_1^{(0)}}{\partial t^2} &= K\left(\frac{\partial^2 u_1^{(0)}}{\partial x_1^2} + \frac{\partial^2 u_2^{(0)}}{\partial x_2 \partial x_1} + \frac{\partial^2 u_3^{(0)}}{\partial x_3 \partial x_1}\right) \\
&+\mu\left(2\frac{\partial^2 u_1^{(0)}}{\partial x_1^2} + \frac{\partial^2 u_1^{(0)}}{\partial x_2^2} + \frac{\partial^2 u_1^{(0)}}{\partial x_3^2} + \frac{\partial^2 u_2^{(0)}}{\partial x_1 \partial x_2} + \frac{\partial^2 u_3^{(0)}}{\partial x_1 \partial x_3}\right) \\
&-\frac{2}{3}\mu\left(\frac{\partial^2 u_1^{(0)}}{\partial x_1^2} + \frac{1}{2}\frac{\partial^2 u_2^{(0)}}{\partial x_2 \partial x_1} + \frac{\partial^2 u_3^{(0)}}{\partial x_3 \partial x_1}\right) \qquad (6.25)
\end{aligned}
$$

Analogously, is posible to calculate for u_2 and u_3, this result is coherent with the solution given by Graff [248], where the speed of sound of longitudinal and shear waves are derived as follows,

$$
\begin{aligned}
c_p &= \sqrt{\tfrac{\lambda+2\mu}{\rho}} \\
c_s &= \sqrt{\tfrac{\mu}{\rho}} \qquad (6.26)
\end{aligned}
$$

The figure 6.1 shows the propagation of P- wave and S-wave through an elastic bar,

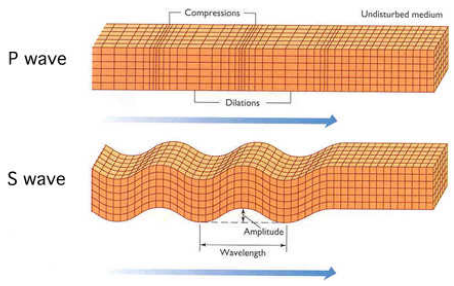

Figure 6.1: Logitudinal P-wave and transversal S-wave propagation. Source: USGS

6.3 Geometric and constitutive origin of acoustic nonlinearity

It is necessary to remark that the nonlinear effects in theory of acoustics, have three main sources affecting the harmonics generation, (1) The nonlinear term inside the compatibility equation 4.1 (this is referred to the the cross term), (2) the nonlinear term from the derivation of Cauchy stress 4.2 and (3) the noninearity from the derivation of strain energy of third order that impacts on TOEC. in Equation 4.13.

The Hamilton expression of nonlinear acoustic parameter β_H can easily illustrate the explained below as follows,

Dynamic equilibrium, $\sigma_{ij,j} = \rho u_{i,tt}$

Constitutive law, $\sigma_{ij} = \lambda\varepsilon_{kk}\delta_{ij} + 2\mu\varepsilon_{ij} \underbrace{+O(\varepsilon_{ij}^2)}_{NL(3)}$

Compatibility equation, $\varepsilon_{ij} = \frac{1}{2}(u_{i,j} + u_{j,i} \underbrace{+u_{k,i}u_{k,j}}_{NL(1)})$

Constraining to a plane wave in 1D ($u(x,t) = u_1, u_2 = 0 = u_3$)

$$\sigma_{,x} = \rho u_{i,tt}$$

$$\sigma = (\lambda + 2\mu)\varepsilon \underbrace{- \left(\beta + \frac{1}{2}\right)(\lambda + 2\mu)\varepsilon^2}_{NL(2)}$$

$$\varepsilon = u_{,x} \underbrace{+\frac{1}{2}u_{,x}^2}_{NL(1)}$$

Substitution yields the equation of motion

$$\frac{\partial^2 u}{\partial t^2} = c_p^2 \frac{\partial^2 u}{\partial x^2} \quad \Rightarrow \quad \frac{\partial^2 u}{\partial t^2} = c_p^2 \underbrace{\frac{\partial^2 u}{\partial x^2}\left(1 - 2\beta\frac{\partial u}{\partial x}\right)}_{NL(2)}$$

Then, the hamilton definition of nonlinear acoustic parameter β_H is obtained by the main three sources of nonlinearity as in Equation 6.27 as follows,

$$\beta_H = -\frac{3}{2} - \frac{\mathcal{A} + 3\mathcal{B} + \mathcal{C}}{\lambda + 2\mu} \tag{6.27}$$

Note that this parameter could variate depending on the of Nonlinear wave equation, as in the Zarembo conception, Gol'dberg case or Guyer. (For more details, See Chapter 5). Then, the fundamental contribution of this chapter connect with the expansion and derivation of nonlinear acoustic parameter assumed as no unique. This extension contribute to distinguish between phases of material or tissue, under this process three sources of nonlinearity have been considered.

7

Exploration of microdamage as possible explanation of nonlinearity

To formulate a posible explanation to the nonlinear origin based on microdamage and microcracks in solid state. This origin starts with developing of the homogenization techniques, constructing a theory that connects micromechanical and heterogeneous elasticity and nonlinear ultrasound tools is possible to derivate and quantify density of microcracks. The aim of this Chapter is extending the theory of Eshelby to solve various cases of geometrical inclusions and provide a method for measuring density of microcracks with a consistent relationship established between the acoustic nonlinearity and homogenization. The results of this chapter are in process of review in Ultrasonics journal [262] with the coauthor William J. Parnell.

In this chapter, a homogenization model is proposed to relate the density of micro-cracks with the acoustic nonlinearity. To this end, the damaged material is idealized as a composite material, that is a dispersion of nonlinear isotropic spheroidal inclusions surrounded by a linear isotropic matrix. A basic hypothesis is that nonlinear properties are strongly sensitive to strength changes and may unveil deeper dimensions of its micro and macrostructure. Particularly, microcracks are a growing type of damage that is predominantly responsible for the eventual mechanical failure. At the micro-scale, the clapping mechanism excited inside each micro-crack during nonlinear ultrasonification is approximated by a Taylor expansion of the bilinear stress-strain constitutive law. This approximation is linked to the acoustic nonlinearity by rearranging the nonlinear Landau constitutive law. The Eshelby theory [249] is applied in the homogenization process, where the clapping micro-cracks are

represented by non-linear penny-shaped inclusions. The penny-shaped cracks are assumed to be aligned, as a consequence of a preferential fatigue load direction of the structure. The nonlinearity of the inclusions can therefore be described by the so-called Landau coefficients, which measure the deviation from the linearity. Finally, the relationships between these Landau coefficients and the measurable acoustic nonlinearity in ultrasound are presented. The complete process is outlined in Figure 7.1, in which the notation is anticipated, but will be introduced below.

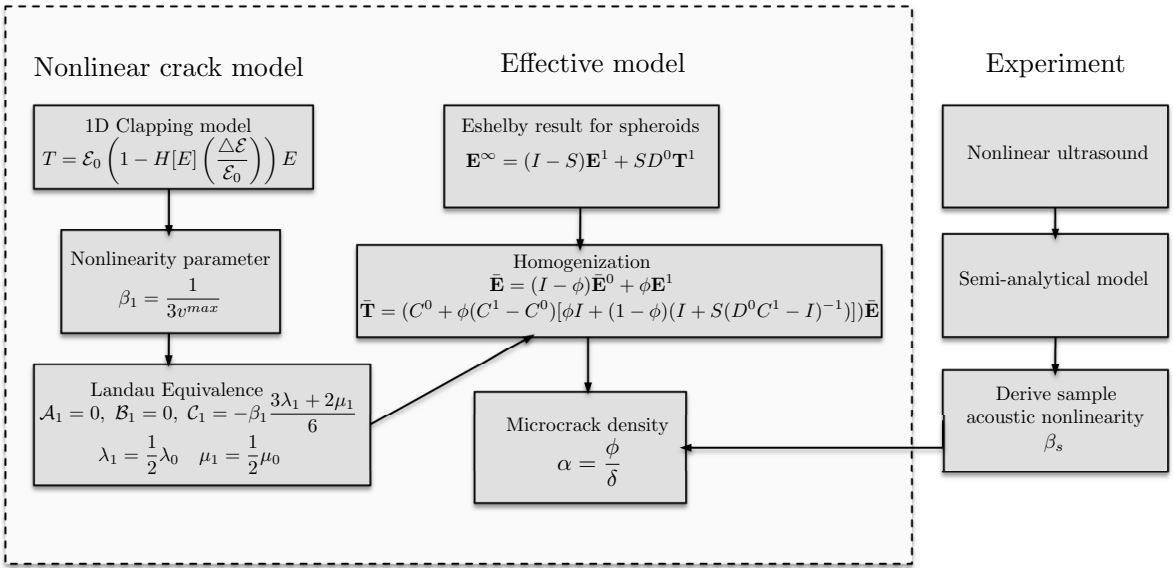

Figure 7.1: Flow chart: homogenization procedure that relates the density of micro-cracks with the acoustic nonlinearity.

Flow chart of the theory, summarizing steps: a crack behaves by contact clapping - the clapping generates nonlinear constitutive law - 1D beta nonlinearity is approximated (bilinear $\rightarrow$ logistic curve $\rightarrow$ Taylor series $\rightarrow$ beta inclusion) - 3D Landau nonlinearity constants are extracted ($\mathcal{A}, \mathcal{B}$ and $\mathcal{C}$ of inclusion) - the crack is treated a nonlinear penny-shaped inclusion - density of inclusions (cracks) are homogenized into equivalent properties ($\mathcal{A}, \mathcal{B}$ and $\mathcal{C}$ effective) - acoustic nonlinearity (β effective) is obtained from them, which is the measurable quantity by nonlinear ultrasound.

7.1 Homogenization framework

We model a damaged material in a similar manner to a composite material, as has been done to good effect many times previously [250, 251, 252]. In particular we are interested in the effect that damage, or more specifically micro-cracks, have on the effective properties and how this subsequently affects the *nonlinear* acoustic response of the material. We suppose that a number of aligned penny shaped cracks are dispersed throughout the linear elastic host phase, see Figure 7.2. We model these cracks as the limit of spheroidal cavities as we shall explain shortly. Furthermore we shall consider these cracks to behave nonlinearly. Let

us deal with various effects sequentially, starting with the classical case of linear, traction free cracks, followed by the linear effect of crack face contact and finally the case of nonlinear effects.

7.1.1 Homogenization for linear elastic particulate media

Here we describe and employ the so-called *Mori-Tanaka* method [202] which attempts to incorporate interaction between inclusions and so can be used as an approximation for the effective properties of inhomogeneous media at finite concentrations of inclusions. Although this approach is standard and well-known, it is important to describe its derivation fully since later we can then describe the departures from this theory.

Consider the case in Figure 7.2 when a medium Ω has within it two linear elastic phases Ω_0 (the host or matrix) and inclusion phase Ω_1 with elastic modulus tensors $\mathbf{C}^0$ and $\mathbf{C}^1$ respectively. We suppose that the inclusions are aligned spheroids with semi-axes $a_1 = a_2 = \ell$ and a_3 in the x_1, x_2 and x_3 directions respectively, defining the aspect ratio $\delta = a_3/\ell$ so that $\delta < 1$ ($\delta > 1$) for oblate (prolate) spheroids.

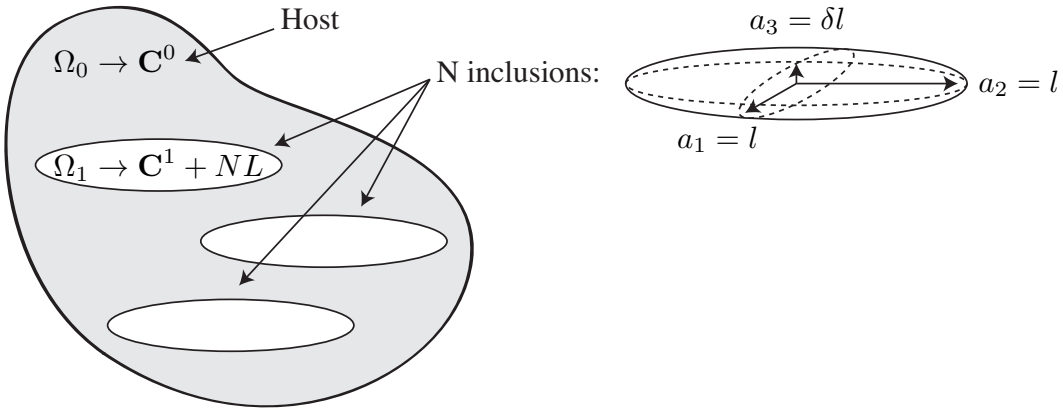

Figure 7.2: Outline of the considered bone medium: dispersion of nonlinear spheroidal inclusions in a linear isotropic host with distribution of microcracks defined by density $\alpha = \phi/\delta$ where ϕ is the volume fraction.

Referring to Figure 7.2, as will be shown later, the volume of cracks vanishes in the strongly oblate limit of spheroidal cavities, i.e. $\delta \to 0$. As such the effective contribution of the vanishing inclusion volume fraction has to be defined in this limit. The standard volume fraction ϕ in homogenization theory is defined by

$$\phi = \frac{|\Omega_1|}{|\Omega|} \tag{7.1}$$

where $|\Omega|$ denotes the volume of the medium Ω and ϕ clearly tends to zero in the limit $\delta \to 0$. This motivates introducing what we call *density* of microcracks $\alpha = \frac{\phi}{\delta}$, which is finite as $\delta \to 0$, and can be interpreted as the volume fraction of the spherical inclusions that would have the same footprint or projection as the flat, zero-volumed, penny-shaped

inclusions. To put it in another way, if the penny-shaped inclusions were inflated to make them spherical, their volume fraction would be α.

Let us denote the Cauchy stress by $\mathbf{T}$ and the linear strain $\mathbf{E}$. The average stress within the medium is easily determined as

$$\begin{aligned}
\bar{\mathbf{T}} &= \frac{1}{|\Omega|}\int_{\Omega_0}\mathbf{T}^0 d\Omega + \frac{1}{|\Omega|}\int_{\Omega_1}\mathbf{T}^1 d\Omega \\
&= \frac{\mathbf{C}^0}{|\Omega|}\int_{\Omega_0}\mathbf{E}^0 d\Omega + \phi\bar{\mathbf{T}}^1 \qquad (7.2)\\
&= \frac{\mathbf{C}^0}{|\Omega|}\left(\int_{\Omega_0}\mathbf{E}^0 d\Omega + \int_{\Omega_1}\mathbf{E}^1 d\Omega - \int_{\Omega_1}\mathbf{E}^1 d\Omega\right) + \phi\bar{\mathbf{T}}^1 \\
&= \mathbf{C}^0\bar{\mathbf{E}} - \phi\mathbf{C}^0\bar{\mathbf{E}}^1 + \phi\bar{\mathbf{T}}^1\{\bar{\mathbf{E}}^1\} \qquad (7.3)
\end{aligned}$$

where $f\{\cdot\}$ denotes an argument of the function f and where $\overline{f}^r$ denotes the volume average over the rth phase, i.e.

$$\overline{f}^r = \frac{1}{|\Omega_r|}\int_{\Omega_r} f(\mathbf{x})\, d\Omega_r. \qquad (7.4)$$

Because here, for now, we assume that the inclusions are linear elastic, we have $\bar{\mathbf{T}}^1 = \mathbf{C}^1\bar{\mathbf{E}}^1$ and so we obtain the classical result that

$$\bar{\mathbf{T}} = \mathbf{C}^0\bar{\mathbf{E}} + \phi(\mathbf{C}^1 - \mathbf{C}^0)\bar{\mathbf{E}}^1 \qquad (7.5)$$

Eshelby's [198] result for spheroids informs us that

$$\begin{aligned}
\mathbf{E}^\infty = \bar{\mathbf{E}}^0 &= (\mathbf{I} - \mathbf{S})\mathbf{E}^1 + \mathbf{S}\mathbf{D}^0\mathbf{T}^1 \\
&= (\mathbf{I} + \mathbf{S}(\mathbf{D}^0\mathbf{C}^1 - \mathbf{I}))\mathbf{E}^1 \qquad (7.6)
\end{aligned}$$

where $\mathbf{I}$ is the fourth order identity tensor, $\mathbf{S}$ is the (uniform) Eshelby tensor, $\mathbf{D}^0$ is the compliance tensor ($\mathbf{D}^0\mathbf{C}^0 = \mathbf{I}$) and we have assumed dilute dispersions so that the average strain in the matrix $\bar{\mathbf{E}}^0 = \bar{\mathbf{E}}^\infty$, the strain in the far field. Importantly for spheroidal inclusions $\bar{\mathbf{E}}^1 = \mathbf{E}^1$ since Eshelby showed that the interior strain is uniform for isolated ellipsoids. Next we determine the average strain in the medium which is

$$\begin{aligned}
\bar{\mathbf{E}} &= (1-\phi)\bar{\mathbf{E}}^0 + \phi\mathbf{E}^1 \qquad (7.7)\\
&= [\phi\mathbf{I} + (1-\phi)(\mathbf{I} + \mathbf{S}(\mathbf{D}^0\mathbf{C}^1 - \mathbf{I}))]\mathbf{E}^1 \qquad (7.8)
\end{aligned}$$

where we have used the Eshelby result to obtain the average strain in terms of the inclusion strain. Finally, inverting (7.8) and substituting in (7.5) yields

$$\begin{aligned}
\bar{\mathbf{T}} &= \left(\mathbf{C}^0 + \phi(\mathbf{C}^1 - \mathbf{C}^0)[\phi\mathbf{I} + (1-\phi)(\mathbf{I} + \mathbf{S}(\mathbf{D}^0\mathbf{C}^1 - \mathbf{I}))]^{-1}\right)\bar{\mathbf{E}} \\
&= \mathbf{C}^*\bar{\mathbf{E}} \qquad (7.9)
\end{aligned}$$

The above approach summarizes the Mori-Tanaka method. Even though we have assumed a dilute dispersion of spheroids, the result (7.9) is *feasible* for non-dilute volume fractions in that it recovers the limit $\mathbf{C}^* \to \mathbf{C}^1$ as $\phi \to 1$.

7.1.2 Linear elasticity: open cracks in a homogeneous matrix

Let us consider how the above theory is modified when we consider the case of penny shaped cracks, which can be considered as the strongly oblate limit of the spheroidal cavity, i.e. $\delta \to 0$ and $\phi \to 0$. Clearly, one cannot simply take these as equalities in the above result (7.9). Instead, one needs to consider the limit carefully. The approach below was employed by Giordano [218] (amongst others) for example.

Let us first derive the result associated with spheroidal cavities or voids of aspect ratio δ, in which case the traction on the void surface is zero by removing the stiffness of the inclusion, $\mathbf{C}^1 = \mathbf{0}$. The average stress (7.3) then becomes

$$\bar{\mathbf{T}} = \mathbf{C}^0 \bar{\mathbf{E}} - \phi \mathbf{C}^0 \mathbf{E}^1. \tag{7.10}$$

and the Eshelby result (7.6) takes the form

$$\mathbf{E}^0 = (\mathbf{I} - \mathbf{S})\mathbf{E}^1. \tag{7.11}$$

Therefore we can write that the induced "cavity strain" is

$$\mathbf{E}^1 = (\mathbf{I} - \mathbf{S})^{-1}\mathbf{E}^0 = \mathbf{F}\mathbf{E}^0. \tag{7.12}$$

Next let us use the relationship for the average strain (7.7) with (7.12) to find that

$$\bar{\mathbf{E}} = [(1-\phi)\mathbf{F}^{-1} + \phi\mathbf{I}]\mathbf{E}^1. \tag{7.13}$$

Inverting this and using in (7.10) we find that

$$\begin{aligned} \bar{\mathbf{T}} &= \mathbf{C}^0\bar{\mathbf{E}} - \phi\mathbf{C}^0[(1-\phi)\mathbf{F}^{-1} + \phi\mathbf{I}]^{-1}\bar{\mathbf{E}}. \\ &= \left(\mathbf{C}^0 - \phi\mathbf{C}^0\mathbf{F}[(1-\phi)\mathbf{I} + \phi\mathbf{F}]^{-1}\right)\mathbf{E} \\ &= \mathbf{C}^*\bar{\mathbf{E}}. \end{aligned} \tag{7.14}$$

where the effective modulus tensor is thus defined as

$$\mathbf{C}^* = \mathbf{C}^0 - \phi\mathbf{C}^0\mathbf{F}[(1-\phi)\mathbf{I} + \phi\mathbf{F}]^{-1}. \tag{7.15}$$

Next let us define

$$\boldsymbol{\mathcal{F}} = \lim_{\delta\to 0}\mathbf{F} = O\left(\frac{1}{\delta}\right) \tag{7.16}$$

where we show the latter in appendix A. The important aspect to (7.15) is that terms involving ϕ and $\mathbf{F}$ are gathered together as products. Note that if we interpret the volume fraction in the sense of spheroidal inclusions, referring back to (7.1) we have

$$\phi = \frac{|\Omega_1|}{|\Omega|} = \frac{N(4\pi/3)a_1a_2a_3}{|\Omega|} = \delta\frac{N(4\pi/3)\ell^3}{|\Omega|} = \delta\alpha \tag{7.17}$$

where N refers to the number of inclusions in the domain Ω, recalling that we are interested in the limit as $\delta \to 0$ to obtain the strongly oblate limit, i.e. penny shaped cracks. Introducing α in this manner ensures that the limit $\delta \to 0$ is sufficient for both $\delta \to 0$ and $\phi \to 0$, and (7.15) becomes

$$\mathbf{C}^* = \mathbf{C}^0 - \alpha\mathbf{C}^0\mathbf{G}[(1-\delta\alpha)\mathbf{I} + \alpha\mathbf{G}]^{-1}. \tag{7.18}$$

where we have defined $\mathbf{G} = \delta\mathbf{F}$. Now take the limit $\delta \to 0$ and introduce

$$\boldsymbol{\mathcal{G}} = \lim_{\delta\to 0}\mathbf{G} = \lim_{\delta\to 0}(\delta\mathbf{F}) = O(1) \tag{7.19}$$

The non-zero components of the transversely isotropic tensor $\boldsymbol{\mathcal{G}}$ are listed in (A.22) of Appendix A. Results are now obtained in terms of the modified volume fraction α, noting that $\boldsymbol{\mathcal{G}}$ is independent of α the effective modulus tensor. The expression for $\mathbf{C}^*$ given in (7.18) therefore becomes, in the penny-shaped crack limit,

$$\mathbf{C}^* = \mathbf{C}^0\big(\mathbf{I} - \alpha\boldsymbol{\mathcal{G}}[\mathbf{I} + \alpha\boldsymbol{\mathcal{G}}]^{-1}\big). \tag{7.20}$$

noting that the term inside the square brackets that was $\delta\alpha\mathbf{I} \to \mathbf{0}$. This is a classical result, as derived in e.g. [218].

We wish to understand how the above is extended to the case of nonlinear inclusions. We will do this shortly, but first as a precursor to this problem, let us consider how one can incorporate more complicated (linear) crack face traction effects.

7.1.3 Linear elasticity: allowing for crack face effects

If the cracks are open, the traction $\mathbf{T}^1$ is identically zero and thus contributes nothing to the effective properties. On the other hand, if it scales with the aspect ratio of the crack, $\mathbf{T}^1 \sim \delta$ then it can affect the overall properties in the penny-shaped crack limit as we now show. Let us assume that as $\delta \to 0$

$$\mathbf{T}^1 = \mathbf{C}^1\mathbf{E}^1 = \delta\tilde{\mathbf{C}}^1\mathbf{E}^1 \tag{7.21}$$

where $\tilde{\mathbf{C}}^1 = O(1)$.[1] Using this, the Eshelby result (7.6) becomes

[1] To show why the scaling of $\mathbf{C}^1$ is needed from a mathematical point of view, consider if we just put $\mathbf{T}^1 = \mathbf{C}^1\mathbf{E}^1$ directly into the Eshelby result (no arguments about scaling of either $\mathbf{C}^1$ or $\mathbf{E}^1$ on δ, then we get

$$\mathbf{E}^\infty = (\mathbf{I} - \mathbf{S} + \tilde{\mathbf{H}})\mathbf{E}^1$$

$$\mathbf{E}^0 = (\mathbf{I} - \mathbf{S} + \delta\mathbf{H})\,\mathbf{E}^1 \tag{7.22}$$

where we have written $\mathbf{H} = \mathbf{S}\mathbf{D}^0\tilde{\mathbf{C}}^1$ which we note is order one as $\delta \to 0$. This is the effect of the "extra stress" associated with the crack. Therefore following analogous steps to the last section we find that

$$\mathbf{E}^1 = \mathbf{F}\left[(1-\alpha\delta)\,(\mathbf{I} + \mathbf{H}\delta\mathbf{F}) + \alpha\delta\mathbf{F}\right]^{-1}\bar{\mathbf{E}} \tag{7.23}$$

where we set $\phi = \alpha\delta$. The equation for the averaged stress then gives

$$\begin{aligned}\bar{\mathbf{T}} &= \mathbf{C}^0\bar{\mathbf{E}} - \phi\mathbf{C}^0\mathbf{E}^1 + \phi\bar{\mathbf{T}}^1,\\ &= \mathbf{C}^0\bar{\mathbf{E}} - \alpha\mathbf{C}^0\delta\mathbf{E}^1 + \alpha\tilde{\mathbf{C}}^1\delta^2\mathbf{E}^1,\end{aligned} \tag{7.24}$$

where again we have set $\phi = \alpha\delta$, anticipating the penny-shaped crack limit being taken. Note that the coefficient of the last term here is $O(\delta^2)$ so that in the limit, this term will tend to zero since $\mathbf{E}^1 \sim O(1/\delta)$. The "extra stress" therefore arises purely due to the Eshelby result and not due to averaged stress.

To understand from a physical point of view the definition of the scaled inclusion stiffness $\mathbf{C}^1$, we should recall that neither $\mathbf{T}^1$, $\mathbf{E}^1$ or $\mathbf{C}^1$ are fully defined inside the crack in a physical sense, simply because the crack is not fully defined due to the unknown δ. Starting from the idea that the measurable physical magnitude which the matrix senses from the crack is the displacement u, and since the strain $\mathbf{E}^1$ is defined from its gradient, it will depend on δ and be of order $O(\delta)$. To transmit the same stress, the stiffness of an equivalent spherical crack (of $\delta = 1$) should rescale to be softer: $\tilde{\mathbf{C}}^1 = \frac{\mathbf{C}^1}{\delta}$, so $\mathbf{T}^1_L = \mathbf{C}^1\mathbf{E}^1 = \delta\tilde{\mathbf{C}}^1\mathbf{E}^1 = \delta\tilde{\mathbf{T}}^1_L$. Figure 7.3 provides a physical interpretation of the three terms that contribute to the average stress in (7.24). In the penny-shaped crack limit we therefore obtain

---

with $\tilde{\mathbf{H}} = \mathbf{S}\mathbf{D}^0\mathbf{C}^1$. But importantly note that there is no δ in front of this $\tilde{\mathbf{H}}$ term. Therefore following the steps through what we will end up with is, instead of 7.26 below, and expanding out brackets,

$$\mathbf{E}^1 = \mathbf{F}\left(\tilde{\mathbf{H}}\mathbf{F} + \mathbf{I} - \alpha\delta - \alpha\tilde{\mathbf{H}}\delta\mathbf{F} + \alpha\delta\mathbf{F}\right)^{-1}\bar{\mathbf{E}}$$

this ends up being multiplied by a δ which is ok for the $\mathbf{F}$ out the front, but the problem is that in the limit $\delta \to 0$, the term $\tilde{\mathbf{H}}\mathbf{F}$ is not bounded, like the other terms in the brackets.

Alternatively if we scaled $\mathbf{E}^1$ as $\mathbf{E}^1 = \tilde{\mathbf{E}}^1/\delta$ then

$$\mathbf{T}^1 = \mathbf{C}^1\mathbf{E}^1 = \frac{1}{\delta}\mathbf{C}^1\tilde{\mathbf{E}}^1$$

so that the Eshelby result becomes

$$\mathbf{E}^\infty = (\mathbf{I} - \mathbf{S} + \tilde{\mathbf{H}})\frac{1}{\delta}\tilde{\mathbf{E}}^1$$

which just creates a different problem. Therefore, to solve it we need is a scaling of $\mathbf{C}^1$.

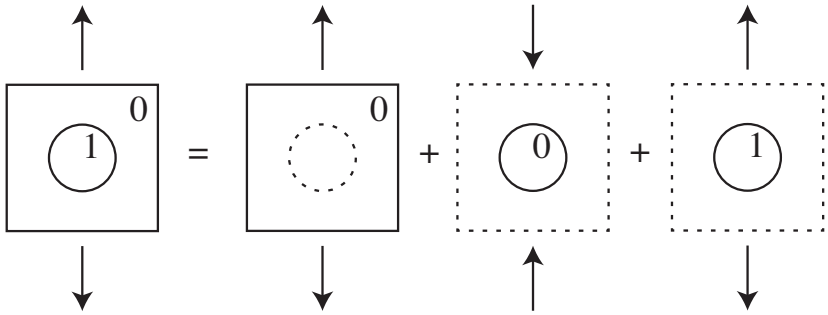

Figure 7.3: Physical interpretation of how the average stress is composed of the addition of the three stress terms in Eq. 7.24.

$$\bar{\mathbf{T}} = \mathbf{C}^0 \left(\mathbf{I} - \alpha \boldsymbol{\mathcal{G}} \left[\mathbf{I} + \mathbf{H}\boldsymbol{\mathcal{G}} + \alpha \boldsymbol{\mathcal{G}} \right]^{-1} \right) \bar{\mathbf{E}} \tag{7.25}$$

noting that if we take $\tilde{\mathbf{C}}^1 \rightarrow 0$ (so that $\mathbf{H} = 0$) we recover (7.20). As should be expected the effect of a non-zero $\mathbf{H}$ has the effect of stiffening the material. In particular for example, in dynamics where a compressive wave will give rise to both open cracks (in tension) and closed cracks (in compression) the effective Young's modulus cannot be that due to the open crack case considered above. Expression (7.25) is the correction to that result.

7.1.4 Homogenization for nonlinear cracks

Let us consider now what happens if we assume that the stress-strain condition for a crack is *nonlinear*. This is reasonable since a number of competing effects occur on the crack face. The form of the nonlinear term will be discussed shortly but we see that it needs an additional δ scaling in order to have an $O(1)$ effect and remain bounded. To understand physically the reason, considering the scaling of $\mathbf{E^1}$ discussed above, in order to contribute equivalently being the nonlinear stress dependent on the square of the strain, $\mathbf{T}^1_{NL} = \delta^2 \tilde{\mathbf{T}}^1_{NL}$, which justifies the scaling of linear and nonlinear stress,

$$\mathbf{T}^1 = \delta \tilde{\mathbf{C}}^1 \mathbf{E}^1 + \delta^2 \tilde{\mathbf{T}}^1_{NL} \tag{7.26}$$

Later on in section 7.2 we justify this scaling from a study of the local crack problem. It has been shown that for constitutive nonlinearity in the strain, the Eshelby result for spheroids holds [218] and gives

$$\mathbf{E}^0 = ((\mathbf{I} - \mathbf{S}) + \delta \mathbf{H}) \mathbf{E}^1 + \delta^2 \mathbf{S} \mathbf{D}^0 \tilde{\mathbf{T}}^1_{NL} \tag{7.27}$$

and using this in the average strain yields (using curly brackets to denote an argument)

$$\bar{\mathbf{E}} = ((1-\phi)((\mathbf{I} - \mathbf{S}) + \delta \mathbf{H}) + \phi \mathbf{I}) \, \mathbf{E}^1 + (1-\phi) \delta^2 \mathbf{S} \mathbf{D}^0 \tilde{\mathbf{T}}^1_{NL} \left\{ \mathbf{E}^1 \right\} \tag{7.28}$$

$$= ((1 - \delta\alpha)(\mathbf{I} + \mathbf{H}\delta\mathbf{F}) + \alpha\delta\mathbf{F}) \, \mathbf{F}^{-1} \mathbf{E}^1 + (\delta^2 - \alpha\delta^3) \mathbf{S} \mathbf{D}^0 \tilde{\mathbf{T}}^1_{NL} \left\{ \mathbf{E}^1 \right\} \tag{7.29}$$

$$= (\mathbf{I} + \mathbf{H}\mathbf{G} + \alpha \mathbf{G}) \, \mathbf{F}^{-1} \mathbf{E}^1 + \mathbf{S} \mathbf{D}^0 \tilde{\mathbf{T}}^1_{NL} \left\{ \delta \mathbf{E}^1 \right\} + O(\delta) \tag{7.30}$$

where we have retained only terms that will become important in the penny shaped limit and we note that we have conveniently put the δ inside the argument of the nonlinear stress term which is quadratic in its argument. Now we have to *formally invert* this expression which gives,

$$\mathbf{E}^1 = \mathbf{F}\left[\mathbf{I} + \mathbf{HG} + \alpha\mathbf{G}\right]^{-1}\bar{\mathbf{E}} - \mathbf{FU}\{\bar{\mathbf{E}}\} \tag{7.31}$$

where $\mathbf{U}\{\bar{\mathbf{E}}\}$ refers to the first, quadratic nonlinear contribution to this equation, which it transpires, takes the form

$$\mathbf{U}\{\bar{\mathbf{E}}\} = (\mathbf{I} + \mathbf{HG} + \alpha\mathbf{G})^{-1}\mathbf{SD}^0\tilde{\mathbf{T}}^1_{NL}\left\{\mathbf{G}(\mathbf{I} + \mathbf{HG} + \alpha\mathbf{G})^{-1}\bar{\mathbf{E}}\right\} \tag{7.32}$$

noting again that the curly brackets denote that this is the argument of the nonlinear isotropic stress term $\tilde{\mathbf{T}}^1_{NL}$.

Finally, using (7.31) in the average stress equation and taking the penny-shaped crack limit, we find

$$\bar{\mathbf{T}} = \mathbf{C}^0\left(\mathbf{I} - \alpha\boldsymbol{\mathcal{G}}\left[(\mathbf{I} + \mathbf{H}\boldsymbol{\mathcal{G}}) + \alpha\boldsymbol{\mathcal{G}}\right]^{-1}\right)\bar{\mathbf{E}} - \mathbf{C}^0\alpha\boldsymbol{\mathcal{G}}\boldsymbol{\mathcal{U}}\left\{\bar{\mathbf{E}}\right\} \tag{7.33}$$

where

$$\boldsymbol{\mathcal{U}}\{\bar{\mathbf{E}}\} = (\mathbf{I} + \mathbf{H}\boldsymbol{\mathcal{G}} + \alpha\boldsymbol{\mathcal{G}})^{-1}\mathbf{SD}^0\tilde{\mathbf{T}}^1_{NL}\left\{\boldsymbol{\mathcal{G}}(\mathbf{I} + \mathbf{H}\boldsymbol{\mathcal{G}} + \alpha\boldsymbol{\mathcal{G}})^{-1}\bar{\mathbf{E}}\right\}. \tag{7.34}$$

Note once again that if we take the limit when nonlinear effects are negligible, $\boldsymbol{\mathcal{U}} \to 0$, we recover the linear limit of the previous section and the result (7.25).

7.2 Nonlinear crack clapping model

This section describes the formulation of the nonlinear model of an individual micro-crack, which is later equated to an inclusion. As opposed to linear crack analysis, which the literature treats as open (since closed cracks transmit compressional forces as if the material were intact), the nonlinear behaviour of cracks correctly models a range of states, either closed (for negative strains) or open (for positive strains). The clapping contact mechanism excited when a cyclic load exerted by the oscillatory movement of the nonlinear ultrasonification behaves as follows: while the cracks tend to be closed at rest, once subject to the cyclic stress, cracks close during the compressional half-cycle, transmitting stress and establishing displacement continuity, whereas during the crack opening, stress inside the crack vanishes and a displacement discontinuity across the crack arises.

7.2.1 Nonlinearity formulation

This local clapping contact phenomenon gives rise to a non-linear stress-strain relation at the defect [253]. Pecorari et al. [254] already proposed a 1D clapping model along direction

3 with different elastic moduli for compression and tension,

$$T_{33} = \mathcal{E}_0 \left(1 - H\{E_{33}^1\} \left(\frac{\Delta\mathcal{E}}{\mathcal{E}_0}\right)\right) E_{33} \tag{7.35}$$

where $H\{E_{33}\}$ is the Heaviside step function, $\mathcal{E}_0$ is the elastic modulus under compression, and $\Delta\mathcal{E}$ is its change under stress reversal to tension.

Given that micro-cracks are small compared to the specimen and ultrasonic wavelength, we assume that the elastic modulus under tension is negligibly small and therefore $\Delta\mathcal{E} = \mathcal{E}_0$. Additionally all other components of stress act, as usual, linearly in the strain components.

By treating only the volumetric components of stress and strain in the way defined in next subsection, we obtain a 1D compressional constitutive law that relates pressure p with volumetric strain v of the form, which captures the compressive or opening states of the crack behavior in a single dimension,

$$p = K\{v\}v \tag{7.36}$$

where $K[v]$ is the non-constant bulk modulus. Hence, from Equation (7.35), the bilinear stiffness of the proposed model with multiple micro-cracks is proposed as,

$$K\{v\} = K_0(1 - H\{v\}) \tag{7.37}$$

where K_0 is the compressibility modulus of the host material. Recall that this form is valid only inside the inclusion, whose spatial domain is defined as coincident with that of the penny-shaped crack, i.e. the limiting case of a spheroid whose transverse axis aspect ratio tends to zero.

In order to bypass the difficulty of engaging with a non-differentiable function for the stress-strain law (via the extraction a Taylor expansion of the Heaviside function) we approximate it by a logistic function, as is widespread in the literature [255, 256, 257]. The Heaviside step function is therefore be smoothly approximated by the logistic function, with a sharpness parameter κ, i.e.

$$K\{v\} \simeq \lim_{\kappa\to 0} K_0 \left(1 - \frac{1}{1 + e^{-\kappa v}}\right). \tag{7.38}$$

When homogenizing, note that the assumption of common alignment of cracks is made, as well as negligible residual stresses that would be responsible for differences in the strain where the kink appears, which would average out as a smoothed bilinear form

Now, the bilinear stiffness is approximated by a Taylor expansion,

$$K[v] \simeq K_0 \left(\frac{1}{2} - \frac{\kappa v}{4} + O[v^2]\right) \tag{7.39}$$

where the parameter κ should be chosen so that the Taylor expansion is valid for the range of volumetric deformation v induced by the ultrasound, whereby $\kappa \simeq \frac{2}{v^{max}}$. These parameters are chosen so as to optimize the fitting of the Taylor expansion around the kink and over the desired range of values. This choice as well as the accuracy of the Taylor expansion is evident from Fig. 3. This result can be validated by reasoning that, on average, the first linear

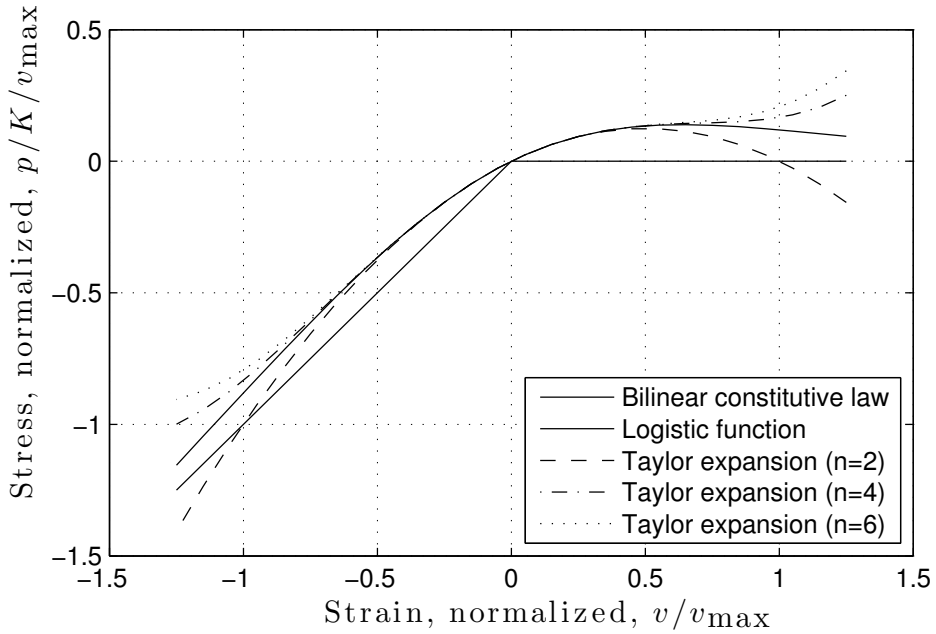

Figure 7.4: Taylor expansion, logistic function and bilinear constitutive law

approximation contains half open (zero modulus) and half closed cracks (intact modulus). This average yields an effective compressibility modulus of the inclusion of $K_0/2$, which coincides with the first linear tangent term of the Taylor expansion. Comparing now with the definition of the acoustic nonlinearity to be compatible with Equation 9.47,

$$K\{v\} = K_1 \left(1 - \frac{3}{2}\beta_1 v\right) \tag{7.40}$$

the origin of both the linear and nonlinear constants can be identified from Equation 7.39, where the equivalent Young modulus is derived as,

$$K_1 = \frac{1}{2}K_0 \tag{7.41}$$

and the nonlinearity parameter β_1 is found to depend only on the maximal induced deformation v^{max} as,

$$\beta_1 = \frac{\kappa}{6} = \frac{1}{3v^{max}} \tag{7.42}$$

7.2.2 Nonlinear Landau coefficients of inclusions

The nonlinear constitutive response of the crack relates the stress $\mathbf{T}^1$ and strain $\mathbf{E}^1$ fields and is assumed to be of the second order form established by Landau et al. [1], valid for any 3D

continuum, which was recently updated in the sense explained below by Parnell et al. [258] based on [259, 260],

$$\mathbf{T}^1_{NL}(\mathbf{E}^1) = \mathcal{A}_1(\mathbf{E}^1)^2 + \mathcal{B}_1\big(\mathrm{tr}\left((\mathbf{E}^1\right)^2)\mathbf{I}_2 + 2\mathrm{tr}(\mathbf{E}^1)\mathbf{E}^1\big) + \mathcal{C}_1(\mathrm{tr}\mathbf{E}^1)^2\mathbf{I}_2 \tag{7.43}$$

the subscript 2 on $\mathbf{I}_2$ indicates that this is the identity tensor of second order, as opposed to $\mathbf{I}$ above which is the identity tensor of fourth order. The penny-crack limit ensures that the macroscopic response is transversely isotropic for aligned cracks. λ and μ are the Lamé constants and $\mathcal{A}_1, \mathcal{B}_1, \mathcal{C}_1$ are the Landau coefficients, where the following approximation has been applied, since the linear constants are negligible when compared to the nonlinear ones,

$$\begin{aligned} \mathcal{A}_1 + 4\mu_1 &\simeq \mathcal{A}_1, \\ \mathcal{B}_1 + \lambda_1 - \mu_1 &\simeq \mathcal{B}_1, \\ \mathcal{C}_1 - \lambda_1 &\simeq \mathcal{C}_1. \end{aligned} \tag{7.44}$$

Since any tensor (stress or strain) can be split into volumetric (scalar) and deviatoric (tensor) parts, the constitutive equations can be rearranged as particular cases of the following general form, by decomposing them into volumetric and deviatoric constituents,

$$\mathbf{T} \;=\; \underbrace{-p\mathbf{I}}_{\text{volumetric}} \;+\; \underbrace{\mathbf{T}^D}_{\text{deviatoric}}, \quad p = -\tfrac{1}{3}\mathrm{tr}\mathbf{T} \tag{7.45}$$

since any tensor is split into volumetric (scalar) and deviatoric (tensor) parts. The strain is therefore also decomposed into volumetric v and deviatoric $\mathbf{D}$ strain,

$$\mathbf{E} = -v\delta_{ij} + \mathbf{D}, \quad v = -\frac{1}{3}\mathrm{tr}\mathbf{E} \tag{7.46}$$

The linear elastic dependency is enriched with quadratic terms, following the series expansion concept put forth by Landau [1]. Only the volumetric part is detailed in terms of the nonlinearity parameter β due to the simplicity of the volumetric strain v being scalar, and since the experimental part only applies compressional ultrasonic waves, i.e. $\mathbf{D} = 0$,

$$\begin{aligned} -p &= -3Kv \;+\; 9\beta_1 K\tfrac{1}{2}v^2 \\ \mathbf{T}^D &= \underbrace{2\mu\,\mathbf{D}}_{\text{Linear}} \quad \underbrace{\qquad}_{\text{Nonlinear}} \end{aligned} \tag{7.47}$$

where $K = \lambda + \frac{2}{3}\mu$ is the bulk modulus, which depends on the Lamé constants.

The definition of the compressional nonlinearity stems from the Taylor expansion of pressure p in Equation 7.36 with respect to volumetric strain v, where the order zero term is zero, the first order term is the linear elastic one proportional to v and the second order term is depends on $\frac{1}{2}v^2$, where β_1 is defined to capture the volumetric constitutive nonlinearity as a consequence of the clapping nonlinearity due to the change of volume during its closing

and opening. Note that this definition of nonlinearity parameter β_1 should not be confused by that used by other authors who expand the compressibility as $K\{v\} = K + 3\beta K v$.

Combining equations (7.45), (7.46) and (9.47), and recalling that $\mathbf{D} = 0$,

$$\mathbf{T} = -K\text{tr}\mathbf{E}\mathbf{I} - \frac{\beta_1 K}{2}(\text{tr}\mathbf{E}^1)^2\mathbf{I}_2 \tag{7.48}$$

which compared to the general form (7.43), allows one to establish that the nonlinear properties are

$$\mathcal{A}_1 = 0, \qquad \mathcal{B}_1 = 0, \qquad \mathcal{C}_1 = -\beta_1\frac{(3\lambda^1 + 2\mu^1)}{6} \tag{7.49}$$

and as such we find that

$$\mathbf{T}^1_{NL}(\mathbf{E}^1) = \mathcal{C}_1(\text{tr}\mathbf{E}^1)^2\mathbf{I}_2. \tag{7.50}$$

The inclusion is simplified to isotropic because the transverse projected area of the penny-shaped spheroid vanishes, and its contribution to the transverse stress components is zero. Therefore, the anisotropic terms of the crack behavior inside the inclusion are negligible for the purpose of the homogenization. The first consequence is that Poisson's ratio is assumed to stay invariant under the presence of the micro-crack, and therefore both Lamé constants behave following Equation 7.41, so that,

$$\lambda_1 = \frac{1}{2}\lambda_0, \qquad \mu_1 = \frac{1}{2}\mu_0 \tag{7.51}$$

7.3 Effective acoustic nonlinearity

Given that we now have a model for the nonlinear behavior of the cracks, let us use this in order to determine the effective nonlinear behavior of the cracked material. For conciseness and computational ease we introduce the notation

$$\mathbf{X} = [(\mathbf{I} + \mathbf{H}\boldsymbol{\mathcal{G}}) + \alpha\boldsymbol{\mathcal{G}}]^{-1} \tag{7.52}$$

together with $\mathbf{Y} = \boldsymbol{\mathcal{G}}\mathbf{X}$ and $\mathbf{Z} = \mathbf{Y}\mathbf{S}\mathbf{D}^0$ which we note both depend on α as well as the effective linear elastic moduli $\mathbf{C}^* = \mathbf{C}^0\,(\mathbf{I} - \alpha\mathbf{Y})$. Referring to (7.34) and (7.50) we can then write

$$\begin{aligned}\boldsymbol{\mathcal{G}}\boldsymbol{\mathcal{U}}(\bar{\mathbf{E}}) &= \mathbf{Z}\tilde{\mathbf{T}}^1_{NL}\{\mathbf{X}\bar{\mathbf{E}}\} \\ &= \mathcal{C}_1(\text{tr}(\mathbf{Y}\bar{\mathbf{E}}))^2\mathbf{Z} : \mathbf{I}_2.\end{aligned} \tag{7.53}$$

The total average stress is written

$$\bar{\mathbf{T}} = \mathbf{C}^*\bar{\mathbf{E}} - \alpha\mathcal{C}_1\mathbf{C}^0(\text{tr}(\mathbf{Y}\bar{\mathbf{E}}))^2\mathbf{Z} : \mathbf{I}_2. \tag{7.54}$$

Importantly note that the same non-zero components of $\mathcal{G}$ are also non-zero in $\mathbf{X}$, $\mathbf{Y}$ and $\mathbf{Z}$. This simplifies the analysis significantly.

Our investigation of nonlinearity focuses on a compressional stress wave propagating in the x_3 direction, with zero lateral stresses. The strains $\bar{E}_{11} = \bar{E}_{22} \neq \bar{E}_{33}$ and all shear strains are zero. We investigate the propagation of longitudinal, compressional waves in the x_3 direction, i.e. the only non-zero stress is $\bar{\mathbf{T}}_{33}$ and the contributions to this stress are therefore from the $\mathbf{Z}_{33kl}$ terms. Given that $Y_{11k\ell} = Y_{22k\ell} = 0$, it is straightforward to show that

$$\bar{E}_{22} = \bar{E}_{11} = -\nu_{A*}\bar{E}_{33} \tag{7.55}$$

where ν_{A*} is known as the (effective) axial Poisson's ratio as determined from the effective linear elastic modulus tensor via

$$\nu_{A*} = \frac{C^*_{1133}}{C^*_{1111} + C^*_{1122}} \tag{7.56}$$

The equation for the tensile/compressive longitudinal stress is rather more complicated thanks to the non-zero components of the tensors introduced above. First note that

$$\begin{aligned} \mathrm{tr}(\mathbf{Y}\bar{\mathbf{E}}) &= Y_{3311}\bar{E}_{11} + Y_{3322}\bar{E}_{22} + Y_{3333}\bar{E}_{33} \\ &= (Y_{3333} - 2\nu_{A*}Y_{3311})\bar{E}_{33} \end{aligned} \tag{7.57}$$

and

$$\begin{aligned} (\mathbf{C}^0\mathbf{Z} : \mathbf{I}_2)_{33} &= C^0_{3311}(Z_{1111} + Z_{1122} + Z_{1133}) + C^0_{3333}(2Z_{3311} + Z_{3333}) \\ &\simeq C^0_{3333}(2Z_{3311} + Z_{3333}). \end{aligned} \tag{7.58}$$

Then, eliminating $\bar{\mathbf{E}}_{11}$ via (7.55) we find

$$\begin{aligned} \bar{T}_{33} &= \mathcal{E}_*\bar{E}_{33} - \beta_*\mathcal{E}_*\bar{E}^2_{33} \\ &= \mathcal{E}_*(1 - \beta_*\bar{E}_{33})\bar{E}_{33} \end{aligned} \tag{7.59}$$

where β_* defines the effective nonlinear parameter that characterizes the compressional nonlinearity in direction 3, and the effective linear elastic Young's modulus is

$$\mathcal{E}_* = (C^*_{3333} - 2C^*_{3311}\nu_{A*}) \tag{7.60}$$

and the effective nonlinear parameter β_* takes the form

$$\beta_* = \mathcal{C}_1\frac{\alpha}{\mathcal{E}_*}(Y_{3333} - 2\nu_{A*}Y_{3311})^2C^0_{3333}(2Z_{3311} + Z_{3333}) \tag{7.61}$$

where $\mathcal{C}_1$ is the Landau parameter of the inclusion derived in Equation 7.49.

Contractions and inversions of transversely isotropic tensors within the tensors **X**, **Y** and **Z** are best carried out in a symbolic package such as Mathematica where such operations can be done straightforwardly by defining the operations with respect to the components of the Hill basis [261].

7.4 Numerical example

A few figures are exposed to understand the relationships between the effective acoustic nonlinearity β_*, the density of microcracks α and the nonlinearity of the inclusion β_1. Note that the nonlinear parameter β_1 depends upon the maximum volumetric strain v_{max} according to Equation 7.42, which can be quantified experimentally. Contractions and inversions of transversely isotropic tensors within the tensors **X**, **Y** and **Z** are computed using Matlab (The MathWorks, Inc., Natick, Massachusetts, United States).

First, we briefly describe how the maximal strain can be calculated. Consider a bone sample immersed in water, which is interrogated by nonlinear ultrasound at a given central frequency f. The incoming pressure p_w in water at the back of the sample is registered by a needle hydrophone. The water displacement U_w can be obtained as,

$$U_w = 3\frac{p_w}{\rho_w c_w 2\pi f} \tag{7.62}$$

where ρ_w and c_w are the density and velocity of water, respectively. Considering that the water gap between the specimen and the hydrophone is small (that is, the water attenuation is negligible), the displacement of the particles in the specimen is obtained as,

$$U_s = \frac{U_w}{T_{sw}} \tag{7.63}$$

where T_{sw} denotes the transmission coefficient from bone to water, defined as,

$$T_{sw} = \frac{2Z_w}{Z_s + Z_w} \tag{7.64}$$

where $Z_i = \rho_i c_i$, with $i = w, s$ is the impedance of a material i. The displacement field in the sample is, as a first approximation, of the form,

$$U(x,t) = U_s \sin(k_s x - \omega t) \tag{7.65}$$

where $k_s = \omega / c_s$ is the wave number. The strain field is the derivative of the displacement field with respect to the x-coordinate along which ultrasound propagates,

$$E_{33}(x,t) = U_s k_s \cos(k_s x - \omega t) \tag{7.66}$$

and thus, the maximal strain is obtained when $\cos(k_s x - \omega t) = 1$, that is $v_{max} = |-\frac{1}{3}E_{33,max}| = \frac{1}{3}U_s k_s$. Table 1 summarizes the values of the obtained variables for a measured pressure $p_w = 85$ [kPa].

Property		Value	
Displacement in water	U_w	40.5	[nm]
Displacement in sample	U_s	75	[nm]
Frequency	f	666.67	[kHz]
Maximum strain in sample	v^{max}	$2.64 \cdot 10^{-5}$	
Lamé constants	(λ_1, μ_1)	$(10, 2.5) \cdot 10^9$	[Pa]
Density	ρ	$1.8 \cdot 10^3$	[kg/m^3]
Nonlinearity of inclusion	β_1	$3.8 \cdot 10^4$	
Landau coefficient of inclusion	$\mathcal{C}_1$	$22 \cdot 10^{13}$	[Pa]

Table 7.1: Elastic parameters of the inclusion.

Figure 7.6 shows the relationship between the effective acoustic nonlinearity and density of micro-cracks.

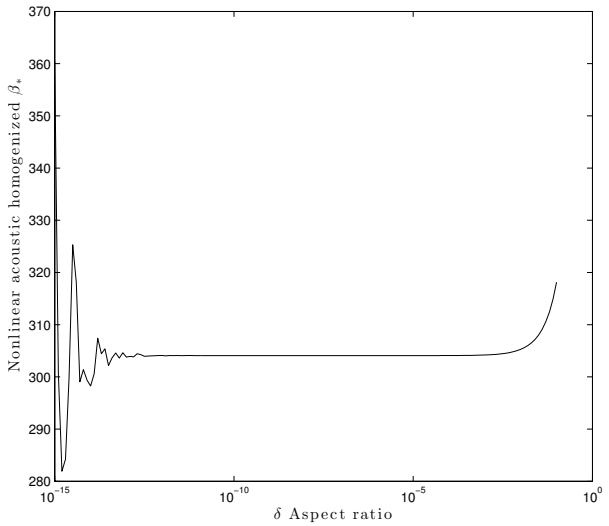

Figure 7.5: Convergence study of the effective acoustic nonlinearity depending on the choice of aspect ratio of the penny shaped inclusions for estimating the limit numerically. Values between $\delta = 10^{-5}$ and $\delta = 10^{-10}$ are chosen.

Figure 7.8 shows the relationship between first effective Lamé lambda parameter and density of micro-cracks.

The main contribution of this chapter resides on the explanation of microdamage as source of nonlinearity with providing a experimental technique that allows quantify the density of microcracks in terms of classical nonlinear effective acoustic parameter.

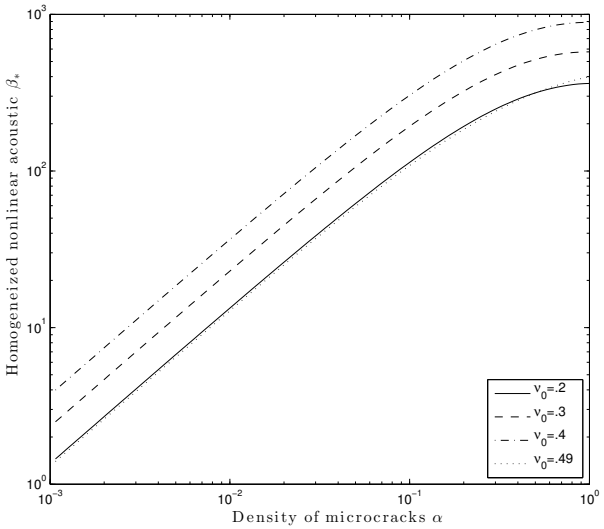

Figure 7.6: Relationship between effective acoustic nonlinearity and density of microcracks.

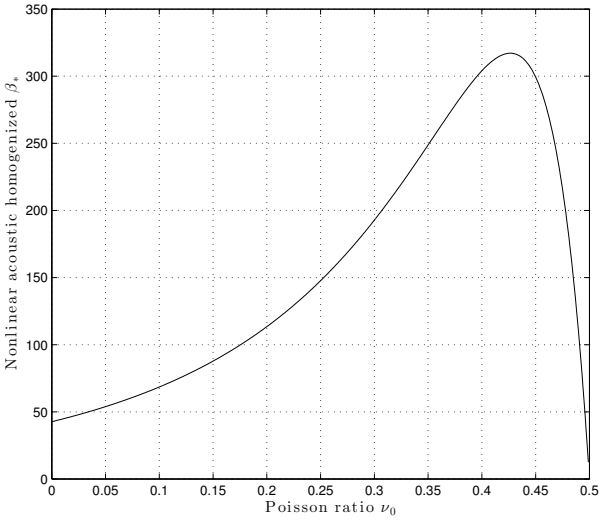

Figure 7.7: Relationship between effective acoustic nonlinearity and Poisson's coefficients

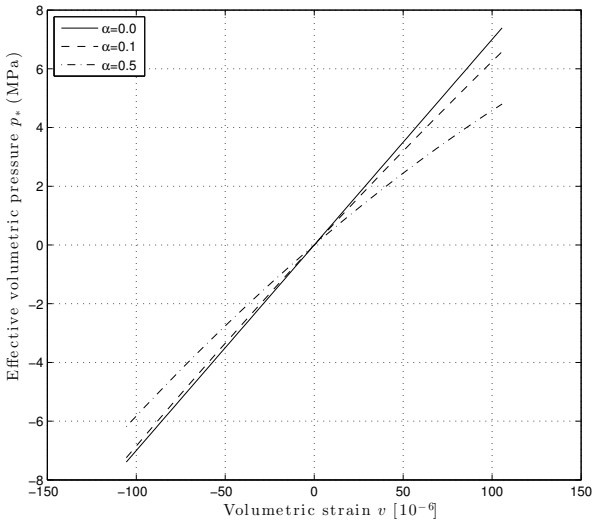

Figure 7.8: Relationship between first effective Lamé parameter and density of micro-cracks.

Eléctrico éxtasis. Movimiento continuo en alta frecuencia, temblor vertical que se sumerge en la clarividencia, ardor, temblor de viva luz.

Tientos de erótica celeste.
Val del Omar-Lagartija Nick, 1993

Part III

RESULTS: EXPERIMENTAL CONTRIBUTIONS

8

Nonlinear mixing to measure acoustic nonlinearities of first order

This Chapter explores all the possibilities of mixing acoustic plane waves from analytical results to experimental procedure to derive nonlinear acoustic parameters extended in Chapter 6. The main aim is to solve the nonlinear acoustic equation extended in 3D by perturbation method and explore the feasibility of measuring these new parameters with ultrasound technology.

8.1 Analytical results

As in Chapter 6, where the linear regime of three dimensional linear wave equation solutions were validated, the perturbation method is formulated with the same framework:

$$u_i = u_i^{(0)} + u_i^{(1)} + \dots \tag{8.1}$$

where $u^{(0)}$ and $u^{(1)}$ denote the zero-order and first-order perturbation solutions, respectively. The zero-order perturbation solution corresponds to the fundamental solution of the linear wave equation (that is, when $\beta = 0$). The first-order perturbation solution is denoted by $u^{(1)}$. Since the effect of the nonlinear term β is small, an approximate solution can be obtained by iteration. Then, the next subsections describe the whole list of detailed cases where the waves interacting inside a material.

8.1.1 Collinear Mixing

This case is presented when two plane waves propagating simultaneously in the same direction and are considering in a semi-infinite elastic layer, the latter is given as,

$$
\begin{aligned}
u_1^{(0)} &= A_1 \cos\left(\omega_1\left(\frac{x_1}{c_p}\right) - t\right) + A_2 \cos\left(\omega_2\left(\frac{x_2}{c_p}\right) - t\right) \\
u_2^{(0)} &= 0 \\
u_3^{(0)} &= 0
\end{aligned} \tag{8.2}
$$

where A_1 and A_2 are the constant amplitudes of the plane waves, c_p, is the velocity of compressional waves, and ω_1 and ω_2 are the angular frequencies. Let us then consider the first-order perturbation equation,

$$
\begin{aligned}
u_1^{(1)} &= B_a x_1 \cos\left(\omega_a\left(\frac{x_1}{c_p}\right) - t\right) + B_b x_1 \cos\left(\omega_b\left(\frac{x_1}{c_p}\right) - t\right) \\
&\quad + B_c x_1 \cos\left(\omega_c\left(\frac{x_1}{c_p}\right) - t\right) + B_d x_1 \cos\left(\omega_d\left(\frac{x_1}{c_p}\right) - t\right) \\
&\quad + B_e x_1 \cos\left(\omega_e\left(\frac{x_1}{c_p}\right) - t\right) + B_f x_1 \sin\left(\omega_f\left(\frac{x_1}{c_p}\right) - t\right) \\
&\quad + B_g x_1 \cos\left(\omega_g\left(\frac{x_1}{c_p}\right) - t\right) + B_h x_1 \sin\left(\omega_h\left(\frac{x_1}{c_p}\right) - t\right) \\
u_2^{(1)} &= 0 \\
u_3^{(1)} &= 0
\end{aligned} \tag{8.3}
$$

Where $|u_{\omega_1}^{(1)}| = B_a x_1$ is the amplitude of the second harmonic, B_a, B_b, B_c, B_d, B_e, B_f, B_g and B_h are the amplitudes of the first order of pertubation, the frequencies for each cases are ω_a, ω_b, ω_c, ω_d, ω_e, ω_f, ω_g and ω_h. Once established zero and first order of perturbation, first order is expanded as follows,

$$
\begin{aligned}
u_L^{(1)} &= \frac{1}{3c_p} 2(3K + 4\mu)\left(2B_1\omega_1 \sin\left(2\omega_1\left(\frac{x_1}{c_p} - t\right)\right)\right) \\
&\quad + \frac{1}{3c_p} 2(3K + 4\mu)\left(2B_2\omega_2 \sin\left(2\omega_2\left(\frac{x_1}{c_p} - t\right)\right)\right) \\
&\quad + \frac{1}{3c_p} 2(3K + 4\mu)\left(B_3\left(\omega_1 + \omega_2\right) \sin\left(\omega_1 + \omega_2\right)\left(\frac{x_1}{c_p} - t\right)\right) \\
&\quad + \frac{1}{3c_p} 2(3K + 4\mu)\left(B_4\left(\omega_1 - \omega_2\right) \sin\left(\left(\omega_1 - \omega_2\right)\left(\frac{x_1}{c_p}\right) - t\right)\right)
\end{aligned} \tag{8.4}
$$

And nonlinear zero-order in nonlinear part results,

$$
\begin{aligned}
u_{NL}^{(0)} &= \frac{1}{9c_p^3}(9(1+12\beta^{dp}+9\beta^{vp})K+4(3-4\beta^{cs}+8\beta^{ds})\mu) \\
&\left(A_1\omega_1^2\cos\left(\omega_1\left(\frac{x_1}{c_p}-t\right)\right)+A_2\omega_2^2\cos\left(\omega_1\left(\frac{x_1}{c_p}-t\right)\right)\right) \\
&\left(A_1\omega_1\sin\left(\omega_1\left(\frac{x_1}{c_p}-t\right)\right)+A_2\omega_1\sin\left(\omega_1\left(\frac{x_1}{c_p}-t\right)\right)\right)
\end{aligned} \tag{8.5}
$$

Expanding the last equation by the product generated in terms of first wave and second compressional waves with both amplitudes and frequencies it results,

$$
u_{NLEXP}^{(0)} = \frac{1}{9c_p^3}(9(1+12\beta^{dp}+9\beta^{vp})K+4(3-4\beta^{cs}+8\beta^{ds})\mu)F(x_1,t) \tag{8.6}
$$

where,

$$
\begin{aligned}
F(x_1,t) &= A_1^2\omega_1^3\cos\left(\omega_1\left(\frac{x_1}{c_p}-t\right)\right)\sin\left(\omega_1\left(\frac{x_1}{c_p}-t\right)\right) \\
&+A_1A_2\omega_1\omega_2^2\cos\left(\omega_2\left(\frac{x_1}{c_p}-t\right)\right)\sin\left(\omega_1\left(\frac{x_1}{c_p}-t\right)\right) \\
&+A_1A_2\omega_1^2\omega_2\cos\left(\omega_1\left(\frac{x_1}{c_p}-t\right)\right)\sin\left(\omega_2\left(\frac{x_1}{c_p}-t\right)\right) \\
&+A_2^2\omega_2^3\cos\left(\omega_2\left(\frac{x_1}{c_p}-t\right)\right)\sin\left(\omega_2\left(\frac{x_1}{c_p}-t\right)\right)
\end{aligned} \tag{8.7}
$$

This result validates the analytical procedure developed in Chapter 6, where the nonlinear mixing is introduced from a classical point of view. In that case $\omega_2-\omega_1$ is neglected by the deduction and it is also possible to be calculated when $u^{(0)}$ is defined as in Equation 8.3, it corresponds to four last terms. Note that trigonometric relations, of sum and difference of two different angles are introduced expanding the products and considering the corresponding factors of each amplitude [263]. Both cases are detailed in Table 8.1 note that $\omega_2-\omega_1$ is introduced with 90^o phase shift.

And then, β is related to the four nonlinear classical nonlinear parameters considering each factor of the sum and comparing as follows,

Combination	B_i	ω_i
a	A_1^2	$2\omega_1$
b	A_2^2	$2\omega_2$
c	A_1A_2	$\omega_1+\omega_2$
d	$\nexists$	$\nexists$
e	A_1^2	$2\omega_1$
f	A_2^2	$2\omega_1$
g	$\nexists$	$\nexists$
h	A_1A_2	$\omega_2-\omega_1$

Table 8.1: The corresponding factors of each amplitude for zero and first order of perturbation

$$\begin{aligned}
\frac{B_a c_p^3}{x_1 A_1^2 \omega_1} &= \frac{1}{9}(9(12\beta^{dp}+9\beta^{vp})K+4(-4\beta^{cs}+8\beta^{ds})\mu) \\
\frac{B_b c_p^3}{x_1 A_2^2 \omega_2} &= \frac{1}{9}(9(12\beta^{dp}+9\beta^{vp})K+4(-4\beta^{cs}+8\beta^{ds})\mu) \\
\frac{B_c c_p^3}{x_1 A_1 A_2(\omega_1+\omega_2)} &= \frac{1}{9}(9(12\beta^{dp}+9\beta^{vp})K+4(-4\beta^{cs}+8\beta^{ds})\mu) \\
\frac{B_h c_p^3}{x_1 A_1 A_2(\omega_2-\omega_1)} &= \frac{1}{9}(9(12\beta^{dp}+9\beta^{vp})K+4(-4\beta^{cs}+8\beta^{ds})\mu)
\end{aligned} \tag{8.8}$$

In each case, β is the classical parameter equal to the left part of the equations i. e. $\beta = \frac{B_a c_p^3}{x_1 A_1^2 \omega_1}$, and if we want to calculated the right part of the equations with the nonlinear acoustic parameter components an experimental design should be considered.

For the liquid case i.e calculating the nonlinearity of water as in the last section, shear modulus is neglected $\mu = 0$, and the Equation 8.8 is

$$\begin{aligned}
\frac{|u_{2\omega_1}^{(1)}|c_p^3}{A_1^2\omega_1} &= (12\beta^{dp}+9\beta^{vp})K \\
\frac{|u_{2\omega_2}^{(1)}|c_p^3}{A_2^2\omega_2} &= (12\beta^{dp}+9\beta^{vp})K \\
\frac{|u_{\omega_1+\omega_2}^{(1)}|c_p^3}{A_1A_2(\omega_1+\omega_2)} &= (12\beta^{dp}+9\beta^{vp})K \\
\frac{|u_{\omega_1-\omega_2}^{(1)}|c_p^3}{A_1A_2(\omega_2-\omega_1)} &= (12\beta^{dp}+9\beta^{vp})K
\end{aligned} \tag{8.9}$$

Nonlinear effect is influenced by a disaggregation that could be decomposed in volumetric pressure and deviatoric pressure. Note that this case of collinear mixing in water has been detailed as in the last section section of this chapter. A single transmitter setup is explored and nonlinear acoustic parameter of water is calculated.

8.1.2 *Noncollinear Mixing: P-P interaction*

This case is presented when two compressional waves are considering in a semi-infinite elastic layer, in an angle θ, the latter is given as,

$$\begin{aligned} u_1^{(0)} &= A_1 \cos\left(\omega_1\left(\frac{x_1}{c_p}\right) - t\right) + A_2 \cos\theta \cos\omega_2\left(\frac{(\cos x_1\theta + x_2 \sin\theta)}{c_p} - t\right) \\ u_2^{(0)} &= A_2 \sin\theta \cos\omega_2\left(\frac{(x_1 \cos\theta + x_2 \sin\theta)}{c_p} - t\right) \\ u_3^{(0)} &= 0 \end{aligned} \tag{8.10}$$

where A_1 and A_2 are the constant amplitudes of the plane waves, c_p, is the velocity of compressional waves, and ω_1 and ω_2 are the angular frequencies. Let us then consider the first-order perturbation equation,

$$\begin{aligned} u_1^{(1)} &= B_a\left((x_1\cos\alpha_1 + x_2\sin\alpha_1)\cos\alpha_1 \sin\omega_a\left(\frac{(x_1\cos\alpha_1 + x_2\sin\alpha_1)}{c_p} - t\right)\right) \\ &\quad + B_b\left((x_1\cos\alpha_2 + x_2\sin\alpha_2)\cos\alpha_2 \sin\omega_b\left(\frac{(x_1\cos\alpha_2 + x_2\sin\alpha_2)}{c_p} - t\right)\right) \\ &\quad + B_c\left((x_1\cos\alpha_3 + x_2\sin\alpha_3)\cos\alpha_3 \sin\omega_c\left(\frac{(x_1\cos\alpha_3 + x_2\sin\alpha_3)}{c_p} - t\right)\right) \\ &\quad + B_d\left((x_1\cos\alpha_4 + x_2\sin\alpha_4)\cos\alpha_4 \sin\omega_d\left(\frac{(x_1\cos\alpha_4 + x_2\sin\alpha_4)}{c_p} - t\right)\right) \\ u_2^{(1)} &= B_e\left((x_1\cos\alpha_1 + x_2\sin\alpha_1)\sin\alpha_1 \sin\omega_e\left(\frac{(x_1\cos\alpha_1 + x_2\sin\alpha_1)}{c_p} - t\right)\right) \\ &\quad + B_f\left((x_1\cos\alpha_2 + x_2\sin\alpha_2)\sin\alpha_2 \sin\omega_f\left(\frac{(x_1\cos\alpha_2 + x_2\sin\alpha_2)}{c_p} - t\right)\right) \\ &\quad + B_g\left((x_1\cos\alpha_3 + x_2\sin\alpha_3)\sin\alpha_3 \sin\omega_g\left(\frac{(x_1\cos\alpha_3 + x_2\sin\alpha_3)}{c_p} - t\right)\right) \\ &\quad + B_h\left((x_1\cos\alpha_4 + x_2\sin\alpha_4)\sin\alpha_4 \sin\omega_h\left(\frac{(x_1\cos\alpha_4 + x_2\sin\alpha_4)}{c_p} - t\right)\right) \\ u_3^{(1)} &= 0 \end{aligned} \tag{8.11}$$

Once established zero and first order of perturbation, $u_{NL}^{(0)}$ and $u_L^{(1)}$, respectively, the first order it is expanded as follows,

$$
\begin{aligned}
u_L^{(1)} &= \frac{1}{3c_p} 2(3K+4\mu)\left(-B_a\omega_a\cos\alpha_1\cos\left(\omega_a\left(\frac{(x_1\cos\alpha_a+x_2\sin\alpha_a)}{c_p}-t\right)\right)\right.\\
&+\left(-B_b\omega_2\cos\alpha_b\cos\left(2\omega_b\left(\frac{(x_1\cos\alpha_b+x_2\sin\alpha_b)}{c_p}-t\right)\right)\right)\\
&+\left(-B_c(\omega_c)\cos\alpha_c\cos\left((\omega_c)\left(\frac{(x_1\cos\alpha_c+x_2\sin\alpha_c)}{c_p}-t\right)\right)\right)\\
&+\left.\left(-B_h(\omega_h)\cos\alpha_h\cos\left((\omega_h)\left(\frac{(x_1\cos\alpha_h+x_2\sin\alpha_h)}{c_p}-t\right)\right)\right)\right)
\end{aligned}
\tag{8.12}
$$

And nonlinear zero-order in nonlinear part results,

$$
\begin{aligned}
u_{NL}^{(0)} &= \frac{1}{18c_p^3}\left(A_1\omega_1^2\left(A_1(9(1+12\beta^{dp}+9\beta^{vp})K+4(3-4\beta^{cs}+8\beta^{ds})\mu)\right.\right.\\
&\left(\omega_1\sin\left(2\omega_1\left(\frac{x_1}{c_p}-t\right)\right)+A_2\omega_2\cos\left(\omega_1\left(\frac{x_1}{c_p}-t\right)\right)\right)\\
&(9(1+6\beta^{dp}+18\beta^{vp})K+4(3-5\beta^{cs}+4\beta^{ds})\mu\\
&+3((3+54\beta^{dp})K-4(-1+\beta^{cs}-4\beta^{ds})\mu)\cos 2\theta)\\
&\sin\left(\omega_2\left(\frac{(x_1\cos\theta+x_2\sin\theta)}{c_p}-t\right)\right)\Big)\\
&+(A_2\omega_2^2\cos\theta)\left(A_1\omega_1(9(1+6\beta^{dp}+18\beta^{vp})K+(21-32\beta^{cs}+28\beta^{ds})\mu\right.\\
&+3(3K+54\beta^{dp}K+\mu+12\beta^{ds}\mu)\cos 2\theta)\\
&\cos\left(\omega_2\left(\frac{(x_1\cos\theta+x_2\sin\theta)}{c_p}-t\right)\right)\sin\left(2\omega_1\left(\frac{x_1}{c_p}-t\right)\right)\\
&+\Big(A_2(9(1+12\beta^{dp}+9\beta^{vp})K)\\
&\left.\left.+(4(3-4\beta^{cs}+8\beta^{ds})\mu)\omega_2\sin\left(2\omega_2\left(\frac{(x_1\cos\theta+x_2\sin\theta)}{c_p}-t\right)\right)\right)\right)\Big)
\end{aligned}
\tag{8.13}
$$

The amplitudes coincides with the collinear mixing case, expanding products and using of trigonometric relations, as in Table 8.1. The non collinear mixing is feasible considering $\alpha_1 = 0$ and $\alpha_2 = \theta$ in the sum of frequencies $\omega_1 + \omega_2$, the direction of harmonics coincides with the advance of wave front. Note that if $\alpha_3 = 0$ the collinear case is recovered. Analogously occurs, when $\omega_1 - \omega_2$ is expanded from $\alpha_4 = 0$.

And then, β is related to the four nonlinear classical nonlinear parameters considering each factor of the sum and comparing as follows,

$$
\begin{aligned}
\frac{B_a c_p^3}{x_1 A_1^2 \omega_1} &= \frac{1}{18}(9(12\beta^{dp}+9\beta^{vp})K+4(-4\beta^{cs}+8\beta^{ds})\mu) \\
\frac{B_b c_p^3}{x_1 A_2^2 \omega_2} &= \frac{1}{18}((9(12\beta^{dp}+9\beta^{vp})K)+(4(-4\beta^{cs}+8\beta^{ds})\mu))\cos\theta \\
\frac{B_c c_p^3}{x_1 A_1 A_2(\omega_1+\omega_2)} &= \frac{1}{18}(9(12\beta^{dp}+9\beta^{vp})K+4(-4\beta^{cs}+8\beta^{ds})\mu \\
&\quad +(3(54\beta^{dp})K-4(+\beta^{cs}-4\beta^{ds})\mu)\cos 2\theta \\
&\quad +(9(6\beta^{dp}+18\beta^{vp})K+(-32\beta^{cs}+28\beta^{ds})\mu) \\
&\quad +(3(54\beta^{dp}K+\mu+12\beta^{ds}))\cos 2\theta) \\
\frac{B_h c_p^3}{x_1 A_1 A_2(\omega_2-\omega_1)} &= \frac{1}{18}(9(12\beta^{dp}+9\beta^{vp})K+4(-4\beta^{cs}+8\beta^{ds})\mu \\
&\quad +(3(54\beta^{dp})K-4(\beta^{cs}-4\beta^{ds})\mu)\cos 2\theta \\
&\quad +(9(6\beta^{dp}+18\beta^{vp})K+(-32\beta^{cs}+28\beta^{ds})\mu) \\
&\quad +(3(54\beta^{dp}K+12\beta^{ds}\mu))\cos 2\theta)
\end{aligned}
\tag{8.14}
$$

Note that this case is not posible experimentally due to the angle extraction is imaginary, it should be introduced modes conversion and $u_{NL}^{(0)}$ as an S-wave. This is detailed in the next section.

8.1.3 Noncollinear Mixing: P-S interaction

This case is presented when two waves one transversal and other compressional are considering interacting in a semi-infinite elastic layer, in an angle θ, the latter is given as,

$$
\begin{aligned}
u_1^{(0)} &= A_1\cos\left(\omega_1\left(\frac{x_1}{c_p}-t\right)\right)-A_h\sin\theta\cos\left(\omega_2\left(\frac{(x_1\cos\theta+x_2\sin\theta)}{c_s}-t\right)\right) \\
u_2^{(0)} &= A_h\cos\theta\cos\left(\omega_2\left(\frac{(x_1\cos\theta+x_2\sin\theta)}{c_s}-t\right)\right) \\
u_3^{(0)} &= 0
\end{aligned}
\tag{8.15}
$$

where A_1 and A_h are the constant amplitudes of the compressional and transversal waves respectively, c_p and c_s, is the velocity of compressional and transversal waves respectively, and ω_1 and ω_2 are the angular frequencies. Then, let us then consider the first-order perturbation equation,

$$
\begin{aligned}
u_1^{(1)} &= B_{ha}(x_1\cos\alpha_a + x_2\sin\alpha_a)\cos\alpha_a\cos\left(\omega_a\left(\frac{(x_1\cos\alpha_a + x_2\sin\alpha_a)}{c_p} - t\right)\right) \\
&\quad -B_{hb}(x_1\cos\alpha_b + x_2\sin\alpha_b)\sin\alpha_b\cos\left(\omega_b\left(\frac{(x_1\cos\alpha_b + x_2\sin\alpha_b)}{c_s} - t\right)\right) \\
u_2^{(1)} &= B_{ha}(x_1\cos\alpha_a + x_2\sin\alpha_a)\sin\alpha_a\cos\left(\omega_a\left(\frac{(x_1\cos\alpha_a + x_2\sin\alpha_a)}{c_p} - t\right)\right) \\
&\quad +B_{hb}(x_1\cos\alpha_b + x_2\sin\alpha_b)\cos\alpha_b\cos\left(\omega_b\left(\frac{(x_1\cos\alpha_b + x_2\sin\alpha_b)}{c_s} - t\right)\right) \\
u_3^{(1)} &= 0
\end{aligned} \tag{8.16}
$$

Once established zero and first order of perturbation, $u_N^{(0)}L$ and $u_L^{(1)}$, respectively, the first order it is expanded as follows,

$$
\begin{aligned}
u_L^{(1)} &= \frac{1}{3c_p^2c_s^2}\left(B_{ha}c_s^2(3K+4\mu)\omega_a^2x_1\cos^4\alpha_a\cos\left(\omega_a\left(\frac{(x_1\cos\alpha_a + x_2\sin\alpha_a)}{c_p} - t\right)\right)\right. \\
&\quad -\frac{1}{2}B_{ha}c_s^2\omega_a^2x_1\cos^2\alpha_a(2(3K+4\mu) + (3K+4\mu)\cos 2\alpha_a) \\
&\quad \cos\left(\omega_a\left(\frac{(x_1\cos\alpha_a + x_2\sin\alpha_a)}{c_p} - t\right)\right) \\
&\quad +B_{ha}c_s^2(3K+4\mu)\omega_a\cos^3\alpha_a\left(\omega_ax_2\cos\left(\omega_a\left(\frac{(x_1\cos\alpha_a + x_2\sin\alpha_a)}{c_p} - t\right)\right)\right. \\
&\quad \left.+2c_p\sin\left(\omega_a\left(\frac{(x_1\cos\alpha_a + x_2\sin\alpha_a)}{c_p} - t\right)\right)\right) \\
&\quad +B_{ha}c_s^2\omega_a\cos\alpha_a\sin\alpha_a\left(\omega_ax_2\cos\left(\omega_a\left(\frac{(x_1\cos\alpha_a + x_2\sin\alpha_a)}{c_p} - t\right)\right)\right. \\
&\quad \left.(-3K-4\mu+(3K+4\mu)\sin^2\alpha_a) + 2c_p(3K+4\mu)\sin\left(\omega_a\left(\frac{(x_1\cos\alpha_a + x_2\sin\alpha_a)}{c_p} - t\right)\right)\right) \\
&\quad \left.+3B_{hb}c_p^2\omega_b\sin\alpha_b\left(-2c_s\mu\sin\left(\omega_b\left(\frac{(x_1\cos\alpha_b + x_2\sin\alpha_b)}{c_s} - t\right)\right)\right)\right)
\end{aligned}
$$

And nonlinear zero-order of perturbation part results,

$$
\begin{aligned}
u_{NL}^{(0)} &= \frac{1}{18c_p^3}\left(A_1^2(9(1+12\beta^{dp}+2\beta^{ds})K+4(3-4\beta^{cs}+8\beta^{ds})\mu)\omega_1^3\sin\left(2\omega_1\left(\frac{x_1}{c_s}-t\right)\right)\right.\\
&+\frac{1}{c_s^3}3A_hc_p\omega_2\left(-A_1c_pc_s\omega_1\omega_2((3+54\beta^{dp})K+(7-4\beta^{cs}+8\beta^{ds})\mu\right.\\
&+((3+54\beta^{dp})K+\mu+12\beta^{ds}\mu)\cos 2\theta)\cos\left(\omega_2\left(\frac{(x_1\cos\theta+x_1\sin\theta)}{c_s}-t\right)\right)\\
&\sin\left(\omega_1\left(\frac{x_1}{c_p}-t\right)\right)\sin\theta\\
&-A_1c_s^2((3+54\beta^{dp})K-4(-1+\beta^{cs}-4\beta^{ds})\mu)\omega_1^2\\
&\cos\left(\omega_1\left(\frac{x_1}{c_p}-t\right)\right)\sin 2\theta\sin\left(\omega_2\left(\frac{(x_1\cos\theta+x_2\sin\theta)}{c_s}-t\right)\right)+\\
&\left.\left.+A_hc_p^2(3K+27\beta^{dp}K+4\mu+6\beta^{ds}\mu)\omega_2^2\cos\theta\sin\left(2\omega_2\left(\frac{(x_1\cos\theta+x_2\sin\theta)}{c_s}-t\right)\right)\right)\right)
\end{aligned}
\tag{8.17}
$$

Then, the amplitudes are described as in Table **??**, and β is related to the four nonlinear classical nonlinear parameters considering each factor of the sum and comparing as follows,

$$
\begin{aligned}
\frac{B_ac_p^3}{x_1A_1^2\omega_1} &= \frac{1}{18}(9(12\beta^{dp}+9\beta^{vp})K+4(-4\beta^{cs}+8\beta^{ds})\mu)\\
\frac{B_bc_s^3}{x_1A_2^2\omega_2} &= \frac{1}{18}(27\beta^{dp}K+6\beta^{ds}\mu)\cos\theta\\
\frac{B_c}{x_1A_1A_2(\omega_1+\omega_2)} &= \frac{1}{18}\left(3\frac{1}{c_s^3}A_hc_p(-A_1c_pc_s((3+54\beta^{dp})K+(7-4\beta^{cs}+8\beta^{ds})\mu\right.\\
&+((3+54\beta^{dp})K+\mu+12\beta^{ds}\mu)\cos 2\theta)\\
&\left.-A_1c_s^2((3+54\beta^{dp})K-4(-1+\beta^{cs}-4\beta^{ds})\mu)\sin 2\theta)\right)\\
\frac{B_h}{x_1A_1A_2(\omega_2-\omega_1)} &= \frac{1}{18}\left(\frac{1}{c_s^3}3A_hc_p(-A_1c_pc_s((3+54\beta^{dp})K+(7-4\beta^{cs}+8\beta^{ds})\mu\right.\\
&+((3+54\beta^{dp})K+\mu+12\beta^{ds}\mu)\cos 2\theta)\\
&\left.-A_1c_s^2((3+54\beta^{dp})K-4(-1+\beta^{cs}-4\beta^{ds})\mu)\sin 2\theta)\right)
\end{aligned}
\tag{8.18}
$$

The nature of transversal waves is relevant to obtain transversal nonlinear acoustic parameter and also to disaggregate them. Longitudinal wave is considered as the reference, and transversal wave as a angle θ. Note that the angle determines the interaction where the velocity is coupled to the disaggregation. To explore the nonlinearity from the wave generated after the interaction, is necessary to neglect S or P influence in the $\omega_1+\omega_2$ or $\omega_2-\omega_1$ in order to receive a pure P or S wave depending on conversing modes. Note that the result is the same when comparing S-P interaction. The different angles are detailed in the experimental section.

8.1.4 Noncollinear Mixing: S-S interaction

This case is presented when two transversal waves are considering in a semi-infinite elastic layer, in an angle θ, the latter is given as,

$$\begin{aligned} u_1^{(0)} &= -A_{h2}\sin\theta\cos\left(\omega_2\left(\frac{(x_1\cos\theta + x_2\sin\theta)}{c_s} - t\right)\right) \\ u_2^{(0)} &= A_{h1}\cos\left(\omega_1\left(\frac{x_1}{c_s}\right) - t\right) + A_{h2}\cos\theta\cos\left(\omega_2\left(\frac{(x_1\cos\theta + x_2\sin\theta)}{c_s} - t\right)\right) \\ u_3^{(0)} &= 0 \end{aligned} \tag{8.19}$$

where A_{h1} and A_{h2} are the constant amplitudes of the transversal waves, c_s, is the velocity of transversal waves, and ω_1 and ω_2 are the angular frequencies. Then, let us then consider the first-order perturbation equation,

$$\begin{aligned} u_1^{(1)} &= B_a(x_1\cos\alpha_a + x_2\sin\alpha_a)\cos\alpha_a\cos\left(\omega_a\left(\frac{(x_1\cos\alpha_a + x_2\sin\alpha_a)}{c_p} - t\right)\right) \\ &\quad -B_{hb}(x_1\cos\alpha_b + x_2\sin\alpha_b)\sin\alpha_b\cos\left(\omega_b\left(\frac{(x_1\cos\alpha_b + x_2\sin\alpha_b)}{c_s} - t\right)\right) \\ u_2^{(1)} &= B_a(x_1\cos\alpha_a + x_2\sin\alpha_a)\sin\alpha_a\cos\left(\omega_a\left(\frac{(x_1\cos\alpha_a + x_2\sin\alpha_a)}{c_p} - t\right)\right) \\ &\quad +B_{hb}(x_1\cos\alpha_b + x_2\sin\alpha_b)\cos\alpha_b\cos\left(\omega_b\left(\frac{(x_1\cos\alpha_b + x_2\sin\alpha_b)}{c_s} - t\right)\right) \\ u_3^{(1)} &= 0 \end{aligned} \tag{8.20}$$

Once established zero and first order of perturbation, $u_{NL}^{(0)}$ and $u_{L}^{(1)}$, respectively, the first order is expanded as follows,

$$
\begin{aligned}
u_L^{(1)} &= \frac{1}{3c_p^2c_s^2}\left(B_a c_s^2(3K+4\mu)\omega_a^2 x_1\cos^4\alpha_a\cos\left(\omega_a\left(\frac{(x_1\cos\alpha_a+x_2\sin\alpha_a)}{c_p}-t\right)\right)\right.\\
&-\frac{1}{2}B_a c_s^2\omega_a^2 x_1\cos^2\alpha_a(2(3K+4\mu)+(3K+4\mu)\cos 2\alpha_a)\\
&\cos\left(\omega_a\left(\frac{(x_1\cos\alpha_a+x_2\sin\alpha_a)}{c_s}-t\right)\right)\\
&+B_a c_s^2(3K+4\mu)\omega_a\cos^3\alpha_a\left(\omega_a x_2\cos\left(\omega_a\left(\frac{(x_1\cos\alpha_a+x_2\sin\alpha_a)}{c_s}-t\right)\right)\right.\\
&\left.+2c_p\sin\left(\omega_a\left(\frac{(x_1\cos\alpha_a+x_2\sin\alpha_a)}{c_p}-t\right)\right)\right)\\
&+B_a c_s^2\omega_a\cos\alpha_a\sin\alpha_a\left(\omega_a x_2\cos\left(\omega_a\left(\frac{(x_1\cos\alpha_a+x_2\sin\alpha_a)}{c_s}-t\right)\right)\right.\\
&\left.(-3K-4\mu+(3K+4\mu)\sin^2\alpha_a)+2c_p(3K+4\mu)\sin\left(\omega_a\left(\frac{(x_1\cos\alpha_a+x_2\sin\alpha_a)}{c_p}-t\right)\right)\right)\\
&+3B_{hb}c_p^2\omega_b\sin\alpha_b\left(-2c_s\mu\sin\left(\omega_b\left(\frac{(x_1\cos\alpha_b+x_2\sin\alpha_b)}{c_s}-t\right)\right)\right)\Bigg)
\end{aligned}
\tag{8.21}
$$

And nonlinear zero-order of perturbation part results,

$$
\begin{aligned}
u_{NL}^{(0)} &= \frac{1}{6c_s^3}\left(A_{h1}\omega_1((3K+4\mu)+3(9\beta^{dp}K+2\beta^{ds}\mu)\cos\left(2\omega_1\left(\frac{x_1}{c_p}-t\right)\right)\right.\\
&+\cos\theta A_{h2}\omega_b((3K+4\mu)+3(9\beta^{dp}K+2\beta^{ds}\mu))\sin\left(2\omega_2\left(\frac{(x_1\cos\theta+x_2\sin\theta)}{c_s}-t\right)\right)\\
&+\Big(2A_{h1}A_{h2}(3K+4\mu)\omega_1^2\omega_2\cos^2\theta+\omega_1\omega_2^2A_{h2}A_{h1}\cos\theta(3K+7\mu+(3K+\mu)\cos 2\theta)\\
&+3A_{h1}A_{h2}\omega_1\omega_2^2(9\beta^{dp}K+2\beta^{ds}\mu)(\cos\theta+\cos 3\theta)\\
&\left.+\sin(\omega_1+\omega_2)\left(\left(\frac{x_1}{c_p}-t\right)\right)+\left(2\omega_2\left(\frac{(x_1\cos\theta+x_2\sin\theta)}{c_s}-t\right)\right)\right)\Big)
\end{aligned}
\tag{8.22}
$$

Then, the amplitudes could be relates as in Table 8.1, and β is related to the four nonlinear classical nonlinear parameters considering each factor of the sum and comparing as follows,

$$
\begin{aligned}
\frac{B_a c_s^3}{x_1 A_1^2\omega_1} &= \frac{1}{2}(3(9\beta^{dp}K+2\beta^{ds}\mu))\\
\frac{B_b c_s^3}{x_1 A_2^2\omega_2} &= \frac{1}{2}(3(9\beta^{dp}K+2\beta^{ds}\mu))\\
\frac{B_c c_s^3}{x_1 A_1 A_2(\omega_1+\omega_2)} &= \frac{1}{2}(3(9\beta^{dp}K+2\beta^{ds}\mu)(\cos\theta+\cos 3\theta))\\
\frac{B_h c_s^3}{x_1 A_1 A_2(\omega_2-\omega_1)} &= \frac{1}{2}(3(9\beta^{dp}K+2\beta^{ds}\mu)(\cos\theta+\cos 3\theta))
\end{aligned}
\tag{8.23}
$$

The results of nonlinear acoustic terms is a linear function of nonlinear classical acoustic transversal parameter β^T. Note that even β^{cs} and β^{vp} are neglected after the derivation procedure, due to the volumetric part does not exist in transversal mode. The collinear S-case could be explored too, under this possibility an experimental setup should be considered in a quasifluid media or in a soft tissue. The procedure should be introduced in the same manner of the collinear for P waves interaction with $\theta = 0$, with a T-junction and the experimental configuration of the chapter 9.

8.2 Experimental methodology

The proposed experimental methodology consists of three elements: An (1) experimental setup used to monitor the nonlinear ultrasound-sample interactions using the harmonic generation technique, a (2) semi-analytical approach to extract the linear and nonlinear sample properties from the measurements, and the (3) implementation of the nonlinear acoustic extension model formulated in previous section to estimate the disaggregation of nonlinearity of first order .

In order to validate the sensitivity of the proposed methodology, the experiment has been conducted on four different shape materials of Aluminum beam, with different geometries (see Figure 8.2) has been analyzed. The difference between samples are due to the angle of incidence of two waves θ and the angle after the interaction ψ based on Korneev and Zarembo estudies and modes conversion [38, 264, 5, 265] (see Figures 8.2 and 8.2 and Equations 8.24 and 8.25), where,

$$\left(\frac{\omega_1 \pm \omega_2}{c_a}\right)^2 = \left(\frac{\omega_1}{c_1}\right)^2 + \left(\frac{\omega_2}{c_2}\right)^2 \pm 2\frac{\omega_1}{c_1}\frac{\omega_2}{c_2}\cos\theta \tag{8.24}$$

where c_a is the velocity for the $c_1 \pm c_2$ case or only c_1 or c_2 ergo, transversal or longitudinal plane wave. The case for the angle after the interaction is described as,

$$\tan\psi = \frac{\pm\frac{c_1\omega_2}{c_2\omega_1}\sin\theta}{1 \pm \frac{c_1\omega_2}{c_2\omega_1}\cos\theta} \tag{8.25}$$

Figures 8.2 and 8.2 represents the geometry of the four shapes design when the different propagation of waves with modes conversion are considered.

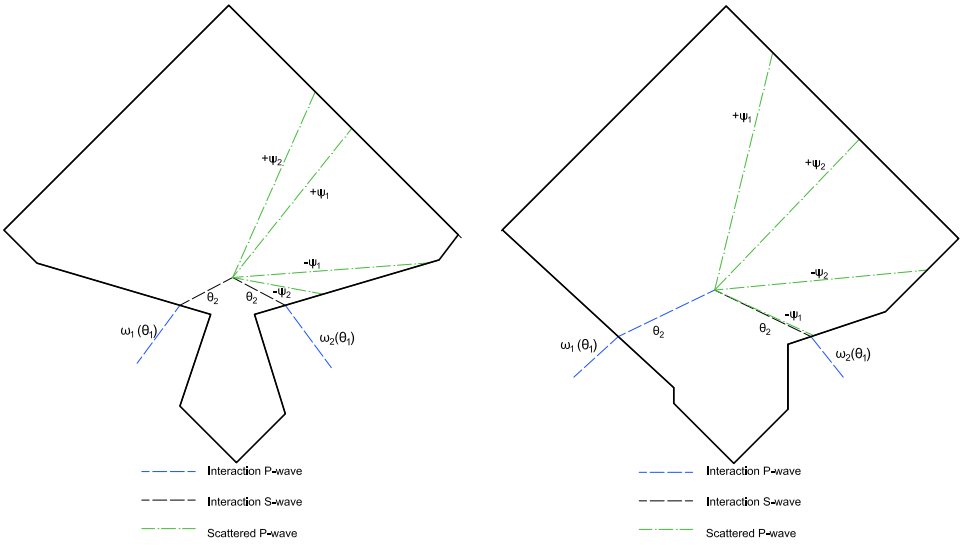

Figure 8.1: Four shapes of aluminium with the calculation of angles for each case of interaction for S with S and P with S, respectively

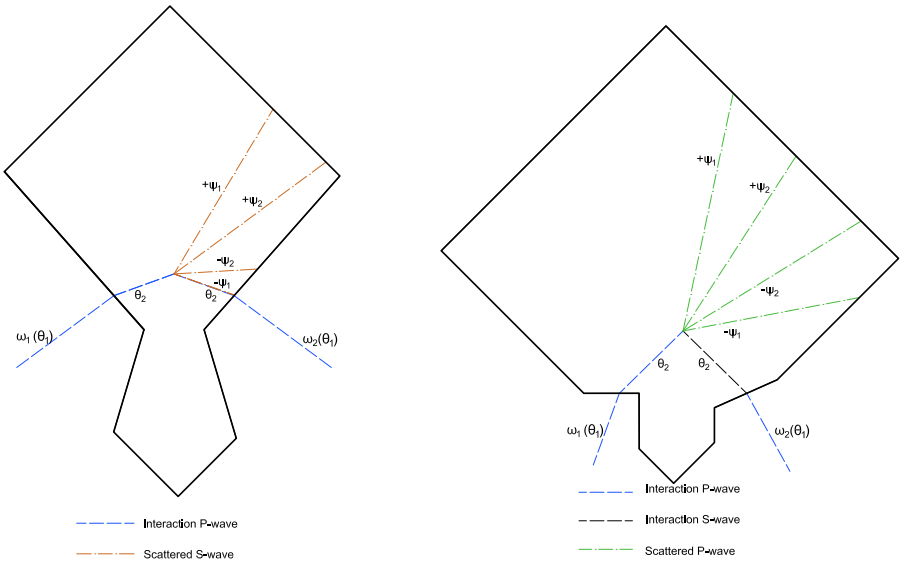

Figure 8.2: Four shapes of aluminium with the calculation of angles for each case of interaction for P with P and S with P respectively

The resulting aluminum samples are photographed in Figure 8.2, before introduced in the immersion tank.

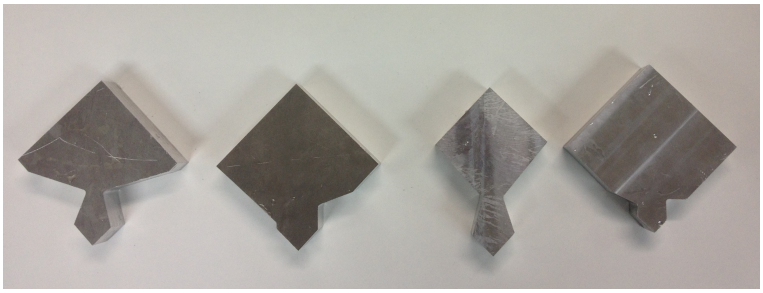

Figure 8.3: Four shapes of Aluminum samples

The experimental calculus of the angles have been carried out in the project of Molina [266], where the study interaction of plane waves from different nature between water and aluminum (see Figure 8.2) was carried out.

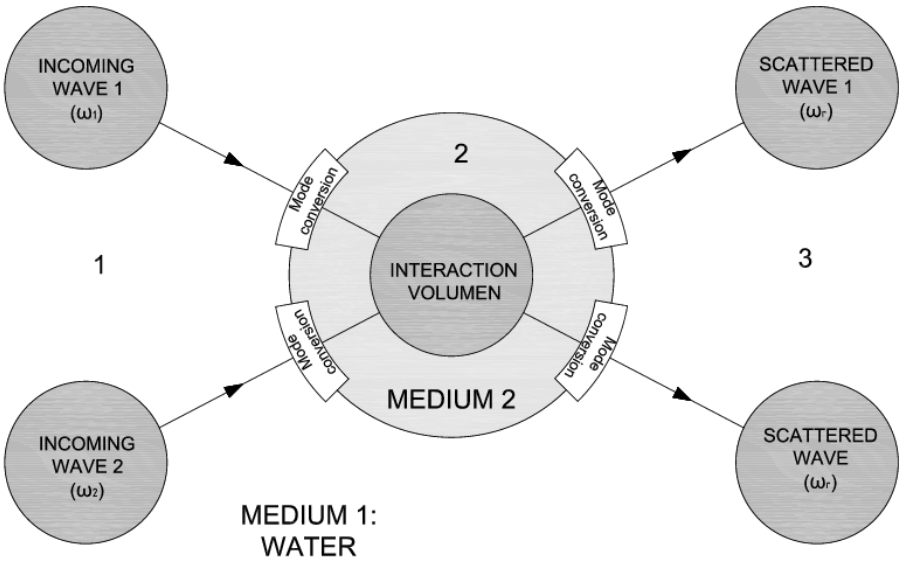

Figure 8.4: Draft of the interaction waves in a medium

At the beginning, the following reference table of wave interactions recently described by Korneev [38] was examined and validated through a device specifically designed to this experiment (See Figure 8.2).

where $=$ is refereed to the collinear case, when the direction of the propagation is the same, $\neq$ when the interaction posible, even when the waves are antili-nears (the direction of the propagation are opposites), $+$ when the interaction is possible, $\times$ when the interaction not possible and white spaces, when the wave is not generated.

		Generated waves			
		$\omega_r = \omega_1 + \omega_2$		$\omega_r = \omega_1 - \omega_2$	
N	Interaction waves	P	S	P	S
1	P(ω_1) y P(ω_2)	=		=	$\neq$
2	P(ω_1) y S(ω_2)	$\neq$		+	$\neq$
3	S(ω_1) y P(ω_2)	+			
4	S(ω_1) y S(ω_2)	$\neq$	$\times$		$\times$

Table 8.2: Types of waves from interaction of two of them with different frequencies

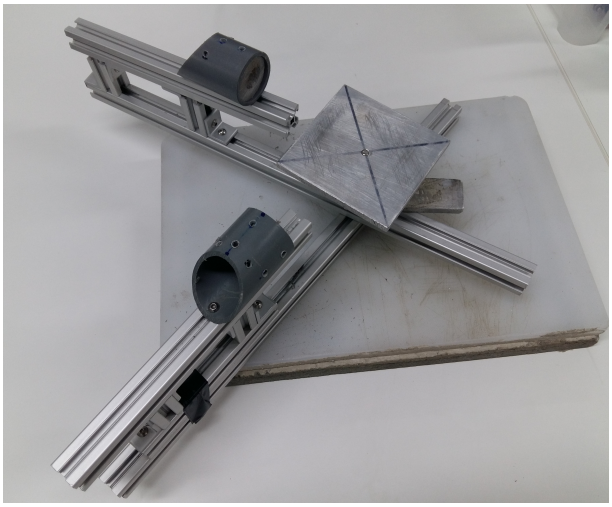

Figure 8.5: Noncollinear mixing device with two transducers.

With the purpose of extract nonlinear parameters experimentally, a prototype has been designed 8.2 in order to find desired angles for each nonlinear mixing case extracted in previous section.

Note that when P propagating from medium one to medium 2 the amplitude of the generating waves should be multiplied by the transmission coefficient $T_P = 0.1641$. In the case of sum of frequencies in aluminum from sum of frequencies in water the registered amplitudes should be divided by the coefficient $T_{P,S}$ (depending on the generating wave after the interaction). This coefficient is defined by Zoeppritz [267, 268] and denotes the nature of the wabe and the angle with normal of the surface.

8.3 Experimental results

The receiver was an ONDA calibrated hydrophone (model HNR- 0500) with a bandwidth of $0.1 - 20$ MHz. The response signals were sampled with a high resolution A/D converter after 40 dB preamplification stage and saved for post-processing. The transmitters were two panametric planar transducers, of central frequency 1 MHz and 0.25 in diameter. We used two arbitrary wave generators (Agilent 33220) to drive the transmitter at two different frequencies. The ultrasonic excitation frequencies were arbitrarily chosen, the only constraints being that both driving frequencies and the sum and difference frequencies lay within the

linear operating region of the transducers, and that f_b was not an integer multiple of f_a. Different frequency combinations were used: $f_a = 6.25$ MHz and $f_b = 4.25$ MHz. The amplitude of the input signal at the high frequency f_b (HF) was kept at 7.5 V, while the amplitude of the input signal at the low frequency f_a (LF) was increasing, 10 V. To avoid unwanted interference effects in the propagation medium, we used short trains of pulses for excitation and a 10 ms pulse duration was used.

We investigated the generated waves as a function of distance. The transmitter-receiver distance was increased in 1-mm increments until a total distance of 250 mm between two mediums water and aluminum. At each distance x from the transmitter, the pressure of the fundamental, $u_a^{(0)}$ and $u_b^{(0)}$, and that of the generated harmonics, $u_a^{(1)}$, $u_b^{(1)}$, u_- and u_+, were determined.

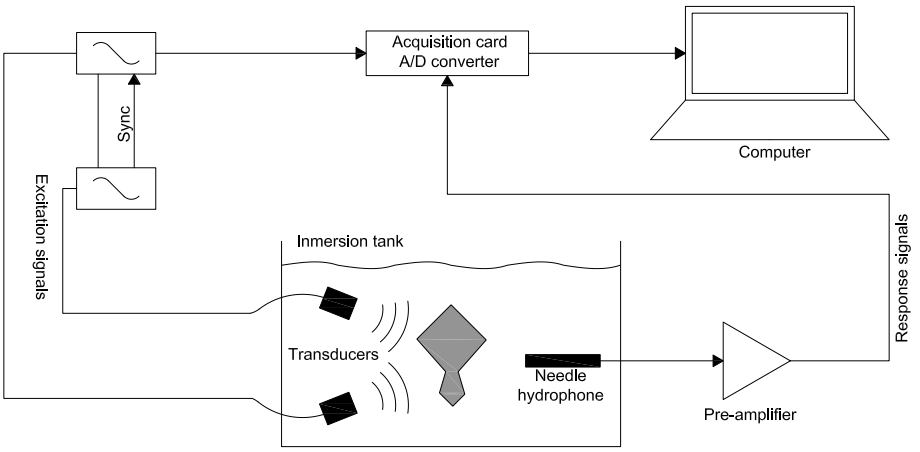

Figure 8.6: Experimental configuration

Figures 8.3 ilustrate a set of measurements carried out in the END lab at the University of Granada. The prototype is introduced into a immersion tank where the values were calculated experimentally.

Figure 8.3 shows when the specimen of aluminum was introduced in the immersion tank and the process of alignment under a laser device and controlling the spirit level with the designed prototype.

The whole cases was calculated with matlab software with an algorithm that calculated the FFT and consequently the amplitude of the harmonics for each aluminum sample. The Figures 8.3, 8.3, 8.3 and 8.3 show the wave received and the FFT for each experiment.

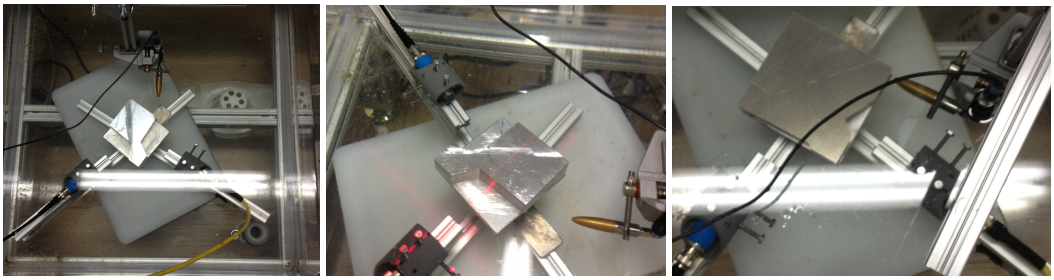

Figure 8.7: Experimental test to obtain nonlinear acoustic parameters in aluminum

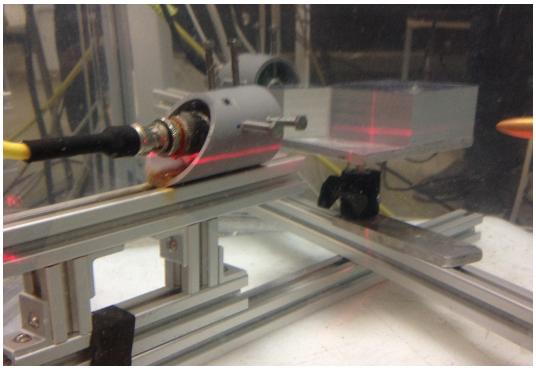

Figure 8.8: Experimental test to obtain nonlinear acoustic parameters in aluminum with a laser aligment

Under this interaction of two P waves, ψ the output angle is obtained for each cases as was showed in Figure 8.2. Note that the case of P wave resulting of the interaction is not posible experimentally.

This interaction of a P wave with a S wave, with ψ as the output angle is obtained for each cases as was showed in Figure 8.2.

This interaction of a S wave with a P wave, with ψ as the output angle is obtained as was showed in Figure 8.2.

This interaction of two S waves, with ψ as the output angle is obtained as was showed in Figure 8.2.

Therefore, after the experimental procedure, the results of classical nonlinear acoustic parameter β^{τ} and β_H and new parameters β^{vp}, β^{dp}, β^{cs} and β^{ds} can be calculated from Figures 8.3, 8.3, 8.3, and 8.3. Note that the disaggregated nonlinear acoustic new extension could be measured by comparing two or more different experiments.

Note that the aluminum nonlinear parameters that were obtained by the different authors is different that is due to the definition of the nonlinear acoustic theory, that converges with the Hamilton one but not with the Zarembo definition detailed in chapter 5. The TOEC can be derived due to the relationship established in Chapter 6, when the different nonlinear acoustic parameters are uncoupled from the analytical results. Note that connects with nonlinear acoustic transversal parameter of Zarembo and Gol'dberg and is the m TOEC of

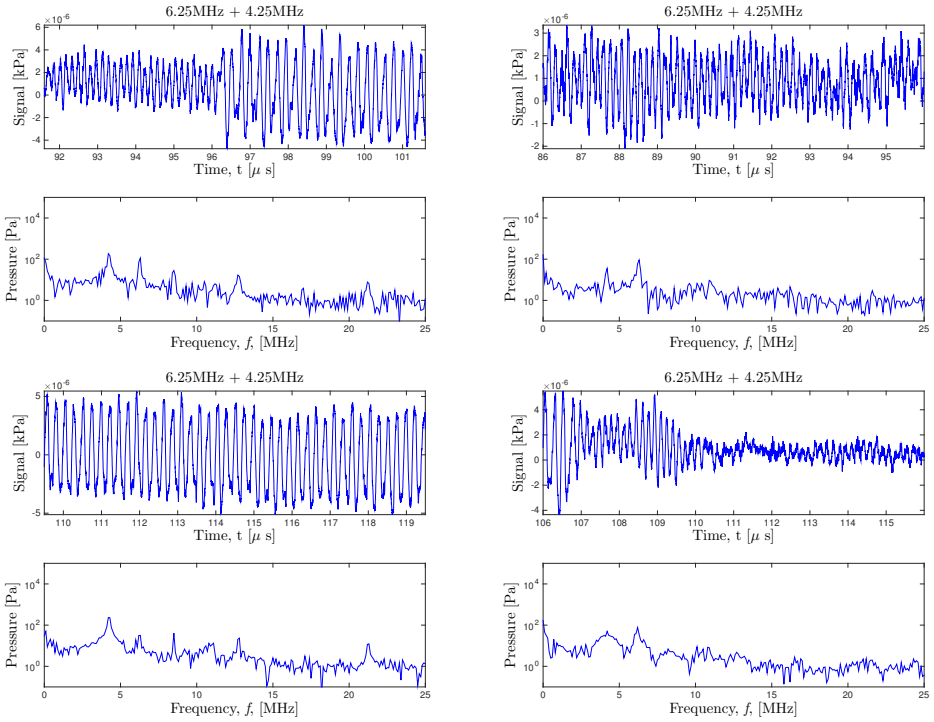

Figure 8.9: Nonlinear acoustic parameters in aluminum with signal and FFT for two P-waves interaction

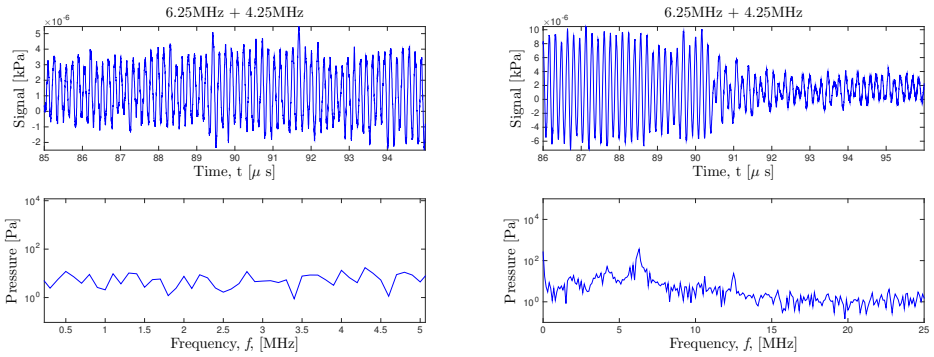

Figure 8.10: Nonlinear acoustic parameters in aluminum with signal and FFT for P and S waves interaction

Murnaghan see Table 4.1. it result converges with the calculation of others authors as Stobbe and Muir, they are shown in Table 4.2.

Note that this method could be relevant in several cases for solid materials and could be relevant to consider damaged materials treating to correlate the values with the internal cracks.

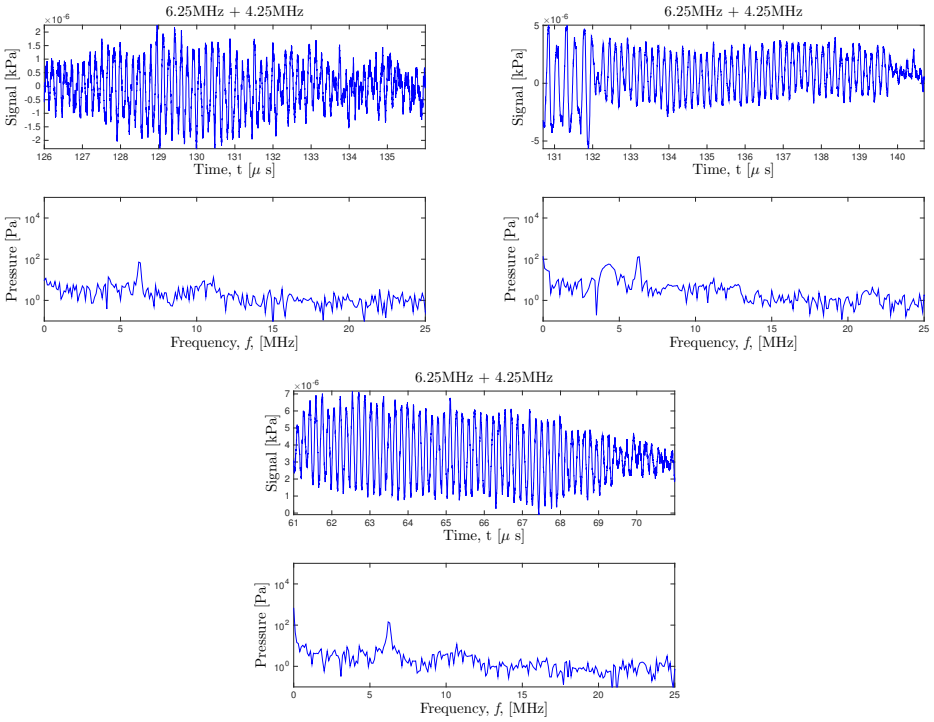

Figure 8.11: Nonlinear acoustic parameters in aluminum with signal and FFT for S and P waves interaction

Wave interaction	*Angle*	$\mathcal{B} + \mathcal{A}/2$ GPa
P-P	$+\psi_1$	-2240.07 $\times$
P-P	$+\psi_2$	-1191.41 $\times$
P-P	$-\psi_1$	-2535.70 $\times$
P-S	$+\psi_1$	-893.10 $\times$
P-S	$-\psi_2$	-1760.13 $\times$
S-P	$+\psi_1$	-373.81
S-P	$-\psi_1$	-484.57
S-P	$-\psi_2$	-244.73
S-S	$+\psi_1$	-435.67
S-S	$+\psi_2$	-481.07
S-S	$-\psi_1$	-491.27
Average		-418.52
Standar Deviation		87.62

Table 8.3: Nonlinear parameters characterization of the aluminum samples

8.4 Single transmitter setup

In this section, the acoustic nonlinearity of water was investigated using a variation of the collinear wave mixing method [269]. One single transducer, driven at two different frequencies f_a and f_b, was used to generate a third frequency component at $f_a - f_b$, $f_a + f_b$, $2f_a$ and $2f_b$. Such a configuration allows to cancel out system nonlinearities since no amplification

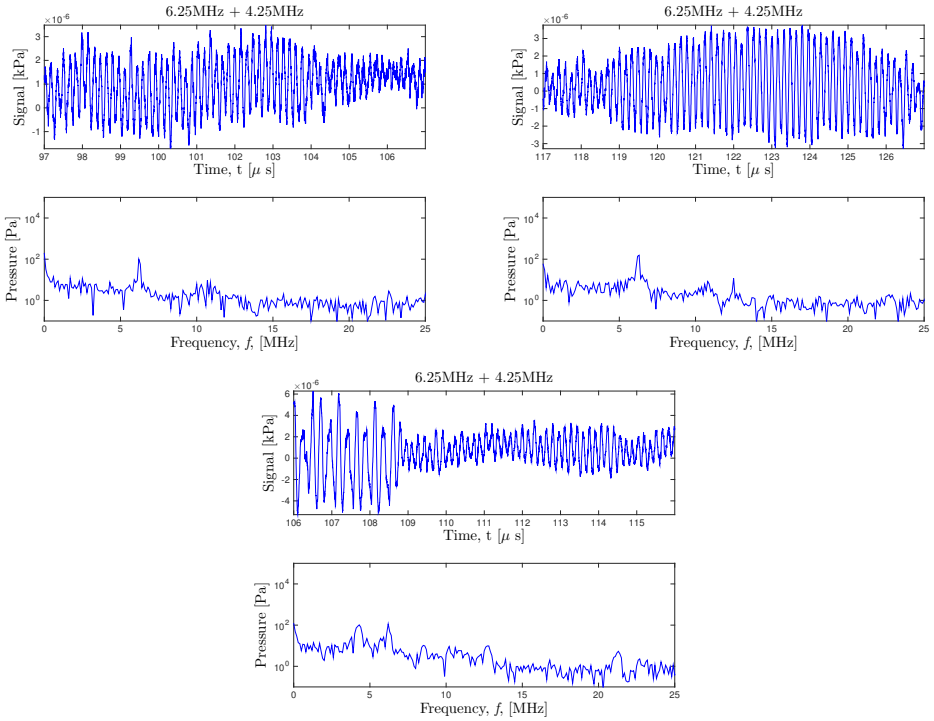

Figure 8.12: Nonlinear acoustic parameters in aluminum with signal and FFT for S waves interaction

of the signal beyond $10V$ is needed. Perturbation solutions of nonlinear parameter in water are analytically calculated and validated with experimental measurements.

8.4.1 Perturbation solutions

Let us considerer the equation of motion for plane elastic waves propagating through a medium, in the absence of body forces, and in index notation as was detailed in the field of Continuum Mechanics Equations 5.2. The first solution under a perturbation method framework can be expressed as,

$$u_0 = A \sin\left(\omega\left(\frac{x}{c_p} - t\right) + \varphi\right) \tag{8.26}$$

where $\omega = 2\pi f$ is the angular frequency, f is the frequency of the wave, A is the amplitude, $A = \sqrt{A_1 + A_2}$, and φ the phase, $\varphi = \tan A_2/A_1$. Now, let us consider two monochromatic waves as zero-order perturbation: $u^{(0)} = u_a^{(0)} + u_b^{(0)}$ at two different frequencies, ω_a and ω_b,

$$u_a^{(0)} = A_1 \sin\left(\omega_a\left(\frac{x}{c_p} - t\right)\right) + A_2 \cos\left(\omega_a\left(\frac{x}{c_p} - t\right)\right) \tag{8.27}$$

$$u_b^{(0)} = B_1 \sin\left(\omega_b\left(\frac{x}{c_p} - t\right)\right) + B_2 \cos\left(\omega_b\left(\frac{x}{c_p} - t\right)\right) \tag{8.28}$$

$$\tag{8.29}$$

or in compact form,

$$\begin{aligned} u_a^{(0)} &= A\sin\left(\omega_a(\tfrac{x}{c_p}-t)+\varphi_a\right) \\ u_b^{(0)} &= B\sin\left(\omega_b(\tfrac{x}{c_p}-t)+\varphi_b\right) \end{aligned} \tag{8.30}$$

Inserting the zero-order perturbation solutions into Equation linear wave equation part, it can be shown that the first-order perturbation solution is the sum of four traveling waves at velocity cp and frequency $2\omega_a$, $2\omega_b$, $(\omega_a+\omega_b)$ and $(\omega_a-\omega_b)$, respectively. Thus, a particular solution may be obtained by the method of variations of parameters as,

$$u^{(1)} = u_a^{(1)} + u_b^{(1)} + u_{ab}^{(1)} + u_{ba}^{(1)} \tag{8.31}$$

where each wave can be written as [270],

$$\begin{aligned} u_a^{(1)} &= \beta\frac{\omega_a^2}{4c_p^2}A^2x\sin(2\omega_a(x/c_p-t)+\varphi_1) \\ u_b^{(1)} &= \beta\frac{\omega_b^2}{4c_p^2}B^2x\sin(2\omega_b(x/c_p-t)+\varphi_2) \\ u_{ab}^{(1)} &= \beta\frac{\omega_a\omega_b}{2c_p^2}BAx\sin((\omega_a+\omega_b)(x/c_p-t)+\varphi_3) \\ u_{ba}^{(1)} &= \beta\frac{\omega_a\omega_b}{2c_p^2}BAx\sin((\omega_a-\omega_b)(x/c_p-t)+\varphi_4) \end{aligned} \tag{8.32}$$

As can be observed, the first-order perturbation solution is generated by the fundamental waves, whose amplitude accumulates with the propagation distance x. In this case, the nonlinear effect is essentially due to frequency-mixing between four spectral components, i.e. the double-frequency components (second harmonics) are generated by a mixing of the fundamental waves with themselves, the sum-frequency component (harmonic at frequency $\omega_a+\omega_b$) and the difference- frequency component (harmonic at frequency $\omega_a-\omega_b$ are generated by a mixing of the two fundamental waves between them.

If we assign $u_a^{(0)}$ as the amplitude of the fundamental wave at frequency ω_a, $u_b^{(0)}$ as the amplitude of the fundamental wave at frequency ω_b, $u^{(1)_a}$ and $u^{(1)_b}$ as the amplitude of the second harmonic, u_+ as the amplitude of the harmonic at frequency $\omega_a+\omega_b$ and u_- as the amplitude of the harmonic at frequency $\omega_a-\omega_b$, we can obtain four different expressions for the acoustical nonlinearity parameter as a function of these four harmonics. Furthermore, these expressions can be written in terms of pressures of the fundamentals $p_a^{(0)}$ and $p_b^{(0)}$, the second harmonics $p_a^{(1)}$, respectively, $p_b^{(1)}$, the sum and difference harmonics p_+, p_-, β can be derived from the acoustic pressures of generated components $f_+=f_a+f_b$, $f_-=f_a-f_b$, $2f_a$, $2f_b$ and fundamental components f_a, f_b as,

$$
\begin{aligned}
\beta &= \frac{\rho c_p^3}{\pi f_a x} \frac{p_{1a}(x)}{p_{0a}^2(x)} \\
\beta &= \frac{\rho c_p^3}{\pi f_b x} \frac{p_{1b}(x)}{p_{0b}^2(x)} \\
\beta &= \frac{\rho c_p^3}{\pi f_+ x} \frac{p_+(x)}{p_{0a}(x) p_{0b}(x)} \\
\beta &= \frac{\rho c_p^3}{\pi f_- x} \frac{p_-(x)}{p_{0a}(x) p_{0b}(x)}
\end{aligned}
\tag{8.33}
$$

8.4.2 Experimental setup

A schematic view of the experimental setup is shown in Figure 8.4.2. Both the transmitter and the receiver were immersed in a tank that contained degassed water at room temperature and mounted on a 3-axes scanner, with guarantees perfect alignment along the propagation direction of the sound.

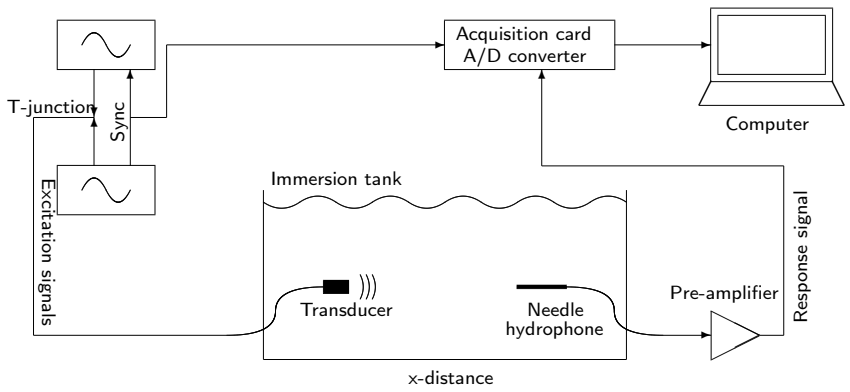

Figure 8.13: Schematic representation of the experimental setup

The receiver was an ONDA calibrated hydrophone (model HNR- 0500) with a bandwidth of $0.1 - 20$ MHz. The response signals were sampled with a high resolution A/D converter after 40 dB preamplification stage and saved for post-processing. The transmitter was a panametric planar transducer, of central frequency 1 MHz and 0.25 in diameter. We used two arbitrary wave generators (Agilent 33220) to drive the transmitter at two different frequencies. The ultrasonic excitation frequencies were arbitrarily chosen, the only constraints being that both driving frequencies and the sum and difference frequencies lay within the linear operating region of the transducers, and that f_b was not an integer multiple of f_a. Different frequency combinations were used: $f_a = [4, 4, 4, 3.6, 5.4, 3.6]$ MHz and $f_b = [5.7, 6.3, 5.5, 4.3, 6.3, 6.3]$ MHz. The amplitude of the input signal at the high frequency f_b (HF) was kept at 7.5 V, while the amplitude of the input signal at the low frequency f_a (LF) was increasing, $[5, 7.5, 10]$ V. To avoid unwanted interference effects in the propagation medium, we used short trains of pulses for excitation and a 10 ms pulse duration was used.

We investigated the generated waves as a function of distance. The transmitter-receiver distance was increased in 1-mm increments until a total distance of 250 mm. At each distance x from the transmitter, the pressure of the fundamental, $u_a^{(0)}$ and $u_b^{(0)}$, and that of the generated harmonics, $u_a^{(1)}$, $u_b^{(1)}$, u_- and u_+, were determined, for the different frequencies and excitation levels.

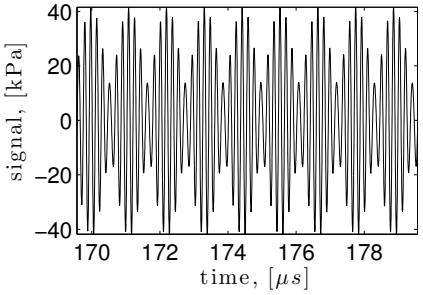

Figure 8.14: Signal received by the hydrophone after 12.5 cm of propagation, for input frequencies and amplitudes $f_a = 5.4$ MHz, $A = 10$ V and $f_b = 6.3$ MHz, $B = 7.5$ V.

8.4.3 Numerical results of collinear mixing

All experimental data were collected in degassed water at room temperature. The sound speed determined from the travel time for several transmitter-receiver distances was 1486 ± 2 m/s. The near field distance (NF) was characterized for each pair of excitation frequencies as,

$$NF = \frac{2\pi f_c r^2}{2c_0} \tag{8.34}$$

where f_c is the called central frequency, defined by the two input frequencies as $f_c = \frac{f_a + f_b}{2}$, r is the radius of the two transducer and c_0 is the compressional sound speed in water. The corresponding values are shown in Table 8.4 with HF and LF.

HF [MHz]	LF [MHz]	NF [m]
4.0	5.7	0.1017
4.0	6.3	0.1080
4.0	5.5	0.0996
3.6	4.3	0.0829
5.4	6.3	0.1227
3.6	6.3	0.1038

Table 8.4: Characterization of the Near field (NF) for each pair of excitation frequencies.

Frequencies farther apart from the central frequency of the transducer presented results with less resolution as the limited frequency band of the transducer. To highlight the frequency mixing, the results for the pair of frequencies $f_a = 5.4$ MHz and $f_b = 6.3$ MHz will be discussed further, since they are within the transducer band frequency. An example of a

collected signal at 12.5 cm from the transducer surface and its amplitude spectrum, for an input signal of frequencies $f_a = 5.4$ MHz and $f_b = 6.3$ MHz, is shown in Figure 8.4.2.

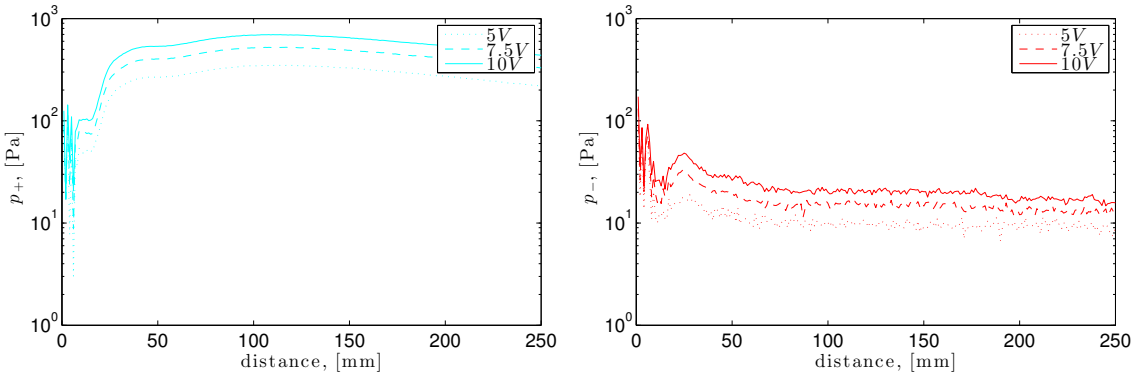

Figure 8.15: Representation of the experimental data used for the acoustic nonlinear parameter determination (sum and difference harmonics), for input frequencies and amplitudes $f_a = 5.4$ MHz, $A = 10$ V and $f_b = 6.3$ MHz, $B = 7.5$V.

The representation of the experimental data for the sum and difference harmonics (p_+, p_-) is depicted in Figure 8.4.3, where the horizontal axe represents the propagation (transmitter-receiver) distance, and the input excitation voltage for the low frequency, respectively. The vertical axe represents the measured pressure of the sum and difference harmonics generated in the propagation through water. As can be seen in Figure 8.4.3, the difference harmonics, p_- is significantly lower than the harmonic of the sum, p_+, which contradicts the analytical solution. According to Equation 8.32, the amplitude of both harmonics, sum and difference, should be the same.

Figure 8.16 shows the pressure of the four different harmonics versus the propagation distance. The amplitude of the harmonics is greatly affected by interference effects in the proximity of the transmitter. These effects are mainly due to the interference of the wave that travels back and forth between the transmitter and the receiver, and due to the diffraction in the close proximity of the transmitter. The pulse trains used in these experiments are short in duration, but interference will occur when the transmitter-receiver distance is shorter than the travel time between the two. Comparing to the classic finite amplitude method widely used in the literature, where additional effects can be generated from the necessary high power to generate the second harmonic, no high power is needed here for the harmonic generation.

As expected from the contradictory measured amplitudes, non reliable value was obtained from the difference harmonics (p_-). Furthermore, it can be noticed that the experimental values are stable in a short distance and beyond the NF distance they diverge from the literature value [271]. Nevertheless, further experimental works are needed to figure out the apparently contradictory results with the difference harmonics, i.e. the one generated at frequency $f_a - f_b$.

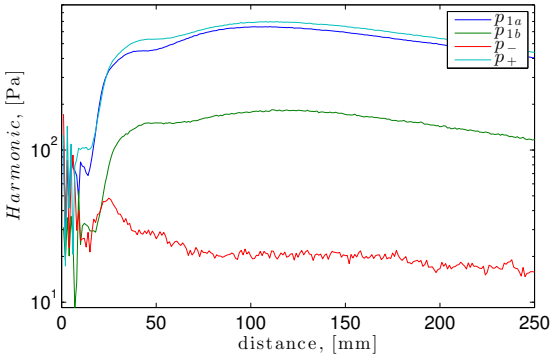

Figure 8.16: *Harmonic pressures vs. transmitter-receiver distance, for input frequencies and amplitudes* $f_a = 5.4$ *MHz,* $A = 10$ *V and* $f_b = 6.3$ *MHz,* $B = 7.5$ *V.*

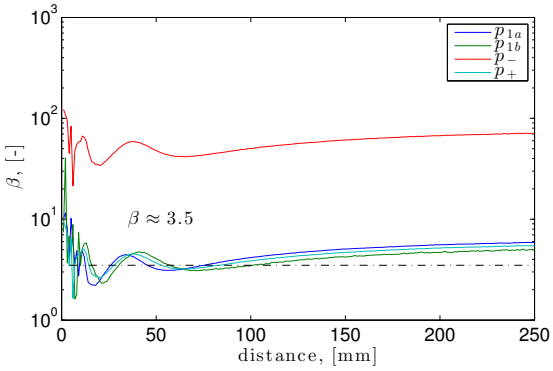

Figure 8.17: *Acoustic nonlinear parameter* β *calculated at different transmitter-receiver distances, for input frequencies and amplitudes* $f_a = 5.4$ *MHz,* $A = 10$ *V and* $f_b = 6.3$ *MHz,* $B = 7.5$ *V.*

Note that the expression of β nolinear acoustic parameter is the same that the one obtained in the previous section, when the collinear mixing was derived as the first case of interaction of two P waves as in Equation 8.9 for water.

Figure 8.17 shows the β parameter calculated using the expressions (8.33). The dashed-line represents the literature value for water, $\beta = 3.5$, which is compatible with values obtained in previous literature by other methods.

Profound study of nature is the most fertile source of mathematical discoveries.

Joseph Fourier 1783-1830

9

Torsional ultrasonic transducer to measure soft tissue nonlinearities

The aim of this chapter is to test the feasibility of a new type of ultrasonic configuration, named torsional ultrasound, to quantify nonlinear parameters of soft tissue. To this end a new concept of sensor is designed and prototyped, based on the theory of piezoelectricity.

9.1 Sensor design and optimization

The piezoelectricity constitutive equations are described in this chapter in the charge-stress and electric field-strain form, because they are necessaries to implement piezoelectric properties. The ultrasonic transducer is made of steel and piezoelectric ceramic taking into account two layers of dermic and connective tissue where the waves are propagated. This process is simulated by FEAP software based on finite element method and it is detailed below.

9.1.1 Piezoelectric formulation

Piezoelectricity is an interaction between mechanical and electric fields, whereby electric charge that accumulates in certain solid materials in response to applied mechanical stress. It is a coupling between the elasticity and the electricity that makes the concept of transduction possible. Linear piezoelectricity is described analytically within constitutive equation, defined how stress (**T**), strain (**S**), charge-density displacement (**D**), and electric field (**E**)

interact by two constitutive equations. The constitutive laws are in Strain-Charge form:

$$\mathbf{T} = \mathbf{C}_E \cdot \mathbf{S} + \mathbf{e}^T \cdot \mathbf{E} \tag{9.1}$$

$$\mathbf{D} = \mathbf{e} \cdot \mathbf{S} - \varepsilon_{\mathbf{S}} \cdot \mathbf{E} \tag{9.2}$$

where $\mathbf{C_E}$ is the piezoelectric stiffness matrix, $\mathbf{e}$ is the piezoelectric coupling coefficient matrix, $\mathbf{e}^T$ is its transposed and $\varepsilon_{\mathbf{S}}$ is permitivity coefficient matrix.

The equilibrium and compatibility equations are stated as:

$$\nabla \cdot \mathbf{D} = 0;\ \mathbf{E} = -\nabla\phi \tag{9.3}$$

$$\nabla^S \cdot \mathbf{T} = 0;\ \mathbf{S} = \frac{1}{2}(\nabla\mathbf{u} + \nabla\mathbf{u}^T) \tag{9.4}$$

where $\mathbf{u} = (u_1, u_2, u_3)$ denotes the displacement vector field, and ϕ is the electric potential or voltage. Finally, the following standard sign criteria is used: the electric field and stress values are considered positive for the direction of polarization of the material and for tractions, respectively.

9.1.2 Finite element formulation

The governing discretized equation of motion of the system using is written in the form,

$$\mathbf{M}\ddot{\mathbf{U}} + \mathbf{K}\mathbf{U} = \bar{\mathbf{F}}(\mathbf{t}) \tag{9.5}$$

$$\mathbf{U}^a = \begin{bmatrix} u_1^a \\ u_2^a \\ u_3^a \\ \phi^a \end{bmatrix} \tag{9.6}$$

where $\mathbf{U}$ and $\ddot{\mathbf{U}}$ are the displacement and acceleration vectors including the three components of the displacements u_i^a and the voltage degree of freedom ϕ^a associated to node a, respectively, $\mathbf{M}$ is the mass matrix, $\mathbf{K}$ is the stiffness matrix, and $\bar{\mathbf{F}}(\mathbf{t})$ is the time history of the applied load.

The global stiffness matrix of the element can be expressed as

$$\mathbf{K} = \int_V \mathbf{B}^{(e)T}\mathbf{D}^*\mathbf{B}^{(e)}d\Omega \tag{9.7}$$

where $\mathbf{D}^*$ is the elasticity matrix that transforms effective strains to stresses including the electric field coupling at every point of the domain. It depends on the piezoelectric constitutive equations, and can be represented in matrix form as described below.

$$\begin{bmatrix} T_{11} \\ T_{22} \\ T_{33} \\ T_{12} \\ T_{13} \\ T_{23} \\ D_1 \\ D_2 \\ D_3 \end{bmatrix} = \underbrace{\begin{bmatrix} C_{E11} & C_{E12} & C_{E13} & 0 & 0 & 0 & e_{11} & e_{21} & 0 \\ C_{E12} & C_{E22} & C_{E23} & 0 & 0 & 0 & e_{12} & e_{22} & 0 \\ C_{E13} & C_{E23} & C_{E33} & 0 & 0 & 0 & e_{13} & e_{23} & 0 \\ 0 & 0 & 0 & C_{E44} & 0 & 0 & 0 & 0 & e_{34} \\ 0 & 0 & 0 & 0 & C_{E55} & 0 & 0 & 0 & e_{35} \\ 0 & 0 & 0 & 0 & 0 & C_{E66} & e_{16} & e_{26} & 0 \\ e_{11} & e_{12} & e_{13} & 0 & 0 & e_{16} & \varepsilon_{11} & \varepsilon_{12} & 0 \\ e_{21} & e_{22} & e_{23} & 0 & 0 & e_{26} & \varepsilon_{12} & \varepsilon_{22} & 0 \\ 0 & 0 & 0 & e_{34} & e_{35} & 0 & 0 & 0 & \varepsilon_{33} \end{bmatrix}}_{\mathbf{D^*}} \begin{bmatrix} S_{11} \\ S_{22} \\ S_{33} \\ S_{12} \\ S_{13} \\ S_{23} \\ E_1 \\ E_2 \\ E_3 \end{bmatrix} \tag{9.8}$$

and,

$$\mathbf{B}^{(e)} = \begin{bmatrix} N^a_{,1} & 0 & 0 & 0 \\ 0 & N^a_{,2} & 0 & 0 \\ 0 & 0 & N^a_{,1} & 0 \\ N^a_{,2} & N^a_{,1} & 0 & 0 \\ N^a_{,3} & 0 & N^a_{,1} & 0 \\ 0 & N^a_{,3} & N^a_{,2} & 0 \\ 0 & 0 & 0 & N^a_{,1} \\ 0 & 0 & 0 & N^a_{,2} \\ 0 & 0 & 0 & N^a_{,3} \end{bmatrix} \tag{9.9}$$

where $\mathbf{B}^{(e)}$ is the strain-displacement matrix of the element (e), and the superscript T denotes the transpose operator, being $N^a_{,i}$, $i = 1, 2, 3$ the shape functions defined for each type of element.

9.1.3 Implementation

The numerical tool selected for solving the response of the model (forward problem) is the Finite Element Method (FEM). A 8-node quadratic finite element is chosen because it improves the ratio between precision of shape functions and the size of the system of equations, with 4 degrees of freedom per node described in equation 8. It has been implemented to solve the model given by the previous constitutive equations. The piezoelectric element was developed and implemented in the research academic finite element code FEAP [163] because it is an open code allowing us to introduce our piezoelectric element formulation. The strain-charge to stress-charge transformation has been used to introduce the piezoelec-

tric properties:

$$\mathbf{C_E} = \mathbf{S_E}^{-1} \tag{9.10}$$

$$\mathbf{e} = \mathbf{d} \cdot \mathbf{S_E}^{-1} \tag{9.11}$$

$$\varepsilon_S = \varepsilon_T - \mathbf{d} \cdot \mathbf{S_E}^{-1} \cdot \mathbf{d^T} \tag{9.12}$$

9.1.4 Parametric geometry

Due to the difficulty that mechanical parameter measurement and detection of soft tissue pathologies may lead to, a torsional S-wave transducer design is proposed in this paper, where the transmitter and the receiver are fit inside a circular crown that can be encapsulated in a clinical diagnostic device.

To model it, the partial differential equations described above require the geometry, material properties and boundary conditions to completed the problem definition. The geometry of the specimen comprises a 90 degree sector of a circular crown 90 degrees. The cyclic boundary conditions ensures that the behavior is equivalent to a complete model.

The boundary conditions are completed with the excitation, which is defined by a 100 [V] peak-to peak voltage difference applied between the upper and lower sides of the piezoelectric ceramics, with a spike function based on Heaviside function time dependency:

$$f = AH(t)H(D_0 - t)\frac{t}{D_0} \tag{9.13}$$

where A is the amplitude, $H(t)$ is Heaviside function, D_0 is the distance to origin in the x axes, and t is the time. The output of the model (signal V), consist of a difference of voltage at the piezo-ceramic blocks ends in the receiver ring.

The PZT-5A laminate is considered as prismatic block of size Lx [mm], Ly [mm] and Lz [mm], as shown in table 9.1 and figure 9.1.

The geometry construction in FEAP consists in 86 blocks comprising the transmitter disc pair, receiver crown pair, set of piezoelectric ceramic blocks and two layers of dermic and connective tissue and piezoelectric ceramic, respectively (see figure 9.2). Mesh size and time increment discretization are chosen in section 5 based on a convergence study (as shown in figures 9.5 and 9.6).

The torque sensor simulation was pre-dimensioned based on the dimensions tested of the simplified analytical model described in the next section, and summarized in the table below.

The top and bottom central discs and external rings material will be selected later, within the optimization procedure.

- Crystal symmetry class: Uniaxial
- Density: 7750 [kg/m^3]
- Relative permitivity:

Description of design parameters	Dimensions [mm]	Label
Piezoelectric ceramic width	1	pw
Piezoelectric ceramic length	1	pl
Piezoelectric ceramic thickness	2	pt
Disc piezoelectric ceramic eccentricity	2.5	dpe
Disc radius	4.25	dr
Ring piezoelectric ceramic eccentricity	7.5	rpe
Ring width	2	rw
Disc and ring thickness	8	drt

Table 9.1: Preliminar dimensions of the sensor design.

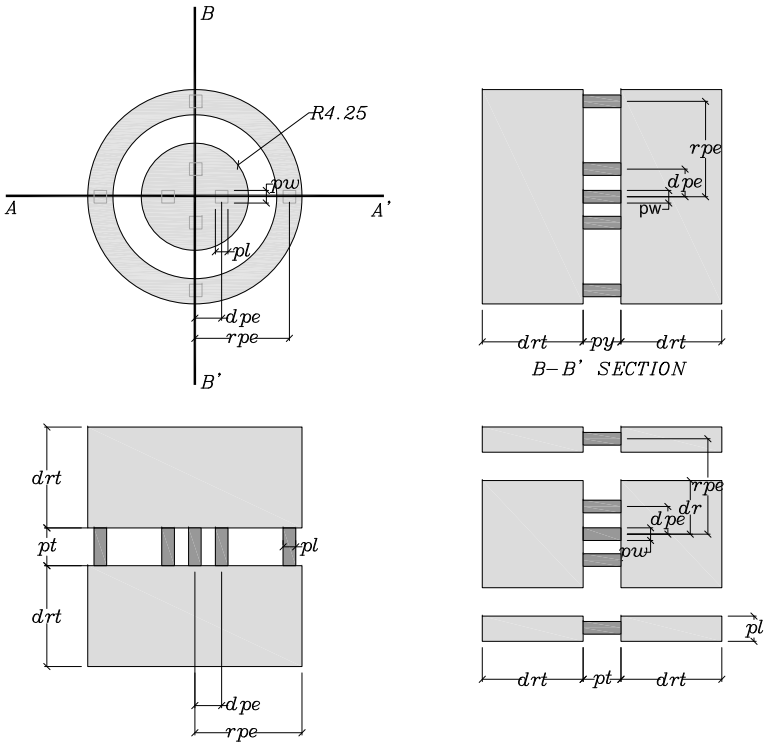

Figure 9.1: The geometry of the transducer describes a scheme with the outline of the transmitter and reception elements. Projections are shown above.

$$\frac{\varepsilon_T}{\varepsilon_0} = \begin{vmatrix} 1730 & 0 & 0 \\ 0 & 1730 & 0 \\ 0 & 0 & 1730 \end{vmatrix}, \tag{9.14}$$

where $\varepsilon_0 = 8.854 * 10^{-12}$ [F/m]

- Flexibility matrix:

$$\mathbf{S_E} = \begin{vmatrix} 16.4 & -5.74 & -7.22 & 0 & 0 & 0 \\ -5.74 & 16.4 & -7.22 & 0 & 0 & 0 \\ -7.22 & -7.22 & 18.8 & 0 & 0 & 0 \\ 0 & 0 & 0 & 47.5 & 0 & 0 \\ 0 & 0 & 0 & 0 & 47.5 & 0 \\ 0 & 0 & 0 & 0 & 0 & 44.3 \end{vmatrix} * 10^{-12} \ [\mathrm{m}^2/\mathrm{N}] \tag{9.15}$$

- Piezoelectric coupling:

$$\mathbf{d} = \begin{vmatrix} 0 & 0 & 0 & 0 & 584 & 0 \\ 0 & 0 & 0 & 584 & 0 & 0 \\ -171 & -171 & 374 & 0 & 0 & 0 \end{vmatrix} * 10^{-12} \ [\mathrm{C}/\mathrm{N}] \tag{9.16}$$

9.1.5 Simplified model of torsion transducer

A simplified analytical model of the fundamental oscillatory movement of the torsion ultrasonic transducer is derived. To this end, a number of assumptions are carried out mainly on the relevance of elements of the design and on their movement shape (eigenmode), in order to arrive at a single degree of freedom system. Second, the piezoelectric element is assumed to have a predominant deformation law uniformly distributed and linearly proportional to the electrical excitation. These assumptions are broken down below to yield the analytical equations of motion:

Assumptions

- Reduction to a single-degree-of-freedom system, where the eigenproblem reduces to a single frequency and a single mode (steady-state movement shape).
- Movement is assumed to be dominated by torsion rotation θ in radians.
- Dynamic equilibrium of torsional moment:

$$k^*\theta + I^*\ddot{\theta} = 0 \tag{9.17}$$

  where k^* is the stiffness in [Nm/rad] and I^* is the inertia.
- Steady-state solution has the form:

$$\theta = \theta^0 \sin(\omega t) \tag{9.18}$$

  as the transient solution is neglected for computing the eigenvalue.
- Natural frequency (eigenvalue that fulfills the equilibrium 9.17):

$$\omega = \sqrt{\frac{k^*}{I^*}} \tag{9.19}$$

  in [rad/s], or $f = \frac{\omega}{2\pi}$ in [Hz].
- Stiffness of piezoceramic due to moment:

$$k* = \frac{M_T}{\theta} \tag{9.20}$$

where M_T is the applied torsional moment.

- Since each of the n piezoceramic elements is dominated by shear deformation, and they are located at distance d from the center of rotation

$$M_T = ndF = ndab\sigma_{xz} \tag{9.21}$$

where F is the resulting force of the shear stress σ_{xz} applied over the area $a \times b$ of the element.

- The element described above deforms due to the shear stress the amount ϵ_{xz}, which creates the differential displacement $u^* = l/\epsilon_{xz}$ between upper and lower sides separated distance l. This links to the rotation of the circular array of piezoceramic elements,

$$\theta = u^*/d = l/d\epsilon_{xz} \tag{9.22}$$

- The effective length of the piezoelectric elements is reduced as $l^{\text{eff}} \simeq 2l$ to account for the flexibility of the clamping into the mass. Hence, $\theta = l^{\text{eff}}/d\epsilon_{xz}$.
- The piezoceramic behaves linearly elastically,

$$\sigma_{xz} = G^*\epsilon_{xz} \tag{9.23}$$

with modified shear stiffness G^* adding piezoelectric coupling [151].

- The inertia against rotation is dominated by the mass blocks of density ρ, which are either cylindrical or annular (ring-shaped) of radius r. The inertia of the piezoelectric and other elements is comparatively neglectible.
- Inertia and mass of cylinder:

$$I = \frac{mr^2}{2}, \;\; m = \pi r^2 h\rho \tag{9.24}$$

where h is the height of the cylinder (in the axial direction).

- Inertia and mass of ring:

$$I = mr^2, \;\; m = 2\pi rhe\rho \tag{9.25}$$

where e is the thickness of the ring (in the radial direction).

- Subsystem eigenfrequency in the case of cylinder mass. Combining equations 9.17 to 9.24,

$$f = \frac{1}{2\pi}\sqrt{\frac{nabd^2G}{\frac{\pi}{2}l^{\text{eff}}hr^4\rho}} \tag{9.26}$$

- Subsystem eigenfrequency in the case of ring mass. Combining equations 9.17 to 9.25,

$$f = \frac{1}{2\pi}\sqrt{\frac{nabd^2G}{2\pi l^{\text{eff}} her^3\rho}} \tag{9.27}$$

When the transducer contains both a cylinder mass and a ring mass for each of the transmitting and receiving subsystems, their eigenfrequencies should be matched in order to maximize the combined resonance amplification.

9.2 Validation

The resonance frequency of the complete system for the final optimized design parameters is given in table **??**. It is computed from the FEM model by measuring the time between peaks of cycles (see figure 9.3). It is found that they coincide with the frequencies of the sensor calculated from the analytical simplified model with a relative error less than 1% in both cases, shown in table 9.2.

Model	Frequency [kHz]	Relative Error to FEM [%]
Analytic Disc	27.977	0.680
Analytic Ring	28.180	0.039
FEM	28.169	-

Table 9.2: Validation analytic design vs. FEM

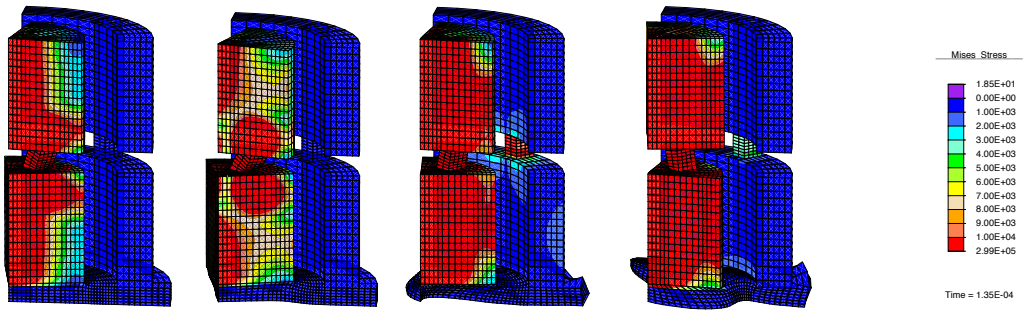

Figure 9.2: Different states of torsional transducer at instants $t = 9, 18, 117, 135$ μs.

9.3 Inverse problem

The physical principle to mechanically characterize soft tissue is the following. A physical magnitude is propagated along the medium to be analyzed, which distorts the wave until it is measured at an accessible surface (see figure 9.4). The mechanical parameters responsible for the modification of the wave can be inferred from the measured one under certain circumstances by means of the inverse problem theory discussed below.

The problem of nondestructive characterization of mechanical tissue properties is solved by a model-based *inverse problem* (IP) approach that consists of two steps: (i) to excite the system applying a dynamic displacement, and (ii) to measure the response (displacements

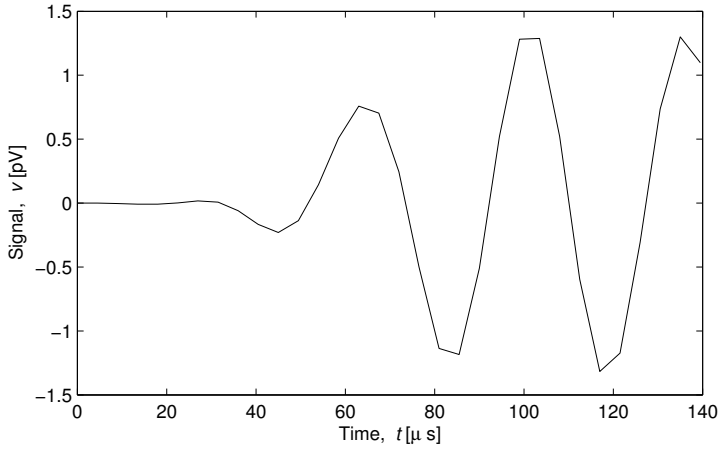

Figure 9.3: example of measurement validating design

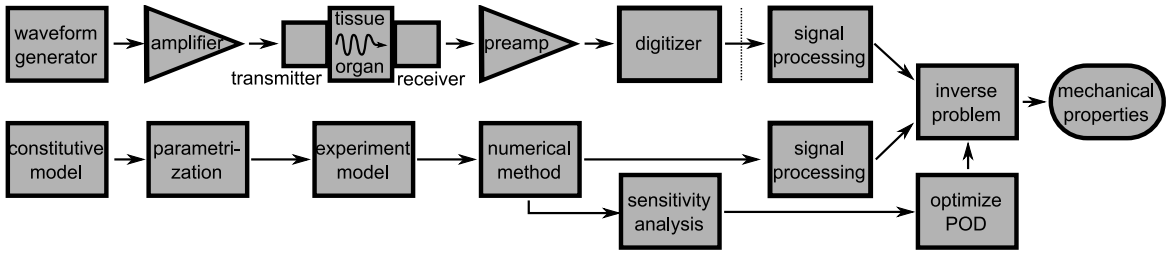

Figure 9.4: Simplified system for measuring ultrasound wave distortion through tissue and reconstruct mechanical properties.

in the time domain). A finite element method model is used in the forward procedure in previous section. We assume the hypothesis that the dynamic behavior of the tissue in its healthy and pathological states is predictable using a well-calibrated model in the sense of faithful reproduction of real measurements.

Then, the measured signal is processed to solve the *inverse problem*, i.e., to determine the changes in the tissue from its original state. A genetic algorithm search tool [272, 164] is used to minimize the discrepancy between the experimental readings and the numerically predicted trial response, by means of a cost functional designed to calibrate for coherent uncertainties and noise, and providing maximal robustness and sensitivity. GA is a heuristic search algorithm that mimics natural selection, where a *population* of candidate solutions are evaluated in terms of their fitness. An iterative process generates, during a number of *generations*, child populations through the processes of *tournament*, *crossover* and *mutation* and *selection*, aimed at converging to the fittest solutions.

9.3.1 Cost functional

The readings from the sensors are time-domain signals denoted by V for the theoretical or synthetic case, and V^x for the experimental case. A reading V^0 in the healthy state of the tissue is defined for calibration, and the measurement to analyze is defined as,

$$\Phi = \frac{V - V^0}{\mathrm{RMS}(V^0)} \tag{9.28}$$

where the RMS values are defined for a discrete function f in time domain $f(t_i)$ at N sampling points as,

$$\mathrm{RMS}(f) = \sqrt{\frac{1}{N}\sum_{i=0}^{N-1} f(t_i)^2} \tag{9.29}$$

A residual γ is defined from the misfit or discrepancy $\Phi^x - \Phi$ between the measurements.

$$\gamma = (\Phi^x - \Phi) \tag{9.30}$$

The cost functional f or fitness function is defined after a residual vector γ of size N_i as the quadratic form,

$$f = \frac{1}{2}|\gamma|^2 = \frac{1}{2}\frac{1}{N_i}\sum_{i=1}^{N_i} \gamma_i^2 \tag{9.31}$$

It is useful to define an alternative version of the cost functional denoted as f^l, with the property of improving the sensitivity while approaching the optimum, just by introducing a logarithm and a small value ϵ to ensure its existence. This definition particularly enhances the convergence speed when the minimization is tackled by with genetic algorithms or other random search algorithms (see Rus *et al.*[273]),

$$f^l = \log(f + \epsilon) \tag{9.32}$$

9.3.2 Probability of detection

The following POD definition is defined to provide an idea of the probability that a pathology is positively detected, given a monitored tissue specimen, when some noise and system uncertainty are present. The detection and characterization of pathologies is based on the interpretation of the alterations of the measurements due to the presence of the pathology. Other model uncertainties such as density value, dermal layer thickness variability or sensor manufacturing geometrical tolerances, and system noises may also alter these measurements, but they are considered to fall outside the scope of this paper because the effect of those uncertainties is grouped in the inserted measurements noise.

We propose to estimate the POD by the probability that the alteration of the measurement caused by the pathology is larger than that caused by the noise. If we label the alteration on the measurement readings caused by the pathology as the SIGNAL component, and the alteration generated by the noise as NOISE, the former definition can be formulated as [272],

$$\text{POD} = P\left(\frac{|\text{SIGNAL}|^2}{|\text{NOISE}|^2} > 1\right) \tag{9.33}$$

Furthermore, three variables are be considered in the problem of maximizing the probability of detection (POD), the level of noise, denoted by σ, the severity of the pathologies in terms of shear stiffness and damping alteration in different tissue layers p considering a reference healthy tissue r, denoted by pat_{pr}, and the cost functional that collects the effects of those in a scalar function f, as defined above.

Nevertheless, we propose a new criterium of POD associated to multivariate pathologies, to consider the case when a sensor should be sensitive to pathologies for a range of different reference or healthy tissues r and a range of tissue layers p, labelled robust POD (RPOD), and defined using a pessimistic criterion as follows,

$$\text{RPOD} = \min_{pat_{pr}} \text{POD}(pat_{pr}) \tag{9.34}$$

$$\text{POD}(pat_{pr}) = P\left(\frac{\left|\text{SIGNAL}(pat_{pr})\right|^2}{\left|\text{NOISE}(pat_{pr})\right|^2} > 1\right) \tag{9.35}$$

where $pat_{pr} = \{\Delta G^c = G^c - \tilde{G}_r^c, \Delta G^d = G^d - \tilde{G}_r^d\}$, G is shear modulus, $\tilde{G}$ correspond to reference healthy tissue, and c and d are refer to connective and dermic tissue respectively.

From the definition of the simulated noise, the dependency of the variation of the measurement with increasing noise is also linear. These two considerations about linearity support the proposal that the measurements on a specimen with noise and with pathology can be expressed as *Taylor series expansion* centered at the case without noise and without pathology , and neglecting higher order terms (*hot*) than linear,

$$\psi_i(pat_{pr}, \sigma) = \psi_i(0,0) + \sum_p \underbrace{pat_{pr}\frac{\mathrm{d}\psi_i}{\mathrm{d}pat_{pr}}(0,0)}_{\text{SIGNAL}} + \underbrace{\sigma\frac{\mathrm{d}\psi_i}{\mathrm{d}\sigma}(0,0)}_{\text{NOISE}} + hot \tag{9.36}$$

where $i = 1, ..., N_i$ are the measuring points for a general case (one in our design). The first term on the right hand side is the measurement at point i without noise nor pathology. The second term is the alteration of that measurement due to the presence of the pathology only, and is labeled SIGNAL, following the reasoning above. The third term is the alteration of the signal originated by the noise only (NOISE).

The second term of the *Taylor* series depends on the sensitivity of the measurements on the pathology, and can be approximated by finite differences,

$$\begin{aligned}&\frac{\mathrm{d}\psi_i}{\mathrm{d}pat_{pr}}(\tilde{pat}_{pr}, 0)\\ &= \psi_{i,_{pat_{pr}}}(\tilde{pat}_{pr}, 0) = \frac{\psi_i(\tilde{pat}_{pr} + \Delta pat_{pr}, 0) - \psi_i(\tilde{pat}_{pr} - \Delta pat_{pr}, 0)}{2\Delta pat_{pr}}\end{aligned} \tag{9.37}$$

where $\tilde{pat}_{pr} \rightarrow 0$ is a small pathology used to guarantee that the FEM captures the perturbations produced at small Δpat_{pr} (since the case $pat_{pr} = 0$ with no pathology needs to be computed with a topologically different mesh), in order to compute $\psi_{i,pat_{pr}}(p_0, 0) \approx \psi_{i,pat_{pr}}(0,0)$. In addition, a central difference scheme, which yields an error of the order $O(\Delta pat_{pr}^2)$, becomes available. Since the noise component is linear by definition, a forward difference scheme is adopted, whose $O(\Delta\sigma)$ error is sufficient.

The third term of the *Taylor* series can be directly derivated if the definition of POD is assumed,

$$\frac{\mathrm{d}\psi_i}{\mathrm{d}\sigma} = \xi_i \mathrm{RMS}(\psi_i^{\mathrm{FEM}}) = \xi_i \mathrm{RMS} \tag{9.38}$$

Equations (9.36), (9.38) and the relationship $|Y_i|^2 = \frac{1}{m}\sum_{i=1}^{m} Y_i^2$, can be combined into (9.33) to obtain,

$$\mathrm{POD}_{pr} = P\left(\frac{{pat_{pr}}^2 \frac{1}{N_i}\sum_{i=1}^{N_i}(\psi_{i,pat_{pr}}(0,0))^2}{\sigma^2 \mathrm{RMS}^2 \frac{1}{N_i}\sum_{i=1}^{N_i}\xi_i^2} > 1\right) \tag{9.39}$$

$$= P\left({pat_{pr}}^2 > \frac{\mathrm{RMS}^2\sigma^2\sum_{i=1}^{N_i}\xi_i^2}{\underbrace{\sum_{i=1}^{N_i}(\psi_{i,pat_{pr}}(0,0))^2}_{S_p}}\right) \tag{9.40}$$

If the noise generator ξ_i is a random variable, the POD is a probability of the stochastic variable ${pat_{pr}}^2$, described by the cumulative probability density function F,

$$\mathrm{POD}_{pr} = F\left(\frac{\mathrm{RMS}^2\sigma^2\sum_{i=1}^{N_i}\xi_i^2}{S_p}\right) \tag{9.41}$$

Using Monte Carlo techniques and error propagation theory the noise in the measurement points can be concluded to follow a normal distribution [272]. Assuming this distribution, the squared sum of the noise ξ_i is known to follow a *Chi-square* distribution, since $\sum_{i=1}^{N_i}\xi_i^2 \longrightarrow \chi^2_{N_i}$ (e.g. [274]). The parameter of the *Chi-square* distribution is the number of degrees of freedom N_i, which in this case is the number of measurement points. In the case that $N_i > 10$, the *Chi-square* distribution can be approximated by a Gaussian or normal N distribution $\chi^2(N_i) \approx N(N_i - 2/3, \sqrt{2N_i})$ with mean $N_i - 2/3$ and standard deviation $\sqrt{2N_i}$. This approximation in (9.41) yields,

$${pat_{pr}}^2 \longrightarrow N\left[\frac{\mathrm{RMS}^2\sigma^2(N_i - 2/3)}{S_p}, \frac{\mathrm{RMS}^2\sigma^2\sqrt{2N_i}}{S_p}\right] \tag{9.42}$$

Since $F(x) = \int_{-\infty}^{x} f(y)\mathrm{d}y$ is the cumulative of the normal probability density function f, whose inverse is $x = G(F(x))$, the useful pathology severity to noise ratio pat_{pr}/σ can be expressed from (9.42) given a POD level as,

$$\frac{pat_{pr}}{\sigma} = \sqrt{\frac{\mathrm{RMS}^2(N_i - 2/3)}{S_p}\left(1 + G[\mathrm{POD}_{pr}]\frac{\sqrt{2N_i}}{N_i - 2/3}\right)} \tag{9.43}$$

Note that the analytical expression (9.42) is only valid for noise with normal distribution at the measurement points.

The central focus of our contribution in this chapter is the optimization of the transducer design with the aim of maximizing the sensitivity to shear properties. Several numerical approaches can be used to evaluate transducer designs for each of the design parameters required, to maintain transducer performance within a specified range [161, 162]. The issue of the probability of detection (POD) has only been addressed independently, under the name of identifiability, in statistics and mathematics, with a wide application in chemistry and physics. In this chapter, the design optimality criteria called Robust Probability of Detection (RPOD) is proposed as a methodology approach (see Chapter 8). It is defined with the goal of maximizing the transducer sensitivity to the tissue properties while minimizing the sensitivity to noise ratio of the multilayered shear elastic constants.

9.3.3 Convergence

In order to select the space and time discretization size, a convergence study is carried out, aimed at finding an acceptable trade-off between computational speed and model error. Two discretization parameters are responsible for convergence: (1) time incremental, and (2) element size, which is inversely proportional to the number of elements.

The time increment convergence was obtained evaluating in a range within 12 [ns] and 3200 [ns] in finite element model and was described by the following figures, where 25 [ns] was chosen as the optimal time step. P waves speedily oscillating were captured with 12 [ns] (see figure 9.6), and S waves slowly oscillating whereas S-waves were only reproduced with 3200 [ns]. Therefore, P waves have been flittering-out numerically.

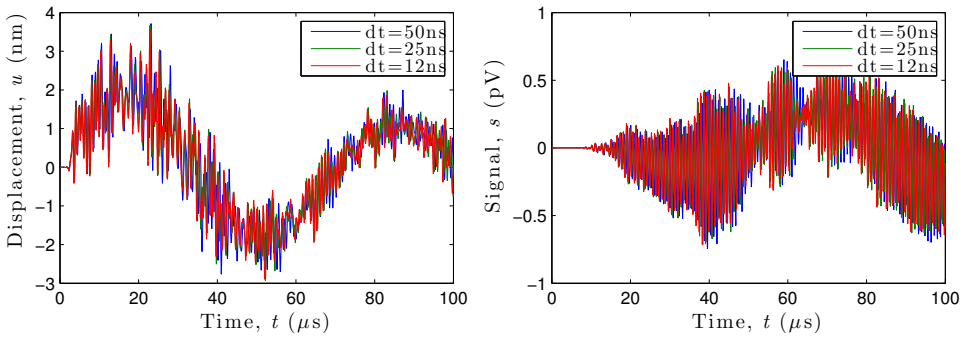

Figure 9.5: Time step convergence

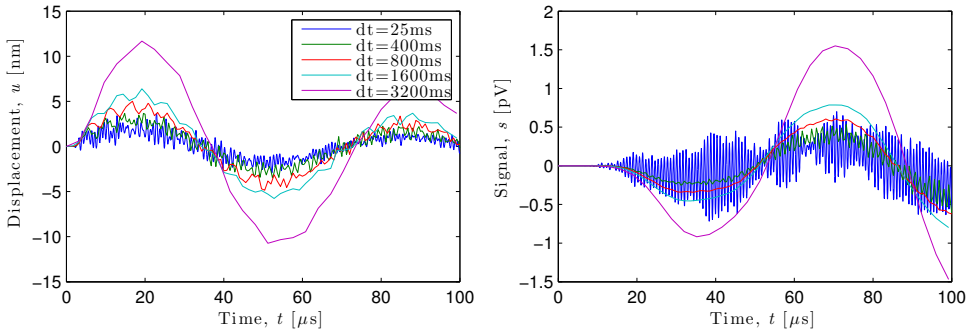

Figure 9.6: High incremental time time step convergence

The study of convergence of the spacial mesh was obtained from twelve mesh refinement parameters q_3, n, m, n_2, q_5, q_2, q_1, q_4, l, p, l_1 and l_2. The final combination of parameters was chosen according to an appropriate error to computational time trade-off, and the final model consists of 1052 nodes, 186 elements and 32 time increments. The following chart describes the geometry of the parametric distribution of the blocks of elements and their mesh parameters (see figure 9.7).

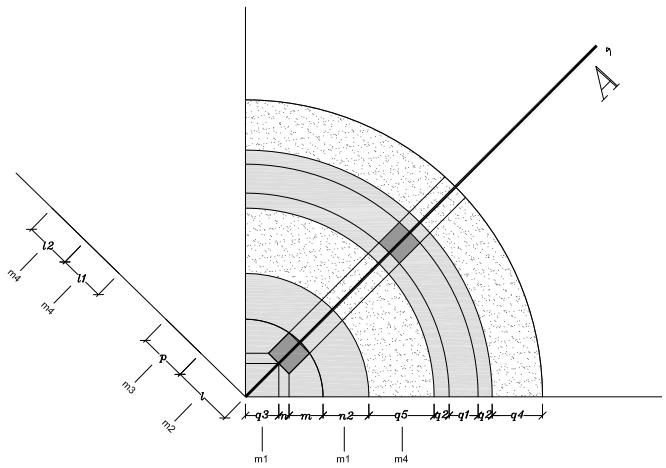

Figure 9.7: Geometry of the blocks and mesh parameters.

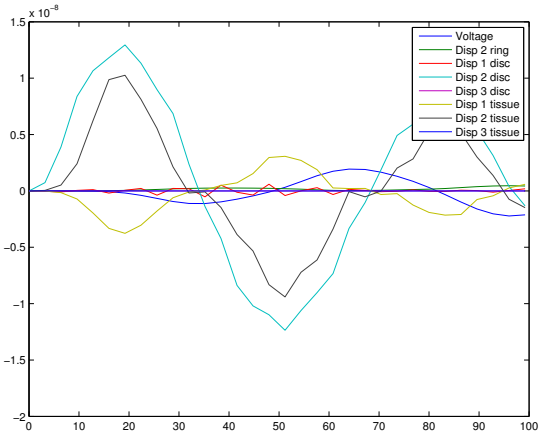

Figure 9.8: Simulation of evolution of several control points of the model.

The purpose of the numerical results is to obtain conclusions about which experimental design is better in characterizing mechanical tissue properties. To the latter end, three independent criteria are evaluated numerically: The effects of the excitation and driving frequency combination on (i) the measurements, (ii) the cost function and (iii) the RPOD, are studied for a set of configurations. The scope is to extract some *a priori* thumb rules that allow to select those with a more accessible minimum in the cost function, and guarantee satisfactory results for a minimization algorithm.

9.3.4 Simulated measurements

Consider the specimen described in previous sections, a sample of resulting measurements is shown in figures 9.8 and 9.9. The simulated signal incorporates a 10% of noise to avoid the inverse crime. The inverse crime consists in using the same model for simulating the measurements than for reconstructing or inverting the unknowns instead of generating the measurements by a different procedure. This is badly regarded in the inverse problem community since a perfect reconstruction is easily achieved, and robustness cannot be assessed, since any small discrepancies between model and reality are not taken into account, which yields an unreal and optimistic result.

9.3.5 Sensitivity analysis

The materials of the disc and ring evaluated in the design were steel, aluminum, carbon fiber, ceramic and PMMA with the following mechanical properties (see table 9.3 below). These materials were chosen according to their mechanical properties and the quality of the simulated received signal in terms of amplitude. The piezoelectric properties of PZT-5A are provided by the material manufacturer, and the Rayleigh stiffness damping is estimated from our experimental experience.

A sensitivity analysis was performed too by assessing the model dimensions according to the ranges chosen with a convergence criteria shown in table 9.4.

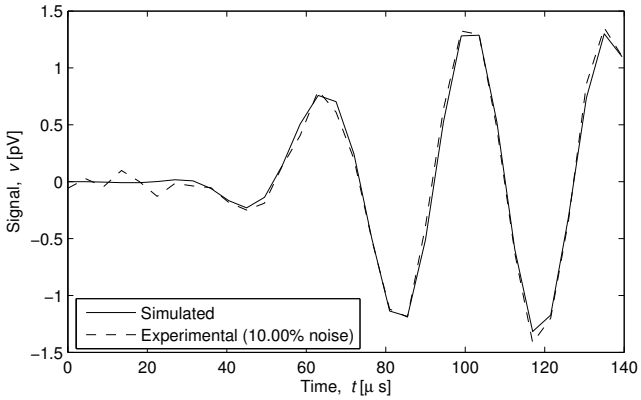

Figure 9.9: Simulated measurements for model design, noise 10%

Material	Young Modulus [MPa]	Poisson coefficient	Density [kg/m^3]
Steel	210	0.3	7800
Aluminium	65	0.3	2700
Carbon	150	0.3	1500
PMMA	3	0.3	1200
Ceramic	80	0.3	1800

Table 9.3: Materials used in the design

Design Parameters	Range	Reference [mm]	Label
Piezoelectric ceramic width	[0.75, 2]	1	pw
Piezoelectric ceramic length	[0.5, 2]	1	pl
Piezoelectric ceramic thickness	[0.5, 4]	2	pt
Disc piezoelectric ceramic eccetricity	[1.5, 3.5]	2.5	dpe
Disc radius	[1.75, 5.75]	4.25	dr
Ring piezoelectric ceramic eccentricity	[5.75, 8.5]	7.5	rpe
Ring width	[1.5, 2.5]	2	rw
Disc and ring ceramic thickness	[3, 13]	8	drt

Table 9.4: Design parameters and their admissible ranges.

The first part of the sensitivity study for the model parameters concerns the design geometrical dimensions of the sensor within their admissible ranges. It follows that, as the width of the piezo *pw* piezoelectric width from 0.75 to 2.00 [mm] increases, the P-wave amplitude for high frequency and frequency increases too. However, the S-wave amplitude at low frequency both outside and inside the ring is indifferent to this range. The same applies to the length of piezoelectric *pl* piezoelectric ceramic length: the P-wave amplitude is directly correlated with it, for both high and low frequency components of the response.

Thereafter, we analyze the sensitivities regarding design ranges for the sensor geometry. *dpe* denotes the disc piezoelectric ceramic eccentricity from the center of the sensor, which varies from 1.50 to 3.50 [mm]. The amplitude of the P-wave amplitude is observed to increase with *dpe*. However the disc radius *dr* shows an opposite trend, as the P-wave amplitude decreases when *dr* increases for frequencies above 1 $[MHz]$ and below 50 $[kHz]$. The

same happens to the amplitude of waves at low frequency S. The voltage signal increases with the disc radius distance dr.

The next parameter to be analyzed is the ring piezoelectric ceramic eccentricity rpe. Here, the range varies between 5.75 and 8.5 [mm], and no change is observed by varying this design parameter.

The following parameter was studied for which sensitivity analysis was rw defined as the width of the ring. The ranges studied varied between 1.50 and 2.50 [mm] and showed no significant differences in the outcome of the movement amplitude either within the interior of the sensor, the ring, or the recorded voltage signal. Notably, only the S wave amplitude at low frequency in radial displacement decreases with this distance.

Finally, the disc radius thickness drt generated a decrease in the P wave amplitude at frequencies above 1 $[MHz]$ and S-wave (circumferential component of the movement) below 50 $[kHz]$. The signal voltage amplitude hardly changes for the studied range of values. Some examples of sensitivity analysis have been calculated and are represented below in figure 9.10.

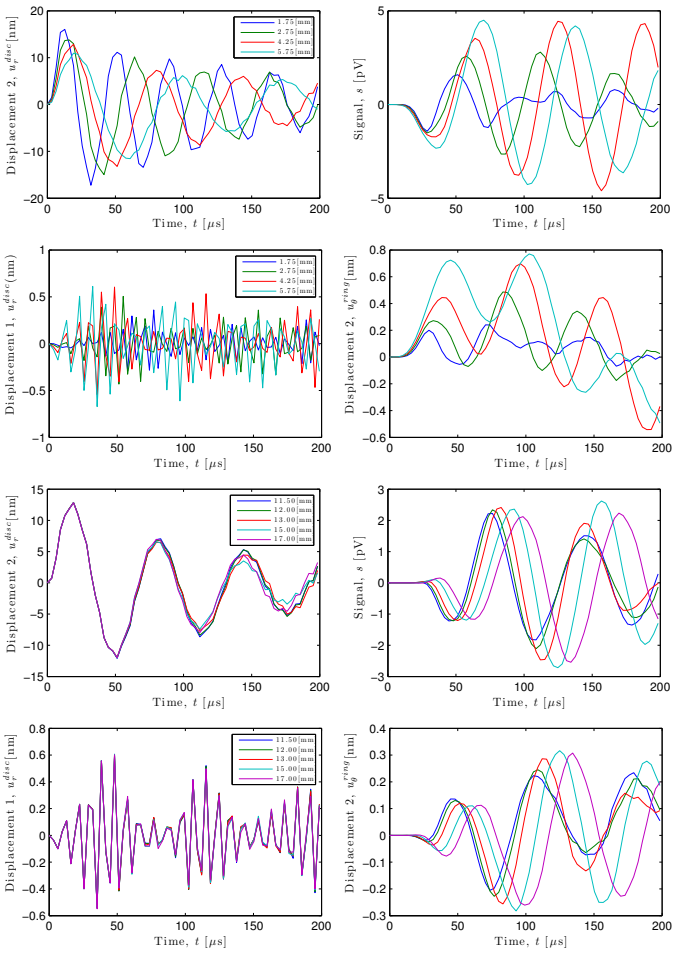

Figure 9.10: Example of sensitivity analysis for rpe and dr parameters with total time 200 μs related to turn displacement disc and radial displacement ring

Tissue sensitivity analysis

Hereinafter, the calculation of the sensitivity of the model parameters that describe the tissue pathology is developed, both for the dermal tissue layer and for the layer of connective tissue, which were chosen as significant within the model. To validate the model, the ranges of values of S-wave velocity in both dermic tissue and connective tissue, as well as the P-wave speed were verified to agree with literature values. Our simulated values ranged for the S wave velocity in $[20, 380]$ [m/s], and for P-waves $[1200, 1800]$ [m/s], while the thicknesses layers in dermic and connective tissue was allowed to range at $[0.3, 0.7]$ [mm].(see [275, 276] and figure 9.11).

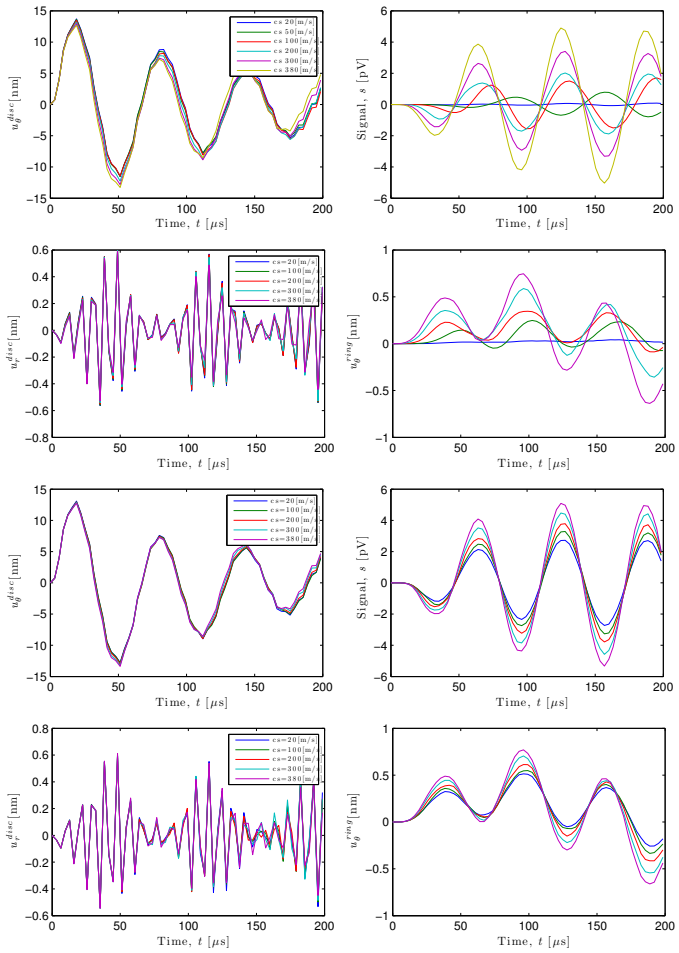

Figure 9.11: Example of sensitivity of connective and dermic tissue with total time 200 [μs] turn radial displacement disc and voltage signal varying secondary wave speed

By varying the shear modulus of dermal tissue, we find that the amplitude of P waves of frequency above 1 $[MHz]$ behaves independently for the allowed range of values. Interestingly, the S-wave amplitude at the ring varies, whereas it does not change at the disc.

9.3.6 Effects on cost functional

The shape of the cost function provides another subjective way to evaluate the sensitivity of the numerically predicted signals, based on the following criteria:

- The existence of local or global minima affects the convergence of the search algorithm.
- Steep minima are better than those providing soft valleys, due to algorithm convergence performance.
- Valleys that present shapes close to circular are considered as an indicator of uncoupled mechanical properties of soft tissue parameters.

Figure 9.12 shows a slice of the multidimensional cost function as functions of the parameters G_d and G_c that are equivalent to C_{E44}, C_{E55} and C_{E66} (see equation 8), for configuration of the model.

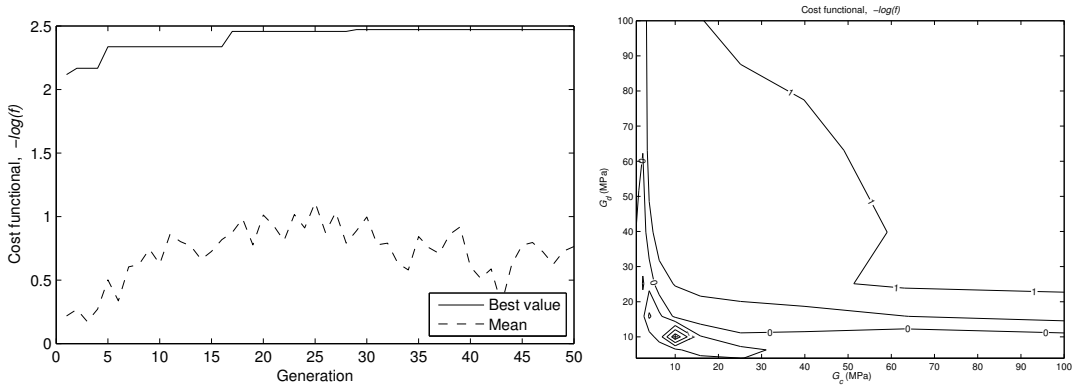

Figure 9.12: Cost functional as a function of the parameters with reference G_d and G_c. The cost function is minima for the model (10,10) noted by +.

9.3.7 Effects on POD

The aforementioned criteria is aimed at evaluating the local behavior of the cost functional, regardless of the noise effects. However, maximizing the POD enables to find the smallest pathology given the presence of experimental noise, independently of the robustness of the convergence of the search. Moreover, the POD serves as a quantifiable and comparable magnitude that can be used as an objective optimality criterion. Figure 9.13 shows an example of the POD estimation for one excitation configuration for increasing pathological values, whereas the dependency of the POD on the pathology extent is illustrated for a fixed noise level that amounts to 10 %.

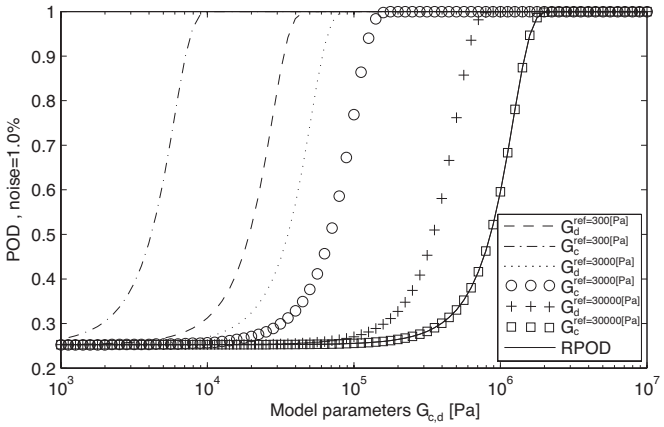

Figure 9.13: Dependency of the POD on the pathology indicator.

9.3.8 POD optimization

Once the effects of the POD are identified, the optimization is calculated to demonstrate how the POD serves as an optimality design criterion. The first four graphs show slices of regions around maximum POD over the 8 parameters of the model. The fifth graph shows the convergence of the genetic algorithms search with a population of 20 individuals and 50 generations of the best value. The last graph shows the optimized parameters for the best POD represented in table 9.5 and in figure 9.14.

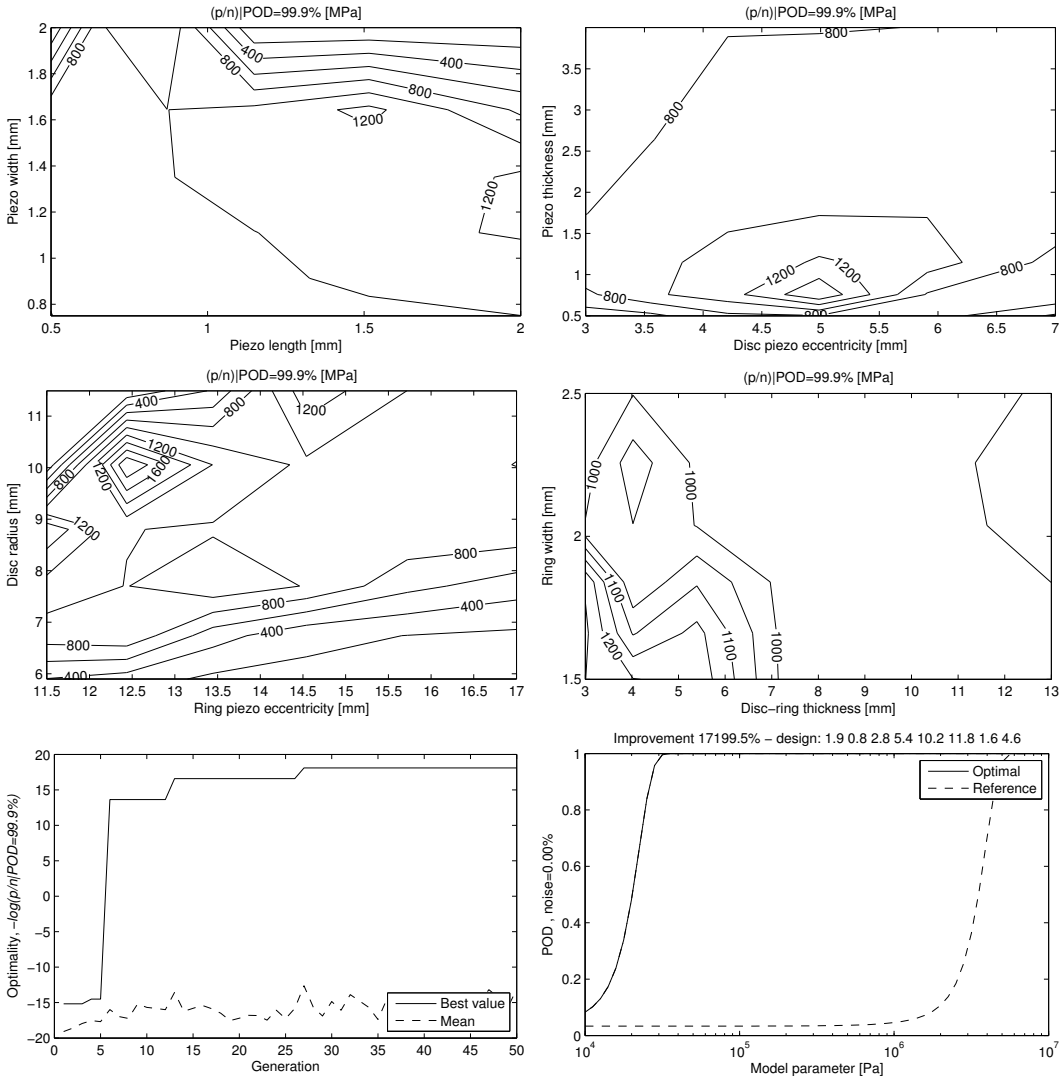

Figure 9.14: POD optimization

Note that the sensitivity of the sensor is increased 172 times with respect to a reference design. Finally, the central frequency of this design results 28 $[kHz]$.

Final dimensions of transducer were introduced in the manufactured design taking into account in the chosen material of steel.

Design Parameters	POD optimization [mm]	Label
Piezoelectric Width	1.9	pw
Piezoelectric Length	0.8	pl
Piezoelectric Thickness	2.8	pt
Disc Piezoelectric Eccentricity	2.7	dpe
Disc Radius	5.1	dr
Ring Piezoelectric Eccentricity	5.9	rpe
Ring Width	1.6	rw
Disc-Ring Thickness	4.6	drt
Disc-Ring Material	Steel	drm

Table 9.5: Final dimensions of transducer based on POD optimization

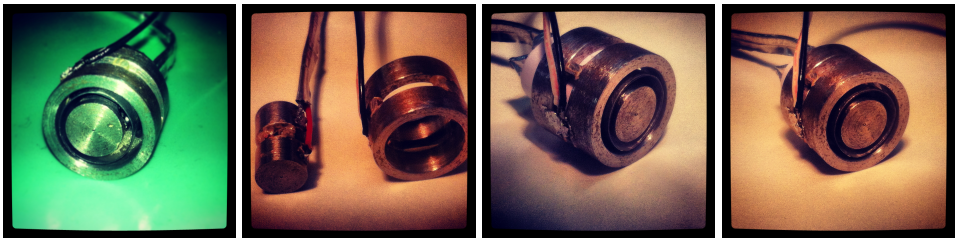

Figure 9.15: Manufactured sensor.

The first torsional ultrasonic transducer was manufactured by END lab team at the University of Granada in 2013 as is shown in Figure 9.15. The next section provides the possibility of measure linear a nonlinear parameters of a material with a quasifluid nature or tissue.

9.4 Torsional waves feasibility and capability for assessing measurements

The aim of this section is to explore the possibility of generate harmonics experimentally with a torsional ultrasonic transducer. The design of this sensor have been developed and improved for this purpose and widely reporter in the precious chapters. The amplitude of harmonics carried out the extraction of nonlinear classical acoustic parameter but taking into account as novelty the deviatoric shear part.

It is well known, the physical study of ultrasonic longitudinal P-waves phenomena vibrating through an isotropic material [277]. The equations that governs this process and their relationship between elasticity are also showed in several cases as was mentioned with detail in the previous chapters. The nonlinear classical extensions interacting with different homogeneous media have given us the idea to formulate the nonlinear shear parameters and validate them with a piezoelectric torsional sensor designed with this propose [39]. Therefore, if we consider S-waves, in particular torsional waves under nonlinear regime and their relative nonlinear classical acoustic parameters harmonics across different materials or soft tissues in the limit of compressibility, the model given by Zarembo [5] could be revisited and improved with a new type of considerations as was deducted in chapter 5. One of this considerations is the direct derivation of TOEC Third Order Elastic Constants [98].

Adding a particular novelty in this study this experimental method provides the Landau $\mathcal{A}$ parameter (See chapter 4) and this means an advance in nonlinear elasticity measurements by ultrasound technology. This is also useful in order to extract a new consequences in the field of tissue mechanics, this characterization improve the understanding of the nature on nonlinear waves and materials. Furthermore, from the point of view of biomedical applications and diagnosis technics, nonlinear shear waves could represent a new challenge due to the relationship proved between micromechanical properties and pathology or damage diagnosis [278, 279].

We have used the piezoelectric torsional design given by [39], in order to configure an experimental design based on three steps, i) validate the design of the transducer in the linear regime, ii) extract the classical nonlinear acoustic parameter β for silicon and soft tissue samples and iii) validate the measurements with a system based on the adjustment of the constitutive nonlinear law by minimum squares.

9.5 Linear measurements of shear modulus

In this section a briefly resume to introduce the linear measurements of shear waves in silicon and gelatin are related based on Valera's grade project in 2015 [280]. Firstly, the previous torsional sensor is experimentally improved by two research lines. On one hand its capsuled from a Faraday jail and prototyped with alignment trials with the whole electronic requirements, and on the other hand, some viscoelastic material are tested and validated with a blending test.

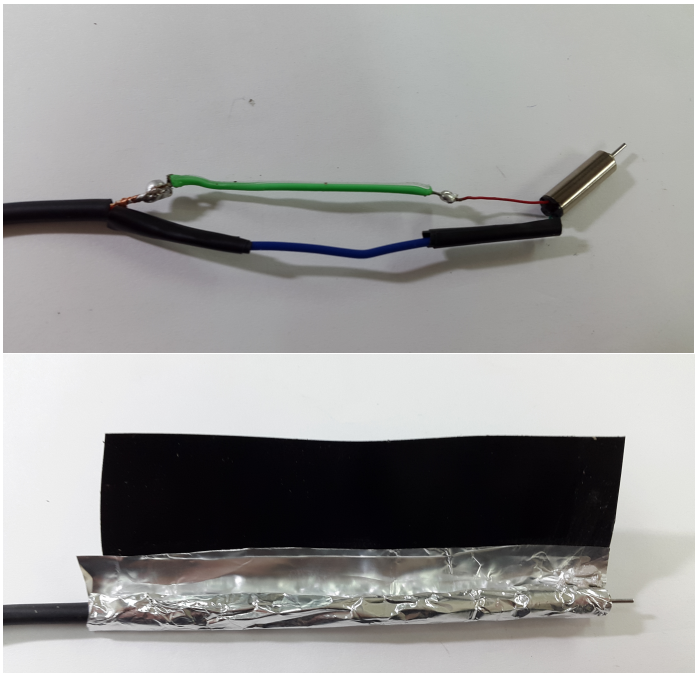

Figure 9.16: Faraday's jails for the capsulated transducer

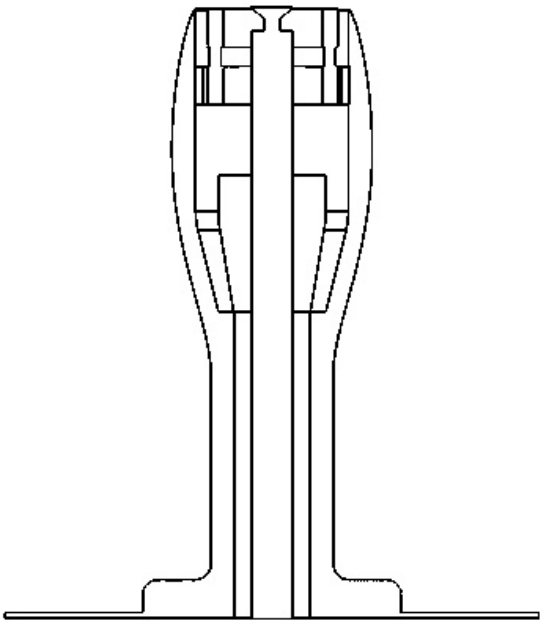

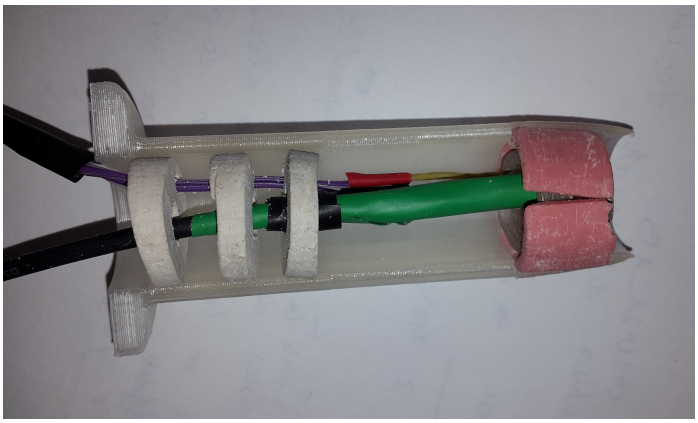

Figure 9.17: Torsional transducer prototyped

The best design is basically the identically but the emisor was changed by a dynamical micro-motor, and the receptor matin equal geometry steel by Polylactic acid (PLA) that could be printed by a classical standard printer. The analytical model developed in chapter 8 is valid for each measurements.

9.5.1 Measurements

The measurements obtained could be resumed in the next two tables, where the Young modulus is approximated to shear modulus with the expression detailed below when Poisson's coefficient is close to 0.5,

$$\frac{E}{3} = \mu \text{ if } \nu \approx 0.5 \tag{9.44}$$

Then the shear wave will be used with the aforementioned velocity of shear waves noted by c_s in the previous chapters as,

$$c_s = \sqrt{\frac{\frac{E}{3}}{\rho}} \tag{9.45}$$

The shear speed is calculated by time of flight t of S_0 initial signal through the sample with a known distance (the distance d from emisor to receptor) from the classical equation $c_s = \frac{d}{t}$. Specifically, the time of flight t is calculated from that signal that travel through the sample S_0, from the receiver signal S_r in the receiver.

$$S_r = S_0 + S_c \tag{9.46}$$

where S_r is the received signal when the sample is measured, S_0 is the initial signal and S_c is the signal transmitted through the capsule. time of flight of S_0 signal is compared with a simulation based on a excitation signal of the electromechanical actuator that been known the calculation of the delay is direct. Then, A cross correlation algorithm have been used to compare the simulated signal and S_0 in terms of plausibility but taking into account the delay of the system.

Energy (mV)	Frequency (Hz)	Delay (μ s)	Velocity (m/s)	Plausibility	μ (KPa)
200	600	450	10.51	0.9998	135.2
200	800	421.5	11.29	0.99986	137.2
200	1000	418.5	11.38	0.99656	158.6
200	2000	394.5	12.16	0.99862	180.9
200	3000	429	11.08	0.98034	150.2
400	600	432	10.99	0.9975	147.9
400	800	447	10.59	0.99986	137.2
400	1000	426	11.26	0.99688	152.5
400	2000	396	12.11	0.99984	179.4
400	3000	391.5	12.26	0.99320	184

Table 9.6: Scanning of frequencies and energies for PLA receiver, in silicone mold material

The final torsional transducer was prototyped in the Nondestructive evaluation (END) lab at the University of Granada and tested for several materials (See figure 9.17). In the case of silicone mold material, the frequency range used started from 600 to 3000 KHz, and the energy used was varied between 200 and 400 mV. The shear modulus was obtained in a range between 135 and 184 KPa with a plausibility of 0.99 for each measurement, see table 9.5.1.

Energy (mV)	Frequency (Hz)	t_S (μ s)	c_s (m/s)	P	μ (KPa)
200	600	585	7.97	0.99974	66.6
200	800	585	7.97	0.99888	66.6
200	1000	570	8.19	0.99427	70.4
400	600	580.5	8.03	0.99967	67.7
400	800	567	8.24	0.99797	71.2
400	1000	567	8.24	0.99754	71.2

Table 9.7: Scanning of frequencies and energies for PLA receiver, in gelatin material, with 92% of water

In the case of gelatin material with 92% of water, the frequency range used started from 600 to 1000 KHz, and the energy used was varied between 200 and 400 mV too. The shear modulus was obtained in a range between 66.6 and 71.1 KPa with a plausibility of 0.99 for each measurement.

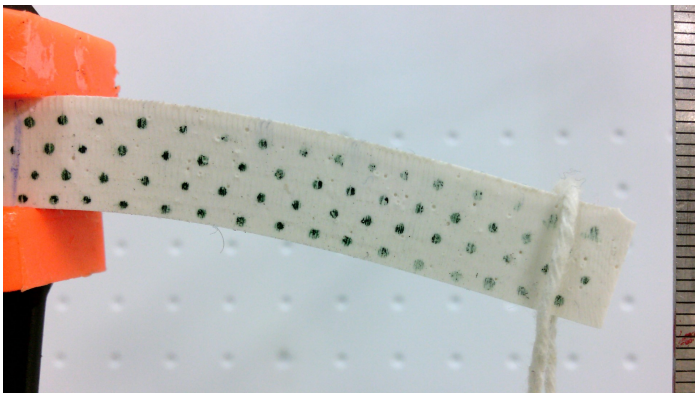

Figure 9.18: Shear modullus validated by a bending test for a silicone mold material

The experimental process to obtain the shear modulus of both materials was validated by a bending test. The figure 9.18 shows a small silicon beam, painted with dots in order to calculate strain based on displacements of these points by a correlation image algorithm and compatibility equation See chapter 4. Navier's law was used for the calculation of stress in a beam, it is commonly used in the strength of materials field [281].

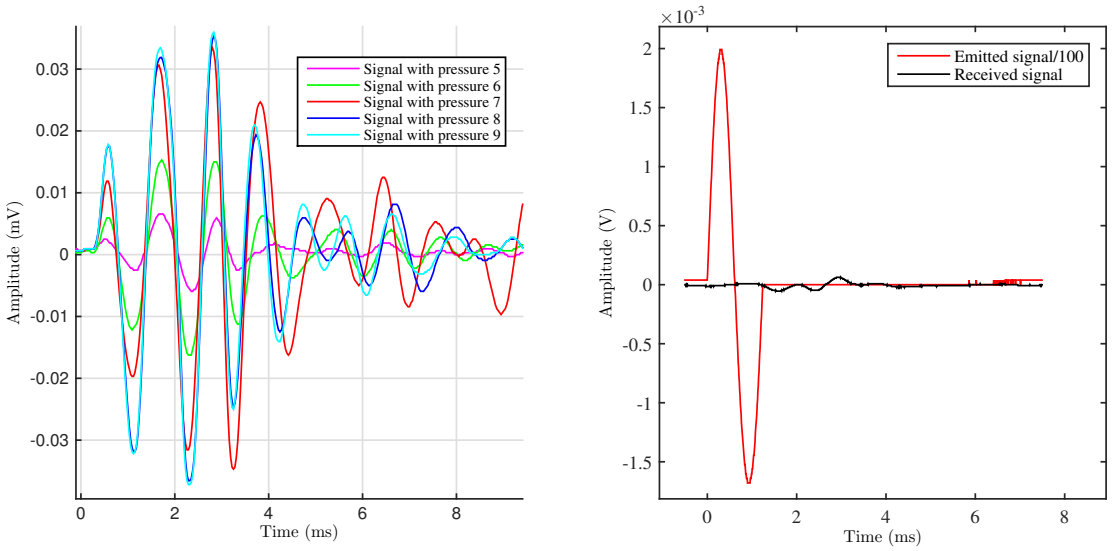

Figure 9.19: Torsional waves signals obtained for empty measurement (1) and several materials (2)

In the figures 9.19 is possible to appreciate the empty signal first and for several materials with different time of flights.

9.6 Nonlinear analytical restrictions to shear components

Following the chapter 6 where the series expansion concept put forth by Landau [98], only volumetric part is detailed in terms of the nonlinear acoustic parameter β,

$$-p \quad = \quad -3Kv + 9K\beta v^2 - 3\eta^v \, \dot{v}. \tag{9.47}$$

There are four combinations of nonlinear parameters β that may explain a different scenario of experimental calculations as in this case where the exploration of quasi-fluids nonlinearity is considered. The concept of the non uniqueness for the classical acoustic parameter β have been recently studied by Bender [75] but without a physical explanation. The aforementioned combinations could be expanded as exploring the whole set of combinations by quadratic terms as follows,

$$\sigma_{ij} = \underbrace{\underbrace{-3Kv\delta_{ij}}_{\text{pressure}} + \underbrace{2\mu D_{ij}}_{\text{shear}}}_{\sigma^L_{ij}\,(Linear)} \underbrace{\underbrace{-3\eta^v \dot{v}\delta_{ij}}_{\text{pressure}} + \underbrace{2\eta \dot{D}_{ij}}_{\text{shear}}}_{\sigma^V_{ij}\,(Viscous)} \tag{9.48}$$

$$\underbrace{\underbrace{+9K\beta^{vp}v^2\delta_{ij} + 9K\beta^{dp}D_{kp}D_{pk}\delta_{ij}}_{\text{pressure}} + \underbrace{4\mu\beta^{ds}D_{ik}D_{kj} + 4\mu\beta^{cs}vD_{ij}}_{\text{shear}}}_{\sigma^{NL}_{ij}\,(Nonlinear)} \tag{9.49}$$

where v and D_{ij} are the volumetric and deviatoric parts of the stress tensor defined in Equation (5). Four nonlinear parameters of first order have been defined as β^{vp}, β^{dp} as the volumetric, the deviatoric and the compound denoting the pressure components and β^{ds}, β^{cs} as the deviatoric, and compound denoting the shear components. Note that the combinations $vD_{kk}\delta_{ij}$ and $(D_{kk})^2\delta_{ij}$ have been neglected due to the definition of D_{ij}, where the deviatoric tensor contains trace equal to zero. The constants in function of K and μ accompanying nonlinear parameters have been chosen in accordance with Equation 9.47, as the quadratic power expansion. However in the case of quasifluids, when compressibility is much higher than shear moduli, it means $K >> \mu$ when the volumetric nonlinear terms could be neglected, this expassion results,

$$\sigma_{ij} = \underbrace{\underbrace{-3Kv\delta_{ij}}_{\text{pressure}} + \underbrace{2\mu D_{ij}}_{\text{shear}}}_{\sigma^{L}_{ij}\ (Linear)} \underbrace{\underbrace{-3\eta^{v}\dot{v}\delta_{ij}}_{\text{pressure}} + \underbrace{2\eta\dot{D}_{ij}}_{\text{shear}}}_{\sigma^{V}_{ij}\ (Viscous)} \tag{9.50}$$

$$\underbrace{\underbrace{9K\beta^{dp}D_{kp}D_{pk}\delta_{ij}}_{\text{pressure}} + \underbrace{4\mu\beta^{ds}D_{ik}D_{kj}}_{\text{shear}}}_{\sigma^{NL}_{ij}\ (Nonlinear)} \tag{9.51}$$

With the aim to find a relationship between this nonlinear expansion of beta parameters and TOEC, we assuming now that the strains are separated in volumetric and deviatoric part to the second order, so ε yields,

$$\begin{aligned} \varepsilon_{ik}\varepsilon_{kj} &= D_{ik}D_{kj} \\ \varepsilon_{ij} &= D_{ij} \\ \varepsilon_{kj} &= D_{kj} \\ \varepsilon_{kp} &= D_{kp} \\ \varepsilon_{pk} &= D_{pk} \end{aligned} \tag{9.52}$$

By making use of Cauchy stress described in Equation (4), in nonlinear regime, an equivalence is deducted in terms of Third Order Elastic Constants TOEC,

$$\begin{aligned} (\mathcal{A}+4\mu)\varepsilon_{ik}\varepsilon_{kj} &= (\mathcal{A}+4\mu)D_{ik}D_{kj} \\ \mathcal{B}\varepsilon_{kp}\varepsilon_{pk}\delta_{ij} &= \mathcal{B}(D_{kp}D_{pk})\delta_{ij} \end{aligned} \tag{9.53}$$

The above analysis is also valid combining nonlinear part of the stress with v and D_{ij} in the constitutive equation,

$$\sigma_{ij}^{NL} = D_{ik}D_{kj}(\mathcal{A}+4\mu) + D_{kp}D_{pk}\mathcal{B}\delta_{ij}$$

Since the relationship is established in the nonlinear constitutive equation, nonlinear acoustic parameters of first order are explicitly deducted as follows in terms of Third Order Elastic Constants,

$$\beta^{dp} = \frac{\mathcal{B}}{9K} \tag{9.54}$$

$$\beta^{ds} = \frac{\mathcal{A}+4\mu}{4\mu} \tag{9.55}$$

For the viscous components, it is shown that the establish definition in Equation. 9.47 matches Landau's one,

$$2\eta\dot{\varepsilon}_{ij} = 2\eta(\dot{D}_{ij}) \tag{9.56}$$

9.6.1 Perturbation method

By adopting the acoustic nonlinear constitutive equation presented above Equations 9.51 in terms of deviatoric a volumetric parts, is possible to establish the three dimensional nonlinear equation of motion up to first-order nonlinearity in terms of four parameters β. This formulation, implies that beta parameter is not unique [246] and it can be defined as the separation between pressure and shear waves written as

$$\begin{aligned}
\rho\frac{\partial^2 u_i}{\partial t^2} = {} & K\left(\frac{\partial^2 u_k}{\partial x_k \partial x_i} + \frac{\partial u_l}{\partial x_k}\frac{\partial^2 u_l}{\partial x_k \partial x_i}\right) \\
& +\mu\left(\frac{\partial^2 u_i}{\partial x_j^2} + \frac{\partial^2 u_j}{\partial x_i \partial x_j} + \frac{\partial^2 u_k}{\partial x_j^2}\frac{\partial u_k}{\partial x_i} + \frac{\partial^2 u_k}{\partial x_i \partial x_j}\frac{\partial u_k}{\partial x_j} - \frac{2}{3}\left(\frac{\partial^2 u_k}{\partial x_k \partial x_i} + \frac{\partial u_l}{\partial x_k}\frac{\partial^2 u_l}{\partial x_k \partial x_i}\right)\right) \\
& +9K\beta^{dp}\left(\frac{1}{2}\left(\frac{\partial^2 u_l}{\partial x_k \partial x_i}\frac{\partial u_l}{\partial x_k} + \frac{\partial^2 u_k}{\partial x_l \partial x_i}\frac{\partial u_k}{\partial x_l} + \frac{\partial^2 u_l}{\partial x_k \partial x_i}\frac{\partial u_k}{\partial x_l} + \frac{\partial^2 u_k}{\partial x_l \partial x_i}\frac{\partial u_l}{\partial x_k}\right) - \frac{2}{3}\frac{\partial^2 u_k}{\partial x_k \partial x_i}\frac{\partial u_l}{\partial x_l}\right) \\
& +4\mu\beta^{ds}\left(\frac{1}{4}\left(\frac{\partial^2 u_i}{\partial x_k \partial x_j}\frac{\partial u_k}{\partial x_j} + \frac{\partial^2 u_k}{\partial x_i \partial x_j}\frac{\partial u_k}{\partial x_j} + \frac{\partial^2 u_i}{\partial x_k \partial x_j}\frac{\partial u_j}{\partial x_k} + \frac{\partial^2 u_k}{\partial x_i \partial x_j}\frac{\partial u_j}{\partial x_k}\right)\right) \\
& +4\mu\beta^{ds}\left(\frac{1}{4}\left(\frac{\partial^2 u_k}{\partial x_j \partial x_j}\frac{\partial u_i}{\partial x_k} + \frac{\partial^2 u_j}{\partial x_k \partial x_j}\frac{\partial u_i}{\partial x_k} + \frac{\partial^2 u_k}{\partial x_j \partial x_j}\frac{\partial u_k}{\partial x_i} + \frac{\partial^2 u_j}{\partial x_k \partial x_j}\frac{\partial u_k}{\partial x_i}\right)\right) \\
& +4\mu\beta^{ds}\left(-\frac{1}{3}\left(\frac{\partial^2 u_k}{\partial x_k \partial x_j}\frac{\partial u_i}{\partial x_j} + \frac{\partial^2 u_k}{\partial x_k \partial x_j}\frac{\partial u_j}{\partial x_i} + \frac{\partial^2 u_i}{\partial x_j^2}\frac{\partial u_k}{\partial x_k} + \frac{\partial^2 u_j}{\partial x_i \partial x_j}\frac{\partial u_k}{\partial x_k}\right) + \frac{2}{9}\frac{\partial^2 u_k}{\partial x_k \partial x_i}\frac{\partial u_l}{\partial x_l}\right)
\end{aligned} \tag{9.57}$$

where K is the Bulk modulus, μ is the shear modulus, ρ is the density and $\beta^{vp}, \beta^{dp}, \beta^{ds}$ and β^{cs} are the four nonlinear parameter of first order explained below in the constitutive

expression. The relevance of this expression is directly linked with the separation of P and S waves and the possibility of design an experimental setup to extract new measurements. Applying the perturbation method [247] allows to write the wave displacement as,

$$u_i = u_i^{(0)} + u_i^{(1)} + \dots \tag{9.58}$$

where $u^{(0)}$ and $u^{(1)}$ denote the zero-order and first-order perturbation solutions, respectively. The zero-order perturbation solution corresponds to the fundamental solution of the linear wave equation (that is, when $\beta = 0$). The first-order perturbation solution is denoted by $u^{(1)}$. Since the effect of the nonlinear term β is small, an approximate solution can be obtained by iteration. When considering a shear wave propagating in a semi-infinite elastic layer, the latter is given as,

$$\begin{aligned}
u_1^{(0)} &= -A_{h2}\sin\theta\cos\left(\omega_2\left(\frac{(x_1\cos\theta + x_2\sin\theta)}{c_s} - t\right)\right) \\
u_2^{(0)} &= A_{h1}\cos\left(\omega_1\left(\frac{x_1}{c_s}\right) - t\right) + A_{h2}\cos\theta\cos\left(\omega_2\left(\frac{(x_1\cos\theta + x_2\sin\theta)}{c_s} - t\right)\right) \\
u_3^{(0)} &= 0
\end{aligned} \tag{9.59}$$

$$\begin{aligned}
u_1^{(1)} &= B_a(x_1\cos\alpha_a + x_2\sin\alpha_a)\cos\alpha_a\cos\left(\omega_a\left(\frac{(x_1\cos\alpha_a + x_2\sin\alpha_a)}{c_p} - t\right)\right) \\
&\quad -B_{hb}(x_1\cos\alpha_b + x_2\sin\alpha_b)\sin\alpha_b\cos\left(\omega_b\left(\frac{(x_1\cos\alpha_b + x_2\sin\alpha_b)}{c_s} - t\right)\right) \\
u_2^{(1)} &= B_a(x_1\cos\alpha_a + x_2\sin\alpha_a)\sin\alpha_a\cos\left(\omega_a\left(\frac{(x_1\cos\alpha_a + x_2\sin\alpha_a)}{c_p} - t\right)\right) \\
&\quad +B_{hb}(x_1\cos\alpha_b + x_2\sin\alpha_b)\cos\alpha_b\cos\left(\omega_b\left(\frac{(x_1\cos\alpha_b + x_2\sin\alpha_b)}{c_s} - t\right)\right) \\
u_3^{(1)} &= 0
\end{aligned} \tag{9.60}$$

where A and B are the constant amplitudes of the shear wave, in zero and first order of perturbation respectively, and ω_1 and ω_2 are the is the angular frequencies. Let us then consider the zero-order perturbation equation in linear regime,

$$\begin{aligned}
\rho\frac{\partial^2 u_1^{(0)}}{\partial t^2} &= K\left(\frac{\partial^2 u_1^{(0)}}{\partial x_1^2} + \frac{\partial^2 u_2^{(0)}}{\partial x_2\partial x_1} + \frac{\partial^2 u_3^{(0)}}{\partial x_3\partial x_1}\right) \\
&\quad +\mu\left(2\frac{\partial^2 u_1^{(0)}}{\partial x_1^2} + \frac{\partial^2 u_1^{(0)}}{\partial x_2^2} + \frac{\partial^2 u_1^{(0)}}{\partial x_3^2} + \frac{\partial^2 u_2^{(0)}}{\partial x_1\partial x_2} + \frac{\partial^2 u_3^{(0)}}{\partial x_1\partial x_3}\right) \\
&\quad -\frac{2}{3}\mu\left(\frac{\partial^2 u_1^{(0)}}{\partial x_1^2} + \frac{1}{2}\frac{\partial^2 u_2^{(0)}}{\partial x_2\partial x_1} + \frac{\partial^2 u_3^{(0)}}{\partial x_3\partial x_1}\right)
\end{aligned} \tag{9.61}$$

Analogously, u_2 and u_3 this result is coherent with the solution given by Graff [277], where the speed of sound of shear waves are derived as follows,

$$c_s = \sqrt{\frac{\mu}{\rho}} \tag{9.62}$$

9.6.2 Analytical solutions

The analytical solution is obtained by the application of perturbation theory, were detailed in Equations 8.21 and 8.22 and the consequent nonlinear acoustic parameter is derived as follows,

$$\frac{B_a c_s^3}{x_1 A_1^2 \omega_1} = 3(9\beta^{dp}K + 2\beta^{ds}\mu) \tag{9.63}$$

This results can be compared with the Zarembo ones [5]. in htat case see chapter 5, the nonlinear transversal acoustic parameter β_Z^τ was formulated through the TOEC,

$$\beta_Z^\tau = \frac{\mu}{\rho_0} + \frac{1}{\rho}\left(\frac{\mathcal{A}}{2} + \mathcal{B}\right) \tag{9.64}$$

So, converting β^{dp} and β^{ds} in the corresponding TOEC is posible to obtain a similar expression as,

$$\beta^T = \frac{(\mathcal{B} + \mathcal{A}/2 + 2\mu)}{4(3K + 4\mu)} \tag{9.65}$$

note that number 2 is due to the nonlinear source of the constitutive expansion introduced in Chapter 4.

In order to validate experimentally the theoretical background, is necessary to design an experimental procedure, for this purpose these results should be convert into a pressure magnitudes. Then, by making use of the conversion to amplitudes of fundamental and first harmonics into transversal stresses, it is posible to calculate the nonlinear shear parameters in terms of transversal stresses.

Then, torsional beta, β^T could be defined by in terms of pressures and disaggregated in two parts, one due to the liquid or water part and the other referred to collagen or fiber undulation part,

$$\beta^T = \frac{(\mathcal{B} + \mathcal{A}/2 + 2\mu)}{4(3K + 4\mu)} = -\frac{\rho c_s^3 T_{12}^{(1)}}{\pi f_1 x (T_{12}^{(0)})^2} \tag{9.66}$$

where the relation $2\pi f = \omega_1$ has been introduced and the relationship between pressure and displacements, used on numerous occasions in Chapter 8. The conversion of T_{12} will be explained in the experimental procedure.

9.7 Experimental setup

A schematic view of the experimental setup is shown in Figure 9.20. The transmiter and receiver are located in the same transducer as was explained in the previous sections. The measurements was taken as in transmission, with guarantees perfect alignment along the propagation direction of sound.

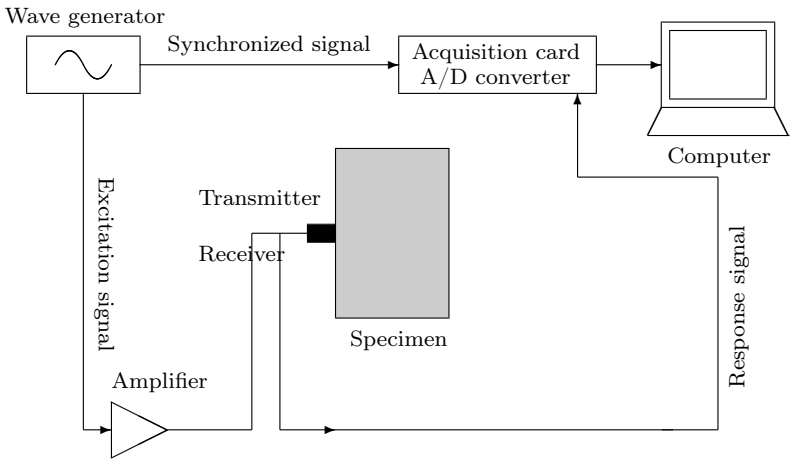

Figure 9.20: Experimental configuration for a nonlinear torsional transducer

The response signals were sampled with a high resolution A/D converter with amplification Fonestar without preamplification stage and saved for post-processing. The transmitter was a torsional transducer manufactured in our END lab at University of Granada of central frequency X Hz and Y in diameter. We used an arbitrary generator (Agilent 33500) to drive the transmitter at different frequencies. The ultrasonic excitation frequencies were arbitrarily chosen. Different frequency combinations were used: $f_1 = [600, 800, 1000]$ Hz. The amplitude of the input signal at the frequency was increasing, $[5, 10]$ V. To avoid unwanted interference effects in the propagation medium, even the risk of burning, we used short trains of pulses for excitation and a 8 ms pulse duration and 3 cycles.

We investigated the generated waves as a function of distance. The transmitter-receiver distance was a total distance of 2.43 mm. At the distance x from the transmitter, the pressure of the fundamental, $u_1^{(0)}$, and that of the generated harmonics, $u_1^{(1)}$, were determined, for the different frequencies and excitation levels.

The material used in this experiment was the silicone mold as a first step. Secondly, a connective tissue was explored with the transducer prototyped as is shown in Figure 9.21.

Figure 9.21: Connective and silicone mold tissue and material, respectively during measurements

Figure 9.23 shows the nonlinear torsional waves through a connective tissue, with the characteristic curved amplitudes as in the longitudinal waves.

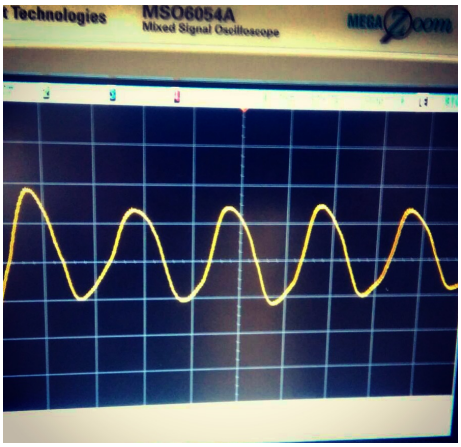

Figure 9.22: Nonlinear torsional signal from oscilloscope view

Note that the nonlinear torsional wave is not generated before with an ultrasonic device according with the literature reviews.

9.8 Experimental results

To obtain the experimental results, is necessary to use the following equation calculated from PZT-5 Piezoelectric material where elastic and electric field are coupled, it was formulated in Chapter 7,

$$T_{12} = C_{E44} S_{12} + e_{24} E_2 \tag{9.67}$$

Neglecting elastic field to found a conversion factor between voltage and Pascal, 122.9 Pa was the multiplication factor for the case of 10V and silicon mold. The conversion factor

is formulated from the analytical simplified model in Chapter 8, where piezoelectric and design material effects were considered interacting with two layers of tissue. For this reason, the stress on the piezoelectric ceramic is approximately the stress on the tissue by a correction factor α_c,

$$T_{12}^{\text{piezo}} = \alpha_c T_{12}^{\text{tissue}} \tag{9.68}$$

Parallel to this, to obtain α_c transmission coefficient should be calculated, by making use of the energy of the transmitter and receiver.

$$T = \frac{4z_1 z_2}{(z_1 + z_2)^2} = \frac{\text{energy,t}}{\text{energy,r}} \tag{9.69}$$

where $energy, t$ is the energy of the transmitter and $energy, r$ is the energy of the receiver. Knowing the different layers of the receiver, the stress and displacement ratios could be deducted as,

$$T_t = T_i \frac{2z_t}{z_i + z_t} \tag{9.70}$$

Analogously, the displacement ratio is given by,

$$u_t = u_i \frac{2z_i}{z_i + z_t} \tag{9.71}$$

Table 9.8 shows the transmission coefficients and the correction factors for the different samples of the test given by the relationship,

$$\frac{T_{12}^{\text{PZT-5A}}}{T_{12}^{\text{tissue}}} = \alpha_c = c_r \cdot \text{transmission PLA-PZT} \cdot \text{transmission PLA-tissue} \tag{9.72}$$

Sample	$\frac{u_t}{u_i}$	$\frac{T_t}{T_i}$	c_r Efficience %	Transmission PLA-PZT	Transmission PLA-Tissue	α_c
Silicon mold	≈2	0.026	≈10	0.78	0.026	≈0.01
Connective tissue	1.21	0.286	≈10	0.78	0.286	≈0.1
Liver tissue	≈2	0.0026	≈10	0.78	0.0026	≈0.001

Table 9.8: Table of transmission coefficients and correction factors for nonlinear torsional measurements

The final experimental results are detailed in Table 9.8 and in Figures 9.23 where nonlinear torsional acoustic parameter β^T was extracted for silicon mold, ligament tissue and liver tissue through the speed of sound of shear waves c_s, density ρ, shear modulus μ and transmission coefficient Z.

Sample	Energy (V)	Frequency (Hz)	ρ (kg/m^3)	c_s (m/s)	Z	μ (KPa)	β^T
Silicon mold	5	800	1100	13.2	13200	0.16	-400±3
Connective tissue	5	800	1000	90	90000	8.1	-8000±0.0
Liver tissue	5	800	1000	4	4000	0.016	-88±20
Silicon mold	10	800	1100	13.2	13200	0.16	-400±3
Connective tissue	10	800	1000	90	90000	8.1	-8000±0.0
Liver tissue	10	800	1000	4	4000	0.016	-88±20

Table 9.9: Nonlinear torsional results for input frequency and amplitude $f_1 = 800$ Hz and $A = 5, 10$ V, respectively, for silicone mold, connective and liver tissue

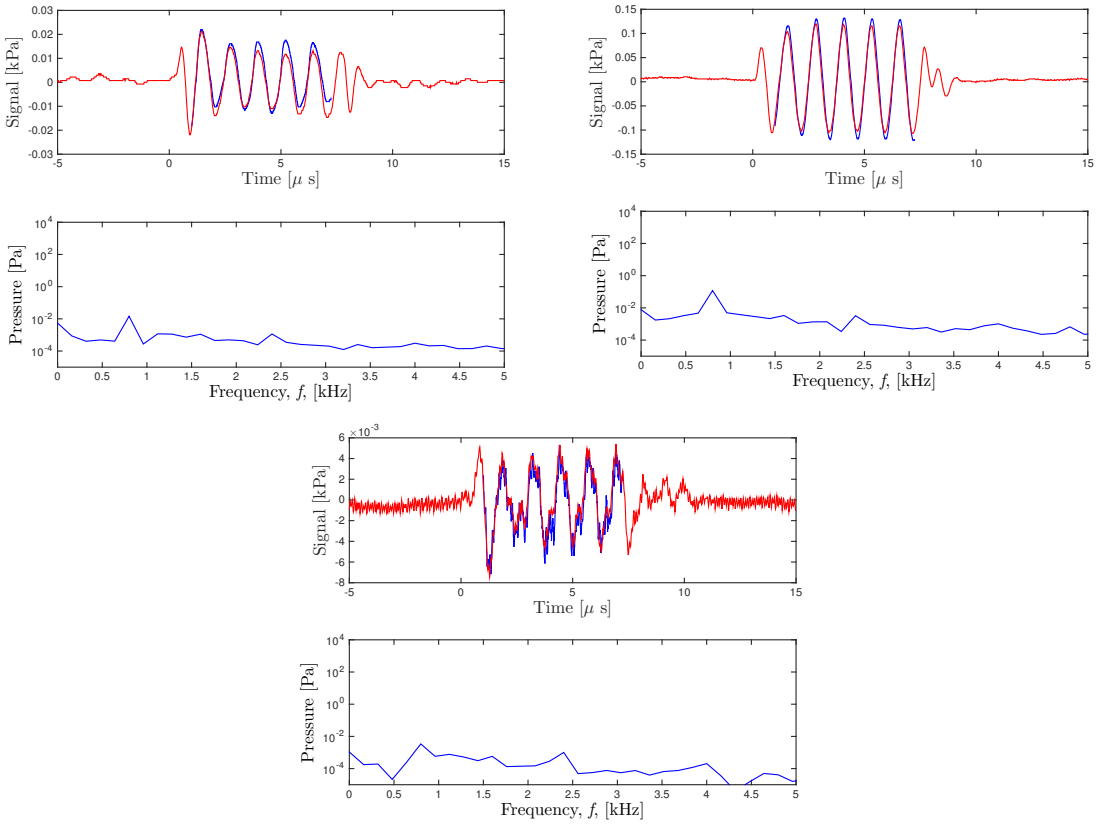

Figure 9.23: Nonlinear torsional signal from silicon and connective with frequency spectrum for 800Hz and 10V

Note that the experimental values of nonlinear torsional acoustic parameter β^T are adimensional and sufficiently small than solid or crystal as it is shown in the tables 5.2, 5.3, 5.4 and 5.5 and this connect with the reference values obtained from the literature, see Chapter 5, the case of tissue in different due to the nature of wave equation considered.

To conclude, a new ultrasonic sensor have been designed, optimized and manufactured based on the piezoelectricity theory, The Robust Probabilty of Detection and Inverse problem. This torsional ultrasonic sensor allows to quantify linear and nonlinear properties in quasifluids and soft tissues.

El tiempo de lo dicho y de los sonidos que lo acompañan son tiempos distintos y a la vez se encuentran en único tempo. La voz parece seguir por momentos un ritmo ternario. Sonidos que se escuchan llegar de otro mundo se mezclan con aquellos en los que se percibe cierta familiaridad. El sonido transporta pero, sobretodo, choca, alza en volandas por unos segundos y luego, deja caer. Sístole y diástole, el sonido atraviesa la piel.

El sonido en la piel: Desbordamiento de Val Del Omar
Carmen Pardo, 2010

Part IV

CONCLUSIONS AND FUTURE WORKS

10
Conclusions and future works

This chapter presents the most relevant conclusions of the obtained results, along with a discussion regarding the exposed contributions. In addition, some future works currently under development are commented.

The analysis of nonlinearity from the point of view of the theory of Elasticity and ultrasonic waves has been considered since the middle of the twentieth century. Nowadays, the relationship between these fields carry out a challenge due to its applications in the biomedical research. This thesis (1) provides a deeper knowledge about the mechanisms that unify nonlinear classical ultrasound and nonlinear elasticity according the references founded, (2) generates a new approach extending the classical nonlinear wave equation which presents a separation of fluid and matrix phases of a material or tissue, (3) suggests microdamage as a possible source of nonlinearity and (4) explores the possibility of measure the nonlinenar acoustic expansion with three experiment designed and validated building and manufacturing the devices.

In addition, the following relevant conclusions are extracted from each of research hypothesis proposed in Chapter 2. Their limitations and future works are also described.

Nonlinear Elasticity Unification

Research objetive 1: Create a new consistent framework where all theories in nonlinear classical elasticity are connected and a set of conversion factors to link to the Third Order Elastic Constants.

Through the unification of Third Order Elastic Constants and its derivation by invariants in nonlinear elasticity, a specific relationship between nonlinear elasticity up to fourth order and nonlinear acoustic parameters until third order have been developed. This allows to formulate the constitutive equation in terms of anisotropy and isotropy. It has been carried out up to third order. The main novelty and contribution of the Chapters 4 and refereed to the Chapter 4 is the understanding of the link of nonlinear acoustic parameter beta and that connect with Hamilton's theories (See [2, 282, 283]), in opposite to Rushchitsky who applied a relationship based on an Taylor extension without invariants (see [284, 285]).

Also, note that large strains have been taken into account in order to obtain a realistic expression of these nonlinear constitutive parameters following the path of Goldberg, Zarembo, Muir, and Stobbe (see [14, 5, 6, 126]). The works of Abelee, Johnson, Muller and Giordano, have been detailed previously and the differences between resides on the mechanical parameters restrictions used due to the nature of the material or tissue (see [286, 130, 287, 288, 117, 289, 290, 291]). Many authors such as Desdrade and Odgen, have stablished a similar definition of nonlinear acoustic parameter beta based on several different invariants but the relationship that they obtained is different to the one given by Hamilton (see [100, 292]).

Nonlinear classical acoustics

Research objetive 2: To unify nonlinear classical acoustic theories to exploring the relationship between this parameters an mechanical ones and extend this to other possible scenarios exploring its physical meaning.

We conclude the Chapter 5 with: a new approach to understand nonlinear acoustics and nonlinear elasticity parameters and their relationship. This connect with the definition developed by Gol'dberg, Zarembo and Hamilton, with the novelty of a new development and extension based on invariants, even so, for anisotropy environment and large strains. The nonlinear sources involved in this formulation are derived from: (1) Constitutive nonlinearity, (2) geometric nonlinearity starting from compatibility equation and (3) geometric nonlinearity beginning with stress of Cauchy definition.

The Westervelt nonlinear acoustics equations are also described in Chapter 5 by making use of the B/A parameter in fluids, under a Taylor expansion of the pressure. Is important to consider these equations as a particular case of nonlinear acoustics in liquids. The general nonlinear elasticity, nonlinear wave equation and their relationship are the main theories that allow the development of this research. Also, the role of small and large displacements are clearly important if we take into account the nonlinear effects on harmonic generation, where the cross term is significant. Note that attenuation has not been included at the moment due to is not necessary for our first assumptions. It will be a future work. The Westervelt equation has recently used in the field of medical ultrasound for tissues and fluids, as was mentioned in previous sections. These allow us to consider future applications

in this field i. e. correlating these nonlinear parameters with tissue characterization or even with different pathologies in tissue.

Nonlinear classical acoustics: Fluid and matrix phases

Research objetive 3: Define nonlinear constitutive constants with physical meaning from the point of view of the interaction of waves depending on fluid and matrix parts, rather than a power series expansion as proposed by Landau.

A new approach is carried out in the field of nonlinear acoustics when non unique beta constants considered. Chapter 6 explore and analyze from a physical and mathematics point of view this possibility and a new theory is exposed. The results are detailed in chapter 8 where the whole parameters are deducted from the interaction of P and S-waves. The perturbation theory is the methodology whose development provides a solution. The nature of this multiple nonlinearity suggest the physical meaning of these variables. Chapter 8 provides new techniques to validate and measure them experimentally. Under this objetive three sources of nonlinearity are exposed as an new approach that never have been explored: (1) Nonlinearity from compatibility cross term or geometric nonlinearity, (2) nonlinearity coming from the derivation of strain energy function and (3) nonlinear constitutive source.

Exploration of microdamage in solids

Research objetive 4: Extending the theory of Eshelby to solve various cases of geometrical inclusions and provide a method for measuring density of microcracks with a consistent relationship established between the acoustic nonlinearity and homogenization.

A nonlinear micro-mechanical approach is proposed in Chapter 7, that relates a distribution of clapping micro-cracks in damaged materials with the macroscopic measurable acoustic nonlinearity in solids. A 1D contact clapping mechanism inside each micro-crack is hypothesized to be responsible for a component of the quadratic nonlinearity. This relationship is formulated by establishing a bilinear clapping constitutive law, which is further approximated by a Taylor expansion, from which the second order constitutive nonlinearity stems. The simplifying assumption to restrict the effect to second order nonlinearity is of course questionable in terms of fully capturing the dynamics of a clapping crack, and even needs extension in a future work. However, there are practical reasons for solving the case of second order components, which is the generation of second harmonics, which are measurable with ultrasonic equipment and could be potentially used to inspecting the structural functionality and damage. It should be clarified that other possible sources of nonlinearity are not treated in this work, such as hysteretic clapping, crack tip plastic zone, partial closure, or atomistic nonlinearities. Their formulations therefore remain for future work.

The distributed micro-cracks are treated as individual penny-shaped inclusions behaving as formulated in Appendix A, embedded into a macroscopic medium through Eshelby's homogenization theory through a nonlinear Mori-Tanaka scheme [293]. The assumption

that penny-shaped inclusions are aligned is justified by the fact that fatigue cracks produced by a preferentially-oriented stress appear to be aligned. However, the case of randomly oriented micro-cracks remains to be solved in a future work.

The relationships between the measurable acoustic nonlinearity and the Landau-type nonlinearity definition required by the homogenization are also proposed. For this purpose, the proposed decomposition of stress and strain tensor into compressional and deviatoric parts plays a key role in redefining several possible acoustic nonlinearities in a convenient way.

There is a future work in progress on measuring the nonlinear cracks under the configuration mentioned at the end of Chapter 7. The control of effective nonlinearity may have be a great impact in the quantification of bone microcracks directly correlated with osseous quality and osteoporosis.

Nonlinear mixing

Research objetive 5: Develop new experimental techniques from ultrasonic sensors and different setups that allow us to measure the deduced theoretically parameters.

To measure experimentally the new parameters two main techniques have been carried out: (1) Based on a two waves mixing, and (2) based on the torsional transducer that has been mentioned below. Then, two waves mixing interaction have been measured in an immersion tank by collinear and nonlinear mixing procedure. For collinear mixing case, just one transducer and two waves are studied with a T-junction, this provides a nonlinear parameter of water that coincides with the literature values. So, a variation of the collinear wave mixing method was investigated to determine the acoustic nonlinear parameter β in water. Perturbation solutions of beta parameter in water were analytically calculated and validated with experimental measurements, for each $2f_a$, $2f_b$, $f_a + f_b$. A nonlinearity β value of 3.5 approximately was obtained, which is consistent with the literature references. However, in the case of the difference harmonic, $f_a - f_b$, contradictory results were obtained, suggesting that the amplitude of this harmonic is not related to the nonlinearity parameter β. In the case of non collinear mixing, this measurements are made from different samples of aluminum with special geometries. This allow integrate the interaction volume of waves inside the sample and validate the Korneev theory introducing the desired angles with a correction given by Zoeppritz. A posible limitation to this technique is the absolute value of FFT Fast Fourier Transform, it occurs when frequency spectrum is calculated by harmonic generation procedure. This explains the ambiguity of the sign phase that has repercussion in the quantification of the nonlinear acoustic parameters.

This technique provides at the first time one method to derive TOEC with ultrasound different of DAET deducting an explanation of nonlinearity from physical point of view.

Soft tissue nonlinearities

Research objetive 6: Evaluate the torsional wave feasibility and capability for assessing linear and nonlinear measurements of tissues.

An optimal piezoelectric transducer design was carried out by combining a piezoelectric finite element model and a robust analytical estimate of the probability of detection, called RPOD in Chapter 9. This allows to estimate the minimum pathology findable given a proposed sensor design, a layered tissue geometry and noise level on measurements. After validation, the RPOD is used as an optimality criterion to feed the used genetic algorithms. An analytical simplified model is formulated and validated with the finite element model, which is aimed at easily predict trends and design parameter dependencies.

The design has the ability to clearly separate P and S wave depending on the frequency and the time when the wave arrives at the receiver. Also, note that the simplified analytical model predicts the frequency response of the sensor with less than 1% error, which is considered validated finite element model. S-waves were only reproduced with 3200 $[ns]$, flittering-out P waves numerically. Even so, amplitude is not predicted by the simplified model, only central frequency and attenuation effects are not considered in the simplified model. The optimization improves 172 times the design. However, after application of the probability of detection of pathologies in the tissue there are several local minima therefore requires a global search algorithm such as genetic algorithms.

A set of sensitivity tests was performed to validate the robustness of the analytical estimates and verify the feasibility, sensitivity and specificity of the designed transducer by the algorithms above. The piezoelectric sensor was eventually manufactured based on the resulting design parameters at Non Destructive Evaluation Laboratory of the University of Granada by the END lab team (see figure 9.15).

Being a relevant approach the design and fabrication of a torsional transducer with several applications in the field of tissue mechanics, the experimental methodology to extract nonlinear shear wave have been rigorously analyzed. It must mention that the linear measurements of shear modulus on cervical tissue are relevant in the problem of preterm birth assessment it is an line of research of the END lab where this prototype is involved [40].

The nonlinear classical acoustics extension have been applied in the Chapter 9, extracting a solution that separates the nonlinear terms that are interpreted as nonlinearity from the matrix and the nonlinearity from the fibers. This is an important conclusion with a main novelty in tissue microstructure. The results suggest that these nonlinear terms that from now can be obtained at real time describe the behavior of the tissue in a new scale. This has triggered an ongoing work with potential impacts on biomedical research and understanding the mechanics of quasifluids and tissues.

11

Conclusiones y trabajos futuros

En este capítulo se presentan las conclusiones más relevantes que se han obtenido a través de los resultados, asimismo una detallada discusión de acuerdo a las contribuciones expuestas. Además, se comentan algunos trabajos futuros que actualmente están desarrollándose en nuestro laboratorio.

The analysis of nonlinearity from the point of view of the Theory of Elasticity and ultrasonic waves has been studied since the middle of the twentieth century. Nowadays, the relationship between these fields carry out a challenge due to its applications in the biomedical research. This thesis (1) provides a deeper knowledge about the mechanisms that unify nonlinear classical ultrasound and nonlinear elasticity according the references founded, (2) generates a new approach extending the classical nonlinear wave equation which presents a separation of fluid and matrix phases of a material or tissue, (3) suggests microdamage as a possible source of nonlinearity and (4) explores the possibility of measure the nonlinenar acoustic expansion with three experiment designed and validated building and manufacturing the devices.

El análisis de la no linealidad desde un punto de vista de la Teoría de la Elasticidad y de la propagación de ondas ultrasónicas ha sido estudiado desde el principio de la segunda mitad del siglo XX. Hoy en día, establecer un vínculo consistente la relación entre estos dos campos conlleva un reto debido su aplicación directa en la investigación biomédica. Esta tesis (1) proporciona un profundo conocimiento sobre los mecanismos que unifican la no linealidad clásica ultrasónica y la no linealidad elástica de acuerdo a las diversas fuentes examinadas, (2) genera un aporte nuevo extendiendo la ecuación de ondas no lineal lo cual

representa una separación en términos de fluido y matriz, diferenciando la no linealidad en fases debidas a la naturaleza del material o tejido, (3) sugiere una posible explicación de la no lineadad a partir del microdaño y (4) explora la posibilidad e realizar mediciones de los parámetros no lineales mediante tres experimentos nuevos y diseñando y construyendo dispositvos para este fin.

Además, en adelante se muestran las siguientes conclusiones extraídas de cada hipótesis propuesta en el capítulo 2. Se describen sus limitaciones y se detallan algunos trabajos actuales y futuros.

Unificación de la no linealidad elástica

Objetivo de investigación 1: Crear un esquema nuevo y consistente donde todas las teorías de nolinealidad clásica elástica se conectan con una serie de factores de conversión que relacionan unas con otras.

A través de la unificación de las TOEC Constantes Elásticas de Tercer Orden y su derivación por invariantes en el régimen de la elasticidad nolineal, se establece una relación con la no linealidad elástica hasta cuarto orden y acústica hasta tercer orden. Esto permite formular la ecuación constitutiva in términos tanto de isotropia como de anisotropia. La principal contribución en los capítulos 4 y 5 es el entendimiento del vínculo entre el parámetro de acústica nolineal clásica beta y su conexión con las teorías de Hamilton (Ver [2, 282, 283]), al contrario que las teorías de Rushchitsky donde se aplican esta relación a partir de un desarrollo en serie de Taylor sin invariantes. (Ver [284, 285]).

Además, las grandes deformaciones en la ecuación de compatibilidad se tienen en cuenta para obtener una expresión realista de estos parámetros constitutivos nolineales siguiento el camino de Gol'dberg, Zarembo, Muir y Stobbe (ver [14, 5, 6, 126]). Los trabajos de Abelee Abelee, Johnson, Muller y Giordano, se analizan con detalle encontrando que la principal diferencia con respecto a la teoría desarrollada reside en las restricciones debidas al tipo de material o tejido (ver [286, 130, 287, 288, 117, 289, 290, 291]). Algunos autores como Desdrade y Odgen, han establecido una definición muy similar a la desarrollada en esta tesis haciendo especial hincapié en el vínculo con la no linealidad acústica a partir de invariantes algebraicos válidos, pero sin encontrar un contexto consistente que apoye y valide las teorías de Hamilton (ver [100, 292]).

No linealidad acústica clásica

Objetivo de investigación 2: Unificar las teorías de no linealidad acústica clásica y explorar la relación entre los parámetros resultantes y los de origen mecánico. Extender dicha relación a otros escenarios posible determinando su significado físico.

Para extrapolar a valores reales estos resultados analíticos, se han extraído resultados numéricos a partir de algunas referencias encontradas. (Ver [6, 126, 5]). En el capítulo 5 se calcula el valor del parámetro nolineal acústico Beta en función de las Constantes Acústicas

de Tercer Orden de Landau y varía entre [-0.51, 8.54] para el caso de los metales, entre [-6.63, -1.88] para cristales, entre [3.5, 6.2] para líquidos, y entre [-3.96, -1.15] para el caso de tejidos biológicos. En el caso de fibra de carbono CRFP y PMMA, estos valores fueron simulados computacionalmente para poder obtener una posible visión de estos parámetros transversalmente isótropos en los distintos supuestos físicos que se detallan en el capítulo 5.

Una vez terminado el capítulo 5 se puede remarcar que el nuevo aporte llevado a cabo en el entendimiento de la no linealidad acústica y la no linealidad elástica proporciona una relación entre sus parámetros de forma consistente. Esto conecta con la definición desarrollada por Gol'dberg, Zarembo y Hamilton, con la novedad de un nuevo desarrollo basado en invariantes de energía y especificamente en la forma que estos se obtienen a través de las ideas de Landau, incluso para casos anisótropos y en grandes deformaciones.

Las ecuaciones de Westervelt se describen en el capítulo 5 haciendo uso del parámetro de no linealidad B/A en fluidos desde una expansión en serie de Taylor de la presión. Es importante considerar estas ecuaciones como un caso particular de no linealidad acústica en líquidos. Tanto la teoría general de la elasticidad como la ecuación no lineal de ondas permiten investigar el vínculo entre ambas en este contexto, donde el rol de los pequeños y grandes desplazamientos son muy relevantes ya que si tenemos en cuenta los efectos de la generación de armónicos el término cruzado en la ecuación de compatibilidad es muy significativo. Hay que tener en cuenta que los términos relativos a la atenuación no han sido tomados en cuenta, ya que no son necesarios en una primera etapa, pero en futuros trabajos serán analizados.

La ecuación de Westervelt se viene usando en el ámbito clínico modelizando dispositivos médicos con ultrasonidos con aplicación en tejidos como se mencionó en la introducción y en capítulos previos. Esto nos permite estimar que el estudio de su extensión e incluso de la ecuación KZK donde aparece un término más podría tener considerables aplicaciones futuras, por ejemplo correlacionando parámetros de no linealidad con la caracterización de tejidos tanto blandos como óseos e incluso ser una clave en el diagnóstico de distintas patologías.

No linealidad clásica en acústica: Fases de fluido y matriz en cuasifluidos y tejidos

Objetivo de investigación 3: Definir las constantes constitutivas no lineales dotándolas de sentido físico desde el punto de vista de la interacción de ondas planas dependiendo de su phase líquida y su phase matricial desde una expansion en serie como propuso Landau.

Si en el contexto de no linealidad acústica clásica consideramos que el parámetro β no es único, esto conlleva un nuevo aporte extendiendo y reescribiendo toda esta teoría. El capítulo 6 explora y analiza desde un punto de vista físico y matemático esta posibilidad y expone una nueva teoría basada en este supuesto. Los resultados están detallados en el capítulo 6 donde todos los parámetros no lineales resultantes se deducen a partir de la

interacción de ondas S y P. La teoría de la perturbación es la metodología encargada de hacer factible las soluciones analíticas del modelo en 3D. La naturaleza de este tipo de no linealidad clásica múltiple inspirador en el sentido de encontrar un significado físico a estos términos. El siguiente paso es encontrar y diseñar nuevas técnicas experimentales donde se validen los resultados conseguidos, cuya repercusión sería muy relevante.

Bajo este objetivo subyace un nuevo aporte donde se exponen tres fuentes de nolinealidad que nunca se han explorado conjuntamente: (1) La no linealidad de la ecuación de compatibilidad a través de su término cruzado o no linealidad geométrica, (2) la fuente de no linealidad que surge tras la derivación de la energía de deformación y (3) la fuente de no linealidad constitutiva.

Exploración del microdaño en sólidos

Objetivo de investigación 4: Explorar la teoría de Eshelby para resolver varios casos de inclusiones geométricas y proporcionar un método para medir densidad de microgrietas estableciendo una relación entre no linealidad acústica y homogeneización.

En el capítulo 7 se propone un nuevo aporte no lineal micromecánico relativo a la distribución de micro grietas de tipo *clapping* en materiales sólidos dañados en los que se pueda medir su parámetro de no linealidad acústica de forma macroscópica.

Bajo la hipótesis de un mecanismo tipo *clapping* por contacto 1D cada microgrieta es responsable de un componente de la no linealidad cuadrática. Esta relación se establece para formular un *clapping* bilineal en la ley constitutiva que se aproxima por una expansión de Taylor desde a partir del sistema constitutivo original. La hipótesis simplificada de restringir el efecto al segundo orden de no linealidad es por supuesto cuestionable en lo referente a la captura completa de la grietas tipo *clapping* de forma dinámica, e incluso necesitaría una extensión en trabajos futuros. Sin embargo, existen razones prácticas para resolver el caso de las componentes de segundo orden, su importancia reside en la generación de armónicos de segundo orden, cuya medida a través de equipos ultrasónicos podría usarse potencialmente para la inspección de funcionamientos estructurales y daño. Debe clarificarse que existen otros posibles orígenes de no linealidad que no se tratan en este capítulo, tales como el *clapping* por histéresis, grietas en zona de plasticidad, daño de tipo cierre parcial o nolinealidad atómicas. Por lo tanto, dichas formulaciones se continuarán en futuros trabajos. Cabe destacar que la distrubución de microgrietas, se tratan como inclusiones de tipo penny-shaped siendo formuladas en el apéndice A, embebidas en un medio macroscópico donde se utiliza la teoría de homogenización de Eshelby a través de un esquema de Mori-Tanaka [293] pero en el caso no lineal. La hipótesis de que las inclusiones tipo penny-shaped están alineadas está justificada por el hecho de que las la aparición de grietas preferentemente orientadas y alineadas en una dirección son debidas a fatiga dada una tensión. Aún así podría darse el caso de que aparecieran microgrietas aleatoriamente orientadas lo cual debería resolver en adelante durante futuros estudios.

La relación entre no linealidad acústica medible y la definición de no linealidad de tipo Landau es una propuesta requerida para utilizar la teoría de homogeneización en el capítulo 7. Con este propósito, la descomposición de la tensión en parte volumétrica y deviatoria, juega un papel clave en la redefinición de varias no linealidades acústicas de una forma conveniente.

Hay un futuro trabajo en este ámbito que se está llevando acabo tratando de medir las grietas no lineales cuya configuración experimental se menciona en el capítulo 7. El control de la no linealidad acústica efectiva u homogeneizada puede tener un gran impacto en la cuantificación de microgrietas óseas directamente correlacionadas con la calidad de los huesos y por tanto con enfermedades como la osteoporosis.

No linealidad por mezcla de ondas

Objetivo de investigación 5: Desarrollar técnicas experimentales de investigación nuevas a partir de sensores ultrasónicos con diferetens configuraciones que nos permitan medir los parámetros deducidos teóricamente.

Para medir experimentalmente estos nuevos parámetros, se han llevado a cabo dos técnicas principalmente: (1) Una basada en en la generación de dos ondas mezcladas, y (2) la otra en un sensor que emite ondas de torsión cuyo diseño se ha mencionado previamente. Entonces, en el caso de la interacción de dos ondas tanto P como S, el procedimiento para medir ha sido en una cuba de inmersión tanto para una emisión superpuesta a través de un transductor y dos ondas P generadas a distinta frecuencia es decir colineal como para la mezcla a un cierto ángulo es decir no colineal. En el supuesto experimental de mezcla colineal las ondas se realiza a través de una unión tipo T, y el resultado es la generación del no linealidad acústica en agua calculado a partir del método de generación de armónicos que coincide con los valores dados en las referencias con un valor aproximado de 3.5. Por lo tanto a través de esta metodología experimental se investiga el cálculo del parámetro de no linealidad β en agua que además, se calculan analíticamente desde la metodología de la teoría de la perturbación tanto en el caso clásico a partir de las teorías de Hamilton, como a través del capítulo de la extensión de no linealidad clásica desglosándolo en los distintos tipos de betas. La validación es calculada para cada, $2f_a$, $2f_b$ y $f_a + f_b$. Sin embargo, en el caso de la diferencia de armónicos debido a la diferencia de frecuencias de entrada, $f_a - f_b$, los resultados que se obtienen son contradictorios ya que sugieren que la amplitud de este armónico no está relacionada con el parámetro de no linealidad β. En el caso de mezcla no colineal, estas medidas no pueden realizarse en agua, supuesto que viene sugerido por los estudios de Korneev [38], así que se han utilizado una serie de muestras de aluminio construidas y cortadas con una geometría especial para realizar las mediciones experimentales. Esto permite tanto integrar el volumen de interacción de las ondas dentro de al muestra y validar la teoría de Korneev 2014 introduciendo los ángulos de entrada y salida de las ondas, algo que hasta el momento no se ha sido posible con esta técnica. Una posible limitación

en este aspecto podría ser el valor absoluto del valor de los armónicos tras calcular la FFT Transformada Rápida de Fourier, esto ocurre cuando se analiza el espectro de frecuencias a través del procedimiento de generación de armónicos. Lo cual explica la ambigüedad de signo en la fase y que repercute en el cálculo directo de la cuantificación de los parámetros acústicos no lineales.

Esta técnica proporciona por primera vez un método para derivar las TOEC con ultrasonidos distinta a la basada en DAET acustoelasticidad dinámica, proporcionando además una explicación desde un punto de físico.

No linealidad en tejido blando

Objetivo de investigación 6: Evaluar la capacidad y factibilidad de las ondas de torsión para valorar las medidas acústicas lineales y no lineales de tejidos blandos.

Se ha diseñado un transductor piezoeléctrico óptimo combinando el uso del modelo de elementos finitos y una estimación robusta de la probabilidad de detección RPOD como criterio de optimización del mismo en el capítulo 9. Esto permite estimar la mínima patología que se pueda encontrar dado un diseño de sensor propuesto dadas una geometría de capas de tejido y un nivel de ruido en las medidas. Después de validarlo, la RPOD se usa como criterio de diseño óptimo sujeto al uso de algoritmos genéticos. Un modelos analítico simplificado se formula y valida con el uso de elementos finitos con el objetivo de predecir y diseñar fácilmente dependencias y tendencias en los parámetros utilizados.

El diseño tiene la capacidad de separar las ondas P y S dependiendo de la frecuencia y el tiempo en el que llegan al receptor. Además, hay que tener en cuenta que el modelo analítico simplificado predice la frecuencia de respuesta del sensor con menos de un 1% de error, con lo que se considera validado el modelo de elementos finitos. Las ondas S solo se reproducen numéricamente en 3200 $[ns]$, a diferencia de las ondas P. Incluso así, la amplitud no se puede predecir con el modelo analítico simplificado, puesto que solo se consideran la frecuencia central, el efecto de la atenuación tampoco se tiene en cuenta. Cabe resaltar que la optimización mejora el diseño 172 veces. Sin embargo, después de aplicar la probabilidad de detección de patologías en tejido existen varios mínimos locales que requiere una búsqueda global a través de algoritmos genéticos,

Se llevaron a cabo un conjunto de ensayos y análisis de sensibilidad para validar la robustez de la estimación analítica y verificar la fiabilidad y especificaciones del diseño del transductor mediante los algoritmos detallados en el capítulo 9. El sensor piezoeléctrico se manufacturó por primera vez en el laboratorio de Evaluación No Destructiva en la universidad de Granada en 2013. (Ver la figura 9.15).

El diseño y fabricación de un sensor de torsión con multitud de aplicaciones en la mecánica tisular, es un aporte muy relevante, así que la metodología experimental para extraer nuevos parámetros tanto mecánicos como acústicos ha sido analizada de forma rigurosa. Se debe mencionar que las medidas lineales del módulo de cizalla en tejido cervical

conllevarán un logro aportando un pronóstico y correlacionándolo el diagnóstico de parto prematuro (una de la mayores causas de mortalidad infantil), mediante técnicas estadísticas [40]. Lo cual es una linea de investigación actual donde está involucrado el diseño de este prototipo.

La extensión de la no linealidad acústica clásica ha sido aplicada en el capítulo 9, extrayendo una solución que separa los términos no lineales que se puede interpretar de la matriz y los generados por las fibras. Esta conclusión representa un aporte muy novedoso en el entendimiento de la microestructura tisular. Los resultados sugieren además, que estos términos no lineales podrían medirse a tiempo real describiendo procesos evolutivos en una nueva escala. Esta línea representará un trabajo futuro cuyo impacto repercutirá en el campo biomédico y en la evaluación de las propiedades mecánicas de los quasifluidos.

Part V

APPENDICES

A

The Eshelby tensor, associated tensors and their strongly oblate limits

TI tensors can be conveniently defined and manipulated by using the Hill basis tensors $\boldsymbol{\mathcal{H}}^{(n)}$ whose components are defined as

$$\mathcal{H}^{(1)}_{ijkl} = \frac{1}{2}\Theta_{ij}\Theta_{kl},\ \mathcal{H}^{(2)}_{ijkl} = \Theta_{ij}\delta_{k3}\delta_{l3},\ \mathcal{H}^{(3)}_{ijkl} = \Theta_{kl}\delta_{i3}\delta_{j3}, \tag{A.1}$$

$$\mathcal{H}^{(4)}_{ijkl} = \delta_{i3}\delta_{j3}\delta_{k3}\delta_{l3},\ \mathcal{H}^{(5)}_{ijkl} = \frac{1}{2}(\Theta_{ik}\Theta_{lj} + \Theta_{il}\Theta_{kj} - \Theta_{ij}\Theta_{kl}) \tag{A.2}$$

$$\mathcal{H}^{(6)}_{ijkl} = \frac{1}{2}(\Theta_{ik}\delta_{l3}\delta_{j3} + \Theta_{il}\delta_{k3}\delta_{j3} + \Theta_{jk}\delta_{l3}\delta_{i3} + \Theta_{jl}\delta_{k3}\delta_{i3}), \tag{A.3}$$

with $\Theta_{ij} = \delta_{ij} - \delta_{i3}\delta_{j3}$ so that the x_1x_2 plane is the plane of isotropy. A fourth order TI tensor $\mathbf{X}$ say, is conveniently written down in terms of the TI basis as

$$\mathbf{X} = \sum_{n=1}^{6} X^n \boldsymbol{\mathcal{H}}^{(n)} \tag{A.4}$$

Further, we find that

$$X^1 = X_{1111} + X_{1122}, \qquad X^2 = X_{1133}, \qquad X^3 = X_{3311}, \tag{A.5}$$

$$X^4 = X_{3333}, \qquad X^5 = X_{1111} - X_{1122}, \qquad X^6 = 2X_{1313} \tag{A.6}$$

The minor (but not major) symmetries hold and furthermore we note that $X_{1212} = (X_{1111} - X_{1122})/2$.

The inverse $\mathbf{X}^{-1}$ of a transversely isotropic tensor $\mathbf{X}$ is straightforwardly determined as

$$\mathbf{X}^{-1} = \sum_{n=1}^{6} \hat{X}^n \boldsymbol{\mathcal{H}}^{(n)} \tag{A.7}$$

where

$$\hat{X}^1 = X_4/\Delta, \qquad \hat{X}^2 = -X_2/\Delta, \qquad \hat{X}^3 = -X_3/\Delta, \tag{A.8}$$

$$\hat{X}^4 = X_1/\Delta, \qquad \hat{X}^5 = 1/X_5, \qquad \hat{X}^6 = 1/X_6 \tag{A.9}$$

and $\Delta = 2(X_1X_4 - X_2X_3)$.

For a spheroid, the non-zero components of the Eshelby tensor are

$$S_{1111} = \frac{1}{8}\frac{-3\delta^2 + 13L - 4\delta^2 L + 8L\nu_0\delta^2 - 8L\nu_0}{(\delta^2-1)(\nu_0-1)}, \tag{A.10}$$

$$S_{1122} = \frac{-1}{8}\frac{\delta^2 + L - 4\delta^2 L + 8L\nu_0\delta^2 - 8L\nu_0}{(\delta^2-1)(\nu_0-1)}, \tag{A.11}$$

$$S_{1133} = \frac{-1}{2}\frac{2\delta^2 L - \delta^2 + L + 2L\nu_0\delta^2 - 2L\nu_0}{(\delta^2-1)(\nu_0-1)}, \tag{A.12}$$

$$S_{3311} = \frac{1}{2}\frac{-L + \delta^2 - 2\delta^2 L - 2L\nu_0\delta^2 + 2\nu_0 + 4L\nu_0\delta^2 - 4L\nu_0}{(\delta^2-1)(\nu_0-1)}, \tag{A.13}$$

$$S_{3333} = \frac{-2\delta^2 + 1 + 4\delta^2 L - L + \nu_0\delta^2 - \nu_0 - 2L\nu_0\delta^2 + 2L\nu_0}{(\delta^2-1)(\nu_0-1)}, \tag{A.14}$$

$$S_{1313} = -\frac{1}{2}\frac{\delta^2 L + 2L - 1 + L\nu_0\delta^2 - L\nu_0 - \nu_0\delta^2 + \nu_0}{(\delta^2-1)(\nu_0-1)}. \tag{A.15}$$

where

$$L = \begin{cases} \frac{\delta}{4(\delta^2-1)^{3/2}}\left[2\delta(\delta^2-1)^{1/2} + \ln\left(\frac{\delta-(\delta^2-1)^{1/2}}{\delta+(\delta^2-1)^{1/2}}\right)\right], & \delta > 1, \\ \frac{\delta}{4(1-\delta^2)^{3/2}}\left[\pi - 2\delta(1-\delta^2)^{1/2} - 2\arctan\left(\frac{\delta}{(1-\delta^2)^{1/2}}\right)\right], & \delta < 1. \end{cases} \tag{A.16}$$

Here we are interested in limits as $\delta \to 0$. Thus we find that

$$L \sim \frac{\pi}{4}\delta - \delta^2 + O(\delta^3)$$

and therefore the components of the Eshelby tensor in the strongly oblate limit, retaining terms of $O(\delta)$ becomes

$$S_{1111} = \delta\frac{\pi(13 - 8\nu_0)}{32(\nu_0-1)}, \qquad S_{1122} = \delta\frac{\pi(8\nu_0 - 1)}{32(\nu_0-1)}, \tag{A.17}$$

$$S_{1133} = \delta\frac{\pi(2\nu_0 - 1)}{8(\nu_0-1)}, \qquad S_{3311} = \frac{\nu_0}{1-\nu_0} - \delta\frac{\pi(1+4\nu_0)}{8(\nu_0-1)}, \tag{A.18}$$

$$S_{3333} = 1 - \delta\frac{\pi(2\nu_0 - 1)}{4(\nu_0-1)}, \qquad S_{1313} = \frac{1}{2} - \delta\frac{\pi(\nu_0 - 2)}{8(\nu_0-1)}. \tag{A.19}$$

so that only $S_{3311} = S_{3322}, S_{3333}$ and S_{1313} (with minor symmetries) have non-zero limits as $\delta \to 0$.

Now define $\mathbf{F}^{-1} = \mathbf{I} - \mathbf{S}$ where $\mathbf{I}$ is the fourth order identity tensor whose components are defined by

$$I_{ijkl} = \frac{1}{2}(\delta_{ik}\delta_{jl} + \delta_{il}\delta_{jk})$$

and we find that as $\delta \to 0$, defining $\hat{\boldsymbol{\mathcal{F}}} = \lim_{\delta\to 0} \mathbf{F}^{-1}$ its only non-zero components are

$$\hat{\mathcal{F}}_{1111} = 1, \qquad \hat{\mathcal{F}}_{3311} = \hat{\mathcal{F}}_{3322} = \frac{8\nu_0}{8\nu_0 - 1}. \tag{A.20}$$

Next given that $\mathbf{F} = (\mathbf{I} - \mathbf{S})^{-1}$ we define

$$\boldsymbol{\mathcal{F}} = \lim_{\delta\to 0} \mathbf{F} = O\left(\frac{1}{\delta}\right). \tag{A.21}$$

We also define $\mathbf{G} = \delta\mathbf{F}$ and $\boldsymbol{\mathcal{G}} = \lim_{\delta\to 0}(\delta\mathbf{F})$, the only non-zero components of which are

$$\mathcal{G}_{3311} = \frac{4\nu_0(1-\nu_0))}{\pi(1-2\nu_0)}, \qquad \mathcal{G}_{3333} = \frac{4(1-\nu_0)^2}{\pi(1-2\nu_0)}, \qquad \mathcal{G}_{1313} = \frac{2(1-\nu_0)}{\pi(2-\nu_0)} \tag{A.22}$$

together with $\mathcal{G}_{3322} = \mathcal{G}_{3311}$ and minor (but not major) symmetries. For finite δ, as should be expected $\mathbf{F}\mathbf{F}^{-1} = \mathbf{I}$ but we note that $\boldsymbol{\mathcal{F}}^{-1}$ does not exist and in particular $\hat{\boldsymbol{\mathcal{F}}}\boldsymbol{\mathcal{F}} \neq \mathbf{I}$.

B

Strain energy function for transversely isotropic materials

Here we show the link between a general expansion and the correct version incorporating the linear elastic moduli k, ℓ, m, n, p as in the results.

STRESS FOR ISO MODEL (THIRD ORDER CASE):

First note that

$$\frac{\partial I_1}{\partial \mathbf{E}} = \mathbf{I}, \qquad \frac{\partial I_2}{\partial \mathbf{E}} = 2\mathbf{E}^T, \qquad \frac{\partial I_3}{\partial \mathbf{E}} = 3(\mathbf{E}^2)^T. \tag{B.1}$$

STRESS FOR TI MODEL(THIRD ORDER CASE):

We need

$$\frac{\partial I_1^2}{\partial \mathbf{E}} = 2\mathrm{tr}(\mathbf{E})\mathbf{I}, \tag{B.2}$$

$$\frac{\partial I_2}{\partial \mathbf{E}} = 2\mathbf{E}^T, \tag{B.3}$$

$$\frac{\partial I_4^2}{\partial \mathbf{E}} = 2(\mathbf{M}\cdot\mathbf{E}\mathbf{M})\mathbf{M}\otimes\mathbf{M}, \tag{B.4}$$

$$\frac{\partial I_4}{\partial \mathbf{E}} = \mathbf{M}\otimes\mathbf{M} \tag{B.5}$$

$$\frac{\partial I_5}{\mathbf{E}} = \mathbf{M}\otimes(\mathbf{E}\mathbf{M}) + (\mathbf{M}\mathbf{E})\otimes\mathbf{M}, \tag{B.6}$$

$$\frac{\partial (I_1 I_4)}{\partial \mathbf{E}} = (\mathbf{M}\cdot\mathbf{E}\mathbf{M})\mathbf{I} + \mathrm{tr}(\mathbf{E})\mathbf{M}\otimes\mathbf{M} \tag{B.7}$$

$$\frac{\partial I_1^3}{\partial \mathbf{E}} = 3(\mathrm{tr}(\mathbf{E}))^2\mathbf{I}, \tag{B.8}$$

$$\frac{\partial (I_1 I_2)}{\partial \mathbf{E}} = (\mathrm{tr}(\mathbf{E}^2))\mathbf{I} + 2(\mathrm{tr}(\mathbf{E}))\mathbf{E}^T, \tag{B.9}$$

$$\frac{\partial I_3}{\partial \mathbf{E}} = 3(\mathbf{E}^2)^T, \tag{B.10}$$

$$\frac{\partial (I_1 I_4^2)}{\partial \mathbf{E}} = (\mathbf{M}\cdot\mathbf{EM})^2\mathbf{I} + 2(\mathrm{tr}(\mathbf{E}))(\mathbf{M}\cdot\mathbf{EM})(\mathbf{M}\otimes\mathbf{M}), \tag{B.11}$$

$$\frac{\partial (I_1 I_5)}{\partial \mathbf{E}} = (\mathbf{M}\cdot\mathbf{E}^2\mathbf{M})\mathbf{I} + (\mathrm{tr}(\mathbf{E}))(\mathbf{M}\otimes(\mathbf{EM}) + (\mathbf{ME})\otimes\mathbf{M}), \tag{B.12}$$

$$\frac{\partial (I_1^2 I_4)}{\partial \mathbf{E}} = 2\mathrm{tr}(\mathbf{E})(\mathbf{M}\cdot\mathbf{EM})\mathbf{I} + (\mathrm{tr}(\mathbf{E}))^2\mathbf{M}\otimes\mathbf{M}, \tag{B.13}$$

$$\frac{\partial (I_2 I_4)}{\partial \mathbf{E}} = 2(\mathbf{M}\cdot\mathbf{EM})\mathbf{E}^T + (\mathrm{tr}(\mathbf{E}^2))\mathbf{M}\otimes\mathbf{M}, \tag{B.14}$$

$$\frac{\partial I_4^3}{\partial \mathbf{E}} = 3(\mathbf{M}\cdot\mathbf{EM})^2\mathbf{M}\otimes\mathbf{M} \tag{B.15}$$

$$\frac{\partial I_4 I_5}{\partial \mathbf{E}} = (\mathbf{M}\cdot\mathbf{E}^2\mathbf{M})\mathbf{M}\otimes\mathbf{M} + (\mathbf{M}\cdot\mathbf{EM})[\mathbf{M}\otimes(\mathbf{E}\cdot\mathbf{M}) + (\mathbf{M}\cdot\mathbf{E})\otimes\mathbf{M}] \tag{B.16}$$

STRESS FOR ISO MODEL (FOURTH ORDER CASE):

$$I_6 = \mathrm{tr}(\mathbf{E}^4) \tag{B.17}$$

$$I_1 I_3 = \mathrm{tr}\mathbf{E}\mathrm{tr}(\mathbf{E}^3) \tag{B.18}$$

$$I_2^2 = \mathrm{tr}(\mathbf{E}^2)^2 \tag{B.19}$$

$$I_1^2 I_2 = \mathrm{tr}(\mathbf{E})^2\mathrm{tr}(\mathbf{E}^2) \tag{B.20}$$

$$I_1^6 = \mathrm{tr}(\mathbf{E})^4 \tag{B.21}$$

$$\frac{\partial I_6}{\partial \mathbf{E}} = 4(\mathbf{E}^3) \tag{B.22}$$

$$\frac{\partial I_1 I_3}{\partial \mathbf{E}} = \mathrm{tr}(\mathbf{E}^3)I + 3\mathrm{tr}\mathbf{E}\mathbf{E}^2 \tag{B.23}$$

$$\frac{\partial I_2^2}{\partial \mathbf{E}} = 4\mathbf{E}\mathrm{tr}(\mathbf{E}^2) \tag{B.24}$$

$$\frac{\partial I_1^2 I_2}{\partial \mathbf{E}} = 2\mathrm{tr}\mathbf{E}I\mathrm{tr}(\mathbf{E}^2) + 2\mathrm{tr}(\mathbf{E})^2\mathbf{E} \tag{B.25}$$

$$\frac{\partial I_1^4}{\partial \mathbf{E}} = 4\mathrm{tr}\mathbf{E}^3 \tag{B.26}$$

C

Homogenization: single inclusion result: spheres and ellipsoids

C.1 Configuration, geometry and description of the model

We consider that the damaged material is of the type depicted on the left of figure C.1 and we wish to perform a homogenization procedure in order to derive an effective nonlinear elastic constitutive law, i.e. the process of going to the homogenized uniform material on the right of the figure. Even for linear elastic materials this procedure is non-trivial. Here however we wish to understand how to determine the resulting *nonlinear* homogenized elastic properties.

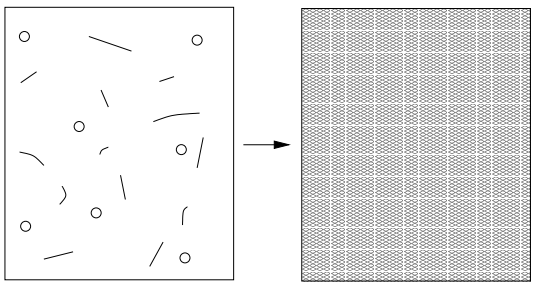

Figure C.1: The required homogenization procedure should take the damaged material which responds macroscopically nonlinear and replace this by an effective homogeneous nonlinear elastic material.

The main difficulty in performing the homogenization step is to understand how to perform the upscaling of the individual contributions to the microstructure. The local stress

and deformation field in the vicinity of the damaged areas in figure C.1 can be tremendously complicated. We shall here adopt the approach of replacing this complicated local region, which we depict as the region enclosed by the spheroidal regions in (b) in figure C.2, with an effective *homogeneous* spheroidal inclusion region with nonlinear elastic behaviour described by the Landau or Murnaghan model as in (4.12) and depicted in (c) of figure C.2.

The corresponding single-inclusion problem for an isolated ellipsoidal nonlinear elastic inclusion embedded in an unbounded linear host medium has recently been considered by Giordano et al. [294] who proved that provided the host material remains linear, the Eshelby result [295] for an isolated nonlinear inclusion still holds. We shall use this property here in order to perform the necessary nonlinear homogenization. The homogenization procedure discussed here is depicted in figure C.2 in the scenario where the damage is purely due to a distribution of aligned, identical microcracks. It is evident that the upscaling from the specific local damage to an effective nonlinear elastic spheroid is non-trivial, although intuitively one can see that there should be mechanisms to achieve this, particularly regarding equivalence of elastic energy within this domain; the specifics of this will be considered elsewhere. Here we assume that this upscaling procedure $(a) - (c)$ in figure C.2 has been achieved and a particular nonlinear damage mechanism can be effectively characterized by a nonlinear elastic effective spheroidal inclusion.

The advantage of the replacement of the local damaged region is self-evident. One can separately consider various types of local damaged regions and consider various analytical or numerical models of what effect this damage region has, the importance being that it may always be characterized by a homogeneous nonlinear spheroid (or more generally ellipsoid). This can then be fed straightforwardly into the resulting homogenization scheme to be developed below in order to derive the macroscopic nonlinear constitutive law.

Since here we wish to motivate this model by a straightforward example, let us restrict attention to distributions of identical aligned spheroidal inclusions corresponding to a distribution of aligned identical damage regions (e.g. microcracks) which have been upscaled into effective nonlinear spheroidal inclusions. We further assume that this behaviour can be accounted for by an *isotropic, spheroidal* inclusion. One could also consider that an anisotropic spherical inclusion or an anisotropic, spheroidal inclusion could also account for the damaged region. However the isotropic spheroid leads to more straightforward results and perhaps more importantly a smaller number of parameters.

C.2 Single inclusion result

C.2.1 The result of Eshelby (1957)

Note first the well known result of Eshelby [295], one of the most cited papers in applied mechanics. Eshelby showed that in the context of linear elasticity, the strain inside an isotropic ellipsoid embedded in an unbounded isotropic host medium with an imposed uniform strain field at infinity is *uniform*. This result was extended to the context of anisotropic

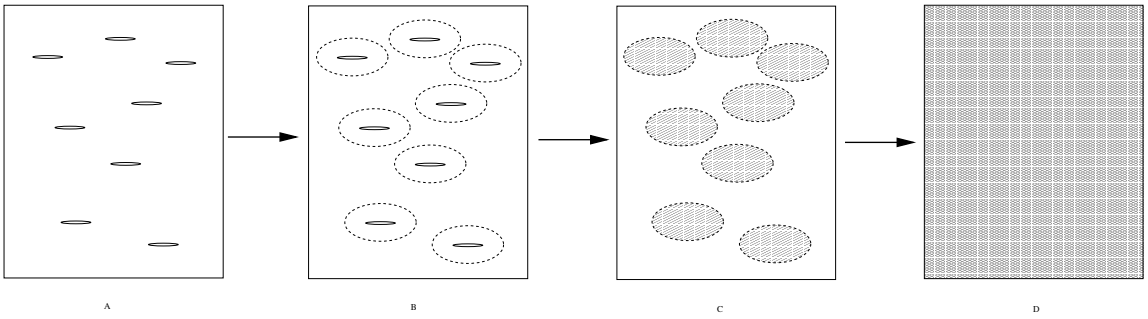

Figure C.2: The homogenization process for a damaged material of the type considered here. (a) shows the actual material which is behaving macroscopically nonlinearly due to the complex response of the damage phase, here pictured as aligned microcracks. (b) We isolate the microcracks by the imaginary spheroidal regions surrounding them. (c) We replace these regions by an effective homogeneous nonlinear inclusion which has the same effect as the microcrack region. (d) We homogenize the distribution of nonlinear inclusions using the modified Eshelby result.

phases by Kneer [296]. The strain inside the inclusion $\mathbf{E}^1$ can then be written in terms of the strain at infinity $\mathbf{E}^\infty$ via the linear relationship

$$\mathbf{E}^\infty = \mathbf{E}^1 - \mathbf{S}(\mathbf{I} - \mathbf{C}_0^{-1}\mathbf{C}_1)\mathbf{E}^1 \tag{C.1}$$

where $\mathbf{C}_0$ and $\mathbf{C}_1$ are the linear elastic moduli tensors of the host and inclusion respectively and where $\mathbf{S}$ is the Eshelby tensor, depending only upon the geometry of the ellipsoidal inclusion and the host modulus tensor $\mathbf{C}_0$. We give the components of the Eshelby tensor for the case of transverse isotropy and a spheroid in the appendix.

C.2.2 The result of Giordano et al. (2007)

Giordano et al. [211] generalized the Eshelby result described above to the case of an inclusion with constitutive *nonlinearity* embedded inside a linear host phase and showed that the strain remains uniform in this case. *Note importantly that the fact that the stress is a derivative of a potential was instrumental in this proof, geometric nonlinearity cannot therefore be incorporated*. Let us suppose that the linear elastic host modulus remains as $\mathbf{C}_0$ but now the inclusion constitutive law is written in the form

$$\mathbf{T}^1 = \mathbf{C}_1(\mathbf{E}^1)\mathbf{E}^1. \tag{C.2}$$

The approach is to *assume* that a solution to (C.1) exists but with $\mathbf{C}_1$ replaced by $\mathbf{C}_1(\mathbf{E}^1)$. To quote [211] "*If such a solution* $\mathbf{E}^1 = \mathbf{E}^1_*$ *exists for a given* $\mathbf{E}^\infty$*, it means that the nonlinear inhomogeneity could be replaced by a linear one with constant stiffness* $\mathbf{C}_0 = \mathbf{C}_0(\mathbf{E}^1_*)$ *without modifications of the elastic fields at any point. Therefore, if* $\mathbf{E}^1_*$ *exists, then* (C.1) *exactly describes, through self-consistency, the elastic behavior of the nonlinear anisotropic inclusion*." In [297] it was shown that such a solution does exist, albeit with a nonlinear association with $\mathbf{E}^\infty$ rather than the simple linear relationship in the linear problem.

The result is therefore that (C.5) still holds, but now provides a nonlinear relationship between the strains inside the inclusion and at infinity:

$$\mathbf{E}^{\infty} = \mathbf{E}^1 - \mathbf{S}(\mathbf{I} - \mathbf{D}_0\mathbf{C}_1(\mathbf{E}^1))\mathbf{E}^1. \tag{C.3}$$

$$= (\mathbf{I} - \mathbf{S})\mathbf{E}^1 + \mathbf{S}\mathbf{D}_0\mathbf{T}^1(\mathbf{E}^1) \tag{C.4}$$

$$\tag{C.5}$$

where we have introduced the notation $\mathbf{D}_0 = \mathbf{C}_0^{-1}$. Let us now describe how we can use this and exploit the weak nonlinearity to derive effective nonlinear stress-strain relationships.

C.2.3 Eshelby's tensor

Here we shall use Eshelby's tensor in a number of different cases. In any of these cases however we restrict attention to the isotropic and transversely isotropic forms, which can conveniently be written as

$$\mathbf{S} = S_1\mathbf{I}^{(1)} + S_2\mathbf{I}^{(2)} \tag{C.6}$$

and

$$\mathbf{S} = \sum_{n=1}^{6} S_n\boldsymbol{\mathcal{H}}^{(n)} \tag{C.7}$$

respectively. The basis tensors $\mathbf{I}^{(n)}$ and $\boldsymbol{\mathcal{H}}^{(n)}$ are defined in Appendix **??**.

C.3 Model implementation via homogenization: A nonlinear Mori-Tanaka scheme

The modified Eshelby result introduced by Giordano (2007) enables us to perform a homogenization procedure. We will assume that at most the host phase is transversely isotropic which means that its constitutive law is written

$$\mathbf{T} = \mathbf{C}_0\mathbf{E} \tag{C.8}$$

where $\mathbf{C}_0$ depends on the five elastic properties k_0, ℓ_0, m_0, n_0 and p_0 were introduced in the (linear) TI form of SEF (5.85). Another reason to ignore geometric nonlinearity is because even for a linear elastic material, the presence of linear elastic moduli in the third order terms when geometric nonlinearity is included means that the stress strain relationship will not be linear!

Let us restrict attention to the case when the (nonlinear) inclusions are *spheroidal* and *isotropic*. Note that we *could* extend to the transversely isotropic scenarios but since the inclusions are intended to represent a nonlinear crack of damage region what we require are parameters and the linear and nonlinear isotropic elastic coefficients together with the aspect ratio of the spheroid already present *six* such parameters which one would feel is

sufficient to represent such a region. The nonlinear constitutive behaviour of the inclusion is thus represented by (4.2).

Giordano used what we view as a modified Mori-Tanaka homogenization procedure (although it was not interpreted as such in that work) in order to determine the effective properties of a medium in which reside a distribution of spherical nonlinear inclusions and both phases are isotropic. Here we wish to extend that result to the case when phases are transversely isotropic and the inclusions are spheroid. This is viewed as both an extension but also due to the fact that we wish to apply this model to the case of predicting damage via nonlinear elastic properties of inhomogeneous media via nonlinear acoustic measurements.

We seek an *effective* nonlinear stress-strain law in the form (5.86)-(5.90) relating average stress to average strain. In particular we use the *body averaged quantities*, e.g. the body averaged stress is defined as

$$\bar{\mathbf{T}} = \frac{1}{|V|}\int_V \mathbf{T} dV \tag{C.9}$$

where V is the domain of the inhomogeneous material we are interested in with volume defined as $|V|$. If we denote the host material as V_0 and the family of inclusions as V_1, we can use (C.8) to write

$$\begin{aligned}
\bar{\mathbf{T}} &= \frac{1}{|V|}\int_{V_0} \mathbf{T}^0\, dV + \frac{1}{|V|}\int_{V_1} \mathbf{T}^1\, dV && \text{(C.10)}\\
&= \frac{\mathbf{C}^0}{|V|}\int_{V_0} \mathbf{E}^0\, dV + \phi\bar{\mathbf{T}}^1 && \text{(C.11)}\\
&= \frac{\mathbf{C}^0}{|V|}\left(\int_{V_0} \mathbf{E}^0\, dV + \int_{V_1} \mathbf{E}^1\, dV - \int_{V_1} \mathbf{E}^1\, dV\right) + \phi\bar{\mathbf{T}}^1 && \text{(C.12)}\\
&= \mathbf{C}^0\bar{\mathbf{E}} - \phi\mathbf{C}^0\bar{\mathbf{E}}^1 + \phi\bar{\mathbf{T}}^1(\bar{\mathbf{E}}^1) && \text{(C.13)}
\end{aligned}$$

where we have defined the volume fraction of the damage phase as $\phi = |V_1|/|V|$. The above is a standard approach in the theory of micromechanics, but here we have had to separate the term involving the inclusion response as this behaves nonlinearly.

What we require to close this system and yield an effective nonlinear stress strain law, is an equation for the averaged strain inside the damage phase in terms of the overall average strain, i.e.

$$\bar{\mathbf{E}}^1 = \bar{\mathbf{E}}^1\left(\bar{\mathbf{E}}\right) \tag{C.14}$$

Substituting this into (C.13) would yield the required equations.

The average strain in the medium can be written

$$\bar{\mathbf{E}} = \phi\bar{\mathbf{E}}^1 + (1-\phi)\bar{\mathbf{E}}^0 \tag{C.15}$$

and we note that for a dilute composite $\bar{\mathbf{E}}^0 \approx \mathbf{E}^{\infty 1}$ so that

$$\bar{\mathbf{E}} = \phi \bar{\mathbf{E}}^1 + (1-\phi)\mathbf{E}^{\infty}. \tag{C.16}$$

Strictly we can drop the "overline" on $\bar{\mathbf{E}}^1$ since it is uniform. However for consistency we retain this here. Eshelby's result for an isolated isotropic (third order) nonlinear inclusion yields

$$\mathbf{E}^{\infty} = \bar{\mathbf{E}}^1 - \mathbf{S}\mathbf{E}^1 + \mathbf{S}\mathbf{D}_0\mathbf{T}^1. \tag{C.17}$$

Since the stress here is a function of strain $\mathbf{E}^1$ we have the strain in the far field in terms of a quadratic expansion in the strain inside the inclusion, i.e.

$$\mathbf{E}^{\infty} = \mathbf{E}^{\infty}(\mathbf{E}^1). \tag{C.18}$$

We substitute this into (C.16) and formally invert the expansion in order to find an expression for $\mathbf{E}^1$ as an expansion in $\bar{\mathbf{E}}$ up to quadratic terms, i.e.

$$\mathbf{E}^1 = \mathbf{E}^1(\bar{\mathbf{E}}). \tag{C.19}$$

Finally, using this in (C.13) yields the desired form

$$\bar{\mathbf{T}} = \mathbf{C}^*(\bar{\mathbf{E}})\bar{\mathbf{E}}$$

where we retain orders up to quadratic terms.

The stress inside the nonlinear, isotropic inclusion is written in the form

$$\mathbf{T}^1 = \mathbf{T}_L + \mathbf{T}_{NL} \tag{C.20}$$

with

$$\mathbf{T}_L = \lambda_1(\mathrm{tr}\mathbf{E}^1)\mathbf{I} + 2\mu\mathbf{E}^1, \tag{C.21}$$

$$\mathbf{T}_{NL} = \mathcal{A}(\mathbf{E}^1)^2 + \mathcal{B}(\mathrm{tr}((\mathbf{E}^1)^2)\mathbf{I} + 2(\mathrm{tr}(\mathbf{E}^1))\mathbf{E}^1) + \mathcal{C}(\mathrm{tr}\mathbf{E}^1)^2\mathbf{I}. \tag{C.22}$$

The tensor $\mathbf{S}(\mathbf{C}^0)^{-1} = \mathbf{S}\mathbf{D}^0$ is either isotropic or transversely isotropic (TI). If the inclusion is spheroidal, there is no additional effort in incorporating a TI matrix phase - we can do this without loss of generality since in any case $\mathbf{S}\mathbf{D}^0$ will be a TI tensor.

[1]This is slightly different to how the Mori-Tanaka method can be explained, see e.g. Appendix C of [298] but this is in fact equivalent and in particular this nonlinear version is more easily explained in this manner. On can explain in the same manner as describedin [298] but this requires second order expansions in strain, etc. In particular we stress that this nonlinear version reduces to the linear Mori-Tanaka approximations when we neglect nonlinear terms

For the isotropic case, we write

$$\mathbf{SD}^0 = S_1\mathbf{I}^{(1)} + S_2\mathbf{I}^{(2)} \tag{C.23}$$

whereas for the TI case we have

$$\mathbf{SD}^0 = \sum_{n=1}^{6} S_n \boldsymbol{\mathcal{H}}^{(n)}. \tag{C.24}$$

C.3.1 Macroscopically isotropic behaviour

Let us assume now that the matrix is isotropic and that the distribution of inclusions is such that the overall response is macroscopically isotropic. Then

$$\mathbf{SD}_0 = \frac{S_1}{3\kappa_0}\mathbf{I}^{(1)} + \frac{S_2}{2\mu_0}\mathbf{I}^{(2)} \tag{C.25}$$

which thus identifies X_1 and X_2. We seek an effective stress strain law in the form

$$\bar{\mathbf{T}} \quad = \quad \lambda_*(\mathrm{tr}\bar{\mathbf{E}})\mathbf{I} \; + \; 2\mu_*\bar{\mathbf{E}} \; + \; \mathcal{A}_*\bar{\mathbf{E}}^2 \; + \; \mathcal{B}_*(\mathrm{tr}(\bar{\mathbf{E}}^2)\mathbf{I} \; + \; 2(\mathrm{tr}\bar{\mathbf{E}})\bar{\mathbf{E}}) \; + \; \mathcal{C}_*(\mathrm{tr}\bar{\mathbf{E}})^2\mathbf{I} \tag{C.26}$$

We have employed the general isotropic Eshelby tensor (C.23). For now we leave this arbitrary so as to enable the incorporation of rather general effects the most simple of which are uniformly distributed spheres. However this approach also enables us to model uniformly distributed and *uniformly oriented* ellipsoidal inclusions, common and useful cases of which are penny cracks, discs and needles, all of which may be very useful in this damage context.

Using (C.25) and (C.20)-(C.22) in (C.17) and we find the following quadratic for the strain at infinity in terms of the strain inside the inclusion:

$$\mathbf{E}^\infty = L\mathbf{E}^1 + M(\mathrm{tr}\mathbf{E}^1)\mathbf{I} + N(\mathbf{E}^1)^2 + O\mathbf{E}^1(\mathrm{tr}\mathbf{E}^1) + P\mathrm{tr}((\mathbf{E}^1)^2)\mathbf{I} + Q(\mathrm{tr}\mathbf{E}^1)^2\mathbf{I} \tag{C.27}$$

where

$$L = 1 + S_2\left(\frac{\mu_1}{\mu_0} - 1\right), \qquad M = \frac{S_1}{3}\left(\frac{K_1}{K_0} - 1\right) - \frac{S_2}{3}\left(\frac{\mu_1}{\mu_0} - 1\right), \tag{C.28}$$

$$N = \frac{S_2}{2\mu_0}\mathcal{A}, \qquad O = \frac{S_2}{\mu_0}\mathcal{B}, \tag{C.29}$$

$$P = \frac{1}{3}\mathcal{A}\left(\frac{S_1}{3K_0} - \frac{S_2}{2\mu_0}\right) + \mathcal{B}\frac{S_1}{3K_0}, \qquad Q = \frac{2}{3}\mathcal{A}\left(\frac{S_1}{3K_0} - \frac{S_2}{2\mu_0}\right) + \mathcal{C}\frac{S_1}{3K_0}. \tag{C.30}$$

Substitute (C.27) in (C.16) to yield

$$\bar{\mathbf{E}} = L'\mathbf{E}^1 + M'\mathrm{tr}(\mathbf{E}^1)\mathbf{I} + N'(\mathbf{E}^1)^2 + O'\mathbf{E}^1\mathrm{tr}\mathbf{E}^1 + P'\mathrm{tr}(\mathbf{E}^1)^2\mathbf{I} + Q'(\mathrm{tr}(\mathbf{E}^1))^2\mathbf{I} \tag{C.31}$$

where

$$L' = \phi + (1-\phi)L, \qquad M' = (1-\phi)M, \qquad N' = (1-\phi)N, \tag{C.32}$$

$$O' = (1-\phi)O, \qquad P' = (1-\phi)P, \qquad Q' = (1-\phi)Q. \tag{C.33}$$

Next we invert (C.27) to yield (correct to quadratic terms)

$$\mathbf{E}^1 = R\bar{\mathbf{E}} + S\text{tr}(\bar{\mathbf{E}})\mathbf{I} + T(\bar{\mathbf{E}})^2 + U\bar{\mathbf{E}}\text{tr}\bar{\mathbf{E}} + V\text{tr}(\bar{\mathbf{E}})^2\mathbf{I} + W(\text{tr}(\bar{\mathbf{E}}))^2\mathbf{I} + ... \tag{C.34}$$

where

$$R = \frac{1}{L'}, \qquad S = \frac{-M'}{L'(L'+3M')}, \qquad T = \frac{-N'}{L'^3}, \tag{C.35}$$

$$U = \frac{2M'N' - O'L'}{L'^3(L'+3M')}, \qquad V = \frac{M'N' - P'L'}{L'^3(L'+3M')}, \tag{C.36}$$

and

$$W = \frac{M'^2}{L'^2(L'+3M')} + \frac{M'^2(3P'-N') + L'M'(2P'+O') - Q'L'^2}{L'^3(L'+3M')^2}. \tag{C.37}$$

We also note the useful relations

$$L' = \frac{1}{\mu_0}(\mu_0 + (1-\phi)(\mu_1 - \mu_0)S_2), \tag{C.38}$$

$$L' + 3M' = \frac{1}{K_0}(K_0 + (1-\phi)(K_1 - K_0)S_1). \tag{C.39}$$

Finally use (C.34) in (C.13) and gather terms in order to find the effective nonlinear stress strain relationship in the form (C.26). We find the effective linear properties

$$\mu_* = \mu_0 + \phi\frac{(\mu_1 - \mu_0)}{L'}, \tag{C.40}$$

$$K_* = K_0 + \phi\left(\frac{K_1 - K_0}{L' + 3M'}\right). \tag{C.41}$$

and effective nonlinear properties

$$\mathcal{A}_* = \frac{\phi\mathcal{A}}{L'^3} \tag{C.42}$$

$$\mathcal{B}^* = \frac{\phi(\phi-1)S_1}{3K_0}\frac{(\lambda_1 - \lambda_0)}{L'^2(L'+3M')}\left(\frac{\mathcal{A}}{3} + \mathcal{B}\right) + \frac{2(\mu_1 - \mu_0)\phi(1-\phi)}{L'^3(L'+3M')}(M'N - L'P) + \frac{\phi\mathcal{B}}{L'^2} \tag{C.43}$$

$$\mathcal{C}^* = \text{derive general form of } \mathcal{C}^* \tag{C.44}$$

and note that

$$M'N - L'P = \frac{1}{3}\mathcal{A}\left(\frac{S_1}{3K_0} - \frac{S_2}{2\mu_0}\right) + \frac{S_1\mathcal{B}}{3K_0} + \frac{1}{3}(1-\phi)S_1S_2\left(\frac{\mathcal{A}}{2\mu_0}\left(\frac{K_1}{K_0}-1\right) - \left(\frac{\mathcal{A}}{3K_0}+\mathcal{B}K_0\right)\left(\frac{\mu_1}{\mu_0}-1\right)\right) \quad \text{(C.45)}$$

When we take the Eshelby tensor for a sphere we recover the results of Giordano [294] (D=0). Alternatively we can also consider a variety of other types of inclusions that are uniformly oriented. We use the results derived by Berryman (1980) for the strain concentration tensor and back-out the Eshelby tensor from these. In particular we find the results list in table C.1.

	S_1	S_2
Sphere	$\frac{3K_0}{3K_0+4\mu_0}$	$\frac{6(K_0+2\mu_0)}{5(3K_0+4\mu_0)}$

Table C.1: Isotropic components of the Eshelby tensor for inclusions averaged over orientations.

Spheres

where

$$L = 1 + S_2\left(\frac{\mu_1}{\mu_0} - 1\right) \quad \text{(C.46)}$$

$$M = \frac{S_1}{3}\left(\frac{K_1}{K_0} - 1\right) - \frac{S_2}{3}\left(\frac{\mu_1}{\mu_0} - 1\right) \quad \text{(C.47)}$$

$$N = \frac{3(\mathcal{A}+4\mu_2)}{5\mu_1}\left(\frac{K_1+2\mu_1}{3K_1+4\mu_1}\right) \quad \text{(C.48)}$$

$$O = \frac{6(K_2 - \frac{5}{3}\mu_2 + \mathcal{B})}{5\mu_1}\left(\frac{K_1+2\mu_1}{3K_1+4\mu_1}\right) \quad \text{(C.49)}$$

$$P = \frac{1}{15(3K_1+4\mu_1)}\left(15\mathcal{B} - (\mathcal{A}+4\mu_2)\left(1+3\frac{K_1}{\mu_1}\right)\right) \quad \text{(C.50)}$$

$$Q = \frac{1}{15(3K_1+4\mu_1)}\left(15\left(\mathcal{C} - K_2 + \frac{2}{3}\mu_2\right) - 2\left(K_2 - \frac{5}{3}\mu_2 + \mathcal{B}\right)\left(1+3\frac{K_1}{\mu_1}\right)\right). \quad \text{(C.51)}$$

Write down linear properties (MT) explicitly.

Spheres

$$S_\kappa = \frac{3K_0}{(3K_0+2\mu_0)}, \qquad S_\mu = \frac{6}{5}\left(\frac{K_0+2\mu_0}{3K_0+4\mu_0}\right) \quad \text{(C.52)}$$

and thus

$$\mathbf{SD} = X_1\mathbf{I}^{(1)} + X_2\mathbf{I}^{(2)} \quad \text{(C.53)}$$

where

$$X_1 = \frac{S_1}{3K_0} = \frac{2}{5K_0}\left(\frac{K_0+2\mu_0}{3K_0+4\mu_0}\right), \qquad X_2 = \frac{S_2}{2\mu_0} = \frac{3K_0}{2\mu_0(3K_0+4\mu_0)} \tag{C.54}$$

C.3.2 Macroscopically transversely isotropic behaviour

In the general TI case, this has the the form of (5.86) with associated effective elastic properties, i.e.

$$\bar{\mathbf{T}} = \bar{\mathbf{T}}_{L1} + \bar{\mathbf{T}}_{L2} + \bar{\mathbf{T}}_{NL1} + \bar{\mathbf{T}}_{NL2} \tag{C.55}$$

where each of the individual contributions, is defined in terms of the body averaged strain and thus defines the effective properties:

$$\bar{\mathbf{T}}_{L1} = (k^* - m^*)(\mathrm{tr}\bar{\mathbf{E}})\mathbf{I} + 2m^*\bar{\mathbf{E}}, \tag{C.56}$$

$$\begin{aligned}\bar{\mathbf{T}}_{L2} = \mathcal{L}_1^*(\bar{\mathbf{M}}\cdot\bar{\mathbf{E}}\bar{\mathbf{M}})\bar{\mathbf{M}}\otimes\bar{\mathbf{M}} + 2(p^*-m^*)(\bar{\mathbf{M}}\otimes\bar{\mathbf{E}}\bar{\mathbf{M}} + \bar{\mathbf{M}}\bar{\mathbf{E}}\otimes\bar{\mathbf{M}}) \\ + \mathcal{L}_2^*((\bar{\mathbf{M}}\cdot\bar{\mathbf{E}}\bar{\mathbf{M}})\mathbf{I} + (\mathrm{tr}\bar{\mathbf{E}})\bar{\mathbf{M}}\otimes\bar{\mathbf{M}})\end{aligned} \tag{C.57}$$

$$\bar{\mathbf{T}}_{NL1} = (\mathcal{A}^* + 4m^*)\bar{\mathbf{E}}^2 + \mathcal{B}^*(\mathrm{tr}(\bar{\mathbf{E}}^2))\mathbf{I} + 2(\mathcal{B}^* - 2m^* + k^*)(\mathrm{tr}\bar{\mathbf{E}})\bar{\mathbf{E}} + (\mathcal{C}^* - k^* + m^*)(\mathrm{tr}\bar{\mathbf{E}})^2\mathbf{I} \tag{C.58}$$

$$\begin{aligned}\bar{\mathbf{T}}_{NL2} = \mathbf{I}(\mathcal{D}^*\bar{I}_4^{\,2} + \mathcal{E}^*\bar{I}_5 + 2\mathcal{F}^*\bar{I}_1\bar{I}_4 - \mathcal{L}_2^*\bar{I}_1\bar{I}_4) \\ + \mathbf{N}^*(2\mathcal{D}^*\bar{I}_1\bar{I}_4 + \mathcal{F}^*\bar{I}_1^{\,2} + \mathcal{G}^*\bar{I}_2 + 3\mathcal{H}^*\bar{I}_4^{\,2} + \mathcal{I}^*\bar{I}_5 - (\mathcal{L}_1^*\bar{I}_1\bar{I}_4 + \mathcal{L}_2^*\bar{I}_1^{\,2})) + \bar{\mathbf{E}}(2\mathcal{G}^*\bar{I}_4 + 2\mathcal{L}_2^*\bar{I}_4) \\ + [\bar{\mathbf{M}}\otimes\bar{\mathbf{E}}\bar{\mathbf{M}} + \bar{\mathbf{M}}\bar{\mathbf{E}}\otimes\bar{\mathbf{M}}](\mathcal{E}^*\bar{I}_1 + \mathcal{I}^*\bar{I}_4 + \mathcal{L}_1^*\bar{I}_4 + \mathcal{L}_2^*\bar{I}_1 - 2(p^*-m^*)\bar{I}_1) \\ + 2(p^*-m^*)[\bar{\mathbf{N}}\bar{\mathbf{E}}^2 + \bar{\mathbf{E}}^2\bar{\mathbf{N}} + \bar{\mathbf{E}}\bar{\mathbf{M}}\otimes\bar{\mathbf{E}}\bar{\mathbf{M}} + \bar{\mathbf{M}}\bar{\mathbf{E}}\otimes\bar{\mathbf{M}}\bar{\mathbf{E}}]\end{aligned} \tag{C.59}$$

where we used the notation $\bar{\mathbf{N}} = \bar{\mathbf{M}}\otimes\bar{\mathbf{M}}$ and it was also convenient to define the moduli combinations

$$\mathcal{L}_1^* = n^* - 4p^* - 2\ell^* + k^* + m^*, \qquad \mathcal{L}_2^* = \ell^* - k^* + m^*. \tag{C.60}$$

Aligned isotropic spheroids

The strain inside the inclusion $\mathbf{E}^1$ can then be written in terms of the strain at infinity $\mathbf{E}^\infty$ via the linear relationship

$$\mathbf{E}^{\infty} = A\mathrm{tn}\mathbf{E}^1 I + B\mathbf{E}^1 + C\mathbf{M}\mathbf{E}^1\mathbf{M}\mathbf{M} \otimes \mathbf{M} + D(\mathbf{M} \otimes \mathbf{E}^1\mathbf{M} + \mathbf{M}\mathbf{E}^1 \otimes \mathbf{M}) \tag{C.61}$$

$$+ E\mathbf{M}\mathbf{E}^1\mathbf{M}I + Ftr\mathbf{E}^1\mathbf{M} \otimes \mathbf{M} + G\mathrm{tn}\mathbf{E}^1\mathbf{E}^1 + H(\mathbf{E}^1)^2 + I\mathrm{tn}(\mathbf{E}^1)^2 I \tag{C.62}$$

$$+ J(tr\mathbf{E}^1)^2 I + Ktr(\mathbf{E}^1)^2\mathbf{M} \otimes \mathbf{M} + L(\mathrm{tn}\mathbf{E}^1)^2\mathbf{M} \otimes \mathbf{M} \tag{C.63}$$

$$+ M\mathbf{M}\mathbf{E}^1\mathbf{M}\mathbf{M} \otimes \mathbf{M}\mathbf{E}^1 + N(\mathbf{M} \otimes \mathbf{E}^1\mathbf{M} + \mathbf{M}\mathbf{E}^1 \otimes \mathbf{M})\mathbf{E}^1 \tag{C.64}$$

$$+ O\mathbf{M}\mathbf{E}^1\mathbf{M}\mathbf{E}^1 I + P\mathrm{tn}\mathbf{E}^1\mathbf{M}\mathbf{E}^1\mathbf{M}I + Q\mathrm{tn}\mathbf{E}^1\mathbf{M}\mathbf{E}^1\mathbf{M}\mathbf{M} \otimes \mathbf{M} \tag{C.65}$$

$$+ R\mathrm{tn}\mathbf{E}^1(\mathbf{M} \otimes \mathbf{E}^1\mathbf{M} + \mathbf{M}\mathbf{E}^1 \otimes \mathbf{M}) + S\mathrm{tn}\mathbf{E}^1\mathbf{E}^1\mathbf{M} \otimes \mathbf{M} \tag{C.66}$$

where

$$A = \frac{2\mu_1 S^C_{1122} + \lambda_1(S^C_{1111} + S^C_{1122} + S^C_{1133} + S^C_{3311})}{3\lambda_0 + 2\mu_0} \tag{C.67}$$

$$B = 1 + \frac{2\mu_1(S^C_{1111} - S^C_{1122})}{3\lambda_0 + 2\mu_0} \tag{C.68}$$

$$C = \frac{2\mu_1(S^C_{1111} - S^C_{1133} - S^C_{3311} + S^C_{3333} - 2S^C_{1313})}{3\lambda_0 + 2\mu_0} \tag{C.69}$$

$$D = \frac{2\mu_1(2S^C_{1313} - S^C_{1111} + S^C_{1212})}{3\lambda_0 + 2\mu_0} \tag{C.70}$$

$$\tag{C.71}$$

$$E = \frac{2\mu_1(S^C_{1133} - S^C_{1122})}{3\lambda_0 + 2\mu_0} \tag{C.72}$$

$$\tag{C.73}$$

$$F = \frac{2\mu_1(S^C_{3311} - S^C_{1122}) + \lambda_1(-S^C_{1111} - S^C_{1122} - S^C_{1133} - S^C_{3311} + S^C_{3333})}{3\lambda_0 + 2\mu_0} \tag{C.74}$$

$$\tag{C.75}$$

$$G = \frac{(\mathcal{A} + 4m)S^C_{1122} + 2(\mathcal{B} + 2m + k)(S^C_{1111} - S^C_{1122})}{3\lambda_0 + 2\mu_0} \tag{C.76}$$

$$H = \frac{(\mathcal{A} + 4m)(S^C_{1111} - S^C_{1122})}{3\lambda_0 + 2\mu_0} \tag{C.77}$$

$$I = \frac{\mathcal{B}(S^C_{1111} + S^C_{1122} + S^C_{1133} + S^C_{3311})}{3\lambda_0 + 2\mu_0} \tag{C.78}$$

$$J = \frac{2(\mathcal{B} - 2m + k)S^C_{1122} + (\mathcal{C} - k + m)(S^C_{1111} + S^C_{1122} + S^C_{1133} + S^C_{3311})}{3\lambda_0 + 2\mu_0} \tag{C.79}$$

$$K = \frac{\mathcal{B}}{3\lambda_0 + 2\mu_0}(-S^C_{1111} - S^C_{1122} - S^C_{1133} - S^C_{3311} + S^C_{3333}) \tag{C.80}$$

$$L = \frac{2(\mathcal{B} - 2m + k)(S^C_{3311} - S^C_{1122}) + (\mathcal{C} - k + m)(-S^C_{1111} - S^C_{1122} - S^C_{1133} - S^C_{3311} + S^C_{3333})}{3\lambda_0 + 2\mu_0} \tag{C.81}$$

$$M = \frac{(\mathcal{A} + 4m)(S^C_{1111} - S^C_{1133} - S^C_{3311} + S^C_{3333} - 2S^C_{1313})}{3\lambda_0 + 2\mu_0} \tag{C.82}$$

$$N = \frac{(\mathcal{A} + 4m)(2S^C_{1313} - S^C_{1111} + S^C_{1212})}{3\lambda_0 + 2\mu_0} \tag{C.83}$$

$$O = \frac{(\mathcal{A} + 4m)(S^C_{1133} - S^C_{1122})}{3\lambda_0 + 2\mu_0} \tag{C.84}$$

$$P = \frac{2(\mathcal{B} - 2m + k)(S^C_{1133} - S^C_{1122})}{3\lambda_0 + 2\mu_0} \tag{C.85}$$

$$Q = \frac{2(\mathcal{B} - 2m + k)(S^C_{1111} - S^C_{1133} - S^C_{3311} + S^C_{3333} - 2S^C_{1313})}{3\lambda_0 + 2\mu_0} \tag{C.86}$$

$$R = \frac{2(\mathcal{B} - 2m + k)(2S^C_{1313} - S^C_{1111} + S^C_{1212})}{3\lambda_0 + 2\mu_0} \tag{C.87}$$

$$S = \frac{(\mathcal{A} + 4m)(S^C_{3311} - S^C_{1122})}{3\lambda_0 + 2\mu_0} \tag{C.88}$$

$$\tag{C.89}$$

$$\bar{\mathbf{E}} = A'\mathrm{tn}\mathbf{E}^1 I + B'\mathbf{E}^1 + C'\mathbf{M}\mathbf{E}^1\mathbf{M}\mathbf{M} \otimes \mathbf{M} + D'(\mathbf{M} \otimes \mathbf{E}^1\mathbf{M} + \mathbf{M}\mathbf{E}^1 \otimes \mathbf{M}) \tag{C.90}$$

$$+ E'\mathbf{M}\mathbf{E}^1\mathbf{M}I + F'\mathrm{tn}\mathbf{E}^1\mathbf{M} \otimes \mathbf{M} + G'\mathrm{tn}\mathbf{E}^1\mathbf{E}^1 + H'(\mathbf{E}^1)^2 + I'\mathrm{tn}(\mathbf{E}^1)^2 I \tag{C.91}$$

$$+ J'(\mathrm{tn}\mathbf{E}^1)^2 I + K'\mathrm{tn}(\mathbf{E}^1)^2\mathbf{M} \otimes \mathbf{M} + L'(\mathrm{tn}\mathbf{E}^1)^2\mathbf{M} \otimes \mathbf{M} \tag{C.92}$$

$$+ M'\mathbf{M}\mathbf{E}^1\mathbf{M}\mathbf{M} \otimes \mathbf{M}\mathbf{E}^1 + N'(\mathbf{M} \otimes \mathbf{E}^1\mathbf{M} + \mathbf{M}\mathbf{E}^1 \otimes \mathbf{M})\mathbf{E}^1 \tag{C.93}$$

$$+ O'\mathbf{M}\mathbf{E}^1\mathbf{M}\mathbf{E}^1 I + P'\mathrm{tn}\mathbf{E}^1\mathbf{M}\mathbf{E}^1\mathbf{M}I + Q't\mathrm{tn}\mathbf{E}^1\mathbf{M}\mathbf{E}^1\mathbf{M}\mathbf{M} \otimes \mathbf{M} \tag{C.94}$$

$$+ R'\mathrm{tn}\mathbf{E}^1(\mathbf{M} \otimes \mathbf{E}^1\mathbf{M} + \mathbf{M}\mathbf{E}^1 \otimes \mathbf{M}) + S'\mathrm{tn}\mathbf{E}^1\mathbf{E}^1\mathbf{M} \otimes \mathbf{M} \tag{C.95}$$

where

$$A' = (1-\phi)\frac{2\mu_1 S^C_{1122} + \lambda_1(S^C_{1111} + S^C_{1122} + S^C_{1133} + S^C_{3311})}{3\lambda_0 + 2\mu_0} \tag{C.96}$$

$$\tag{C.97}$$

$$B' = \phi + (1-\phi)\frac{2\mu_1(S^C_{1111} - S^C_{1122})}{3\lambda_0 + 2\mu_0} \tag{C.98}$$

$$C' = (1-\phi)\frac{2\mu_1(S^C_{1111} - S^C_{1133} - S^C_{3311} + S^C_{3333} - 2S^C_{1313})}{3\lambda_0 + 2\mu_0} \tag{C.99}$$

$$D' = (1-\phi)\frac{2\mu_1(2S^C_{1313} - S^C_{1111} + S^C_{1212})}{3\lambda_0 + 2\mu_0} \tag{C.100}$$

$$E' = (1-\phi)\frac{2\mu_1(S^C_{1133} - S^C_{1122})}{3\lambda_0 + 2\mu_0} \tag{C.101}$$

$$F' = (1-\phi)\frac{2\mu_1(S^C_{3311} - S^C_{1122})}{3\lambda_0 + 2\mu_0} \tag{C.102}$$

$$G' = (1-\phi)\frac{(\mathcal{A} + 4m)S^C_{1122} + 2(\mathcal{B} + 2m + k)(S^C_{1111} - S^C_{1122})}{3\lambda_0 + 2\mu_0} \tag{C.103}$$

$$H' = (1-\phi)\frac{(\mathcal{A} + 4m)(S^C_{1111} - S^C_{1122})}{3\lambda_0 + 2\mu_0} \tag{C.104}$$

$$I' = (1-\phi)\frac{\mathcal{B}(S^C_{1111} + S^C_{1122} + S^C_{1122} + S^C_{1133} + S^C_{3311})}{3\lambda_0 + 2\mu_0} \tag{C.105}$$

$$J' = (1-\phi)\frac{2(\mathcal{B} - 2m + k)S^C_{1122} + (\mathcal{C} - k + m)(S^C_{1111} + S^C_{1122} + S^C_{1133} + S^C_{3311})}{3\lambda_0 + 2\mu_0} \tag{C.106}$$

$$K' = (1-\phi)\frac{\mathcal{B}}{3\lambda_0 + 2\mu_0}(-S^C_{1111} - S^C_{1122} - S^C_{1133} - S^C_{3311} + S^C_{3333}) \tag{C.107}$$

$$L' = (1-\phi)\frac{\mathcal{B} - 2m + k)(S^C_{3311} - S^C_{1122}) + (\mathcal{C} - k + m)(-S^C_{1111} - S^C_{1122} - S^C_{1133} - S^C_{3311} + S^C_{3333})}{3\lambda_0 + 2\mu_0} \tag{C.108}$$

$$M' = (1-\phi)\frac{(\mathcal{A} + 4m)(S^C_{1111} - S^C_{1133} - S^C_{3311} + S^C_{3333} - 2S^C_{1313})}{3\lambda_0 + 2\mu_0} \tag{C.109}$$

$$N' = (1-\phi)\frac{(\mathcal{A} + 4m)(2S^C_{1313} - S^C_{1111} + S^C_{1212})}{3\lambda_0 + 2\mu_0} \tag{C.110}$$

$$O' = (1-\phi) = \frac{(\mathcal{A} + 4m)(S^C_{1133} - S^C_{1122})}{3\lambda_0 + 2\mu_0} \tag{C.111}$$

$$P' = (1-\phi)\frac{2(\mathcal{B} - 2m + k)(S^C_{1133} - S^C_{1122})}{3\lambda_0 + 2\mu_0} \tag{C.112}$$

$$Q' = (1-\phi)\frac{2(\mathcal{B} - 2m + k)(S^C_{1111} - S^C_{1133} - S^C_{3311} + S^C_{3333} - 2S^C_{1313})}{3\lambda_0 + 2\mu_0} \tag{C.113}$$

$$R' = (1-\phi)\frac{2(\mathcal{B} - 2m + k)(2S^C_{1313} - S^C_{1111} + S^C_{1212})}{3\lambda_0 + 2\mu_0} \tag{C.114}$$

$$S' = (1-\phi)\frac{(\mathcal{A} + 4m)(S^C_{3311} - S^C_{1122})}{3\lambda_0 + 2\mu_0} \tag{C.115}$$

$$\tag{C.116}$$

$$\bar{\mathbf{T}} = C_0\bar{\mathbf{E}} - \phi C_0\mathbf{E}^1 + \phi\bar{\mathbf{T}}^1(\bar{\mathbf{E}}^1) \tag{C.117}$$

Next we invert to yield (correct quadratic terms)

$$\begin{aligned}
\mathbf{E}^1 = {} & \hat{A}tr\bar{\mathbf{E}}I + \hat{B}\bar{\mathbf{E}} + \hat{C}\mathbf{M}\bar{\mathbf{E}}\mathbf{M}\mathbf{M}\otimes\mathbf{M} + \hat{D}(\mathbf{M}\otimes\bar{\mathbf{E}}\mathbf{M} + \mathbf{M}\bar{\mathbf{E}}\otimes\mathbf{M}) && \text{(C.118)}\\
& + \hat{E}\mathbf{M}\bar{\mathbf{E}}\mathbf{M}I + \hat{F}tr\bar{\mathbf{E}}\mathbf{M}\otimes\mathbf{M} + \hat{G}tr\bar{\mathbf{E}}\bar{\mathbf{E}} + \hat{H}(\bar{\mathbf{E}})^2 + \hat{I}tr(\bar{\mathbf{E}})^2I && \text{(C.119)}\\
& + \hat{J}(tr\bar{\mathbf{E}})^2I + \hat{K}tr(\bar{\mathbf{E}})^2\mathbf{M}\otimes\mathbf{M} + \hat{L}(tr\bar{\mathbf{E}})^2\mathbf{M}\otimes\mathbf{M} && \text{(C.120)}\\
& + \hat{M}\mathbf{M}\bar{\mathbf{E}}\mathbf{M}\mathbf{M}\otimes\mathbf{M}\bar{\mathbf{E}} + \hat{N}(\mathbf{M}\otimes\bar{\mathbf{E}}\mathbf{M} + \mathbf{M}\bar{\mathbf{E}}\otimes\mathbf{M})\bar{\mathbf{E}} && \text{(C.121)}\\
& + \hat{O}\mathbf{M}\bar{\mathbf{E}}\mathbf{M}\bar{\mathbf{E}}I + \hat{P}tr\bar{\mathbf{E}}\mathbf{M}\bar{\mathbf{E}}\mathbf{M}I + \hat{Q}tr\bar{\mathbf{E}}\mathbf{M}\bar{\mathbf{E}}\mathbf{M}\mathbf{M}\otimes\mathbf{M} && \text{(C.122)}\\
& + \hat{R}tr\bar{\mathbf{E}}(\mathbf{M}\otimes\bar{\mathbf{E}}\mathbf{M} + \mathbf{M}\bar{\mathbf{E}}\otimes\mathbf{M}) + \hat{S}tr\bar{\mathbf{E}}\bar{\mathbf{E}}\mathbf{M}\otimes\mathbf{M} && \text{(C.123)}
\end{aligned}$$

where

$$\hat{A} = -\frac{A'}{B'(B' + 3A' + F')} \tag{C.124}$$

$$\hat{B} = \frac{1}{B'} \tag{C.125}$$

$$\hat{C} = -\frac{C'\hat{B} + C'\hat{E} + 2D'\hat{E} + 3F'\hat{E} + 2E'\hat{D} + 2F'\hat{D} + 2D'\hat{D}}{B' + C' + D' + E' + F'} \tag{C.126}$$

$$\hat{D} = -\frac{D'}{B'(2D' + B')} \tag{C.127}$$

$$\hat{E} = -\frac{A'\hat{C} + 2A'\hat{D} + 2C'\hat{D} + E'\hat{B}}{B' + 3A'} \tag{C.128}$$

$$\hat{F} = -\frac{C'\hat{A} + 2D'\hat{A} + F'\hat{B} + 3F'\hat{A}}{A' + B' + C' + 2D' + E' + F'} \tag{C.129}$$

$$\hat{G} = -\frac{A'\hat{J} + A'\hat{K} + 4G'\hat{D} + G'\hat{B}}{B' + 3A' + C' + E'} \tag{C.130}$$

$$\hat{H} = -\frac{H'}{B'^2} \tag{C.131}$$

$$\hat{I} = -\frac{A'\hat{H}}{B' + 3A' + C' + E'} \tag{C.132}$$

$$\hat{J} = -\frac{J'}{B'^2} \tag{C.133}$$

$$\hat{K} = -\frac{2D'\hat{G} + 3F'\hat{G} + F'\hat{J} + K'\hat{B} + 4K'\hat{D} + S'\hat{F} + A'\hat{S}}{B' + 2D' + E' + F' + C'} \tag{C.134}$$

$$\hat{L} = -\frac{2D'\hat{I} + F'\hat{H} + F'\hat{I} + H'\hat{F} + I'\hat{F} + J'\hat{F} + G'\hat{F} + 3K'\hat{A}}{B' + C' + 2D' + F'} \tag{C.135}$$

$$- \frac{K'\hat{F} + L'\hat{B} + 3L'\hat{A} + G'\hat{F} + P'\hat{F} + 3Q'\hat{A} + Q'\hat{F} + 6R'\hat{A} + 2R'\hat{F} + S'\hat{A} + F'\hat{S}}{B' + C' + 2D' + F'} \tag{C.136}$$

$$\hat{M} = -\frac{2D'\hat{P} + M'\hat{E} + M'\hat{C} + M'\hat{B} + 2N'\hat{C} + 2N'\hat{E} + O'\hat{C} + O'\hat{D} + 3Q'\hat{E}}{B'} \tag{C.137}$$

$$\hat{N} = -\frac{D'\hat{J} + N'\hat{B} + O'\hat{E}}{B' + E'} \tag{C.138}$$

$$\hat{O} = -\frac{2M'\hat{D} + 3P'\hat{E} + O'\hat{B}}{B'} \tag{C.139}$$

$$\hat{P} = -\frac{A'(\hat{M} + 2\hat{N} + 3\hat{O} + \hat{Q} + 2\hat{R}) + 2C'\hat{R} + E'\hat{H} + H'\hat{E} + G'\hat{C} + 2N'\hat{A}}{B' + 3A' + E'} \tag{C.140}$$

$$- \frac{2N'\hat{F} + P'\hat{B} + O'\hat{F} + M'\hat{F}}{B' + 3A' + E'} \tag{C.141}$$

$$\hat{Q} = -\frac{C'\hat{H} + C'\hat{P} + 2D'\hat{P} + 2D'\hat{C} + 2E'\hat{R} + F'\hat{M} + 2F'\hat{N} + 3F'\hat{J}}{B' + C' + 2D' + E' + F'} \tag{C.142}$$

$$- \frac{3F'\hat{O} + 2F'\hat{R} + H'\hat{C} + Q'\hat{B} + S'\hat{C} + S'\hat{E} + C'\hat{S} + E'\hat{S}}{B' + C' + 2D' + E' + F'} \tag{C.143}$$

$$\hat{R} = -\frac{D'\hat{H} + H'\hat{D} + R'\hat{B}}{B'} \tag{C.144}$$

$$\hat{S} = -\frac{S'\hat{B} + M'\hat{A} + O'\hat{A} + O'\hat{F} + 2N'\hat{F}}{B'} \tag{C.145}$$

$$\tag{C.146}$$

Assuming bound uniformity $\bar{\mathbf{T}}^1(\bar{\mathbf{E}}^1) = \mathbf{T}^1(\mathbf{E}^1)$ we obtained the next configuration of stress average.

$$\bar{\mathbf{T}} = \underbrace{2m^*\bar{\mathbf{E}} + (k^* - m^*)tr\bar{\mathbf{E}}I}_{\bar{\mathbf{T}}_{L1}} \tag{C.147}$$

$$+ \underbrace{\mathcal{L}_1^*((\mathbf{M}\bar{\mathbf{E}}\mathbf{M})\mathbf{M}\otimes\mathbf{M}) + 2(p^* - m^*)(\mathbf{M}\otimes\bar{\mathbf{E}}\mathbf{M} + \mathbf{M}\bar{\mathbf{E}}\otimes\mathbf{M}) + \mathcal{L}_2^*(tr\bar{\mathbf{E}}\mathbf{M}\otimes\mathbf{M} + \mathbf{M}\bar{\mathbf{E}}\mathbf{M}I)}_{\bar{\mathbf{T}}_{L2}} \tag{C.148}$$

$$+ \underbrace{\tilde{\mathcal{A}}^*(\bar{\mathbf{E}})^2 + \mathcal{B}^*tr(\bar{\mathbf{E}})^2 + 2\tilde{\mathcal{B}}^*tr\bar{\mathbf{E}}\bar{\mathbf{E}} + \tilde{\mathcal{C}}^*(tr\bar{\mathbf{E}})^2 I}_{\bar{\mathbf{T}}_{NL1}} \tag{C.149}$$

$$+ \mathbf{M}\bar{\mathbf{E}}\mathbf{M}\mathbf{M}\otimes\mathbf{M}\bar{\mathbf{E}} + (\mathbf{M}\otimes\bar{\mathbf{E}}\mathbf{M} + \mathbf{M}\bar{\mathbf{E}}\otimes\mathbf{M})\bar{\mathbf{E}} \tag{C.150}$$

$$+ tr\bar{\mathbf{E}}\bar{\mathbf{E}}\mathbf{M}\otimes\mathbf{M} + tr(\bar{\mathbf{E}})^2\mathbf{M}\otimes\mathbf{M} + (tr\bar{\mathbf{E}})^2\mathbf{M}\otimes\mathbf{M} + \mathbf{M}\bar{\mathbf{E}}\mathbf{M}\mathbf{E}^1 I \tag{C.151}$$

$$+ \underbrace{tr\bar{\mathbf{E}}\mathbf{M}\bar{\mathbf{E}}\mathbf{M}\mathbf{M}\otimes\mathbf{M} + tr\bar{\mathbf{E}}(\mathbf{M}\otimes\bar{\mathbf{E}}\mathbf{M} + \mathbf{M}\bar{\mathbf{E}}\otimes\mathbf{M}) + tr\bar{\mathbf{E}}\mathbf{M}\bar{\mathbf{E}}\mathbf{M}I}_{\bar{\mathbf{T}}_{NL2}} \tag{C.152}$$

$$\tag{C.153}$$

D

Contributions

The results, trasversal applications and contributions from this Thesis, are reflected in the refereed journal publications, international conferences, patens and books enumerated below.

- Refereed journal publications:
  - ▷ G. Rus, J. Melchor, N. Bochud, L. Peralta and W. Parnell. *A micro-mechanical approach for bone nonlinear quantitative ultrasound.* Submitted to *Ultrasonics*.
  - ▷ L. Peralta, F.S. Molina, J. Melchor, L.F. Gómez, J. Florido, P. Massó, G. Rus. Transient Elastography to Assess the Cervical Ripening during Pregnancy: A Preliminary Study. *Ultrashall In Der Medizin*.
  - ▷ J. Melchor, L. Peralta, G. Rus, A. Valera, E. Sánchez, A. Gómez and N. Saffari. *Torsional Sensor Design On Layered Tissue*. Journal of Biomechanics.
  - ▷ G. Rus, L. Peralta, J. Melchor, J. Baena, N. Bochud, J. Marchal, E. Ruiz, C. Artich, G. Jiménez, J. Soto *In-Bioreactor probabilistic model-based monitoring of tissue properties*. Journal of Biomechanics.
  - ▷ L. Peralta, F.S. Molina, J. Melchor, L.F. Gómez, J. Florido, P. Massó, G. Rus. *In-vivo Assessment of the pregnant cervix using transient elastography* Journal of Biomechanics.
  - ▷ J. Melchor. *Review: Exploitation of the linear theory in the non-linear modelling of soft tissue* AMS 2015.
  - ▷ J. Melchor, L. Peralta, G. Rus, N. Saffari, J. Soto *Single-transmitter setup on nonlinear mixing to measure acoustic nonlinearity of first order.* ESUCB 2015, minipaper indexado en IEEE.

- ▷ Rafael Muñoz, Nicolas Bochud, Guillermo Rus, Laura Peralta, Juan Melchor, Juan Chiachío, Manuel Chiachío, Leonard. J. Bond, *Model-Based Damage Evaluation of Layered CFRP Structures. AIP Publishing*
- ▷ J. Melchor, G. Rus. *Piezoelectric transducer computational design optimization. Ultrasonics* 2014 *Elsevier*.
- ▷ J. Melchor, N. Bochud, L. Peralta, M. González, M. Alaminos, A. Campos. Low-Intensity Ultrasound stimulation to enhance the recellularization process of corneal stroma. *Histology and Histopathology cellular and molecular biology 2012*
- ▷ N. Bochud, J. Melchor, L. Peralta, J. Chiachio, M. Chiachio, G. Rus, M. González, M. Alaminos. Ultrasonic monitoring of the decellularization process of porcine corneal stroma. *Histology and Histopathology cellular and molecular biology 2012*
- ▷ L. Peralta, G. Rus, N. Bochud, J. Melchor, J. Chiachio, M. Chiachio, J. Florido, F. Molina. Multiscale mechanical model for the cervical tissue. *Biomechanics 2012*.
- ▷ J. Chiachio, M. Chiachio, G. Rus, N. Bochud, L. Peralta, J. Melchor. A stochastic model for tissue consistence evolution based on the inverse problem. *Biomechanics 2012*.
- ▷ N. Bochud, J. Melchor, L. Peralta, J. Chiachio, M. Chiachio, G. Rus, M. González, M. Alaminos. Ultrasonic monitoring of the decellularization process of porcine corneal stroma. *Biomechanics 2012*.
- ▷ N. Bochud, J. Melchor, G. Rus, M. Alaminos, and A. Campos. Low-Intensity Ultrasound for stimulation os tissue culture *Histology and Histopathology cellular and molecular biology V26 (12.O3) 2011*
- ▷ J. Melchor, N. Bochud, and G. Rus. Specify of piezoelectric tissue stiffness sensor: modelling. *Histology and Histopathology cellular and molecular biology V26 (12.P2) 2011*

- International conferences:
  - ▷ R. Muñoz, G. Rus, J. Melchor, J. Chiachío, M. Chiachío, N. Bochud, L. Peralta. *Predicción de vida remanente de componentes con ultrasonidos*. Congreso Nacional de Ensayos No Destructivos. 2015.
  - ▷ G. Rus, J. Melchor, A. Ionescu. De la Ingeniería a la Medicina. Noche europea de los investigadores. 2014
  - ▷ G. Rus, J. Melchor. *Mecánica Tisular Ultrasónica y Biorreactores. Proceeding of Workshop on Acoustic Emission and other NDT Methods.*
  - ▷ G. Rus, J. Melchor, A. Callejas, S. Cantero, M. Chiachío, J. Chiachío, L. Peralta. *Nonlinear ultrasonics for early damage assessment. Proceeding of Workshop on Acoustic Emission and other NDT Methods.*
  - ▷ J. Melchor, G. Rus, L. Peralta, N. Bochud, J. Chiachío, M. Chiachío, J. Suárez and A. Gómez. *Optimization of torsion transducer sensitivity on layered tissue. Proceeding of World Congress on Computational Mechanics 2014.*

- ▷ G. Rus, F.S. Molina, L.M. Peralta, J. Florido, J. Melchor, A. Gómez, N. Bochud, J. Chiachío and M. Chiachío. *Mechanical Characterization of Cervical Tissue by Shear wave Ultrasound. World Congress on Biomechanics 2014*
- ▷ J. Melchor, G. Rus, N. Bochud, L. Peralta, J. Chiachío, M. Chiachío, A. Gómez. *Model-based probability of detection of pathologies in soft tissue. IWBBIO 2014*
- ▷ G. Rus, N. Bochud, J. Melchor, L. Peralta, J. Chiachío, M. Chiachío, A. Gómez. *Ultrasonic monitoring of artificial tissue mechanical properties in bioreactor. IWBBIO 2014*
- ▷ L. Peralta, G. Rus, N. Bochud, J. Melchor, J. Chiachío, M. Chiachío. *FDTD simulations for ultrasound propagation in a 2-D cervical tissue model. IWBBIO 2014*
- ▷ J. Chiachío, M. Chiachío, G. Rus, N. Bochud, L. Peralta, J. Melchor. *Information-theory approach to model class assessment for tissue-engineered cultures consistence evolution. IWBBIO 2014*
- ▷ G. Rus, N. Bochud, L. Peralta, J. Melchor, J. Chiachio, M. Chiachio. *Nonlinear ultrasonic imaging of cortical bone. Anglo-French Physical Acoustics Conference 2014*
- ▷ L. Peralta, J. Melchor, G. Rus, J. Chiachio, M. Chiachio. *Mecánica tisular ultrasónica. ESBESP 2013*.
- ▷ J. Melchor, G. Rus, N. Bochud, L. Peralta, J. Chiachio, M. Chiachio. *Optimization of torsion ultrasound piezoelectric transducer. CMNE 2013*.
- ▷ G. Rus, J. Melchor, N. Bochud, L. Peralta, J. Chiachio, M. Chiachio, M. Andrades, A. C. Ximenez, M. Alaminos, A. Campos. *Mechanical properties monitorization in bioreactor by ultrasound. CMNE 2013*.
- ▷ N. Bochud, J. Chiachio. M. Chiachio, G. Rus, J. Melchor, L. Peralta. *Model-based inverse problem for damage reconstruction in composites. CMNE 2013*.
- ▷ J. Chiachio, M. Chiachio, G. Rus, N. Bochud, L. Peralta, J. Melchor, A. Gomez. *Robust fatigue damage prognostics in composites. CMNE 2013*.
- ▷ J. Melchor, W. J. Parnell, G. Rus, N. Bochud, L. Peralta, A. Gómez, M. Chiachio, J. Chiachio. *Relationship between acoustic and homogenized Landau nonlinearity constant in anisotropic bone ESUCB 2013*
- ▷ M. Chiachío, J. Chiachío, G. Rus, N. Bochud, J. Melchor, L. Peralta, M. Membrilla, A.Gómez. *A stochastic model for bone mechanical evolution based on the inverse problem ESUCB 2013*
- ▷ L. Peralta, A. Gómez, N. Bochud, J. Melchor, G. Rus, M. Chiachío, J. Chiachío, G. Ruiz-Cabello, C. Reyes, M.V. Olmedo. *Evolution of implant osseointegration by nonlinear ultrasound ESUCB 2013*
- ▷ G. Rus, J. Melchor, J. Baena, J. Marchal, G. Jimenez, E. Lopez-Ruiz, M. Peran, N. Bochud, L. Peralta, A. Gómez, D. Castello, M. Chiachio, J. Chiachio *Real-time probabilistic model-based monitoring biorreactor for engineered cartilage ESUCB 2013*
- ▷ N. Bochud, M. Membrilla, L. Peralta, J. Melchor, and G. Rus. *Nonlinear ultrasonic imaging for cortical bone damage assessment ESUCB 2013*

- ▷ A. J. Gómez, G. Rus, F. J. Suárez, D. Arcoya, N. Bochud, J. Melchor, L. Peralta, J. Chiachío, M. Chiachío *Biomechanical Shear Moduli recovery from ultrasound in multilayered half-space media ICU 2013*
- ▷ G. Rus, N. Bochud, J. Melchor, L. Peralta, J. Chiachío, M. Chiachío, A. J. Gómez, A. C. Ximenez, M. Alaminos, A. Campos. *In-bioreactor ultrasonic monitoring of tissue mechanical properties ICU 2013*.
- ▷ J. Melchor, G. Rus. Tissue Ultrasound Mechanics. Capítulo nacional de *ESBESP* Sevilla, Octubre, 2012
- ▷ W. Parnell, J. Melchor, G. Rus. Nonlinearity in bone: a micromechanics approach. *ECCOMAS* Viena 2012.
- ▷ J. Melchor, N. Bochud, L. Peralta, G. Rus, M. González, M. Alaminos. Corneal stroma recellularization process advantaged by ultrasound. *ECCOMAS* Viena 2012.
- ▷ N. Bochud, J. Melchor, L. Peralta, J. Chiachio, M. Chiachio, G. Rus, M. González, M. Alaminos. Ultrasonic monitoring of the decellularization process of porcine corneal stroma. *ECCOMAS* Viena 2012.
- ▷ G. Rus, N. Bochud, J. Melchor, M. Alaminos, A. Campos. Dispersive model selection and reconstruction for tissue culture ultrasonic monitoring. AIP Conf. Proc. 1433, 375-378. 2012.
- ▷ J. Melchor, W. Parnell, G. Rus. Damage due to bone : effective nonlinear constitutive behavior. Manchester bone and homogenization workshop, Marzo 2012.
- ▷ G. Rus., N. Bochud and J. Melchor. Ultrasonic monitoring and parameters identification of simulated tissue culture. *4th European symposium on Ultrasonic Characterization of Bone*, Jyvskyla, Finland, June 2011.
- ▷ N. Bochud, J. Melchor, and G. Rus. Reconstruction of nonlinear constitutive models from 1D ultrasound propagation. *Proceedings of the CMNE 2011*, Coimbra, June 2011.
- ▷ G. Rus, N. Bochud, J. Melchor, Ultrasound-based monitoring of simulated tissue culture. *Proceedings of the CMNE 2011*, Coimbra, June 2011.
- ▷ J. Melchor, N. Bochud, and G. Rus. Piezoelectric transducer design optimization. *Proceedings of the CMNE 2011*, Coimbra, June 2011.

- Patents:
  - ▷ G. Rus, J. Melchor, N. Bochud, L. Peralta, M. Chiachío, N. Bochud, M. González. "Bioreactor para terapias avanzadas"
  - ▷ G. Rus, J. Melchor, L.Peralta, J. Chiachío, M. Chiachío, N. Bochud, J. Florido, F. Molina."Sensor ultrasónico anular de torsión"
  - ▷ G. Rus, J. Melchor, N. Bochud, J. Florido. "Transductor ultrasónico de torsión para diagnóstico tisular." P201100700. 14/06/2011.

- ▷ G. Rus, N. Bochud, J. Melchor, J. Chiachío, M. Chiachío, C. Ureña, L. Pérez, A. Campos y M. Alaminos, "Dispositivo y método de monitorización de muestras" . ES. Patente P-04263. 2011

- Books chapters:
  - ▷ R. Muñoz, G. Rus, N. Bochud, D. Barnard, J. Melchor, J. Chiachío, M. Chiachío, S. Cantero, A. Callejas, L. Peralta. *Nonlinear ultrasonics as an early damage signature*, Aprobado para publicación en: Emerging Design Solutions in Structural Health Monitoring Systems, Advances in Civil and Industrial Engineering Series, *Ed. IGI Global.*

References

[1] L. D. Landau and E. M. Lifshitz. *Theory of Elasticity*. Pergamon, Oxford, USA, 1986.

[2] Mark F Hamilton, David T Blackstock, et al. *Nonlinear acoustics*, volume 237. Academic press San Diego, 1998.

[3] J.D. Eshelby. The continuum theory of lattice defects. In E. Seitz and D. Turnbull, editors, *Progress in Solid State Physics*. Academic Press, 1956.

[4] K.E.A. Van Den Abeele, P.A. Johnson, and A. Sutin. News techniques to discern material damage, part i: Nwms (nonlinear wave modulation spectroscopy). *Research in Nondestructive Evaluation*, 12:17–30, 2000.

[5] L.K. Zarembo and V.A. Krasil'Nikov. Nonlinear phenomena in the propagation of elastic waves in solids. *Physics-Uspekhi*, 13(6):778–797, 1971.

[6] Dave D Muir. *One-sided ultrasonic determination of third order elastic constants using angle-beam acoustoelasticity measurements*. Dissertation, Georgia Institute of Technology, May 2009.

[7] Francis A. Duck. *Physical properties of tissues: a comprehensive reference book*. Academic press, 2013.

[8] Gerhard A Holzapfel. *Nonlinear solid mechanics*, volume 24. Wiley Chichester, 2000.

[9] Gerhard A Holzapfel, T Christian Gasser, and M Stadler. A structural model for the viscoelastic behavior of arterial walls: continuum formulation and finite element analysis. *European Journal of Mechanics-A/Solids*, 21(3):441–463, 2002.

[10] Gerhard A Holzapfel, Thomas C Gasser, and Ray W Ogden. A new constitutive framework for arterial wall mechanics and a comparative study of material models. *Journal of elasticity and the physical science of solids*, 61(1-3):1–48, 2000.

[11] Gerhard A Holzapfel and Juan C Simo. A new viscoelastic constitutive model for continuous media at finite thermomechanical changes. *International Journal of Solids and Structures*, 33(20):3019–3034, 1996.

[12] F.D. Murnaghan. *Finite deformation of an elastic solid, 1951*. Chapman & Hall, London, 1951.

[13] Do S Hughes and JL Kelly. Second-order elastic deformation of solids. *Physical review*, 92(5):1145, 1953.

[14] ZA Gol?dberg. Interaction of plane longitudinal and transverse elastic waves. *Sov. Phys. Acoust*, 6:306–310, 1961.

[15] RN Thurston and K Brugger. Third-order elastic constants and the velocity of small amplitude elastic waves in homogeneously stressed media. *Physical Review*, 133(6A):A1604, 1964.

[16] G Douglas Meegan Jr, Paul A Johnson, Robert A Guyer, and Katherine R McCall. Observations of nonlinear elastic wave behavior in sandstone. *The Journal of the Acoustical Society of America*, 94(6):3387–3391, 1993.

[17] E Koen and A Van Den Abeele. Elastic pulsed wave propagation in media with second-or higher-order nonlinearity. part i. theoretical framework. *The Journal of the Acoustical Society of America*, 99(6):3334–3345, 1996.

[18] James A TenCate, Koen EA Van Den Abeele, Thomas J Shankland, and Paul A Johnson. Laboratory study of linear and nonlinear elastic pulse propagation in sandstone. *The Journal of the Acoustical Society of America*, 100(3):1383–1391, 1996.

[19] KR McCall and RA Guyer. A new theoretical paradigm to describe hysteresis, discrete memory and nonlinear elastic wave propagation in rock. *Nonlinear processes in geophysics*, 3(2):89–101, 1930.

[20] V Gusev, Christ Glorieux, Walter Lauriks, and Jan Thoen. Nonlinear bulk and surface shear acoustic waves in materials with hysteresis and end-point memory. *Physics Letters A*, 232(1):77–86, 1997.

[21] Veniamin E Nazarov, Lev A Ostrovsky, Irina A Soustova, and Aleksandr M Sutin. Nonlinear acoustics of micro-inhomogeneous media. *Physics of the Earth and Planetary Interiors*, 50(1):65–73, 1988.

[22] Igor Yu Solodov. Ultrasonics of non-linear contacts: propagation, reflection and ndeapplications. *Ultrasonics*, 36(1):383–390, 1998.

[23] RA Guyer, KR McCall, and Koen Van Den Abeele. Slow elastic dynamics in a resonant bar of rock. *Geophysical research letters*, 25(10):1585–1588, 1998.

[24] CD Bertram, F Pythoud, N Stergiopulos, and J-J Meister. Pulse wave attenuation measurement by linear and nonlinear methods in nonlinearly elastic tubes. *Medical engineering & physics*, 21(3):155–166, 1999.

[25] Jun-ichi Kushibiki and Mototaka Arakawa. Diffraction effects on bulk-wave ultrasonic velocity and attenuation measurements. *The Journal of the Acoustical Society of America*, 108(2):564–573, 2000.

[26] G Renaud, M Talmant, S Callé, M Defontaine, and P Laugier. Nonlinear elastodynamics in micro-inhomogeneous solids observed by head-wave based dynamic acoustoelastic testing. *The Journal of the Acoustical Society of America*, 130(6):3583–3589, 2011.

[27] J Rivière, G Renaud, RA Guyer, and PA Johnson. Pump and probe waves in dynamic acousto-elasticity: comprehensive description and comparison with nonlinear elastic theories. *Journal of Applied Physics*, 114(5):054905, 2013.

[28] G Renaud, J Rivière, S Haupert, and P Laugier. Anisotropy of dynamic acoustoelasticity in limestone, influence of conditioning, and comparison with nonlinear resonance spectroscopy. *The Journal of the Acoustical Society of America*, 133(6):3706–3718, 2013.

[29] Hélène Moreschi, Samuel Callé, Sophie Guerard, David Mitton, and Marielle Defontaine. Détection du micro-endommagement dans le tissu osseux trabéculaire par une méthode d?acousto-élasticité dynamique. *IRBM*, 32(5):269–273, 2011.

[30] Guillaume Renaud, Samuel Calle, J-P Remenieras, and Marielle Defontaine. Exploration of trabecular bone nonlinear elasticity using time-of-flight modulation. *Ultrasonics, Ferroelectrics and Frequency Control, IEEE Transactions on*, 55(7):1497–1507, 2008.

[31] Guillaume Renaud, Samuel Callé, Jean-Pierre Remenieras, and Marielle Defontaine. Non-linear acoustic measurements to assess crack density in trabecular bone. *International Journal of Non-Linear Mechanics*, 43(3):194–200, 2008.

[32] Jeremiah J Rushchitsky et al. *Nonlinear Elastic Waves in Materials*. Springer, 2014.

[33] PJ Westervelt. Acoustical impedance in terms of energy functions. *The Journal of the Acoustical Society of America*, 23(3):347–348, 1951.

[34] Gunnar Taraldsen. A generalized westervelt equation for nonlinear medical ultrasound. *The Journal of the Acoustical Society of America*, 109(4):1329–1333, 2001.

[35] Xiaozhou Liu, Junlun Li, Xiufen Gong, and Dong Zhang. Nonlinear absorption in biological tissue for high intensity focused ultrasound. *Ultrasonics*, 44:e27–e30, 2006.

[36] P Gélat, G Ter Haar, and N Saffari. A comparison of methods for focusing the field of a hifu array transducer through human ribs. *Physics in medicine and biology*, 59(12):3139, 2014.

[37] Anthony J Croxford, Paul D Wilcox, Bruce W Drinkwater, and Peter B Nagy. The use of non-collinear mixing for nonlinear ultrasonic detection of plasticity and fatigue. *The Journal of the Acoustical Society of America*, 126(5):EL117–EL122, 2009.

[38] VA Korneev and A Demčenko. Possible second-order nonlinear interactions of plane waves in an elastic solid. *The Journal of the Acoustical Society of America*, 135(2):591–598, 2014.

[39] J Melchor and G Rus. Torsional ultrasonic transducer computational design optimization. *Ultrasonics*, 54(7):1950–1962, 2014.

[40] L Peralta, FS Molina, J Melchor, LF Gómez, P Massó, J Florido, and G Rus. Transient elastography to assess the cervical ripening during pregnancy: A preliminary study. *Ultraschall in der Medizin (Stuttgart, Germany: 1980)*, 2015.

[41] Pier Paolo Delsanto. *Universality of nonclassical nonlinearity*. Springer, 2006.

[42] Guillermo Rus. Nature of acoustic nonlinear radiation stress. *Applied Physics Letters*, 105(12):121904, 2014.

[43] John Douglas Eshelby. The force on an elastic singularity. *Philosophical Transactions of the Royal Society of London A: Mathematical, Physical and Engineering Sciences*, 244(877):87–112, 1951.

[44] JOHN D Eshelby. The determination of the elastic field of an ellipsoidal inclusion, and related problems. *Proceedings of the Royal Society of London. Series A. Mathematical and Physical Sciences*, 241(1226):376–396, 1957.

[45] JD Eshelby. The elastic model of lattice defects. *Annalen der Physik*, 456(1-3):116–121, 1957.

[46] P Ponte Castañeda. Exact second-order estimates for the effective mechanical properties of nonlinear composite materials. *Journal of the Mechanics and Physics of Solids*, 44(6):827–862, 1996.

[47] Luc Dormieux, Djimedo Kondo, and Franz-Josef Ulm. A micromechanical analysis of damage propagation in fluid-saturated cracked media. *Comptes Rendus Mecanique*, 334(7):440–446, 2006.

[48] William J Parnell. Effective wave propagation in a prestressed nonlinear elastic composite bar. *IMA journal of applied mathematics*, 72(2):223–244, 2007.

[49] William James Parnell. *Homogenization techniques for wave propagation in composite materials*. PhD thesis, University of Manchester, 2006.

[50] Jüri Engelbrecht and Arkadi Berezovski. On modelling of wave propagation in microstructured solids. *Estonian Journal of Engineering*, 19(3):171–182, 2013.

[51] William J Parnell and Quentin Grimal. The influence of mesoscale porosity on cortical bone anisotropy. investigations via asymptotic homogenization. *Journal of the Royal Society Interface*, 6(30):97–109, 2009.

[52] Torsten Hauck, Wolfgang H Mueller, and Ilko Schmadlak. Fracture risk assessment for interface flaws in the 3d-interconnect systems of a cmos chip. In *Thermal and Thermomechanical Phenomena in Electronic Systems, 2008. ITHERM 2008. 11th Intersociety Conference on*, pages 756–761. IEEE, 2008.

[53] J Rahmoun, J Halgrin, H Naceur, E Markiewicz, F Chaari, and P Drazetic. Multi-scale modeling of the trabecular bone mechanical behaviour.

[54] V Sansalone, V Bousson, S Naili, C Bergot, F Peyrin, JD Laredo, and G Haïat. Effects of the axial variations of porosity and mineralization on the elastic properties of the human femoral neck. *Computer Modeling in Engineering & Sciences(CMES)*, 87(5):387–409, 2012.

[55] Guillermo Rus, Nicolas Bochud, Laura Peralta, Juan Melchor, Juan Chiachio, and Manuel Chiachio. Nonlinear ultrasonic imaging of cortical bone.

[56] G Rus, J Melchor, A Callejas, S Cantero, M Chiachio, J Chiachio, and L Peralta. Nonlinear ultrasonics for early damage assessment.

[57] Frank E Barber, Donald W Baker, Arthur WC Nation, D Eugene Strandness, and John M Reid. Ultrasonic duplex echo-doppler scanner. *Biomedical Engineering, IEEE Transactions on*, (2):109–113, 1974.

[58] Joseph D Bronzino. *Biomedical engineering handbook*, volume 2. CRC press, 1999.

[59] W Murr. Pressure sensing system and method, December 10 1974. US Patent 3,853,117.

[60] Yariv Porat, Avi Penner, and Eyal Doron. Implantable acoustic bio-sensing system and method, August 13 2002. US Patent 6,432,050.

[61] Michael J Vellekoop. Acoustic wave sensors and their technology. *Ultrasonics*, 36(1):7–14, 1998.

[62] Jonathan M Cannata, Timothy Ritter, Wo-Hsing Chen, Ronald H Silverman, K Kirk Shung, et al. Design of efficient, broadband single-element (20-80 mhz) ultrasonic transducers for medical imaging applications. *Ultrasonics, Ferroelectrics, and Frequency Control, IEEE Transactions on*, 50(11):1548–1557, 2003.

[63] John Denis Enderle and Joseph D Bronzino. *Introduction to biomedical engineering*. Academic press, 2012.

[64] Pascal Laugier and Guillaume Haèiat. *Bone quantitative ultrasound*. Springer, 2011.

[65] Ahmad Safari and E Koray Akdogan. *Piezoelectric and acoustic materials for transducer applications*. Springer Science & Business Media, 2008.

[66] Roderic Lakes, Hyo Sub Yoon, and J Lawrence Katz. Ultrasonic wave propagation and attenuation in wet bone. *Journal of biomedical engineering*, 8(2):143–148, 1986.

[67] K Kirk Shung and Gary A Thieme. *Ultrasonic scattering in biological tissues*. CRC Press, 1992.

[68] Emmanuel Bossy, Maryline Talmant, Marielle Defontaine, Frédéric Patat, and Pascal Laugier. Bidirectional axial transmission can improve accuracy and precision of ultrasonic velocity measurement in cortical bone: a validation on test materials. *Ultrasonics, Ferroelectrics, and Frequency Control, IEEE Transactions on*, 51(1):71–79, 2004.

[69] Robert Rohling, Andrew Gee, and Laurence Berman. A comparison of freehand three-dimensional ultrasound reconstruction techniques. *Medical image analysis*, 3(4):339–359, 1999.

[70] Naima Sebaa, Naima Sebaa, Mohamed Fellah, Erick Ogam, Farid G Mitri, Claude Depollier, and Walter Lauriks. Application of the biot model to ultrasound in bone: inverse problem. *Ultrasonics, Ferroelectrics, and Frequency Control, IEEE Transactions on*, 55(7):1516–1523, 2008.

[71] Guillermo Rus, Shi-Chang Wooh, and Rafael Gallego. Design of ultrasonic wedge transducer. *Ultrasonics*, 43(5):391–395, 2005.

[72] Juan Melchor, Guillermo Rus, Nicolas Bochud, Laura Peralta, Juan Chiachio, and Manuel Chiachio. Model-based probability of detection of pathologies in soft tissue.

[73] TG Muir and EL Carstensen. Prediction of nonlinear acoustic effects at biomedical frequencies and intensities. *Ultrasound in medicine & biology*, 6(4):345–357, 1980.

[74] Francis A Duck. Nonlinear acoustics in diagnostic ultrasound. *Ultrasound in medicine & biology*, 28(1):1–18, 2002.

[75] Frank A Bender, Jin-Yeon Kim, Laurence J Jacobs, and Jianmin Qu. The generation of second harmonic waves in an isotropic solid with quadratic nonlinearity under the presence of a stress-free boundary. *Wave Motion*, 50(2):146–161, 2013.

[76] JW Ju and X Lee. Micromechanical damage models for brittle solids. part i: tensile loadings. *Journal of Engineering Mechanics*, 117(7):1495–1514, 1991.

[77] CM Sayers. *Ultrasound in Solids with Porosity, Microcracking and Polycrystalline Structuring*. Springer, 1993.

[78] C Payan, V Garnier, J Moysan, and PA Johnson. Applying nonlinear resonant ultrasound spectroscopy to improving thermal damage assessment in concrete. *The Journal of the Acoustical Society of America*, 121(4):EL125–EL130, 2007.

[79] Kyung-Young Jhang. Nonlinear ultrasonic techniques for nondestructive assessment of micro damage in material: a review. *International journal of precision engineering and manufacturing*, 10(1):123–135, 2009.

[80] A Bauer, P Hauff, J Lazenby, P Von Behren, M Zomack, M Reinhardt, and R Schlief. Wideband harmonic imaging: a novel contrast ultrasound imaging technique. *European radiology*, 9(3):S364–S367, 1999.

[81] Ray W Ogden. *Nonlinear elasticity, anisotropy, material stability and residual stresses in soft tissue*. Springer, 2003.

[82] Guillaume Picinbono, Herve Delingette, and Nicholas Ayache. Nonlinear and anisotropic elastic soft tissue models for medical simulation. In *Robotics and Automation, 2001. Proceedings 2001 ICRA. IEEE International Conference on*, volume 2, pages 1370–1375. IEEE, 2001.

[83] Gerhard A Holzapfel. Biomechanics of soft tissue. *The handbook of materials behavior models*, 3:1049–1063, 2001.

[84] Walter Maurel, Yin Wu, Nadia Magnenat Thalmann, and Daniel Thalmann. *Biomechanical models for soft tissue simulation*. Springer, 1998.

[85] Francis A Duck. *Physical properties of tissues: a comprehensive reference book*. Academic press, 2013.

[86] Ray W Ogden and Gerhard A Holzapfel. *Mechanics of biological tissue*. Springer, 2006.

[87] A Menzel. *Anisotropic remodelling of biological tissues*. Springer, 2006.

[88] Jeffrey A Weiss, Bradley N Maker, and Sanjay Govindjee. Finite element implementation of incompressible, transversely isotropic hyperelasticity. *Computer methods in applied mechanics and engineering*, 135(1):107–128, 1996.

[89] JL Ericksen and RS Rivlin. Large elastic deformations of homogeneous anisotropic materials. *Journal of rational mechanics and analysis*, 3(3):281–301, 1954.

[90] Jerald Laverne Ericksen. Deformations possible in every isotropic, incompressible, perfectly elastic body. *Zeitschrift für Angewandte Mathematik und Physik (ZAMP)*, 5(6):466–489, 1954.

[91] TC Doyle and JL Ericksen. Nonlinear elasticity. *Advances in applied mechanics*, 4:53–115, 1956.

[92] JR Willis. Bounds and self-consistent estimates for the overall properties of anisotropic composites. *Journal of the Mechanics and Physics of Solids*, 25(3):185–202, 1977.

[93] Zvi Hashin. Analysis of properties of fiber composites with anisotropic constituents. *Journal of Applied Mechanics*, 46(3):543–550, 1979.

[94] Robert F Landel and Lawrence E Nielsen. *Mechanical properties of polymers and composites*. CRC Press, 1993.

[95] VD Azzi and SW Tsai. Anisotropic strength of composites. *Experimental mechanics*, 5(9):283–288, 1965.

[96] Derek Hull and TW Clyne. *An introduction to composite materials*. Cambridge university press, 1996.

[97] Stephen W Tsai and Edward M Wu. A general theory of strength for anisotropic materials. *Journal of composite materials*, 5(1):58–80, 1971.

[98] Lev D Landau and EM Lifshitz. Theory of elasticity, vol. 7. *Course of Theoretical Physics*, 3:109, 1986.

[99] Francis Dominic Murnaghan. *Finite deformation of an elastic solid*. Dover Publications Inc., 1951.

[100] Michel Destrade and Raymond W Ogden. On the third-and fourth-order constants of incompressible isotropic elasticity. *The Journal of the Acoustical Society of America*, 128(6):3334–3343, 2010.

[101] M Destrade, B Mac Donald, JG Murphy, and G Saccomandi. At least three invariants are necessary to model the mechanical response of incompressible, transversely isotropic materials. *Computational Mechanics*, 52(4):959–969, 2013.

[102] Pasquale Ciarletta, Ivano Izzo, Silvestro Micera, and Frank Tendick. Stiffening by fiber reinforcement in soft materials: a hyperelastic theory at large strains and its application. *Journal of the mechanical behavior of biomedical materials*, 4(7):1359–1368, 2011.

[103] Pasquale Ciarletta, Michel Destrade, and Artur L Gower. Shear instability in skin tissue. *The Quarterly Journal of Mechanics and Applied Mathematics*, 66(2):273–288, 2013.

[104] Jia Lu and Liang Zhang. Physically motivated invariant formulation for transversely isotropic hyperelasticity. *International journal of solids and structures*, 42(23):6015–6031, 2005.

[105] John C Criscione, Andrew S Douglas, and William C Hunter. Physically based strain invariant set for materials exhibiting transversely isotropic behavior. *Journal of the Mechanics and Physics of Solids*, 49(4):871–897, 2001.

[106] John C Criscione, Andrew D McCulloch, and William C Hunter. Constitutive framework optimized for myocardium and other high-strain, laminar materials with one fiber family. *Journal of the Mechanics and Physics of Solids*, 50(8):1681–1702, 2002.

[107] A.N. Norris. *Nonlinear acoustics*, chapter Finite amplitude waves in solids, pages 263–277. Academic Press, San Diego, 1998.

[108] David Russell Bland. *Nonlinear dynamic elasticity*, volume 42. Blaisdell Waltham, 1969.

[109] AC Eringen and ES Suhubi. Elastodynamics, voi. i, 1974.

[110] JG Murphy and G Saccomandi. Exploitation of the linear theory in the non-linear modelling of soft tissue. *Mathematics and Mechanics of Solids*, 20(2):190–203, 2015.

[111] Francis Dominic Murnaghan. Finite deformations of an elastic solid. *American Journal of Mathematics*, pages 235–260, 1937.

[112] Sergio Kostek, Bikash K Sinha, and Andrew N Norris. Third-order elastic constants for an inviscid fluid. *The Journal of the Acoustical Society of America*, 94:3014, 1993.

[113] MA Breazeale and Joseph Ford. Ultrasonic studies of the nonlinear behavior of solids. *Journal of Applied Physics*, 36(11):3486–3490, 1965.

[114] Koen Van Den Abeele, PY Le Bas, Bart Van Damme, and Tomasz Katkowski. Quantification of material nonlinearity in relation to microdamage density using nonlinear reverberation spectroscopy: Experimental and theoretical study. *The Journal of the Acoustical Society of America*, 126(3):963–972, 2009.

[115] Mark F Hamilton and David T Blackstock. On the coefficient of nonlinearity β in nonlinear acoustics. *The Journal of the Acoustical Society of America*, 83(1):74–77, 1988.

[116] Mark F Hamilton, Yurii A Ilinskii, and Evgenia A Zabolotskaya. Separation of compressibility and shear deformation in the elastic energy density (l). *The Journal of the Acoustical Society of America*, 116:41, 2004.

[117] Robert A Guyer and Paul A Johnson. Nonlinear mesoscopic elasticity: evidence for a new class of materials. *Physics today*, 52(4):30–36, 2008.

[118] Christian Clason, Barbara Kaltenbacher, and Slobodan Veljović. Boundary optimal control of the westervelt and the kuznetsov equations. *Journal of Mathematical Analysis and Applications*, 356(2):738–751, 2009.

[119] Athanasios Karamalis, Wolfgang Wein, and Nassir Navab. Fast ultrasound image simulation using the westervelt equation. In *Medical Image Computing and Computer-Assisted Intervention–MICCAI 2010*, pages 243–250. Springer, 2010.

[120] Francois Varray, Christian Cachard, Alessandro Ramalli, Piero Tortoli, and Olivier Basset. Simulation of ultrasound nonlinear propagation on gpu using a generalized angular spectrum method. *EURASIP journal on Image and Video Processing*, 2011(1):1–6, 2011.

[121] Maxim A Solovchuk, Tony WH Sheu, and Marc Thiriet. Effects of acoustic nonlinearity and blood flow cooling during hifu treatment. In *12TH INTERNATIONAL SYMPOSIUM ON THERAPEUTIC ULTRASOUND*, volume 1503, pages 83–88. AIP Publishing, 2012.

[122] Chen Xiaorui, Zhang Xiaojing, Wang Shaolin, and Jian Xiqi. Simulation of the therapeutic region during hifu therapy. In *Biomedical Engineering and Informatics (BMEI), 2011 4th International Conference on*, volume 2, pages 986–989. IEEE, 2011.

[123] Marc Thiriet, Maxim Solovchuk, and Tony Wen-Hann Sheu. Hifu treatment of liver cancer–reciprocal effect of blood flow and us studied from a patient-specific configuration. In *Computational Modeling of Objects Presented in Images. Fundamentals, Methods, and Applications*, pages 1–11. Springer, 2014.

[124] Kenneth W Winkler and Xingzhou Liu. Measurements of third-order elastic constants in rocks. *The Journal of the Acoustical Society of America*, 100(3):1392–1398, 1996.

[125] M Dubuget, R El Guerjouma, Sylvain Dubois, JC Baboux, and Alain Vincent. Characterization of the non-linear elastic properties of aluminium alloys using ultrasonic evaluation under load. In *Materials Science Forum*, volume 217, pages 951–956. Trans Tech Publ, 1996.

[126] David M Stobbe. Acoustoelasticity in 7075-t651 aluminum and dependence of third order elastic constants on fatigue damage. Master's thesis, Mechanical Engineering Georgia Institute of Technology, August 2005.

[127] Ming Hong, Zhongqing Su, Qiang Wang, Li Cheng, and Xinlin Qing. Modeling nonlinearities of ultrasonic waves for fatigue damage characterization: Theory, simulation, and experimental validation. *Ultrasonics*, 54(3):770–778, 2014.

[128] Zhongqing Su, Chao Zhou, Ming Hong, Li Cheng, Qiang Wang, and Xinlin Qing. Acousto-ultrasonics-based fatigue damage characterization: Linear versus nonlinear signal features. *Mechanical Systems and Signal Processing*, 45(1):225–239, 2014.

[129] MA Mironov, PA Pyatakov, II Konopatskaya, GT Clement, and NI Vykhodtseva. Parametric excitation of shear waves in soft solids. *Acoustical Physics*, 55(4-5):567–574, 2009.

[130] David Linton Johnson, Sergio Kostek, and Andrew N Norris. Nonlinear tube waves. *The Journal of the Acoustical Society of America*, 96:1829, 1994.

[131] KR McCall and RA Guyer. Equation of state and wave propagation in hysteretic nonlinear elastic materials. *JOURNAL OF GEOPHYSICAL RESEARCH-ALL SERIES-*, 99:23–887, 1994.

[132] Brian O'Neill and Roman G Maev. Acousto-elastic measurement of the fatigue damage in waspaloy. *Research in Nondestructive Evaluation*, 17(3):121–135, 2006.

[133] Chloé Trarieux, Samuel Callé, Hélène Moreschi, Guillaume Renaud, and Marielle Defontaine. Modeling nonlinear viscoelasticity in dynamic acoustoelasticity. *Applied Physics Letters*, 105(26):264103, 2014.

[134] AL Gower, M Destrade, and RW Ogden. Counter-intuitive results in acoustoelasticity. *Wave Motion*, 50(8):1218–1228, 2013.

[135] Pham Chi Vinh and Jose Merodio. On acoustoelasticity and the elastic constants of soft biological tissues. *Journal of Mechanics of Materials and Structures*, 8(5):359–367, 2013.

[136] Cristian Pantea, Curtis F Osterhoudt, and Dipen N Sinha. Determination of acoustical nonlinear parameter β of water using the finite amplitude method. *Ultrasonics*, 53(5):1012–1019, 2013.

[137] Andrew J Hillis, Simon A Neild, Bruce W Drinkwater, and Paul D Wilcox. Bispectral analysis of ultrasonic inter-modulation data for improved defect detection. In *QUANTITATIVE NONDESTRUCTIVE EVALUATION*, volume 820, pages 89–96. AIP Publishing, 2006.

[138] Minghe Liu, Guangxin Tang, Laurence J Jacobs, and Jianmin Qu. Measuring acoustic nonlinearity parameter using collinear wave mixing. *Journal of Applied Physics*, 112(2):4908, 2012.

[139] RM D?Angelo, KW Winkler, and DL Johnson. Three wave mixing test of hyperelasticity in highly nonlinear solids: Sedimentary rocks. *The Journal of the Acoustical Society of America*, 123(2):622–639, 2008.

[140] David L Johnson, Kenneth Winkler, and Ralph D'Angelo. Three wave mixing test of hyperelasticity in sedimentary rocks. *The Journal of the Acoustical Society of America*, 123(5):3396–3396, 2008.

[141] SJH Van Kervel and JM Thijssen. A calculation scheme for the optimum design of ultrasonic transducers. *Ultrasonics*, 21(3):134–140, 1983.

[142] Barbara L McFarlin et al. Ultrasound insertion loss of the rat cervix. *American Journal of Obstetrics and Gynecology*, 193(6):S154, 2005.

[143] Barbara L McFarlin, William D O'Brien, Michael L Oelze, James F Zachary, and Rosemary C White-Traut. Quantitative ultrasound assessment of the rat cervix. *Journal of ultrasound in medicine*, 25(8):1031–1040, 2006.

[144] Matthias Lebertre, Frédéric Ossant, Loïc Vaillant, Stéphane Diridollou, and Frédéric Patat. Spatial variation of acoustic parameters in human skin: an in vitro study between 22 and 45 mhz. *Ultrasound in medicine & biology*, 28(5):599–615, 2002.

[145] F Sebag, J Vaillant-Lombard, J Berbis, V Griset, JF Henry, P Petit, and C Oliver. Shear wave elastography: a new ultrasound imaging mode for the differential diagnosis of benign and malignant thyroid nodules. *Journal of Clinical Endocrinology & Metabolism*, 95(12):5281–5288, 2010.

[146] Jung Min Chang, Woo Kyung Moon, Nariya Cho, Ann Yi, Hye Ryoung Koo, Wonsik Han, Dong-Young Noh, Hyeong-Gon Moon, and Seung Ja Kim. Clinical application of shear wave elastography (swe) in the diagnosis of benign and malignant breast diseases. *Breast cancer research and treatment*, 129(1):89–97, 2011.

[147] D.L. Bader and P. Bowker. Mechanical characteristics of skin and underlying tissues in vivo. *Biomaterials*, 4(4):305–308, 1983.

[148] Avtar S. Ahuja. Tissue as a voigt body for propagation of ultrasound. *Ultrasonic Imaging*, 1(2):136–143, 1979.

[149] J.M. Pereira, J.M. Mansour, and B.R. Davis. Dynamic measurement of the viscoelastic properties of skin. *Journal of Biomechanics*, 24(2):157–162, 1991.

[150] T.A. Bigelow, B.L. McFarlin, W.D. O'Brien Jr., and M.L. Oelze. In vivo ultrasonic attenuation slope estimates for detecting cervical ripening in rats: Preliminary results. *Journal of the Acoustical Society of America*, 123(3):1794–1800, 2008. cited By (since 1996) 0.

[151] J.O. Kim and O.S. Kwon. Vibration characteristics of piezoelectric torsional transducers. *Journal of sound and vibration*, 264(2):453–473, 2003.

[152] S. Kaneko, S. Nomoto, H. Yamamori, and K. Ohya. Load characteristics of a bolted langevin torsional transducer. *Ultrasonics*, 34(2):239–241, 1996.

[153] Stephen C Butler. A 2.5 khz magnetostrictive tonpilz sonar transducer design. *The Journal of the Acoustical Society of America*, 109(5):2459–2459, 2001.

[154] J. Li, P. Liu, H. Ding, and W. Cao. Modeling characterization and optimization design for pzt transducer used in near field acoustic levitation. *Sensors and Actuators A: Physical*, 2011.

[155] H.Y. Lin and W. Fang. A rib-reinforced micro torsional mirror driven by electrostatic torque generators. *Sensors and Actuators A: Physical*, 105(1):1–9, 2003.

[156] AE Glazounov, QM Zhang, and C. Kim. Torsional actuator based on mechanically amplified shear piezoelectric response. *Sensors and Actuators A: Physical*, 79(1):22–30, 2000.

[157] P. Harkness, A. Cardoni, and M. Lucas. A comparison of coupling and degenerating mode in longitudinal-torsional step horns. *IEEE Transactions on Ultrasonics, Ferroelectrics and Frequency Control*, 2011.

[158] S. Lin. Study on the langevin piezoelectric ceramic ultrasonic transducer of longitudinal–flexural composite vibrational mode. *Ultrasonics*, 44(1):109–114, 2006.

[159] M. Aoyagi, T. Suzuki, and Y. Tomikawa. Characteristics of a bolt-clamped torsional vibrator using shear-mode piezo-ceramics sandwiched in the axial direction. *Ultrasonics*, 34(2):219–222, 1996.

[160] JM Thijssen, WA Verhoef, and MJ Cloostermans. Optimization of ultrasonic transducers. *Ultrasonics*, 23(1):41–46, 1985.

[161] H. Kwun, WD Jolly, GM Light, and E. Wheeler. Effects of variations in design parameters of ultrasonic transducers on performance characteristics. *Ultrasonics*, 26(2):65–72, 1988.

[162] CS Dutcher and DC Venerus. Compliance effects on the torsional flow of a viscoelastic fluid. *Journal of Non-Newtonian Fluid Mechanics*, 150(2-3):154–161, 2008.

[163] R.L. Taylor. *FEAP-ein finite element analysis programm*. Ing.-Gemeinschaft Klee & Wrigges, 1987.

[164] D. Goldberg. *Genetic algorithms in search, optimization and machine learning*. Addison-Wesley Publ, Reading, Massachussets, etc., 1989.

[165] F. Wang, X. Zhao, D. Zhang, and Y. Wu. Development of novel ultrasonic transducers for microelectronics packaging. *Journal of materials processing technology*, 209(3):1291–1301, 2009.

[166] A. Schröder, J. Rautenberg, and B. Henning. Evaluation of cost functions for fea based transducer optimization. *Physics Procedia*, 3(1):1003–1009, 2010.

[167] E. Heikkola and M. Laitinen. Model-based optimization of ultrasonic transducers. *Ultrasonics sonochemistry*, 12(1):53–57, 2005.

[168] Pei-Ling Liu and Cheng-Chieh Chen. Parametric identification of truss structures by using transient response. *Journal of sound and vibration*, 191(2):273–287, 1996.

[169] Albert Tarantola. *Inverse problem theory and methods for model parameter estimation*. siam, 2005.

[170] Albert Tarantola and Bernard Valette. Inverse problems= quest for information. *J. geophys*, 50(3):150–170, 1982.

[171] HF Lam, Ching-Tai Ng, and M Veidt. Experimental characterization of multiple cracks in a cantilever beam utilizing transient vibration data following a probabilistic approach. *Journal of Sound and Vibration*, 305(1):34–49, 2007.

[172] G Rus, SY Lee, SY Chang, and SC Wooh. Optimized damage detection of steel plates from noisy impact test. *International journal for numerical methods in engineering*, 68(7):707–727, 2006.

[173] G Rus, R Palma, and JL Pérez-Aparicio. Optimal measurement setup for damage detection in piezoelectric plates. *International Journal of Engineering Science*, 47(4):554–572, 2009.

[174] Theodore E Matikas. Damage characterization and real-time health monitoring of aerospace materials using innovative nde tools. *Journal of Materials Engineering and Performance*, 19(5):751–760, 2010.

[175] Roger J Zemp, Jahangir Tavakkoli, and Richard SC Cobbold. Modeling of nonlinear ultrasound propagation in tissue from array transducers. *The Journal of the Acoustical Society of America*, 113(1):139–152, 2003.

[176] Ketil Hokstad. Nonlinear and dispersive acoustic wave propagation. *Geophysics*, 69(3):840–848, 2004.

[177] MA Breazeale and DO Thompson. Finite-amplitude ultrasonic waves in aluminum. *Applied Physics Letters*, 3(5):77–78, 2004.

[178] H. Krautkramer J. Krautkramer. *Ultrasonic Testing of Materials*. Springer, New York, 1983.

[179] R. Guyer M. Talmant P. Laugier P. A. Johnson M. Muller, A. Sutin. Nonlinear resonant ultrasound spectroscopy (NRUS) applied to damage assessment in bone. *jasa*, 118.

[180] A. Sutin K.-A. Van Den Abeele, P. A. Johnson. Nonlinear elastic wave spectroscopy (NEWS) techniques to discern material damage, part i: nonlinear wave modulation spectroscopy (NEMS). *Research in nondestructive evaluation*, 12(1):17–30, 2000.

[181] J.-P. Remenieras M. Defontaine G. Renaud, S. Callé. Non-linear acoustic measurements to assess crack density in trabecular bone. *International Journal of Non-Linear Mechanics*, 43(3):194–200, 2008.

[182] K.-Y. Jhang and K.-C. Kim. Evaluation of material degradation using nonlinear acoustic effect. *Ultrasonics*, 37(1):39–44, 1999.

[183] Alexander M Sutin. Nonlinear acoustic nondestructive testing of cracks. *The Journal of the Acoustical Society of America*, 99(4):2539–2574, 1996.

[184] AM Sutin and VE Nazarov. Nonlinear acoustic methods of crack diagnostics. *Radiophysics and quantum electronics*, 38(3-4):109–120, 1995.

[185] LK Zarembo, VA Krasil'nikov, and IE Shkol'nik. Nonlinear acoustics in a problem of diagnosing the strength of solids. *Strength of Materials*, 21(11):1544–1551, 1989.

[186] Caterina Letizia Elisabetta Bruno, AS Gliozzi, M Scalerandi, and Paola Antonaci. Analysis of elastic nonlinearity using the scaling subtraction method. *Physical Review B*, 79(6):064108, 2009.

[187] Jeong K Na, William T Yost, and John H Cantrell. Variation of sound velocity in fatigued aluminum 2024-t4 as a function of hydrostatic pressure. In *Review of Progress in Quantitative Nondestructive Evaluation*, pages 2075–2082. Springer, 1993.

[188] John H Cantrell and William T Yost. Acoustic harmonic generation from fatigue-induced dislocation dipoles. *Philosophical magazine A*, 69(2):315–326, 1994.

[189] D Donskoy, A Sutin, and A Ekimov. Nonlinear acoustic interaction on contact interfaces and its use for nondestructive testing. *Ndt & E International*, 34(4):231–238, 2001.

[190] I Yu Solodov, N Krohn, and G Busse. Can: an example of nonclassical acoustic nonlinearity in solids. *Ultrasonics*, 40(1):621–625, 2002.

[191] Arkadi Berezovski, Mihhail Berezovski, and Jüri Engelbrecht. Numerical simulation of nonlinear elastic wave propagation in piecewise homogeneous media. *Materials Science and Engineering: A*, 418(1):364–369, 2006.

[192] M.H̃ori S. Nemat-Nasser. *Micromechanics: overall properties of heterogeneous materials*. North-Holland, Elsevier, 1999.

[193] S. Torquato. *Random Heterogeneous Materials*. Springer Verlag, 2001.

[194] G.W. Milton. *The Theory of Composites*. Cambridge University Press, 2002.

[195] Z Hashin. Analysis of composite materials. *Journal of Applied Mechanics*, 50:481–505, 1983.

[196] LJ Walpole. Analysis of composite materials. *Adv. Appl. Mech*, 21:169–242, 1981.

[197] JK Mackenzie. The elastic constants of a solid containing spherical holes. *Proceedings of the Physical Society. Section B*, 63:2–11, 1950.

[198] J.D. Eshelby. The determination of the elastic field of an ellipsoidal inclusion. *Proc. R. Soc. A*, 241, 1957.

[199] S.K. Kanaun and V.M. Levin. *Self-Consistent methods for composites. Volume 1 - Static problems*. Springer, Dordrecht, 2008.

[200] R. McLaughlin. Differential schemes for the elastic characterisation of dispersions of randomly oriented ellipsoids. *International Journal of Engineering Science*, 15:237–244, 1977.

[201] S Giordano. Differential schemes for the elastic characterisation of dispersions of randomly oriented ellipsoids. *European Journal of Mechanics-A/Solids*, 22:885, 2003.

[202] Y. Benveniste. A new approach to the application of mori–tanaka theory in composite materials. *Mech. Materials*, 6, 1987.

[203] J.R. Willis. Bounds and self-consistent estimates for the overall moduli of anisotropic composites. *J. Mech. Phys. Solids*, 25:185–202, 1977.

[204] P Ponte-Castaneda. The effective mechanical properties of nonlinear isotropic composites. *Journal of the Mechanics and Physics of Solids*, 39:45–71, 1991.

[205] M Kachanov and I I Sevostianov. On quantitative characterization of microstructures and effective properties. *International Journal of Solids and Structures*, 42(2):309–336, 2005.

[206] C Mauge and M Kachanov. Interacting arbitrarily oriented cracks in anisotropic matrix. stress intensity factors and effective moduli. *International Journal of Fracture*, 65(2):79–74, 1992.

[207] C Mauge and M Kachanov. Anisotropic material with interacting arbitrarily oriented cracks. stress intensity factors and crack-microcrack interactions. *International Journal of Fracture*, 65(2):115–139, 1994.

[208] M Kachanov. On the effective moduli of solids with cavities and cracks. *International journal of fracture*, 59(1):R17–R21, 1993.

[209] E.A. Berger R. Spatschek, C. Gugenberger. Effective elastic moduli in solids with high density of cracks,. *Phys. Rev. B*, 80.

[210] S.W. Yu X.Q. Feng. Estimate of effective elastic moduli with microcrack interaction effects. *Theoret. Appl. Fracture Mechanics*, 34.

[211] S Giordano and L Colombo. Effects of the orientational distribution of cracks in solids. *Applied Phys. Letters*, 98:055503, 2007.

[212] D.R.S. Talbot and J.R. Willis. Variational principles for nonlinear inhomogeneous media. *IMA J. Appl. Math.*, 35:39–54, 1985.

[213] Oscar Lopez-Pamies. An exact result for the macroscopic response of particle-reinforced neo-hookean solids. *Journal of Applied Mechanics*, 77(2):021016, 2010.

[214] G DeBotton, I Hariton, and EA Socolsky. Neo-hookean fiber-reinforced composites in finite elasticity. *Journal of the Mechanics and Physics of Solids*, 54(3):533–559, 2006.

[215] I Hariton, G Debotton, TC Gasser, and GA Holzapfel. Stress-modulated collagen fiber remodeling in a human carotid bifurcation. *Journal of theoretical Biology*, 248(3):460–470, 2007.

[216] L Gibiansky and S Torquato. Effective energy of nonlinear elastic and conducting composites: Approximations and cross-property bounds. *Journal of applied physics*, 84:5969–5976, 1998.

[217] H Moulinec and P Suquet. Intraphase strain heterogeneity in nonlinear composites: a computational approach. *European Journal of Mechanics-A/Solids*, 22:751–770, 2003.

[218] S Giordano, PL Palla, and L Colombo. Nonlinear elasticity of composite materials. *The European Physical Journal B*, 68:89–101, 2009.

[219] Raymond W Ogden. *Non-linear elastic deformations*. Courier Corporation, 1997.

[220] W Domanski. Weakly nonlinear elastic plane waves in a cubic crystal. *Contemporary Mathematics*, 255:45–62, 2000.

[221] RA Toupin and B Bernstein. Sound waves in deformed perfectly elastic materials. acoustoelastic effect. *The Journal of the Acoustical Society of America*, 33(2):216–225, 2005.

[222] A.C. Erigen and E.S. Suhubi. *Elastodynamics*, volume I and II. Academic Press, New York, and London, 1974-5.

[223] S.H. Smith. Random-loading fatigue crack growth behavior of some aluminum and titanium alloys. In *Fifth Pacific Area National Meeting of the American Society for Testing and Materials*, number 5, pages 1–35. American Society for Testing and Materials, May 1966.

[224] Andrei D Polyanin and Valentin F Zaitsev. *Handbook of nonlinear partial differential equations*. CRC press, 2003.

[225] R.A. Guyer and P.A. Johnson. Nonlinear mesoscopic elasticity: evidence for a new class of materials. *Physics Today*, 52(4):30–36, 1999.

[226] David J Holcomb. Memory, relaxation, and microfracturing in dilatant rock. *Journal of Geophysical Research: Solid Earth (1978–2012)*, 86(B7):6235–6248, 1981.

[227] KR McCall and RA Guyer. A new theoretical paradigm to describe hysteresis, discrete memory and nonlinear elastic wave propagation in rock. *Nonlinear processes in geophysics*, 3(2):89–101, 1999.

[228] Koen EA Van Den Abeele, Paul A Johnson, Robert A Guyer, and Katherine R McCall. On the quasi-analytic treatment of hysteretic nonlinear response in elastic wave propagation. *The Journal of the Acoustical Society of America*, 101(4):1885–1898, 1997.

[229] Sylvain Haupert, Guillaume Renaud, Jacques Riviere, Maryline Talmant, Paul A Johnson, and Pascal Laugier. High-accuracy acoustic detection of nonclassical component of material nonlinearity. *The Journal of the Acoustical Society of America*, 130(5):2654–2661, 2011.

[230] Rafael Munoz, Guillermo Rus, Nicolas Bochud, Daniel J Barnard, Juan Melchor, Juan Chiachío Ruano, Manuel Chiachío, Sergio Cantero, Antonio M Callejas, Laura M Peralta, et al. Nonlinear ultrasonics for early damage detection.

[231] HM Ledbetter and Richard Palmer Reed. Elastic properties of metals and alloys, i. iron, nickel, and iron-nickel alloys. *Journal of Physical and Chemical Reference Data*, 2(3):531–618, 1973.

[232] Michael J Mehl, Barry M Klein, and Dimitri A Papaconstantopoulos. *First principles calculations of elastic properties of metals*, volume 1. Citeseer, 1994.

[233] Jean Lemaitre. A continuous damage mechanics model for ductile fracture. *Journal of Engineering Materials and Technology*, 107(1):83–89, 1985.

[234] Jearl Walker, Robert Resnick, and David Halliday. *Fundamentals of physics*. Wiley, 2008.

[235] Kemal Arda, Nazan Ciledag, Elif Aktas, Bilgin Kadri Arıbas, and Kenan Köse. Quantitative assessment of normal soft-tissue elasticity using shear-wave ultrasound elastography. *American Journal of Roentgenology*, 197(3):532–536, 2011.

[236] ME Carr and SHERYL L Zekert. Abnormal clot retraction, altered fibrin structure, and normal platelet function in multiple myeloma. *American Journal of Physiology-Heart and Circulatory Physiology*, 266(3):H1195–H1201, 1994.

[237] Marco PE Wenger, Laurent Bozec, Michael A Horton, and Patrick Mesquida. Mechanical properties of collagen fibrils. *Biophysical journal*, 93(4):1255–1263, 2007.

[238] GF Smith and RS Rivlin. The strain-energy function for anisotropic elastic materials. *Transactions of the American Mathematical Society*, 88(1):175–193, 1958.

[239] R. Hill. Theory of mechanical properties of fibre-strengthened materials: I. Elastic behaviour. *J. Mech. Phys. Solids*, 12:199–211, 1964.

[240] D.H. Kim. *Composite structures for civil and architectural engineering*. Taylor & Francis, 1994.

[241] Pichai Rusmee. High strength composites. *Utah University*, page 2, 2005.

[242] BA Konyukhov and GM Shalashov. Third-order effects in the propagation of elastic waves in isotropic solids generation of higher harmonics. *Journal of Applied Mechanics and Technical Physics*, 15(4):535–540, 1974.

[243] Karan S Surana. *Advanced mechanics of continua*. CRC Press, 2014.

[244] Meir Shinitzky and Michael Inbar. Microviscosity parameters and protein mobility in biological membranes. *Biochimica et Biophysica Acta (BBA)-Biomembranes*, 433(1):133–149, 1976.

[245] Anja Vinckier and Giorgio Semenza. Measuring elasticity of biological materials by atomic force microscopy. *Febs Letters*, 430(1):12–16, 1998.

[246] C. Pantea, C.F. Osterhoudt, and D.N. Sinha. Determination of acoustical nonlinear parameter β of water using the finite amplitude method. *Ultrasonics*, page http://dx.doi.org/10.1016/j.ultras.2013.01.008, 2013.

[247] M.F. Hamilton and D.T. Blackstock. *Nonlinear acoustics*, volume 237. 1998.

[248] K. F. Graff. *Wave motion in elastic solids*. Dover, 1975.

[249] T. Mura, T. Koya, C. Hsieh, Z. A. Moschovidis, and Z. Gao. Inverse problems associated with nondestructive evaluation of plastic damages in solids.

[250] F Lene and D Leguillon. Homogenized constitutive law for a partially cohesive composite material. *International Journal of Solids and Structures*, 18(5):443–458, 1982.

[251] P De Buhan and A Taliercio. A homogenization approach to the yield strength of composite materials. *European journal of mechanics. A. Solids*, 10(2):129–154, 1991.

[252] D Fujii, BC Chen, and Noboru Kikuchi. Composite material design of two-dimensional structures using the homogenization design method. *International Journal for Numerical Methods in Engineering*, 50(9):2031–2051, 2001.

[253] JB Walsh. The effects of cracks on the uniaxial elastic compression of rocks. *Journal of geophysical*, 70:399–411, 1965.

[254] C. Pecorari and I. Solodov. Nonclassical nonlinear dynamics of solid surfaces in partial contact for nde applications. *Universality of Nonclassical Nonlinearity. Springer New York*, pages 309–326, 2006.

[255] Joseph Berkson. Application of the logistic function to bio-assay. *Journal of the American Statistical Association*, 39(227):357–365, 1944.

[256] Joseph Berkson. A statistically precise and relatively simple method of estimating the bio-assay with quantal response, based on the logistic function. *Journal of the American Statistical Association*, 48(263):565–599, 1953.

[257] Nicolas Robeyst, Elke Gruyaert, Christian U Grosse, and Nele De Belie. Monitoring the setting of concrete containing blast-furnace slag by measuring the ultrasonic p-wave velocity. *Cement and Concrete research*, 38(10):1169–1176, 2008.

[258] W.J. Parnell, Melchor J., and Rus G. Non linear elastic constitutive behavior of cracked and damaged materials. In preparation for submission to JASA, 2013.

[259] S Catheline, J-L Gennisson, and M Fink. Measurement of elastic nonlinearity of soft solid with transient elastography. *The Journal of the Acoustical Society of America*, 114:3087, 2003.

[260] Zaki Abiza, Michel Destrade, and Ray W Ogden. Large acoustoelastic effect. *Wave Motion*, 49(2):364–374, 2012.

[261] SK Kanaun, VM Levin, and James G Berryman. Self-consistent methods for composites, volume 1 static problems. *Acoustical Society of America Journal*, 123:4027, 2008.

[262] G Rus, J Melchor, W Parnell, N Bochud, and L Peralta. Damage prediction via nonlinear quantitative ultrasound: a micro-mechanical approach. *Ultrasonics*, pages –, 2016.

[263] Murray Spiegel. *Schaum's mathematical handbook of formulas and tables*. McGraw-Hill Osborne Media, 1999.

[264] Valeri A Korneev, Kurt T Nihei, and Larry R Myer. Nonlinear interaction of plane elastic waves. Technical report, Lawrence Berkeley National Lab., CA (United States), 1998.

[265] Joseph L Rose. *Ultrasonic waves in solid media*. Cambridge university press, 2004.

[266] R Molina and G Rus. Nonlinear mixing: Evaluación de parámetros de no linealidad ultrasónica. *UGR*, 1:1–74, 2015.

[267] Michael Schoenberg and Joao Protazio. Zoeppritz rationalized, and generalized to anisotropic media. *The Journal of the Acoustical Society of America*, 88(S1):S46–S46, 1990.

[268] Karl Zoeppritz. Erdbebenwellen vii. *Nachrichten von der Gesellschaft der Wissenschaften zu Göttingen, Mathematisch-Physikalische Klasse*, 1919:57–65, 1919.

[269] J Melchor, L Peralta, G Rus, N Saffari, and J Soto. Single-transmitter setup on nonlinear mixing to measure acoustic nonlinearity of first order. In *Ultrasonic Characterization of Bone (ESUCB), 2015 6th European Symposium on*, pages 1–4. IEEE, 2015.

[270] Nonlinear Acoustics. Mf hamilton and dt blackstock. *Academic, Boston*, page 245, 1998.

[271] Christophe Barriere and Daniel Royer. Diffraction effects in the parametric interaction of acoustic waves: application to measurements of the nonlinearity parameter b/a in liquids. *Ultrasonics, Ferroelectrics, and Frequency Control, IEEE Transactions on*, 48(6):1706–1715, 2001.

[272] G. Rus, S. Y. Lee, S. Y. Chang, and S. C. Wooh. Optimized damage detection of steel plates from noisy impact test. *International Journal for Numerical Methods in Engineering*, 68:707–727, 2006.

[273] R. Gallego and G. Rus. Identification of cracks and cavities using the topological sensitivity boundary integral equation. *Computational Mechanics*, 33:154–163, 2004.

[274] L. Rade and B. Westergren. *Mathematics Handbook for Science and Engineering*. Springer, 1999.

[275] EA Barannik, A Girnyk, V Tovstiak, AI Marusenko, SY Emelianov, and AP Sarvazyan. Doppler ultrasound detection of shear waves remotely induced in tissue phantoms and tissue in vitro. *Ultrasonics*, 40(1):849–852, 2002.

[276] Marko Orescanin, Muqeem A Qayyum, Kathleen S Toohey, and Michael F Insana. Complex shear modulus of thermally-damaged liver. In *Ultrasonics Symposium (IUS), 2009 IEEE International*, pages 127–130. IEEE, 2009.

[277] Karl F Graff. *Wave motion in elastic solids*. Courier Corporation, 2012.

[278] Evgenia A Zabolotskaya, Mark F Hamilton, Yurii A Ilinskii, and G Douglas Meegan. Modeling of nonlinear shear waves in soft solids. *The Journal of the Acoustical Society of America*, 116(5):2807–2813, 2004.

[279] Armen P Sarvazyan, Oleg V Rudenko, Scott D Swanson, J Brian Fowlkes, and Stanislav Y Emelianov. Shear wave elasticity imaging: a new ultrasonic technology of medical diagnostics. *Ultrasound in medicine & biology*, 24(9):1419–1435, 1998.

[280] A Valera and G Rus. Diseño y validación de un nuevo transductor ultrasónico de ondas de torsión. *UGR*, 1:1–104, 2015.

[281] Ferdinand P Beer and E Russell Johnston Jr. Mechanics of materials, 1992.

[282] Mark F Hamilton. Fundamentals and applications of nonlinear acoustics. *Volume HI: Background Materials*, page 82, 1986.

[283] Timothy S Hart and Mark F Hamilton. Nonlinear effects in focused sound beams. *The Journal of the Acoustical Society of America*, 84(4):1488–1496, 1988.

[284] JJ Rushchitsky and C Cattani. Evolution equations for plane cubically nonlinear elastic waves. *International Applied Mechanics*, 40(1):70–76, 2004.

[285] Jeremiah J Rushchitsky. *Nonlinear elastic waves in materials*, volume 3582. Springer, 2014.

[286] KE-A Van Den Abeele, Paul A Johnson, and Alexander Sutin. Nonlinear elastic wave spectroscopy (news) techniques to discern material damage, part i: nonlinear wave modulation spectroscopy (nwms). *Research in nondestructive evaluation*, 12(1):17–30, 2000.

[287] PA Johnson and PNJ Rasolofosaon. Nonlinear elasticity and stress-induced anisotropy in rock. *Journal of Geophysical Research: Solid Earth (1978–2012)*, 101(B2):3113–3124, 1996.

[288] Christoph Klieber, David Johnson, et al. Nonlinear tube waves. *Acoustics 2012 Nantes*, 2012.

[289] Marie Muller and Guillaume Renaud. Nonlinear acoustics for non-invasive assessment of bone micro-damage. In Pascal Laugier and Guillaume Haïat, editors, *Bone Quantitative Ultrasound*, pages 381–408. Springer Netherlands, 2011.

[290] S Giordano, PL Palla, and L Colombo. Effective permittivity of materials containing graded ellipsoidal inclusions. *The European Physical Journal B-Condensed Matter and Complex Systems*, 66(1):29–35, 2008.

[291] S Giordano, PL Palla, and L Colombo. Nonlinear elasticity of composite materials. *The European Physical Journal B-Condensed Matter and Complex Systems*, 68(1):89–101, 2009.

[292] Michel Destrade, Michael D Gilchrist, and Raymond W Ogden. Third-and fourth-order elasticities of biological soft tissues. *The Journal of the Acoustical Society of America*, 127(4):2103–2106, 2010.

[293] S Mercier and A Molinari. Homogenization of elastic–viscoplastic heterogeneous materials: Self-consistent and mori-tanaka schemes. *International Journal of Plasticity*, 25(6):1024–1048, 2009.

[294] S Giordano, PL Palla, and L Colombo. Nonlinear elasticity of composite materials. *The European Physical Journal B*, 68(1):89–101, 2009.

[295] J.D. Eshelby. The determination of the elastic field of an ellipsoidal inclusion. *Proc. Roy. Soc. Lond. A*, 241:376–396, 1957.

[296] G Kneer. Die elastischen konstanten quasiisotroper vielkristallaggregate. *physica status solidi (b)*, 3(9):K331–K335, 1963.

[297] Stefano Giordano and Luciano Colombo. Effects of the orientational distribution of cracks in solids. *Physical review letters*, 98(5):055503, 2007.

[298] William J Parnell, MB Vu, Q Grimal, and S Naili. Analytical methods to determine the effective mesoscopic and macroscopic elastic properties of cortical bone. *Biomechanics and modeling in mechanobiology*, 11(6):883–901, 2012.

[...] por la materia que me une a ti [...]

La ley del desierto, la ley del mar.
Santiago Auserón, 1984